

Institute of Biomechanics and Orthopaedics
German Sport University Cologne
Head of Institute: Univ.-Prof. Dr. Gert-Peter Brüggemann

**Application of Digital Human Modeling
for the Ergonomic Evaluation
of Handbrakes in Passenger Vehicles**

An academic dissertation approved by the
German Sport University Cologne
and
submitted for the degree
Dr. rer. nat.

by
Andrea Upmann
from Cologne, Germany

Cologne, 2016

Referees

First Referee: Univ.-Prof. Dr. Gert-Peter Brüggemann

Institute of Biomechanics and Orthopaedics
German Sport University Cologne, Germany

Second Referee: Prof. i. R. Dr. rer. nat. Heiner Bubb

Institute of Ergonomics and Division of Sports Equipment and Materials
Technical University of Munich, Germany

Chair of the doctorate committee: Univ.-Prof. Dr. med. Wilhelm Bloch

Institute of Cardiology and Sports Medicine
German Sport University Cologne, Germany

The dissertation was defended on December 15th, 2016.

Declaration

Hereby I declare:

The work presented in this thesis is the original work of the author except where acknowledged in the text.

This thesis is a result of a project accomplished in collaboration with several teams. Thus, in “Foreword & Acknowledgement” a summary is provided which parts of the overall project were achieved by the author and which ones by others.

This material has not been submitted either in whole or in part for a degree at this or any other institution. Those parts or single sentences, which have been verbatim from other sources, are identified as citations. I further declare that I complied with actual guidelines of qualified scientific work of the German Sport University Cologne.

Cologne, 2016

A handwritten signature in black ink, reading "Andrea Upmann", written in a cursive style.

Andrea Upmann

Foreword & Acknowledgement

This dissertation is based on my work as an employee of Ford-Werke GmbH, Cologne, Germany, within the framework of research studies on modeling the human for questions of ergonomic design in vehicle development.

Interdisciplinary collaboration is required for the successful completion of biomechanical and ergonomic tasks within the development of cars. Therefore, thoughts and expert knowledge of several colleagues and project partners were introduced in this work.

This publication is based on research studies about handbrake application, which were enabled by the cooperation between the Institute of Biomechanics and Orthopaedics (IBO), German Sport University Cologne, Germany, and three Ford departments. The departments are Vehicle Interior Technologies (VIT, Ford Research Center, Aachen, Germany), Chassis Engineering and Accommodation & Usage (A&U, Ford Product Development Center, Cologne, Germany).

One of my tasks in A&U was to initiate and lead a project to develop a reliable CAE based assessment procedure for handbrake ergonomics. This procedure is aimed to be applied by engineers during the development of vehicles to reduce the number of subjective evaluation studies, to increase objectivity of ergonomic assessments and to enable evaluations at an early stage in the development.

The entire project consisted of five major subprojects:

1. Two empirical studies with subjects.
2. The reconstruction of motion capturing data and development of an AMS (AnyBody Modeling System) handbrake application model.
3. The development of a RAMSIS procedure for realistic posture prediction.
4. The analysis of AMS results (which were calculated based on RAMSIS postures) and their relation to the subjective ratings from the second empirical study.
5. The development of a mathematical transfer function to predict discomfort ratings for new handbrake variants based on RAMSIS and AMS simulation.

The first, second and third subproject were completed by several teams. This thesis focuses on the fourth and fifth subproject.

In the course of the overall project several master theses, project reports and presentations as well as this doctoral thesis were finalized. Completing my dissertation was a challenging activity and I am very thankful for the support I have received.

First and foremost, I would like to express my deepest gratitude to Univ. Prof. Dr. Gert-Peter Brüggemann, Institute of Biomechanics and Orthopaedics (IBO), German Sport University Cologne, for enabling the collaboration and supervising this thesis. Thank you for the valuable, stimulating and inspiring discussions which were always helpful for me and expanded my engineering view with a biomechanical perspective. Your joy about biomechanical research and your enthusiasm for new findings were very motivating for me! Sincere thanks goes to Prof. i. R. Dr. rer. nat. Heiner Bubb for assessing my thesis as second referee.

I am very thankful to my manager, Paul van den Broek, my supervisor Igor Fischbein and my team leader Milda Park (all A&U) for supporting this thesis by adjusting my workload.

I sincerely thank you, Igor, for being a demanding, encouraging and caring supervisor and mentor for me. I highly appreciate your commitment and passion for vehicle development and smart details as well as your “out of the box” views in discussions. Thank you also for your detailed feedback on this thesis.

Special thanks goes to Igor Fischbein (A&U) and Jessica Rausch (VIT) for numerous fruitful discussions and great collaboration. I also would like to thank you, Jessica, for the reconstruction of motion capturing data and for the development of an AMS handbrake application model. I am deeply grateful to you for sharing your enormous AMS and Matlab knowledge and experiences as well as for helping to overcome challenging tasks regarding these tools. Many thanks to AnyBody Technology and Philipp Wolf for also assisting me in case of AMS related questions.

Sincere thanks to Philipp Raiber for developing a RAMSIS procedure as a part of this project and to Ralf Nürnberg (both A&U) as well as Human Solutions GmbH for sharing their extensive RAMSIS expertise.

I also would like to thank the team from IBO for performing the empirical studies and contributing with their knowledge about motion capturing and analysis. I would like to representatively name Kai Heinrich, Johannes Lietmeyer and Peter Rzepka.

Furthermore, my gratitude goes to my colleagues from Chassis Engineering for sharing their knowledge on handbrake design. I also would like to thank the staff from the metrology team as well as the mechanical and electrical workshops at Ford and IBO for their support to prepare the ErgoBuck for the studies.

Last but not least, I would like to thank my family, close colleagues and friends who have always encouraged and supported my dreams and ambitions, most importantly my parents Mathilde und Klaus Upmann, my sister Claudia Margner and my partner Michael Mauk.

DANKE, dass ihr immer für mich da wart und da seid!

Abstract

Comfort is an important factor in product buying decision. Therefore vehicle manufacturers aim to develop ergonomic vehicles which minimize occupants' discomfort. The handbrake is an essential control in vehicles. This work provides the first demonstration that the perceived discomfort of the handbrake application can reliably be predicted based on postural, biomechanical and mathematical modelling.

In two studies 117 respectively 40 subjects rated the discomfort for several handbrake variants while their motion was recorded. Afterwards, the handbrake application was modeled in the Digital Human Modeling software RAMSIS and the biomechanical software AnyBody Modeling System (AMS). Calculated biomechanical parameters included joint reactions, joint muscle moment measures, muscle activities, joint angles as well as metabolic power and energy. Stepwise regression was applied to develop a prediction model for discomfort. The herewith calculated discomfort was well in line with the subjects' ratings ($r^2 = 0.96$, $r^2_{adj} = 0.94$).

As a result, a user-friendly procedure has been proposed to quantify handbrake discomfort with DHMs which are typically available in automotive development. This method can be applied at early stages of the automotive development to enhance the ergonomics of the vehicle interior. It allows for increasing efficiency and objectivity as well as for saving resources and budget.

Abstrakt

Komfort ist ein wichtiger Faktor bei Kaufentscheidungen. Deswegen streben Fahrzeughersteller die Entwicklung ergonomischer Fahrzeuge, die den Diskomfort der Insassen minimieren, an. Die Handbremse ist ein wesentliches Bedienelement in Fahrzeugen. Diese Arbeit beinhaltet den ersten Nachweis, dass der empfundene Diskomfort bei der Betätigung der Handbremse durch Haltungssimulation sowie biomechanische und mathematische Modellierung zuverlässig vorhergesagt werden kann.

In zwei Studien beurteilten 117 beziehungsweise 40 Probanden den Diskomfort für mehrere Handbremsvarianten. Dabei wurde ihre Bewegung aufgezeichnet. Danach wurde die Handbremsbetätigung im Menschmodell RAMSIS und in der biomechanischen Software AnyBody Modeling System (AMS) simuliert. Die berechneten biomechanischen Parameter umfassen Gelenkreaktionen, Gelenkmuskelmomente, Muskelaktivitäten, Gelenkwinkel sowie metabolische Leistung und Energie. Schrittweise Regression wurde angewendet, um eine Vorhersagegleichung für den Diskomfort zu entwickeln. Der damit berechnete Diskomfort spiegelt die Bewertungen der Probanden sehr gut wieder ($r^2 = 0.96$, $r^2_{adj} = 0.94$).

Somit wurde eine benutzerfreundliche Methode entwickelt, um den Handbremsdiskomfort mit Menschmodellen, welche üblicherweise in der Automobilindustrie verwendet werden, zu quantifizieren. Diese Methode kann bereits früh im Entwicklungsprozess angewendet werden, um die Ergonomie des Fahrzeuginnenraums zu verbessern. So können Effizienz und Objektivität erhöht sowie Ressourceneinsatz und Kosten reduziert werden.

Contents

1 INTRODUCTION, OBJECTIVE AND OUTLINE	1
1.1 Introduction	1
1.2 Objective	4
1.3 Outline	4
2 LITERATURE REVIEW	5
2.1 Classification and interaction of biomechanics, ergonomics, comfort & discomfort	5
2.1.1 Biomechanics.....	5
2.1.1.1 Introduction to the musculoskeletal system.....	6
2.1.2 Ergonomics	8
2.1.3 Comfort and discomfort.....	10
2.2 Comfort and discomfort models.....	12
2.2.1 Comfort and discomfort model by Zhang et al. (1996)	12
2.2.2 Comfort pyramid by Krist (1993)	14
2.2.3 Comfort and discomfort model by de Looze et al. (2003).....	14
2.2.4 Discomfort model by Vink & Hallbeck (2012)	16
2.2.5 Conclusions	17
2.3 Factors influencing discomfort	18
2.3.1 Human characteristics	18
2.3.1.1 Anthropometry including inertial characteristics	18
2.3.1.2 Physical capabilities	19
2.3.2 Biomechanical characteristics	22
2.3.2.1 Kinematics	22
2.3.2.2 Kinetics	23
2.3.3 Product and usage characteristics.....	25
2.3.3.1 Geometrical dimensions and shape	26
2.3.3.2 Forces and interface design	26
2.3.3.3 Time.....	26
2.3.4 Conclusions	27
2.4 Evaluation of comfort and discomfort	27
2.4.1 Subjective evaluation methods with examples	28
2.4.2 Objective evaluation methods and examples	30
2.5 Discomfort of handbrake application and seated reach	30
2.5.1 Handbrake application discomfort	31
2.5.2 Discomfort of seated reach and grasp.....	33
2.5.3 Discomfort evaluation using Digital Human Models	36
2.5.4 Conclusions	36
2.6 Movement strategies.....	38
2.6.1 Driving posture	39

2.6.2 Seated reach	40
2.6.2.1 Reach and grasp	41
2.6.2.2 Movement regularity and variability	41
2.6.2.3 Reach movement hypotheses, influence factors and empirical studies	42
2.6.2.4 Influence of age	45
2.6.3 Conclusions	48
2.7 Digital Human Models	51
2.7.1 Advantages, limitations and challenges	51
2.7.2 Development history	53
2.7.3 Selected categories of DHMs	54
2.7.3.1 Anthropometric models	54
2.7.3.2 Biomechanical models	54
2.7.3.3 Posture and motion models	55
2.7.3.4 Models providing discomfort prediction	60
2.7.3.5 Combination of DHMs for discomfort prediction	64
2.7.4 Conclusions	67
2.8 RAMSIS	68
2.8.1 Internal and external model	69
2.8.2 RAMSIS platforms	70
2.8.3 RAMSIS NextGen plug-ins	71
2.8.3.1 The BodyBuilder plug-in	71
2.8.3.2 The Ergonomics plug-in and posture calculation	72
2.8.4 The Car Driver Model (CDM)	75
2.8.4.1 Posture prediction	75
2.8.4.2 Discomfort prediction	77
2.8.5 Conclusions	79
2.9 The AnyBody Modeling System (AMS)	79
2.9.1 User Interface	81
2.9.2 Applications	82
2.9.3 Body Models	82
2.9.3.1 Arm and shoulder model	82
2.9.3.2 Trunk model	84
2.9.3.3 Leg and foot models	84
2.9.4 Muscle modeling	85
2.9.4.1 Muscle types	85
2.9.4.2 Muscle models	85
2.9.5 Scaling methods	87
2.9.5.1 Geometrical scaling	87
2.9.5.2 Muscle strength scaling	89
2.9.6 Kinematic analysis	90
2.9.7 Inverse dynamics	91

2.9.7.1 Muscle recruitment	92
2.9.7.2 Mechanical model.....	94
2.9.8 Simulation results.....	94
2.9.8.1 Metabolic power consumption and total metabolic energy	94
2.9.8.2 Muscle activity	95
2.9.8.3 Joint reactions and joint moment measure.....	96
2.9.8.4 Joint angles	97
2.9.9 Validation	97
2.9.10 Limitations	98
2.9.11 Conclusions	99
2.10 The handbrake.....	99
2.10.1 Brake systems	99
2.10.2 Legal requirements	100
2.10.3 Automotive standards and key indicator method.....	101
2.10.3.1 Automotive standards and guidelines	101
2.10.3.2 Key indicator methods for manual handling operations	105
2.10.4 Handbrake lever design	106
2.10.5 Relevance of the handbrake design	107
2.10.6 Discomfort perception of handbrake application	108
2.10.7 Conclusions	109
3 RESEARCH PROBLEM AND OBJECTIVE OF THE THESIS	111
3.1 Research problem	111
3.2 Objective of the thesis	112
3.3 Hypotheses	113
4 DESIGN OF THE STUDY	115
5 PRELIMINARY STUDY	117
5.1 Methods.....	118
5.1.1 Study design	118
5.1.2 Test vehicle	118
5.1.3 Testrig ErgoBuck	119
5.1.4 Handbrake locations	120
5.1.5 Subjects	121
5.1.6 Procedure	123
5.1.6.1 Pre-questionnaire	123
5.1.6.2 Test drive	123
5.1.6.3 Anthropometric measurements	124
5.1.6.4 Handbrake application.....	124
5.1.6.5 Maximal force measurement and post-questionnaire	127
5.1.7 Data analysis	127
5.1.7.1 Cluster analysis	127

5.2 Results	128
5.2.1 Subjective evaluation	128
5.2.1.1 Reproducibility	131
5.2.2 Movement patterns	131
5.2.2.1 Identification of outliers	131
5.2.2.2 Selection of relevant variables	132
5.2.2.3 Selection of cluster merging algorithm	132
5.2.2.4 Classification of subjects in clusters	133
5.2.2.5 Analysis of cluster variables	133
5.2.2.6 Analysis of the cluster composition	134
5.2.3 Inclusion criteria of subjects for the main study	135
5.2.3.1 Repeatability of subjective ratings	135
5.2.3.2 Conformity with cluster means of movement variables	136
5.2.3.3 Ranking list and selection	136
5.3 Discussion and conclusions	137
5.3.1 Subjective evaluation	137
5.3.2 Movement patterns	138
5.3.3 Inclusion criteria of subjects for the main study	140
6 MAIN STUDY	141
6.1 Methods	141
6.1.1 Study design	141
6.1.2 Motion analysis	142
6.1.3 Handbrake locations	145
6.1.4 Subjects	146
6.1.5 Procedure	146
6.1.5.1 Pre-questionnaire	147
6.1.5.2 Anthropometric measurements	147
6.1.5.3 Preparation of the subjects	147
6.1.5.4 Handbrake application	147
6.1.5.5 Post-questionnaire	150
6.1.5.6 Measurement data processing	150
6.1.6 Data analysis	151
6.2 Results	151
6.2.1 Subjective evaluation	151
6.2.1.1 Reproducibility	151
6.2.1.2 Handbrake locations	151
6.2.2 Joint angles	154
6.3 Discussion and conclusions	158
6.3.1 Subjective evaluation	158
6.3.2 Joint angles	160

7 POSTURE MODELING	163
7.1 Preliminary considerations	164
7.2 Prediction of driving posture	164
7.3 Prediction of hand posture for handbrake application	165
7.4 Prediction of the handbrake application posture	167
8 BIOMECHANICAL MODELING AND CORRELATION TO DISCOMFORT	173
8.1 Methods.....	173
8.1.1 AMS setup	173
8.1.2 Modeled handbrake applications	175
8.1.3 Analyzed biomechanical parameters calculated with AMS	175
8.1.3.1 Metabolic power consumption and energy.....	176
8.1.3.2 Muscle activity	176
8.1.3.3 Joint reaction forces and moment measures	176
8.1.3.4 Joint angles	176
8.1.4 Relation of biomechanical parameters and discomfort perception.....	176
8.1.5 Mathematical procedure	178
8.2 Results and discussion	179
8.2.1 Metabolic power consumption (P_{met}) and total metabolic energy (E_{met}).....	182
8.2.2 Muscle activity.....	186
8.2.2.1 Maximum and mean muscle activity for body regions	186
8.2.2.2 Maximum and mean muscle activity for the trunk	186
8.2.2.3 Maximum and mean muscle activity for right shoulder and arm muscles.....	188
8.2.3 Joint reactions.....	192
8.2.4 Joint moment measures.....	196
8.2.5 Joint angles	197
8.2.6 Body height and gender.....	200
8.3 Conclusions	200
9 DISCOMFORT MODELING	201
9.1 Methods.....	201
9.2 Results and discussion	202
9.2.1 Stepwise regression.....	202
9.2.2 Predictors	203
9.2.3 Prediction quality.....	208
9.3 Conclusions	213
10 PROCEDURE TO PREDICT DISCOMFORT PERCEPTION	215
11 DISCUSSION AND OUTLOOK	219
11.1 Discussion	219
11.2 Limitations and potential topics for future research	221
11.2.1 Validation	221

11.2.2 Subjects' demographics and anthropometry.....	222
11.2.3 Subjects' handbrake application habits.....	222
11.2.4 Handbrake and application characteristics	222
11.2.5 Subjective evaluation and motion analysis	223
11.2.6 RAMSIS.....	223
11.2.7 AMS.....	224
11.2.8 Mathematical model	224
11.2.9 Pressure distribution	224
11.2.10 Ergonomics and discomfort evaluation of other applications.....	224
12 SUMMARY	225
13 GERMAN SUMMARY - DEUTSCHE ZUSAMMENFASSUNG	229
14 APPENDIX.....	235
14.1 Nomenclature.....	235
14.2 Preliminary study	237
14.2.1 Pre-questionnaire	237
14.2.2 Variables from the video analysis	238
14.2.2.1 Anteversion/retroversion of the Arm (AntRet).....	238
14.2.2.2 Abduction of the upper arm (Abd)	239
14.2.2.3 Flexion of the elbow joint (Eflex).....	239
14.2.2.4 Wrist abduction (HG)	239
14.2.2.5 Vertical position of the shoulder (SGv)	240
14.2.2.6 Dorsal-ventral movement of the shoulder (SGh)	240
14.2.2.7 Vertical shoulder movement (dSGv).....	241
14.2.2.8 Dorsal-ventral movement of the elbow (dESx)	241
14.2.2.9 Vertical movement of the elbow (dESz)	241
14.2.2.10 Dorsal-ventral movement of the elbow (dETx)	242
14.2.2.11 Medio-lateral movement of the elbow (dETz)	242
14.2.2.12 Range of the anteversion/retroversion of the arm (dAntRet).....	243
14.2.2.13 Range of abduction of the upper arm (dAbd)	243
14.2.2.14 Range of dorsal-ventral position of the shoulder (dSGh)	243
14.2.2.15 Range of elbow flexion/extension (dEflex)	243
14.2.2.16 Range of abduction of the wrist (dHG)	243
14.2.3 Post-questionnaire	244
14.2.4 Preliminary study subjective evaluation	245
14.2.5 Dendogram for outlier selection	249
14.2.6 Dendogram for classification of subjects into clusters	250
14.2.7 Correlation of movement variables and clusters.....	251
14.2.8 Correlation of body height and further subject characteristics	252
14.3 Main study.....	252
14.3.1 Marker setup	252

14.3.2 Pre-questionnaire.....	255
14.3.3 Post-questionnaire	256
14.3.4 Subjective evaluation	257
14.4 Posture modeling	259
14.4.1 Sternoclavicular joint.....	259
14.4.2 Glenohumeral joint (shoulder joint)	259
14.4.3 Elbow joint.....	260
14.4.4 Wrist	261
14.4.5 Vertebral column (spine / pelvis thorax angles	261
14.4.6 Changes in joint angles during the handbrake application	263
14.5 Biomechanical modeling and correlation to discomfort.....	264
14.5.1 Muscles	264
14.5.2 Muscle anatomy	266
14.5.3 Joint reactions and joint moment measures	270
14.5.4 Joint angles	275
14.5.5 Correlations with $p \leq 0.06$	276
14.6 Discomfort modeling	277
14.6.1 Stepwise regression.....	277
14.6.2 Discomfort index	279
15 REFERENCES	281
16 CURRICULUM VITAE	299

1 INTRODUCTION, OBJECTIVE AND OUTLINE

1.1 Introduction

The automotive industry is a very important global industry branch with increasing annual international car sales for years. In 2015, 66.3 millions of passenger vehicles have been sold globally (OICA, 2016). With sales of 389.525 million euros and 815.128 employees in 2013, the automotive industry a leading branch in Germany (Statistisches Bundesamt, 2015). For several years in a row, the German automotive industry has spent about one third of German's industry internal research and development budget (Kladroba & Stenke, 2013).

The comfort perception of a vehicle can be a major selling argument. The long term comfort experience of a car can be the main reason for future car buying decisions (Hartung, 2006). Considerable efforts have been made in recent years to study how to optimize comfort and minimize discomfort (De Looze, Kuijt-Evers & Dieën, 2003; Hartung, 2006). Several objective and subjective measurement methods are in use to assess comfort or discomfort (de Looze et. al, 2003). Many papers have been published on relationships between objective measurements and subjective evaluations (de Looze et al., 2003). Numerous studies have shown that physical discomfort is linked to biomechanical parameters and the musculoskeletal system (Zhang, Helander & Drury, 1996; Helander & Zhang, 1997; Kyung, 2008).

Hence, it is crucial to include the analysis of musculoskeletal load and biomechanical parameters in discomfort assessments. Both are influenced by kinematics (posture, motion) and kinetics (relation between forces and motion) (Chaffin, Andersson & Martin, 1999a).

Several Digital Human Models (DHMs) enable the simulation of humans and modelling kinematics and kinetics (Bubb & Fritzsche, 2009). The application of DHMs – with the purpose to develop more ergonomic vehicles and minimize occupants' discomfort – has increased. The main reason is that the application of DHMS has numerous advantages in comparison to the conventional method of completing subjective evaluation studies. DHMs enable assessments and comparisons of several variants at an early stage of development as well as objective, reproducible, efficient and fast evaluations (Geuß, 1995; Naumann & Rötting, 2007; Bonin et al., 2014; Upmann & Raiber, 2014). So, they allow for reducing or completely avoiding expensive studies with subjects and prototypes.

The Digital Human Modal RAMSIS allows creating desired percentile models for numerous regions with its anthropometric databases. RAMSIS posture prediction is based on empirical studies of joint angles. It is task-related and enables the prediction of the most probable posture based on geometrical constraints. RAMSIS was developed for vehicle design and is applied by more than 75 % of car manufacturers. (Bubb & Fritzsche, 2009)

AMS (AnyBody Modeling System) is an open musculoskeletal modeling system. Body models – consisting of bones, joints and tendon muscle units – and their interactions with the environment can be modeled with a script language. Based on body postures/movements and external reactions, kinematic and inverse dynamics analyses are completed to calculate biomechanical parameters such as joint reactions, muscular forces and activities. AMS is applied at several automotive companies. (Damsgaard, Rasmussen, Christensen, Surma & Zee, 2006; AnyBody Technology A/S, 2015b)

A number of studies has been published on discomfort predictions based on Digital Human Modeling, e.g. Wang et al. (2008). Research is ongoing on combining DHMs for more holistic discomfort assessments (Paul & Lee, 2011; Ulherr & Bengler, 2014).

An extensive portion of the automotive comfort and discomfort research has focused on sitting discomfort (De Looze et al., 2003) and comfortable joint angles while driving (Kyung & Nussbaum, 2009). Further core areas of automotive discomfort research are the operation of the pedals (Wang, Le Breton-Gadegbeku & Bouzon, 2004), ingress/egress (Dufour & Wang, 2005) and reach (Wang & Trasbot, 2011).

For reach, a lot has been published about biomechanical parameters influencing reach posture and reach discomfort as well as their prediction with DHMs, e.g. Jung & Choe (1996). In contrast, little information has been published about handbrake application. Lietmeyer emphasizes the absence of research on discomfort criteria for the handbrake application in vehicles (Lietmeyer, 2013). Raiber underlines that the handbrake application movement and its prediction have not been documented in literature so far (Raiber, 2015).

Vehicle drivers need to be able to apply the handbrake in all situations, e.g. for parking a car on a gradient. Since the occupants can adjust their seat and have different anthropometries, they are in different positions relative to the handbrake. Movement patterns and discomfort perceptions can vary significantly due to unique relative position to the handbrake and different human characteristics such as anthropometry and

strength. All these factors make it a challenging task to minimize discomfort of handbrake application for the main portion of potential customers.

A handbrake is typically located in the center console where trade-offs between many vehicle components and attributes have to be achieved. Late design changes are expensive and unbalanced compromises may result in customer complaints. This makes it extremely important to understand and objectively quantify – early in the vehicle development – how changes in the handbrake design affect the discomfort perception of the customers.

Wang (2009) emphasizes that the discomfort evaluation required for ergonomic assessments of complex movements is a challenge for Digital Human Modeling researchers. He describes the following fundamental questions:

“How to measure the discomfort perceived by a subject, knowing that it is subjective and that there is no other measurement instrument than the subject himself?”

How to define discomfort criteria based on biomechanical parameters, such as joint angles, joint forces, work, energy, muscle efforts, ...” (Wang, 2009, p. 25-1)

Furthermore, Wang (2009) highlights the need to include the simulation of muscle activities in discomfort modeling:

“Until now, discomfort, induced by internal biomechanical constraints that affect the human musculoskeletal system, has not adequately been taken into account in Digital Human Modeling.

We believe that discomfort modeling requires a detailed muscular activities simulation.” (Wang, 2009, p. 25-6)

The objective of this doctoral thesis is to provide an answer to Wang’s fundamental questions while considering the need to include the simulation of muscle activities.

Handbrake application in passenger vehicles has been chosen as an example for the reasons mentioned above.

RAMSIS and AMS have been chosen as Digital Human Models due to their modeling capacities and as they are typically applied in automotive industry.

1.2 Objective

There is a lack of publications on handbrake application postures respectively movements and their simulation as well as on the factors influencing the perception of handbrake application discomfort and its prediction by using DHMs.

The aim of this thesis is to develop an efficient and reliable procedure to predict the discomfort perception of the handbrake application in passenger vehicles – as an example of a complex activity – based on biomechanical criteria derived from the application of Digital Human Models (DHMs) typically used in automotive industry.

To achieve the overall objective, a multistep study has been accomplished which is reflected in the outline.

1.3 Outline

This thesis is divided into 13 chapters.

This section (chapter 1) presents the introduction to the topic, the objective and the outline. After the review of the relevant literature (chapter 2), the research problem and objective are specified in detail (chapter 3). Based on these chapters, the design of the multistep study is defined (chapter 4). A dedicated chapter is provided for each of the six steps:

- Preliminary study with subjects (chapter 5).
- Main study with subjects (chapter 6).
- Posture modeling (chapter 7).
- Biomechanical Modeling and correlation to discomfort (chapter 8).
- Discomfort modeling (chapter 9).
- Development of a procedure to predict discomfort (chapter 10).

Discussion and outlook conclude the thesis (chapter 11). The summary is provided in English (chapter 12) and in German (chapter 13).

2 LITERATURE REVIEW

The literature review aims to summarize state of the art knowledge beyond the basics of engineering and biomechanics. Still, relevant basic principles are briefly recapped.

The topic of this thesis is the simulation of handbrake application with the Digital Human Models RAMSIS and AMS to predict perceived discomfort. Purpose is to create a procedure which can be applied in vehicle development to assure ergonomic handbrake design with minimum discomfort based on the analysis of biomechanical parameters.

The key terms of biomechanics, ergonomics, comfort and discomfort are described in the following subchapters to clarify the differences between them and how they interact with each other.

2.1 Classification and interaction of biomechanics, ergonomics, comfort & discomfort

In a modern view “Biomechanics is the science that examines forces acting upon and within a biological structure and effects produced by such forces” (Nigg & Herzog, 1999, p. 2). Ergonomics aims to adapt workplaces and products to the humans (Bhise, 2012). So, biomechanics is dedicated to the inner processes of the human, especially the musculoskeletal system, whereas ergonomics focusses on a wise interface design to the human (Senner, 2001). Discomfort and comfort are subjective feelings which are influenced by a variety of factors including physical respectively biomechanical ones (Zhang et al., 1996). Good ergonomics shall prevent respectively lower discomfort, typically by reducing the physical load.

Reducing mental load is also an aspect of ergonomics. However it is not addressed in this thesis, which focuses on physical characteristics of biomechanics and discomfort.

2.1.1 Biomechanics

Senner (2001) underlines two aims of biomechanics in a technical environment. One is to determine the reactions of the human's organism to external stimuli, e.g. the reaction forces and moments in the elbow joint when applying the handbrake. The second one is to develop models of human substructures to finally be able to simulate the whole body. Both aims of biomechanics can support ergonomic design of products and workplaces by understanding the human's internal processes and modeling the human interacting with a product or workplace. The science of biomechanics requires applying the laws of

physics and engineering methodologies to the human body. Therefore, knowledge of the structure and function of the musculoskeletal system is essential (Chaffin et al., 1999a). Subchapter 2.1.1.1 describes basics of the musculoskeletal system.

2.1.1.1 Introduction to the musculoskeletal system

2.1.1.1.1 Physical and physiological force

Physical force can be defined by three Newton' laws (Grehn & Krause, 2006). Any force is a vector and completely defined by magnitude, direction and force application point (Grehn & Krause, 2006). When force is viewed physiologically (as natural process and function of the body), it can be described as an ability of the neuromuscular system to generate contraction by innervation and metabolism processes. This is illustrated in Figure 2.1. (Grosser, 1987; Hamill, Knutzen & Derrick, 2015)

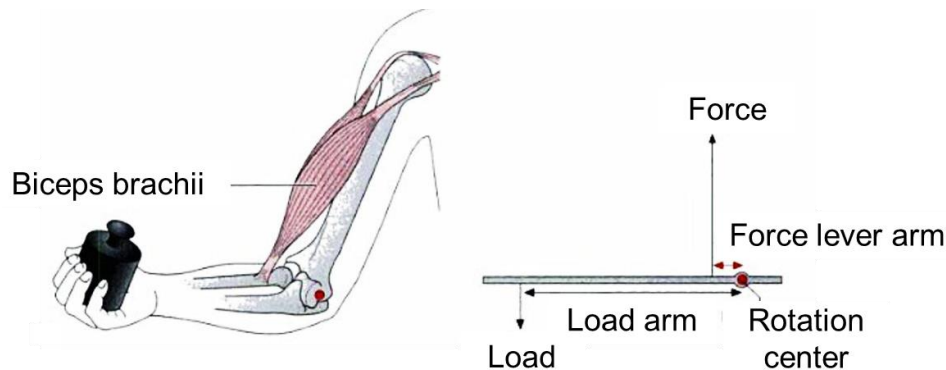


Figure 2.1: Principle of force transmission via muscle contraction (Schünke, 2000), extracted and adopted from Koch (2013, p. 4).

2.1.1.1.2 Structure and function of the musculoskeletal system

The musculoskeletal system can be classified in a passive and an active part.

The passive part is connective tissue, which provides support, transmits forces and assures the structural integrity of the body parts. Bones, ligaments, tendons, fascia and cartilage are connective tissues.

Muscles, which voluntarily contract, are the active part of the musculoskeletal system and move the passive part (Chaffin et al., 1999a). They are also called skeletal muscles or striated muscles. Contraction (shortening the muscle) is the only active action a muscle can perform. Contraction leads to a tension, also called tensile force. Muscles cannot produce compressive force (Kroemer, Kroemer & Kroemer-Elbert, 2010).

Skeletal muscles have several different functions. The three functions to “stabilize joints”, to “maintain postures and positions” of the body and to “produce movements”

(which is to accelerate and decelerate the joints) are related to the human movement (Hamill & al., 2015, p. 62). Furthermore, muscles enable to transmit force to objects outside the human, e.g. controls or tools (Damon, Stoudt & McFarland, 1966).

Muscles are usually arranged in groups. The prime movers (agonists) drive the movement whereas the antagonists have the property to oppose the movement. The muscle bellies transmit the tensile forces to the skeleton by tendons. (Chaffin et al., 1999a)

Muscles consist of connective tissue, muscle cells ("muscle fibers") and nerve elements. Their shape, size, length and architecture depend on the task they perform (Chaffin et al., 1999a). Their contraction is triggered by electrochemical stimuli (Mense, 2010).

A skeletal muscle contains two main types of muscle fiber, „white“ and „red“ fibers. White fibers twitch fast and fatigue quickly. They enable movements of high velocity and short duration. Red fibers contract with slower twitches and better resist to fatigue. The proportion of red and white fibers varies between muscles. (Mense, 2010; Hamill & al., 2015)

Various muscle types are distinguished based on the arrangement of the muscle fibers related to the tensile direction of the tendon (Hamill & al., 2015). The angle between the direction of the muscle fibers and the tensile direction of the tendons is called pennation angle. A pennation angle of zero means that muscle fibers and tensile direction of the tendons are parallel. The physiological cross-section of a muscle is measured perpendicular to its fibers. (Houglum, Bertoti & Brunnstrom, 2012)

The resting length or neutral length of a muscle is the length in which the relaxed muscle is not shortened or elongated (Houglum et al., 2012). The tensile force of muscles depends on several factors (Chaffin et al., 1999a; Houglum et al., 2012):

1. Physiological cross section.
2. Length of muscle fibers.
3. Muscle type and pennation angle.
4. Composition of muscle fiber types.
5. Length of the muscle compared to its resting length (length tension relation).
6. Velocity of contraction (velocity tension relationship).

The length tension relationship (5.) and velocity tension relationship (6.) are illustrated in Figure 2.2. The length tension relationship is shown on the left hand side. The highest tension is reached for the resting length (Caldwell et al., 1974; Mense, 2010). Since the

length of a muscle is depending on the joint angles for a given posture or movement, joint angles can have a significant influence on tensile force.

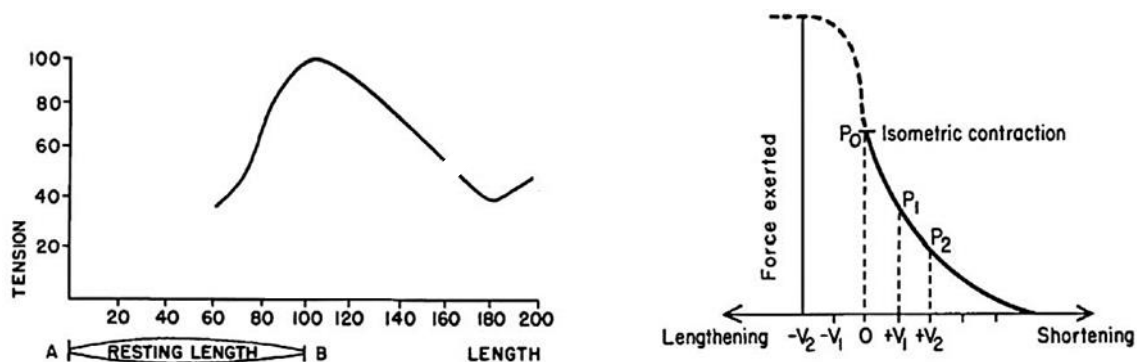


Figure 2.2: Left: Length tension relationship of a muscle with tendon for maximum activation. Right: Velocity tension relationship at maximum muscle activity (Houglum et al., 2012). Extracted and modified from Koch (2013, p. 6).

On the right hand side of Figure 2.2, the velocity tension relationship is shown for maximum muscle activity. The isometric contraction (no change in muscle length), is provided as a reference. The faster a muscle contracts, the smaller is its force. If a muscle is elongated contrary to its exerted force, it can generate a force even larger than at isometric contraction. (Chaffin et al., 1999a; Houglum et al., 2012)

Muscle fatigue describes the decrease of the ability of the muscle to exert force when executing voluntary efforts. Fatigue is considered as a function of the neuromuscular system to prevent serious damage to muscles. Muscle fatigue is a complex mechanism which is influenced by the composition of fibers within the muscle, metabolic factors and the activation (including rests) itself. (Chaffin et al., 1999a)

This excursion about the musculoskeletal system presents most relevant basics. For more detailed explanations of the musculoskeletal system including mechanisms of muscle contraction, stimulation, control, energy supply, fatigue etc. see e.g. Chaffin et al. (1999), Nigg & Herzog (1999), Brüggemann (2005) or Hamill & al. (2015).

2.1.2 Ergonomics

In this chapter the science of ergonomics is described. Ergonomics applies biomechanical methods to optimize tasks, workplaces and products to the human.

Bhise defines (automotive) ergonomics with the following sentences:

“Ergonomics is a multidisciplinary science involving fields that have information about people (e.g., psychology, anthropometry, biomechanics, anatomy,

*physiology, psychophysics). It involves studying human characteristics, capabilities, and limitations and applying this information to design and evaluate the equipment and systems that people use. The basic goal of ergonomics is to design equipment that will achieve the best possible fit between the users (drivers) and the equipment (vehicle) such that the users' safety (freedom from harm, injury, and loss), **comfort**, convenience, performance, and efficiency (productivity or increasing output/input) are improved.” (Bhise, 2012, p. 3)*

This thesis focuses on physical and psychophysical ergonomics. Still, there are other aspects of ergonomics to be considered in the interaction of the human and technical systems, such as cognitive ergonomics (Gunzelmann et al., 2014).

It is not the aim of ergonomics to adapt people to a product or process, but to design the product or process considering the user groups, so that most individual within the target customer group can use the product respectively fit within the product. When designing a product, the human should be treated as an integral element of the product. So, when designing a vehicle, three major elements need to be considered as illustrated in Figure 2.3: the occupant(s), the vehicle and the environment. (Bhise, 2012)

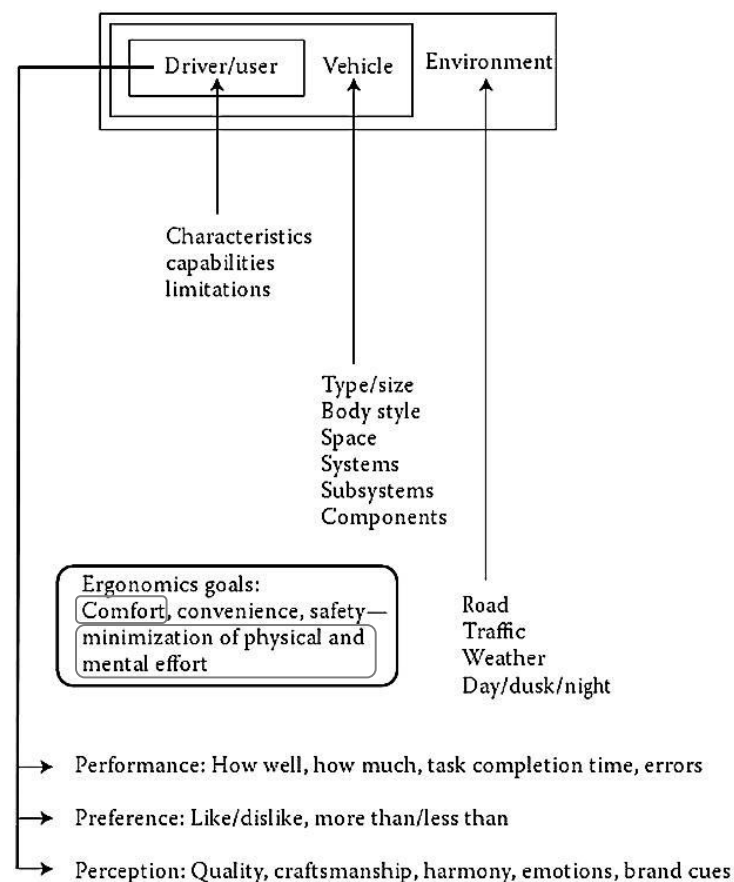


Figure 2.3: “Ergonomics engineer’s considerations related to characteristics of the driver, the vehicle, and the environment and their relationship to driver performance, preference, and perception”, Bhise (2012, p. 5), illustration modified.

As indicated in Figure 2.4, the three basic approaches to solve ergonomic “problems” are guessing, performing an experiment or applying a model (Bhise, 2012). The least time-consuming approach, guessing, is not objective. In this thesis, experiments (subjective evaluation studies) and modeling are conducted to establish a pure modeling procedure to be applied in automotive development. Modeling has several advantages, e.g. is less time and resources consuming, more objective and allows for earlier investigations in the vehicle development.

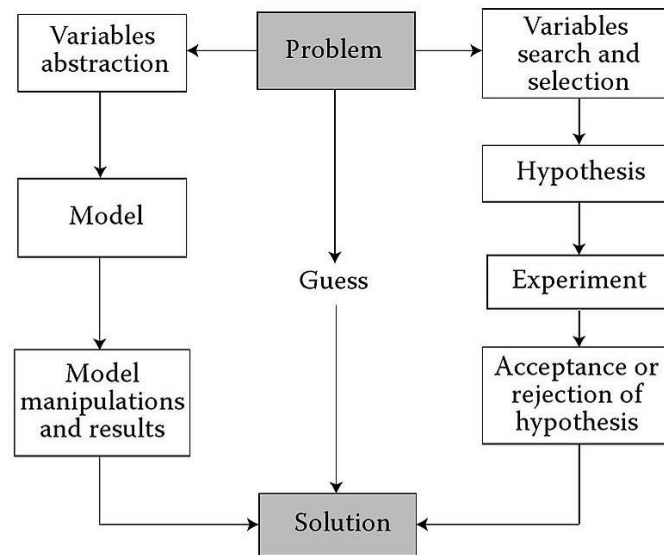


Figure 2.4: Approaches for problem-solving (Bhise, 2012, p. 6).

As mentioned above, the users’ comfort is one objective of ergonomics (Bhise, 2012).

In Western cultures, end user comfort of products becomes an important topic in product buying decisions and thus for the product manufacturers who acknowledge comfort as a selling argument. Comfort and ergonomics are also in the focus of employers, who intend to create a healthful and stimulative environment by providing comfortable equipment. (de Looze et al., 2003)

Since comfort can only be perceived when the level of discomfort is sufficiently low (see 2.2.1), the driver’s perceptions of comfort and discomfort are crucial aspects of ergonomics in the automotive industry (Raiber, 2015).

2.1.3 Comfort and discomfort

Comfort and discomfort are words which are used in everyday life communication and also in scientific context. There is no single universally accepted definition or model describing their meanings. However, there are many definitions of comfort and discomfort, their relationship, influencing factors and models (Kyung, 2008). For

thorough descriptions, e.g. Krist (1993), Kyung (2008) and Zenk (2008) can be referred. In this thesis, only an overview of mostly cited definitions respectively models of discomfort and comfort is provided.

In everyday life, comfort means coziness, convenience and contentedness. Comfort additionally refers to the assessment of the luxury of a product (Bubb, 2004). The word comfort is often used in marketing with respect to a variety of end user products such as chairs, vehicles and clothes (Vink & Hallbeck, 2012).

Vink and Hallbeck's search for the word "discomfort" via "Science Direct" in publications from 1980 to 2010 delivered 108.794 papers (Vink & Hallbeck, 2012). A "Science Direct" search using journals from 2011 to 2014 results in 34.879 papers containing the word "discomfort" and 61.628 papers containing the words "discomfort" respectively "comfort". Many of the studies about discomfort refer to temperatures, patient comfort or musculoskeletal injuries (Vink & Hallbeck, 2012). Studies about comfort often refer to seat comfort.

While comfort is not yet clearly defined (Helander & Zhang, 1997; Zhang et al., 1996), there is wide consensus that:

- "(1) comfort is a construct of a subjectively-defined personal nature;*
- (2) comfort is affected by factors of a various nature (physical, physiological, psychological); and*
- (3) comfort is a reaction to the environment."* (de Looze et al., 2003, p. 986)

These characteristics are considered to be applicable to discomfort, too. Vink & Hallbeck (2012) define comfort as a "pleasant state or relaxed feeling of a human being in reaction to its environment". They define discomfort as an "unpleasant state of the human body in reaction to its physical environment". Paul, Helander & Morrow (1997) indicate with their proposed nurturing/pampering paradigm the need for differentiating approaches to decrease discomfort (nurturing) and increase comfort (pampering) (de Looze et al., 2003). However, the separation between comfort and discomfort has only partly established in literature (Hartung, 2006). The words comfort and discomfort are not consistently applied in publications.

Bubb (2007) does not classify in comfort and discomfort but in the aspects pleasure and suffering. A small sports vehicle ("roadster") can make drivers suffer from little head clearance and awkward ingress/egress, but still please the customer due to its shape and image (Bubb, 2007), see Figure 2.6.

2.2 Comfort and discomfort models

Although many papers have been published on comfort and discomfort, there are only few providing explanations of their concepts, in particular when related to products and product design (Vink & Hallbeck, 2012).

Vink & Hallbeck (2012) present and compare the concepts/models of comfort and discomfort from inter alia Zhang et al. (1996); Helander & Zhang (1997); de Looze et al. (2003); Kuijt-Evers, Groenesteijn, de Looze & Vink (2004) and Moes (2005). At the end, Vink & Hallbeck (2012) propose a new model, which is expanded in a later publication (Naddeo, Cappetti, Vallone & Califano, 2014).

In the following subchapters a selection of comfort and discomfort concepts is described. Although they have been established mainly with regards to sitting comfort, the underlying principles are considered to be applicable to other products (e.g. cars, shoes and sports equipment) and workplace design.

2.2.1 Comfort and discomfort model by Zhang et al. (1996)

Zhang et al. (1996) have shown that comfort and discomfort are described by independent factors. Figure 2.5 illustrates the results of their cluster analysis.

Discomfort was found to be related to biomechanical parameters such as joint angles, muscle activation or pressure distributions (between human and seat). This results in sensations such as pain, fatigue, soreness and numbness. Discomfort tends to increase over time and with fatigue. (Zhang et al., 1996)

The perception of comfort was mainly associated with sensations of relaxation and wellbeing. Also impressions such as luxuriousness and spaciousness positively influence comfort perception (Zhang et al., 1996). Aesthetical design of products was also observed to amplify the sensation of comfort (Helander & Zhang, 1997). As the impressions and aesthetics depend on individual expectations and preferences, it is hardly possible to measure them physically, whereas discomfort is influenced largely by physically measurable factors (Hartung, 2006).

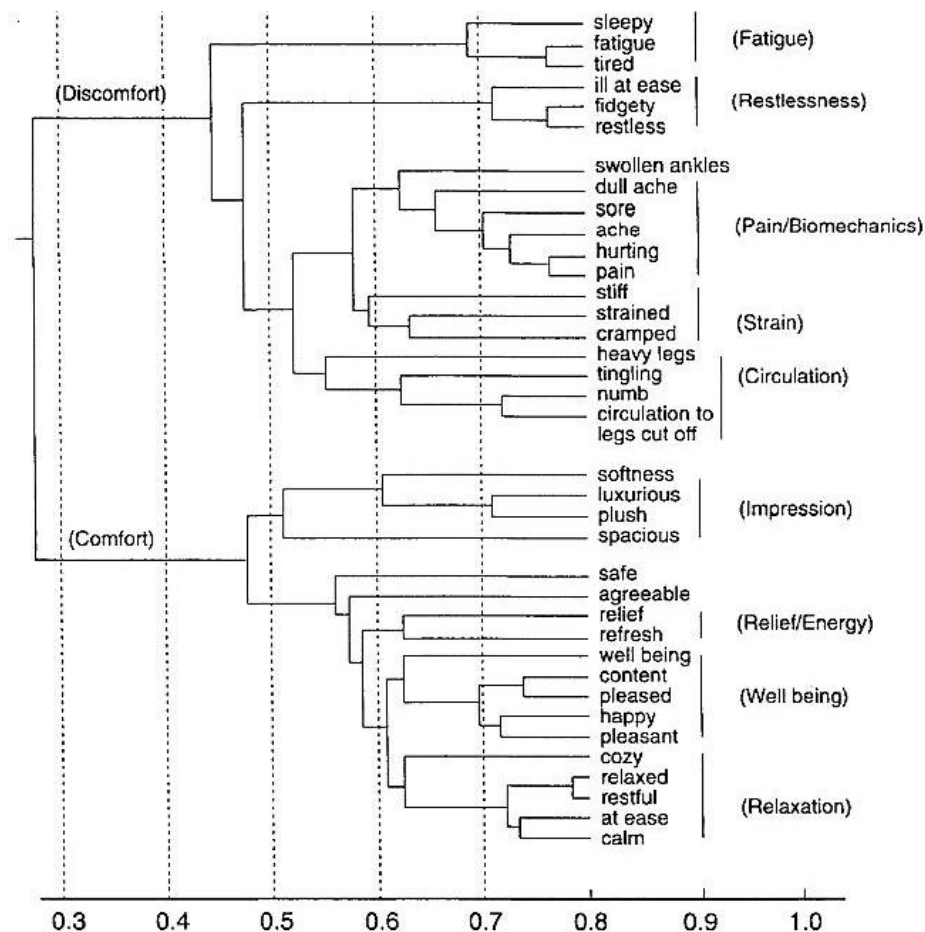


Figure 2.5: Results of a cluster analysis related to comfort and discomfort. Extracted from Zhang et al. (1996, p. 387).

Figure 2.6 demonstrates the interaction of comfort and discomfort. Comfort and discomfort have to be considered as separate, orthogonal, dimensions of perceptions (Zhang et al., 1996; Lietmeyer, 2013) and need to be treated as different and complementary items (de Looze et al., 2003).

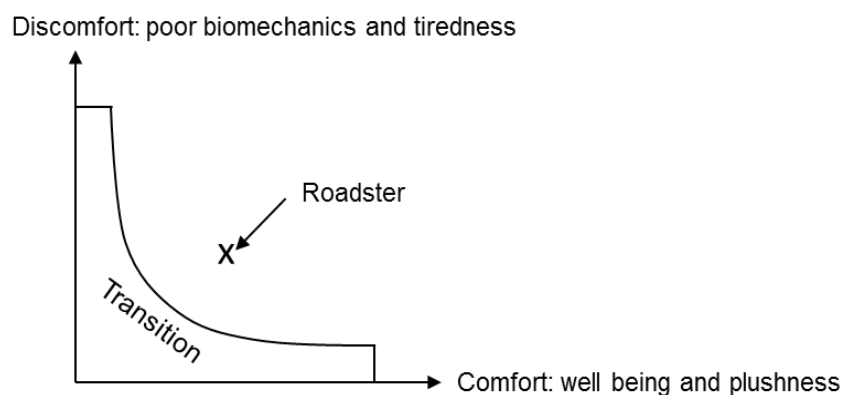


Figure 2.6: Model of comfort and discomfort. Modified from Zhang et al. (1996) and Bubb (2007, p. 242).

With the increase of discomfort, comfort will be reduced. With the reduction of discomfort, comfort may be experienced. Good biomechanical conditions can reduce discomfort, but may not necessarily result in comfort. In presence of adverse biomechanical parameters the focus will be directed on discomfort: the perception changes from comfort into discomfort (Zhang et al., 1996).

So, discomfort is the dominant perception: when discomfort factors arise, comfort factors become second-ranked in the human perception (Zhang et al., 1996; Helander & Zhang, 1997; de Looze et al., 2003).

These conclusions are considered to apply to most products. However, there are products with rather high discomfort and rather high comfort (for different product attributes) at once, such as a roadster (Figure 2.25).

2.2.2 Comfort pyramid by Krist (1993)

In analogy to Maslow's Pyramid of Needs (Maslow, 1943; Maslow, 1978), a pyramid of comfort (Figure 2.7) was developed based on a questionnaire study by Krist (1993). It suggests that basic needs (lower in the pyramid) for comfort and discomfort have to be fulfilled before the higher ones can be perceived. Anthropometrics is on the top of the pyramid (Bubb, 2007; Hartung, 2006; Lietmeyer, 2013). It implies a design of products and tasks for the range of user anthropometries and capabilities.

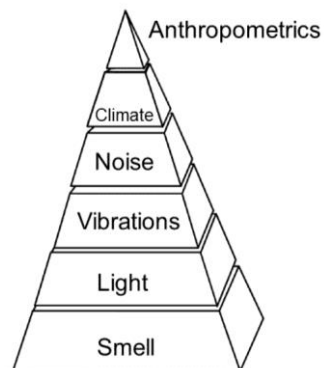


Figure 2.7: Comfort pyramid, translated from Hartung (2006, p. 7) and Bubb (2007, p. 242), who modified from Krist (1993, p. 9).

2.2.3 Comfort and discomfort model by de Looze et al. (2003)

The comfort model by de Looze et al. (2003) is often cited in the context of product comfort. In agreement with Zhang et al. (1996) comfort and discomfort are considered as separate perceptions (Figure 2.8). The left hand side of the model is about discomfort, the right hand side about comfort. The arrows from left (discomfort) to right

(comfort) indicate the dominant role of discomfort proposed by Helander & Zhang (1997).

For both, comfort and discomfort, the model considers the human level, the product level and the context (environment) level. On the discomfort side, the physical characteristics of the product (e.g. handbrake geometry and application force), the environment (e.g. seat adjustment, clearances, driving situation) and the task (handbrake application) expose a person with external loads (e.g. forces to apply handbrake, joint angles changes). These external stresses lead to an internal level of strain/load, e.g. muscle activity as well as internal forces and moments, which result in chemical, physiological and biomechanical responses. The internal dose and response depend on the characteristics (such as anthropometry and physical capabilities) of the individual.

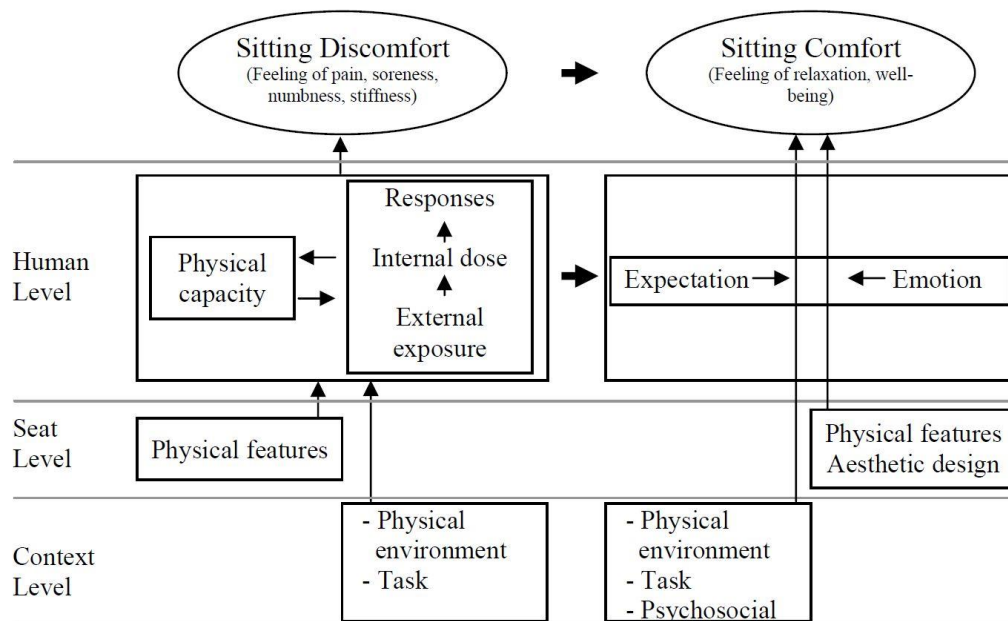


Figure 2.8: Theoretical model of sitting comfort and discomfort (de Looze et al., 2003), adapted from Kyung (2008, p. 15).

The right hand side of the model is about comfort. Again the comfort perception is influenced by the human, product and environment. For the environment physical and psychosocial factors (e.g. satisfaction with job and social life) are relevant in addition to the task.

At the product level, physical features and aesthetics of the product can influence the perception of comfort. At the human level, the influencing factors such as experiences, expectations and emotions are very individual. (de Looze et al., 2003; Vink & Hallbeck, 2012).

So, just looking at – and not yet using – a product or workplace can lead to positive or negative emotions, affecting the perception of comfort and discomfort during and after use (de Looze et al., 2003).

The model illustrated in Figure 2.8 shows that discomfort is closer linked to physical parameters (exposure, dose, capacity) than comfort. This can lead to the expectation that discomfort may have a stronger relationship with physical respectively biomechanical measures than comfort. However, de Looze et al. (2003) could not verify this expectation in their literature review. One potential reason is that in the studies they reviewed the words comfort and discomfort were not consistently used. Another reason is that the subjects did only rate discomfort or comfort – and not both, comfort and discomfort on different scales. (de Looze et al., 2003)

2.2.4 Discomfort model by Vink & Hallbeck (2012)

Vink & Hallbeck (2012) have reviewed the findings from 10 papers and propose a new model (Figure 2.9). It is strongly inspired by the comfort models of Moes (2010) and de Looze et al. (2003).

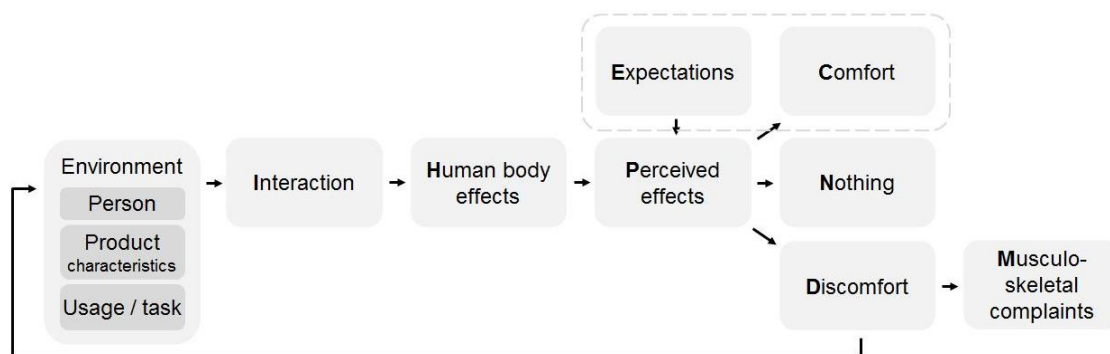


Figure 2.9: Illustration of the comfort model by Vink & Hallbeck (2012, p. 275, adapted).

Applying this model to the handbrake application, interaction includes force transfer and pressure distribution at the contact area between hand and handle as well as joint angles changes. Effects in the body are e.g. joint load and muscle activity, tissue deformation, compression of nerves and blood vessels at contact surfaces between the human and the vehicle (e.g. handbrake, seat, steering wheel). The body effects are perceived and interpreted, which is influenced by the expectations. (Moes, 2005; Vink & Hallbeck, 2012)

According to Vink & Hallbeck (2012), the perceived effects can be interpreted as feelings of comfort and/or discomfort or nothing. The author of this dissertation proposes to add “neutral” or “neither/nor” to “nothing”. The circle around expectations and comfort

illustrates Vink's and Hallbeck's position that expectations are often related to comfort (Vink & Hallbeck, 2012).

2.2.5 Conclusions

In the previous subchapters, several influencing factors and models of comfort and discomfort were described. There is wide consensus that comfort and discomfort are subjective feelings (de Looze et al., 2003).

Comfort or discomfort perceptions are influenced by the human, the product characteristics, the usage of the product and the context respectively environment (Moes, 2005; Vink & Hallbeck, 2012).

The interaction between the human and the environment when using a product leads to effects inside the human body. They are perceived and interpreted. Discomfort respectively comfort can be felt as a result. (Moes, 2005; Vink & Hallbeck, 2012)

Discomfort and comfort are associated with physical (biomechanical), emotional (e.g. expectations) and psychosocial (e.g. satisfaction with social life) aspects (de Looze et al., 2003). These aspects can influence each other and contribute to a person's comfort and discomfort perception (Kyung, 2008).

Several papers have shown that physical discomfort is linked to biomechanical parameters (Zhang et al., 1996; Helander & Zhang, 1997; Kyung, 2008). Discomfort is influenced by several physically measurable factors (Hartung, 2006), whereas comfort influencing aspects such as aesthetics are difficult to measure.

This thesis will focus on discomfort for two main reasons. Firstly, comfort can only be perceived if discomfort is reduced below a certain limit (dominance of discomfort) (de Looze et al., 2003; Helander & Zhang, 1997). For the handbrake application, the level of force and range of postures are anticipated to cause discomfort perception. Secondly, discomfort has shown to be related to biomechanical values (Zhang et al., 1996; Helander & Zhang, 1997; Kyung, 2008) and measureable characteristics (Hartung, 2006). This is relevant for the development of an assessment procedure based on subjective evaluation studies as well as RAMSIS and AMS simulation.

For the nature of subjective evaluation studies, it can be assumed that the musculoskeletal discomfort ratings of the subjects may be influenced by emotional and psychosocial aspects of discomfort and comfort. To minimize their effect on the ratings, discomfort sources of a lower level in the discomfort pyramid (Krist, 1993) such as smell, light, vibrations, noise and climate have to be minimized and kept constant.

2.3 Factors influencing discomfort

In this chapter, an overview is provided about factors which influence discomfort perception. As illustrated in the comfort models mentioned above, the human, biomechanical and environmental characteristics can influence discomfort perception.

2.3.1 Human characteristics

First, of all, human characteristics including anthropometry and physical capabilities will be described.

2.3.1.1 Anthropometry including inertial characteristics

Chaffin et al. (1999, p. 65) define anthropometry as “the science that deals with the measurement of size, mass, shape and inertial properties of the human body”.

Anthropometric measurements are crucial for ergonomic investigations and biomechanical modeling. Anthropometry is an empirical science. Quantitative methods are used to measure properties of populations (Chaffin et al., 1999a) as the data can highly differ from one human to another (Huston, 2009). The results are statistically analyzed (Chaffin et al., 1999a). Resulting patterns are used for ergonomic or biomechanical analyses (Huston, 2009). Commonly used patterns in automotive development are percentiles. The 5th percentile female body height (5F) of a population is the body height so that 5% of the females in that female population are smaller than this value and 95% taller (Bhise, 2012).

There are static and dynamic anthropometric measures. Examples of static anthropometric length measures are body height, upper arm length and waist circumference. Dynamic measures are often taken in working postures, examples are reaches, clearances and visual geometry (Damon et al., 1966). Figure 2.10 shows hand grasping reaches for selected percentiles.

Some studies on working postures also provide range of motion data (see chapter 2.3.1.2).

Inertial properties of the human body and its segments – such as mass, volume, density, center of gravity (CG) – are often based on few cadaver measurements and mathematical modelling (Braune, 1877; Miller & Nelson, 1973; Braune & Fischer, 1988; Chaffin et al., 1999a).

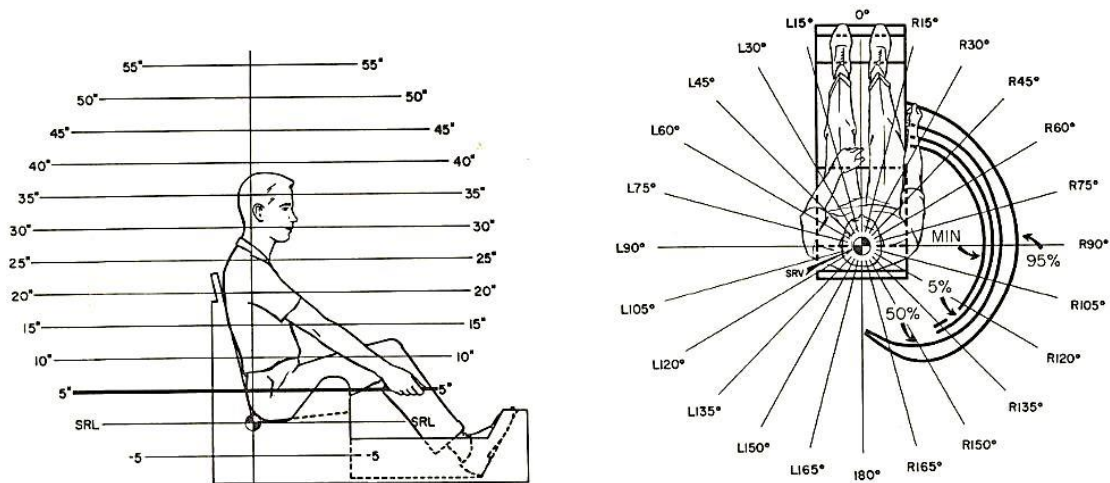


Figure 2.10: Illustration of grasping reach of the right arm to a horizontal plane, 5 inches above SGRP, for selected percentiles (Kennedy, 1964). Extracted from Damon et al. (1966, p. 141).

Anthropometric measures are available in tables, standards and Digital Human Models (Godil & Ressler, 2009). Values often differ due to discrepancies in the measured populations and differences in the measurement procedures. Thus, they should be applied thoughtfully.

Anthropometric characteristics can be influenced by several factors including age, gender, ethnics, body build/physique, occupation, diet, health, physical activity and exercise, body posture, voluntary changes (e.g. stature reduction by crouching), time of the day, long term changes and clothing (Damon et al., 1966).

Many of those factors also influence the physical capabilities which are described in chapter 2.3.1.2.

2.3.1.2 Physical capabilities

This chapter is about most relevant biomechanical properties of the healthy musculoskeletal system: muscle strength, endurance and joint range of motion (Chaffin et al., 1999a).

2.3.1.2.1 Strength and endurance

Muscle strength is “the maximum force that a group of muscles can develop under prescribed conditions” (Chaffin et al., 1999a, p. 101). Figure 2.11 shows types of strength, which are involved in static and dynamic tasks.

HUMAN PERFORMANCE TASK DESCRIPTION:	TYPE OF MUSCULAR STRENGTH:	CONDITIONS:	TYPE OF MUSCLE ACTION:
Static Exertions: (e.g., hold, carry, initiate motions) Dynamic Exertions (e.g., lifting, pushing, pulling, etc.)	Static Strength	Fixed Postures	Isometric Contractions
	Isoinertial Strength	Body Movement with Constant External Load	Concentric (shortening) or Eccentric (lengthening) Contractions
	Isokinetic Strength	Body Movement with Constant Velocity at Specific Joint	Concentric (shortening) or Eccentric (lengthening) Contractions
	Isotonic Strength	Body Movement with Constant Muscle Tension (laboratory only)	Concentric (shortening) or Eccentric (lengthening) Contractions

Figure 2.11: Types of strength involved in static and dynamic tasks (Chaffin et al., 1999, p. 103).

Similar to the measurement and application of anthropometric data, precautions have to be taken to measure and use strength data with success (Chaffin et al., 1999a).

For measuring muscular strength of a person, the muscle (group) has to be voluntarily activated by the person. Therefore some authors use the term “maximum voluntary exertion strength”. Psychophysical methods are required for the determination of the human attribute muscular strength. Even with well-motivated subjects, the measured values are probably lower than the actual physiological capabilities. (Chaffin et al., 1999a)

Muscular strength need to be distinguished from muscular endurance, which can also be measured using psychophysical methodologies (Chaffin et al., 1999a). “Endurance can be defined as the ability to maintain a submaximal force over a given period of time” (Damon et al., 1966, p. 199) or with a predefined frequency over a period of time.

An occasional short exertion (for a few seconds) depends on muscular strength, whereas repeated or sustained exertions depend also on muscular endurance. To determine muscular endurance of a person an exertion is performed – at a submaximal level - for a period of time or at a defined frequency. (Chaffin et al., 1999a)

There is a positive relation between strength and endurance: in general, strong people are able to continue predefined submaximal efforts for longer periods of time than weak people. (Chaffin et al., 1999a)

The instruction plays an important role for determining strength and endurance. Subjects, told to apply maximum force and hold it, reach their maximum force later than subjects who are told to apply the force as rapidly as possible. (Caldwell et al., 1974)

The velocity of motion during dynamic strength tests influences the peak values: the faster a muscle shortens, the lower is the generated tension (Chaffin et al., 1999a), compare chapter 2.1.1.1.2. Complex exertion (e.g. lifting a heavy, large object) requires the coordination of many muscles, so additional time is needed to apply the necessary force. Practice will shorten the time. (Chaffin et al., 1999a)

There are numerous factors influencing muscular strength and endurance. Damon et al. (1966) list many of them and describe their influences: for example anthropometry (and its influence factors), handedness, fatigue, fitness/training, drugs and day-to-day variation contribute. Also environmental factors (such as temperature, altitude and acceleration), psychological factors (e.g. motivation and emotional state) and occupational factors (intellectual vs. manual work, clothing and workspace equipment) have an effect.

On average, females have 30 % to 35 % less strength than males. Age related decrease of force-producing capabilities (including strength) begins at the age of 25 years and is about 5 % to 10 % per decade. (Bhise, 2012)

2.3.1.2.2 Range of motion

Several factors influence the range of joint mobility, e.g. the anthropometry and its influencing characteristics (e.g. gender and age). Damon et al. (1966) list further influencing factors such as ethnical background, body build, training, occupation, fatigue, disease, motivation, handedness and clothing.

The range of motion of a joint can differ depending on the adjacent joint(s). This is in particular the case when the “joint is spanned by two joint muscles” (Chaffin et al., 1999a, p.100). For example, a small study by Laubach (Webb Associates, 1978) has shown a significant reduction in available shoulder flexion while flexing the elbow. For some subjects also a decrease in elbow flexion, while flexing the shoulder, was documented. For this reason, it is crucial to pay attention to potential limitations of the tabulated data, e.g. to consider in which posture the range of motion of a joint was determined.

Joint angles are typically measured between the longitudinal axes of two adjacent body segments or between a body segment and a plane. The range of motion is determined between the two extreme joint angles. (Damon et al., 1966)

The range of motion can be measured for active joint movements (performed by the subject) and passive joint movements (joint is “forced” in the extreme position).

Studies on joint mobility have been published by numerous researchers (Chaffin et al., 1999a). It is difficult to compare them and discrepant values exist for the following reasons: variations in measurements (e.g. the amount of “forcing” the joint or body segments in the position) as well as differences in body postures, in the joint “component” moved and/or in measuring gauges (Damon et al., 1966). Also factors of the investigated population and individuals (e.g. age, gender and anthropometry) have an effect (Chaffin et al., 1999a).

Discomfort can begin for postures respectively exertions much lower than the subject’s maximum capabilities. Correlations between active joint motion (below maximum) and discomfort respectively comfort ratings have been published, e.g. in Kee & Karwowski (2001). Apostolico et al. (2014) experimentally determined postural ranges perceived comfortable for several joints for seating and standing.

2.3.2 Biomechanical characteristics

This chapter describes biomechanical characteristics and methods applied to reduce discomfort and/or to develop ergonomic guidelines.

Biomechanical studies often include a kinematic description of a posture or movement and kinetic analysis. Kinematics is about location respectively displacement, velocity and acceleration – but not about the forces. Forces, moments of forces and how they can initiate and alter movements or contribute to postures are the focus of kinetics. (Chaffin et al., 1999a; Miller & Nelson, 1973)

Following the nomenclature of AMS, the term “moment” stands for “moment of force” respectively “torque” in this thesis.

2.3.2.1 Kinematics

As mentioned above in chapter 2.3.1.2.2, discomfort can occur for joint angles much smaller than the maximum range of motion (Kee & Lee, 2012).

Joint locations, angles and their changes over time can be determined by kinematic analyses. There are several non-invasive (peripheral) methods of 2D and 3D motion capturing and analyses (Chaffin et al., 1999a; Nigg & Herzog, 1999; Senner, 2001).

Senner (2001) classifies them, describes how they work and lists advantages, disadvantages and commercially available systems. He references studies in which the methods have correctly been applied or have been compared to other methods.

The effect of posture or movement on discomfort has extensively been studied for several applications (Kee & Karwowski, 2001b; Kyung & Nussbaum, 2009) but not for the handbrake application.

2.3.2.2 Kinetics

In this chapter, factors and methods related to kinetics are in focus.

2.3.2.2.1 Forces and pressure distribution at area of contact

Reactions are measured at the interface between the human and its environment, e.g. the ground and/or objects such as machine controls or consumer products. These forces/moments are also referred to as external forces/moments or external reactions. Based on the reaction forces (defined by magnitude, direction and point of application) and geometric conditions (e.g. derived by motion capturing), mathematical models can be applied to calculate strains within the body. There are several types of force measurement devices available on the market. (Senner, 2001)

There is more to discomfort than the magnitude of a load. The way how a load reacts on the human and the resulting stress within the human body are also important factors of influence. The pressure distribution at the interfaces between human and environment can be an important influencing factor for comfort respectively discomfort; this has been proven for seat comfort (Shen & Parsons, 1997; Mergl, Klendauer, Mangen & Bubb, 2005; Mergl, 2006). Pressure distribution measuring devices are available e.g. in form of mats and shoe soles (Senner, 2001).

The testrig ErgoBuck (see chapter 5.1.3) used for this study allows for measuring interface forces between several of its elements (such as floor, seat and handbrake) and the human by load cells. This equipment was implemented by employees of Technical University Ilmenau (Sendler & Kirchner, 2012) and German Sport University Cologne (Heinrich et al., 2014).

2.3.2.2.2 Biomechanical load in the human body

In this work, the term “internal load” stands for loads such as forces, pressure, moments and strain in human joints and forces and strain of the muscles.

To determine a subject's internal loads, which can contribute to discomfort perception (see chapter 2.2), there are several methods:

1. In vivo measurements of forces, moments, stress, strain etc.
2. External measurements which relate to internal loads.
3. (Digital) Human Modeling.

All three methods have advantages, disadvantages and limitations.

2.3.2.2.2.1 In vivo measurements

There are several examples of human body instrumentation with the purpose to measure e.g. forces in tendons (Komi, 1990) and bones (tibia, femur, patella) (Koh, Grabiner & De Swart, Robert J., 1992) or to measure disc pressure (Chaffin et al., 1999a). There are also cases in which implants have been equipped with measuring capabilities (Bergmann et al., 2007; Zander, Dreischarf, Schmidt, Bergmann & Rohlmann, 2015) e.g. to validate biomechanical models.

However, in many cases implementation of measurement equipment into the human body is ethically questionable.

2.3.2.2.2.2 Measurements and methods related to internal load

Since in vivo measurements are often not possible, methods have been developed to measure related parameters.

2.3.2.2.2.3 Muscle dynamometry

In vivo, it is not possible to measure the isolated force of a single muscle because joint motion is always driven by several muscles.

It is common practice to measure the strength/force of groups of muscles, which contribute to a specific task respectively function, for different postures or movement conditions. (Gyr, 2011; Koch, 2013)

This method is referred to as muscle dynamometry and enables to determine joint specific net moments (moments resulting from muscle forces). It provides parameters for force laws to describe the muscle contraction and for the determination of joint specific maximum moments. (Senner, 2001)

The joint specific maximum moments can also be used for plausibility checks of Digital Human Models (Senner, 2001, Koch, 2013). Correlations between perceived discomfort and the level of external forces respectively moments were documented by e.g. Zacher & Bubb (2004).

2.3.2.2.2.4 Electromyography

Electromyography (EMG) is a method to determine the status of muscle contraction via measuring the voltage causing it (Senner, 2001). The fundamental research paper by De Luca, Carlo J.(1997) provides a detailed description of the technology and its limitations. They are summarized in the following excerpt:

“Electromyography is a seductive muse because it provides easy access to physiological processes that cause the muscle to generate force, produce movement, and accomplish the countless functions that allow us to interact with the world around us. The current state of surface electromyography is enigmatic. It provides many important and useful applications, but it has many limitations that must be understood, considered, and eventually removed so that the discipline is more scientifically based and less reliant on the art of use. To its detriment, electromyography is too easy to use and consequently too easy to abuse.” (de Luca, 1997, p. 1)

EMG allows to assess the muscle activity, e.g. to understand if – respectively when – a muscle is active and at what activation level. EMG is applied to assess muscle fatigue, e.g. for workplace and task design as well as in sports (de Luca, 1997; Senner, 2001) and to validate DHMs such as AMS (Siebertz, Christensen, Damsgaard & Rasmussen, 2004). Correlations of EMG values and perceived reach discomfort have been presented in Jung & Choe (1996).

Assessing the strength of a muscle based on EMG is difficult (Senner, 2001).

2.3.2.2.3 Energy considerations

“The balance of work and power describes inner and outer energy status of the body and its change when interacting with the environment.” (Senner, 2001, p. 32)

Energy parameters offer high information content and can be used to optimize sports and workplace equipment and other products. There are several types of energy exchange and parameters; and there is a confusing variety of terms. Depending on the application, mechanical, chemical or thermodynamic principles and models are applied. Epstein (1995) and Winter (1990) provide detailed overviews of energy considerations. (Senner, 2001)

2.3.3 Product and usage characteristics

In addition to the human characteristics, the design of a product and its usage (respectively of a workplace corresponding tasks) has an influence on the

biomechanical load and thus discomfort perception. In this chapter, examples are provided – mainly related to vehicle interior.

2.3.3.1 Geometrical dimensions and shape

The geometric arrangement of products or workplaces has an influence on the joint angles during a posture or movement of the user respectively worker. The joint angles directly influence the lever arms of acting external forces and the length of muscles, which influences their strength (see 2.1.1.1.). So, the joint angles and their effect on muscle lever arms and muscle length can influence the discomfort perception.

In case of a vehicle handbrake, e.g. its location in the vehicle interior, its lever arm length and its pivot point influence the driver's joint angles and thus the available strength level. The geometric arrangement of its environment is important because sufficient clearances are required to apply the handbrake without surrounding elements (e.g. armrest, beverages in a cup holder, seat) interfering.

Obviously, human anthropometry and resulting seat adjustment have an effect on the joint angles, too.

2.3.3.2 Forces and interface design

Forces between human and environment are transferred at areas of contact. The magnitude and direction of the forces are relevant for resulting biomechanical load in the body (such as joint loads, disc pressures and muscle activities). The design of the contact area (such as size, shape and mechanical properties) influences the pressure distribution on the human tissue and its deformation. So, the force and interface design can influence the discomfort perception.

Referring to the handbrake, the force required for handbrake application, the execution of the handbrake handle and the driver's seat can influence the discomfort perception.

2.3.3.3 Time

The discomfort perception can be influenced by time characteristics (Zhang et al., 1996) such as the duration of postures or movements, the velocity of movements, the frequency of exertion and breaks. E.g. Estermann (1999) found that the discomfort of the back increasing over driving time.

Maintaining a posture or performing an exerting task lead to muscle fatigue. A high movement velocity can reduce the maximum strength (see 2.3.1.2.1) which accelerates

fatigue. The proportions of exertion and break intervals also influence biomechanical load and discomfort perception.

There are psychological memory effects which can also play a role in the discomfort perception: The primacy and recency effects increase relevance of the first and last information in a situation (Atkinson & Shiffrin, 1968). The peak-end rule was proposed as patients' memories of painful medical treatments mainly reflect the maximum intensity of pain during a medical treatment and the intensity of pain at the end of the treatment (Redelmeier & Kahneman, 1996).

2.3.4 Conclusions

Discomfort can occur in exertions much lower than the maximum capability of a person. Humans' anthropometry and capabilities (such as strength, endurance and range of motion) differ. Published values have to be applied with precaution due to differences in measurement procedures and studied populations.

Consequently, for the subjective evaluation study of handbrake applications, participants have to be selected pursuing a clinic population representative for driving population in Germany.

In the subjective evaluation studies, the sequence of handbrake variations has to be randomized to minimize effects of order such as fatigue and learning.

The primacy, recency and peak-end memory effects may influence the discomfort ratings of the handbrake evaluations. Thus, motion capturing key frames respectively time points of detailed analysis have to be selected accordingly.

The mechanical behavior within in the human still shows many unknowns (Komi, 1990). Its measurement methods are expensive, subject to limitations and/or ethically questionable. So, modeling the human is a useful method to obtain biomechanical parameters which might influence the discomfort perception. Consequently, Digital Human Modeling (DHM) is applied in this thesis in addition to subjective evaluation studies.

2.4 Evaluation of comfort and discomfort

In the previous chapter (2.3), factors influencing discomfort have been described.

This chapter is about methods and examples of assessing comfort and discomfort. There are two types of measurement methods to determine discomfort: subjective and objective ones.

2.4.1 Subjective evaluation methods with examples

Manifold methods are applied for the assessment of subjective perceptions such as discomfort, comfort, workload, effort, fatigue, exertion etc. (Annett, 2002). Asking people is the most direct methodology, especially since comfort and discomfort are subjective experiences (de Looze et al., 2003; Richards, 1980). On the other hand, well-known sources of error and bias in human subjective judgment can affect the ratings (Annett, 2002).

In recent years, numerous types of rating scales have been applied to capture general or local comfort and discomfort. Examples are 5 and 10 point scales and visual analog scales. (de Looze et al., 2003; Kyung, 2008)

Shen & Parsons (1997) have investigated the validity and reliability of six types of rating scales for seated pressure discomfort. Their selection of scales is based on considerations which are also important for the discomfort evaluation of the handbrake: The scales shall measure one dimension and enable quantifying the ratings.

The following scales were tested:

- A category partitioning (CP) scale (cf. Figure 2.12).
- The Borg CR-10 scale.
- An 8-point ordinal scale.
- A 21-point ratio scale.
- The visual analog discomfort scale by Corlett and Bishop (see Figure 2.13).
- A modified version of it (see Figure 2.14).

Twelve subjects participated in two test sessions which were one week apart. Four levels of stimulus were presented to the mid-thigh region of the seated subjects. The subjects rated pressure intensity, discomfort level due to the pressure and overall discomfort. (Shen & Parsons, 1997)

In general, the subjects were able to assess their sensation by using either of the scales. However, the type of rating scale had a strong influence on the accuracy of ratings. Furthermore, different scales were not equally liked by the subjects.

The category partitioning scale (Figure 2.12) performed best. It “was found to be highly reliable and most valid for rating pressure intensity and perceived discomfort. This scale was also preferred by subjects when compared with the other five scales.” (Shen & Parsons, 1997, p 441)

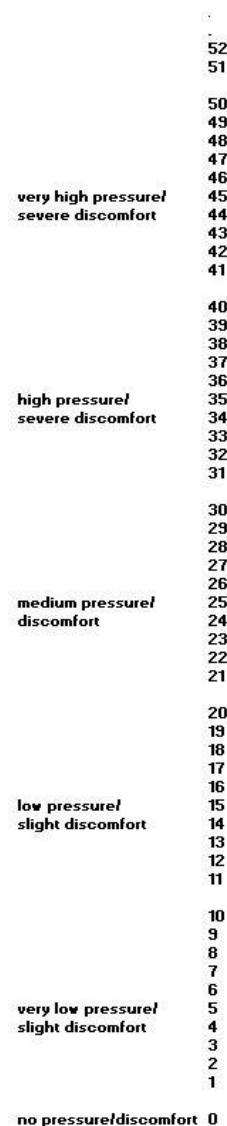


Figure 2.12: Category Partitioning (CP-50) scale, extracted from Shen & Parsons (1997, p. 459), origin in Heller (1985).

The visual analog scales (see Figure 2.13 and Figure 2.14) were also liked by the subjects for clarity, simplicity and ease of use. However, the reliability ranged from fair to poor and the validity from good to poor – depending on the details of scale execution. The scale in Figure 2.13 performed better than the one shown in Figure 2.14. This indicates the importance of the anchors. (Shen & Parsons, 1997)

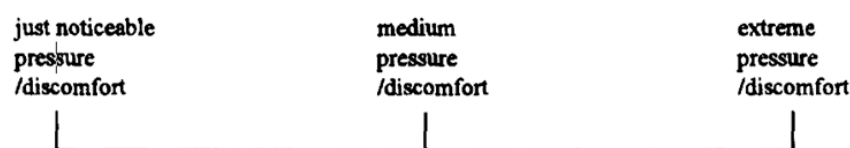


Figure 2.13: Visual analog scale by Corlett & Bishop (1976), adapted by Congleton (1983). Extracted from Shen & Parsons (1997, p. 459). In case of no pressure or discomfort a zero "0" shall be written on the most left end of the scale.

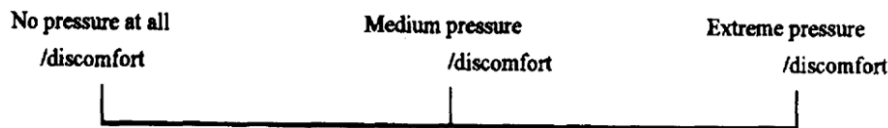


Figure 2.14: Visual analog scale similar to the one in Figure 2.13, but with different left anchor. Extracted from Shen & Parsons (1997, p. 460).

Visual analog scales allow for a continuous mapping of the subjects' perception and have been extensively applied for comfort and discomfort evaluation of chairs and seats (de Looze et al., 2003; Shen & Parsons, 1997). This type of scale was also applied by Krist (1993) providing foundation to the RAMSIS discomfort assessment. For these reasons, in the preliminary study a visual analog scale was applied. In the main study, it was decided to apply the CP 50 scale considering the results of Shen & Parsons (1997) and feedback of the subjects participating the preliminary study.

2.4.2 Objective evaluation methods and examples

Objective methods (such as posture analysis) show advantages when compared to subjective assessments. In general, they are less prone to errors or bias in the measurements and often require a lower number of subjects (de Looze et al., 2003; Lee & Ferraiuolo, 1993). A limitation of objective measurements is that they are indirect: The measurement applies to a parameter (e.g. posture) which shows a clear and plausible correlation with the comfort and discomfort perception. Only in this case, an objective method can be a viable addition to subjective methods (de Looze et al., 2003) or even substitute them. Further limitation respectively disadvantages are, that in some cases, measurements are not possible, not adequate or too resource consuming (see also chapter 2.3).

In the following examples of objective measures related to discomfort are described.

2.5 Discomfort of handbrake application and seated reach

Human, biomechanical and product usage characteristics and their interactions can influence discomfort perception. Therefore, they may correlate to subjective discomfort assessments. The geometric layout, interface design, force level and time constraints characterize the usage of a product, the execution of a task and the design of different studies. These factors and the choice of subjects influence the level of comparability between the studies.

In studies about biomechanical discomfort selected anthropometric and demographic parameters (such as body height, segment lengths, gender and age) are typically recorded because they have an effect on many human characteristics. In some studies, additionally physical capability measurements are recorded such as isometric strength respectively maximum isometric moments and ROM values (Zacher & Bubb, 2004). Joint angles are often captured to quantify their influence on discomfort, e.g. in Wang & Trasbot (2008) and Zacher & Bubb (2004). While external forces can be measured, internal (biomechanical) load is mainly assessed indirectly, e.g. by EMG (Jung & Choe, 1996), muscle dynamometry (Zacher & Bubb) or Digital Human Modeling (Seitz, Recluta, Zimmermann & Wirsching, 2005).

The guidelines for handbrake positioning (see 2.10.3.1) and legal requirements, which define maximum application forces (see 2.10.2), are neither intended nor sufficient to design handbrakes with minimum discomfort for the majority of customers. In literature, little information could be found on handbrake application in general and on the factors influencing correspondent discomfort perception. Most of the literature has focused on seated reach, the underlying principles are considered to be applicable to handbrake reach, too.

The next subchapters are about selected studies on handbrake application and seated reach/grasp discomfort.

2.5.1 Handbrake application discomfort

Fetter et al. (2005) investigated subjective perception of the handbrake location. 30 subjects, divided into 4 groups (representing the 2.5th and 50th female as well as the 50th and 97.5th male body height percentile) participated. After adjusting the seat, they assessed handbrake application for nine different locations. The location of the complete handbrake lever unit was varied. The motion trajectory of the handbrake lever, force angle curve and other parameters were maintained. The handbrake was applied to simulate holding the vehicle at a very steep grade. The subjects applied the handbrake up to a force respectively to an angle they considered appropriate.

Fetter et al. (2005) recommend a range for the handbrake location based on the subjective assessment of predefined locations plus the favorite location, chosen by the subjects themselves within a predefined range. The influence of the handbrake location (in x, y and z) on the subjective perception is described in another paper on the same

study (Augsburg, Heimann & Fetter, 2004). The authors suggest an optimum and a compromised handbrake location range.

While this results can help to position handbrakes with the investigated handbrake geometry and kinematics, they may be not valid for other geometries respectively kinematics. They may also be not fully appropriate for handbrake application on a slight grade, which is probably a more frequent use case.

In another investigation, handbrake locations were subjectively assessed in different Ford and competitor vehicles across passenger vehicle segments (Yilmaz, Heimann, Fingberg, Marek & Fischbein, 2012). As in Augsburg et al. (2004), linear relations between the handbrake location (in x, y and z) and the subjective ratings were documented. The different executions of vehicle interior package and handbrake design as well as their interactions may have influenced the ratings (Yilmaz et al., 2012).

Chateauroux & Wang (2012) compared maximum static handbrake application forces (F_{ST}) and forces exerted during normal dynamic handbrake pull (F_{DY}) for different handle locations and subject characteristics. Handbrake location and resulting body posture, age and gender influence both forces, F_{DY} and F_{ST} . As anticipated, females and elder subjects exerted lower forces than young males. Force generating capabilities were highest for the rear down and lowest for the rear up handbrake location.

“Nearly 94 % of the force was exerted in the handbrake motion direction. It depended on handle position and subject group.” (Chateauroux & Wang, 2012, p. 1309). F_{DY} was significantly lower than F_{ST} ; thus handbrake application usually does not utilize full muscle capability. The ratio F_{DY} divided by F_{ST} was higher for females: they reach a higher level of their strength capability for handbrake application. Handbrake location also showed an effect on the ratio. (Chateauroux & Wang, 2012)

So, the distance – in x, y and z direction – between the shoulder joint (also the hip location if torso motion is required) and the handbrake force application point (FAP) influences the body posture and therefore the force generating capabilities. The location of the FAP in a vehicle is fixed and the driver can adjust the seat. Thus, the distance between shoulder, hip and FAP is influenced by design location of FAP, seat position adjustment and anthropometry. Consequently, the handbrake location and the seat position can influence force capability and therefore the discomfort rating. (Lietmeyer, 2013; Raiber, 2015)

Apart from the above mentioned studies (Augsburg et al., 2004; Fetter et al., 2005; Chateauroux & Wang, 2012; Yilmaz et al., 2012), no further research on handbrake

application could be identified. So, there is a lack of information about the influence of many factors on handbrake application discomfort.

2.5.2 Discomfort of seated reach and grasp

A number of studies have been published focusing on seated reach respectively grasp in general (e.g. Jung & Choe, 1996; Zacher & Bubb, 2004; Wang, Chevalot & Trasbot, 2008; Wang & Trasbot, 2011). The studies are often not related to a particular control element of e.g. a vehicle or an airplane. It is assumed that some findings are partly applicable to the handbrake.

In many publications, there is no clear separation between “reach” and “grasp” (see 2.6). Reaching (out) serves different purposes, such as to push a button with one finger or to grasp a lever with the hand. The type of reaching/grasping target can influence the grip type and reach movement (see 2.6.2).

There are many studies on reach envelopes, e.g. Chaffee (1969) or Sengupta & Das (2000), and on motion analysis with the aim to understand and partly also to simulate movement strategies, e.g. Jung & Choe (1996) or Chateauroux & Wang (2008). Maximum reach envelopes are available as tables and graphics (Figure 2.10; SAE J287, 2007), e.g. for driver hand controls. (Wang & Trasbot, 2011)

Reach envelopes help to design the workspace layout, but not to optimize control location within the reach zones.

Engineers often have to find trade-offs between several requirements (aesthetics, safety, comfort, grouping multiple controls and other elements in a tight space). Thus, they need to know the least uncomfortable location for a control in a predetermined zone and how the discomfort changes if the location is varied. (Wang & Trasbot, 2011)

Wang & Trasbot (2011) deduce the need for models which can predict maximum reach surface and “iso-comfort and discomfort rating surfaces” (Wang & Trasbot, 2011, p. 466). Digital Human Modeling tools, which are able to predict discomfort, would help to determine the least uncomfortable location for a control or to understand discomfort differences between two locations or two tasks.

Kee (2002) developed a methodology to establish three dimensional iso-comfort surfaces based on perceived discomfort ratings. His regression equations between discomfort perception and joint angles were based on experiments with four different controls (lever, push button, knob, track ball). The joint angles were control variables, but only three joint angles were considered. So, it is barely possible to expand the

results to a more detailed Digital Human Model with more degrees of freedom. (Wang & Trasbot, 2011)

In Kee (2002), shoulder flexion, abduction/adduction, elbow flexion as well as the type of control show highly significant influence on perceived postural discomfort. The model of reach capability and difficulty by Reed et al. (2003) predicts reach difficulty depending on the target location for push-buttons. Both models do not have the capability to test if a target is out of reach. (Wang & Trasbot, 2011)

Wang & Trasbot (2011) investigated the effects of target location, body height ("stature") and hand grip type (index fingertip reach, three finger grip, five finger grip) on in-vehicle reach discomfort. They found a strong quadratic effect of the target distance and a less strong quadratic effect of target azimuth and elevation (see Figure 2.15). The effect of subjects' body height was small but significant, in particular for its interaction with target elevation and distance. The three different grip types lead to significantly different discomfort ratings for a similar target. The reproducibility of discomfort ratings was found to be low. (Wang & Trasbot, 2011)

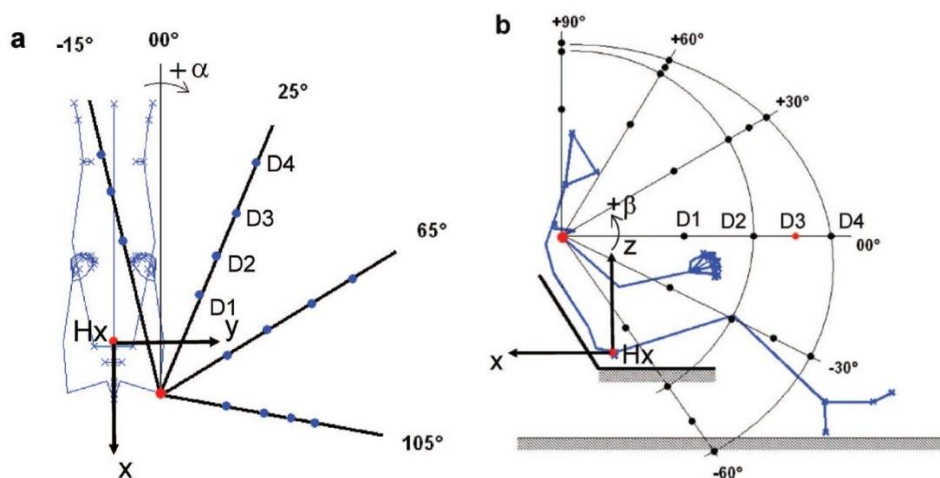


Figure 2.15: Target azimuth (α) and elevation (β) are defined to the sagittal and transverse planes passing through the right acromion marker. Target distance is also calculated to acromion marker. (Wang & Trasbot, 2011, p. 469).

Chateauroux & Wang (2008) found that older subjects' reach capacity was lower. It was more difficult for them to reach eccentric targets which can be explained by the loss of joint mobility.

Anthropometric characteristics and corresponding reach capacity of 24 subjects as well as their ratings were utilized in a DHM database approach. Aim was to predict reach and discomfort related to given targets (Chevalot, Monnier & Trasbot, 2006; Wang, Chateauroux & Chevalot, 2007; Wang; Wang, Chevalot & Trasbot, 2008).

Wang et al. (2008) present the application of this approach to the prediction of in-vehicle reach capacity and discomfort. The use of the model is limited: the reach envelopes are based on reconstructed reach postures from a particular experiment with its specific reach conditions, limited number and anthropometry range of subjects as well as quality of reconstruction (Wang et al., 2008).

Chevalot & Wang (2004) studied the effects of gender, age and target location on perceived discomfort. Target distance, height and azimuth had a quadratic effect on discomfort. Minimum discomfort was perceived at mid-height between seat and shoulder in the sagittal plane. Elder participants perceived higher discomfort than the young. The reproducibility of discomfort ratings was found to be low which might explain why only 49 % of the variance could be explained with the proposed regression equation. (Chevalot & Wang, 2004)

In-vehicle reach tasks (such as handbrake application) mostly begin with the movement from a driving posture. Drivers have different anthropometries and adjust the seat and steering wheel accordingly. Their relative location to the vehicle control has an influence on their individual postures and thus the discomfort perception. (Wang & Trasbot, 2011)

Car interior components (such as seat, steering wheel, armrest, elements of the center console) might interfere with reach movements and affect the discomfort perception, too. The interferences and resulting effects on discomfort perception can vary depending on the driver's anthropometry (Wang & Trasbot, 2011) and on the individual movement pattern. These patterns can differ due to the high variability of human postural and motion control (Wang & Trasbot, 2011). People with a high BMI tend to be more effected from interferences with the car interior (Wang & Trasbot, 2011).

Jung & Choe (1996) have investigated the quantitative relationship between posture, external load, EMG measurements and perceived reach discomfort. They found a Person correlation coefficient of 0.73 for the normalized discomfort rating and the sum of normalized EMG of eight muscles. They proposed a regression model ($r^2 = 0.79$) based on seven joint angles (hip flexion and lateral bending; shoulder flexion, abduction/adduction, rotation; elbow flexion, wrist flexion/extension), external load and several interactions of joint angles or joint angles with external load. (Jung & Choe, 1996)

Zacher & Bubb (2004) have studied the effect of joint angles and external load on perceived discomfort for several joint angles of shoulder, elbow, knee, spine, ankle, hip and wrist.

They identified discomfort dependencies from the percentage of utilization of:

1. The individual maximum range of motion of a joint.
2. The individual maximum moment of a joint.

The corresponding mathematical interrelationships were found to be dependent on the joint and the direction of the external force (Zacher & Bubb, 2004).

Zacher & Bubb (2004) also investigated a complete movement task, going up and down a step. They determined that the discomfort assessment of a complete movement is depending on the maximal discomfort perceived in a single joint or other body part: "The body part where the maximal discomfort is felt is either the body part with the muscles which are stressed most to perform the movement or the joint with the most unpleasant angle." (Zacher & Bubb, 2004, p. 6). They underline the difference between static discomfort and dynamic discomfort, which can be influenced by a lot of impetus. (Zacher & Bubb, 2004)

2.5.3 Discomfort evaluation using Digital Human Models

Several factors influencing discomfort perception have been described in the previous chapters. Studying the effect of these factors on perceived discomfort (for using a product or completing a task) is often a time consuming process. Human anthropometry and capabilities as well as the level of interaction between them often have effects on biomechanical measures and comfort perception. Comparison of studies can show discrepancies in results originating from different test populations or experimental setups. Thus, Digital Human Models have several advantages: they are resource saving and tend to be of higher objectivity. They allow to model characteristics which cannot be measured directly respectively at all or which have disadvantages/limitations when being measured (e.g. joint load, muscle activity).

See chapter 2.7 to 2.9 for more detailed information.

2.5.4 Conclusions

In summary, influence on reach/grasp discomfort has been show for:

- Body height (Chevalot & Wang, 2004; Wang & Trasbot, 2011).
- Age (Chevalot & Wang, 2004).
- Target location respectively distance (Reed, Parkinson & Chaffin, 2003; Chevalot & Wang, 2004; Chateauroux & Wang, 2008; Wang & Trasbot, 2011).
- Type of control and hand grip (Kee, 2002; Wang & Trasbot, 2011).

- Joint angles (Jung & Choe, 1996; Kee, 2002; Zacher & Bubb, 2004).
- External loads (Jung & Choe, 1996), joint loads (Zacher & Bubb, 2004).
- EMG values (Jung & Choe, 1996).

For the handbrake application, the influence of the handbrake location on discomfort (Augsburg et al., 2004; Fetter et al., 2005; Yilmaz et al., 2012) and on force generating capabilities (Chateauroux & Wang, 2012) has been documented.

The effect of target location on reach discomfort was observed quadratic (Chevalot & Wang, 2004; Wang & Trasbot, 2011). However, the relation between handbrake location and application discomfort was found linear (Fetter et al., 2005; Yilmaz et al., 2012). It is anticipated that for a wide range of reach/control locations (from very close to very remote in x, y and z) the relation between location (respectively distance) and discomfort is quadratic. Potential reason is that the discomfort level is high for too close and too distant locations with the optimum and thus lowest discomfort value in between. For a smaller range of reach/control locations, a linear model approximates the relation sufficiently accurately.

Age reinforces the discomfort perception in general and for eccentric targets in particular (Chateauroux & Wang, 2008).

A low reproducibility of ratings was noted in some studies (Chevalot & Wang, 2004; Wang & Trasbot, 2011). However, high reproducibility was observed in Fetter et al. (2005). Differences in experimental setup, rating scales, study participants and definitions of high respectively low reproducibility may explain the apparently contradictory findings. Compared to subjective evaluation studies, assessments with DHMs are typically more consistent and have several other advantages.

At the beginning of chapter 2.5, the little available information about handbrake application has been described. The considerably more findings on reach have been summarized. The special type of handle and thus hand grip type, the movement and forces related to handbrake application are above and beyond reach and cannot be assessed directly with the available models and equations. However, it can be assumed that factors influencing reach discomfort will also influence discomfort of handbrake application.

2.6 Movement strategies

Choudry et al. (2013) introduce movement strategies the following way:

“Due to the large number of joints in the human body, multiple movement strategies can be employed to execute a given task. Movement strategy differences can be exhibited both through different muscle recruitment patterns and differing kinematic trajectories. This flexibility is advantageous because it allows individuals to adapt to varying environments, execute a variety of tasks, and compensate for morphological (e.g., body size and shape) or functional movement constraints (e.g., joint range of motion, strength, fatigue, etc.). However, inter- and intraindividual variations in movement strategies pose significant methodological challenges for human motion analysis, as it becomes difficult to objectively identify and classify movement strategies.” (Choudry, Beach, Callaghan & Kulic, 2013, p. 314)

Movement strategies for handbrake application need to be considered in vehicle development: they can influence the force generation capabilities (Chateauroux & Wang, 2012) due to the length tension relationship (see 2.1.1.1.2), the required clearances to surrounding elements (to operate the handbrake without touching them) and finally the perceived discomfort.

The handbrake operation comprises several movements: reaching from the steering wheel to the handbrake (reach), grasping the handle (grasp) and pulling the handbrake (object manipulation, handbrake application). This study focuses on the process of pulling the handbrake. Still, reaching and grasping can influence the discomfort perception. Reaching and grasping are considered as a single task in parts of the literature referenced in chapter 2.6.2. In this thesis reach is used referring to both, reach and reach to grasp.

A lot of literature has been published on driving posture (see 2.6.1), seated reach and grasp (see 2.6.2). However, little could be found about the reaching, grasping and pulling the handbrake: only one publication (Fetter et al., 2005) which documents the ability of a test rig to run motion analysis during handbrake application. The study is based on a small number of subjects and individual favorite locations of a handbrake. Findings on a single joint angle are exemplarily described. The study does not allow drawing general conclusions about movement strategies for different subjects and/or handbrake designs (e.g. location).

The reach movement toward the handbrake is influenced by the initial driver posture prior to reaching for the handbrake handle. Driver's seat and steering wheel adjustments/positions – as well as the placement of the hands on the steering wheel – influence the reach posture.

2.6.1 Driving posture

Driving postures and related joint angles have been in focus of extensive research (Andreoni, Rabuffetti & Pedotti, 1999; Reed, Manary, Flannagan & Schneider, 2000; He, Xia, Chen & Cui, 2008; Kyung & Nussbaum, 2009; Kyung, Nussbaum & Babski-Reeves, 2010; Mohamad, Deros, Wahab, Daruis & Ismail, 2010). Schmidt et al. (2014) reviewed 30 scientific sources, published between 1940 to 2012, on optimum respectively selected (preferred) human joint angles for automotive sitting posture. Influencing factors such as body height, gender, age, vehicle class, seat design and driving venue are discussed. Large differences in study designs were found. It is emphasized that most of the studies were about adopted respectively preferred postures. They may not necessarily represent the optimum posture regarding biomechanical or physiological factors. This may be valid also for studies on seat adjustment respectively seating position (Parkin, Mackay & Cooper, 1995; de Leonardis, Ferguson & Pantula, 1998; Welsh, Clift, Morris, Cook & Watson, 2003; Jonsson, Stenlund, Svensson & Björnstig, 2008; Fröhmel, 2010) and placement of the hands on the steering wheel (Reed, Manary, Flannagan & Schneider, 2000; Walton & Thomas, 2005).

The leg length and therefore body height influence the fore-aft adjustment of the seat. Several studies have shown that smaller people adjust their seat more forward than taller ones (Parkin et al., 1995; de Leonardis et al., 1998; Welsh et al., 2003; Jonsson et al., 2008; Fröhmel, 2010). This can be explained by the need to operate the pedals. The correlation between body height and height adjustment of the seat was found to be weaker (Jonsson et al., 2008). Smaller people tend to adjust the seat higher for better exterior visibility.

Repeatability of the seat adjustment is subject depending. Individual adjustment range can vary considerably: Jonsson et al. (2008) found a 95 % probability that two seat adjustments of a subject differ up to 50 mm in fore-aft direction.

Kyung et al. (2010) completed a cluster analysis of driving postures for sedans and SUVs. They describe three prevalent postural strategies (lower limb flexed, upper limb flexed and extended, see Figure 2.16) which are influenced by body height, gender (in

that study correlating with body height) and age. They observed that some participants change their postural strategy depending on the vehicle class.

Study results show that most – but not all – drivers hold their hands on the top half of the steering wheel (Walton & Thomas, 2005; Jonsson, 2011; Mossey et al., 2014).

Although the drivers sit in a confined space, they tend to adopt diverse driving postures. Even two drivers of similar anthropometry may demonstrate different postures (Kolic, 2008). Additional to “reaching and controlling movements, drivers tend to change their driving posture intermittently in order to reduced discomfort induced by postural fixity” (Akerblom, 1948; Andreoni et al., 1999; Kyung et al., 2010, p. 376). The driving posture, resulting in the specific seat and steering wheel adjustment, defines the occupant’s distance to the vehicle controls.

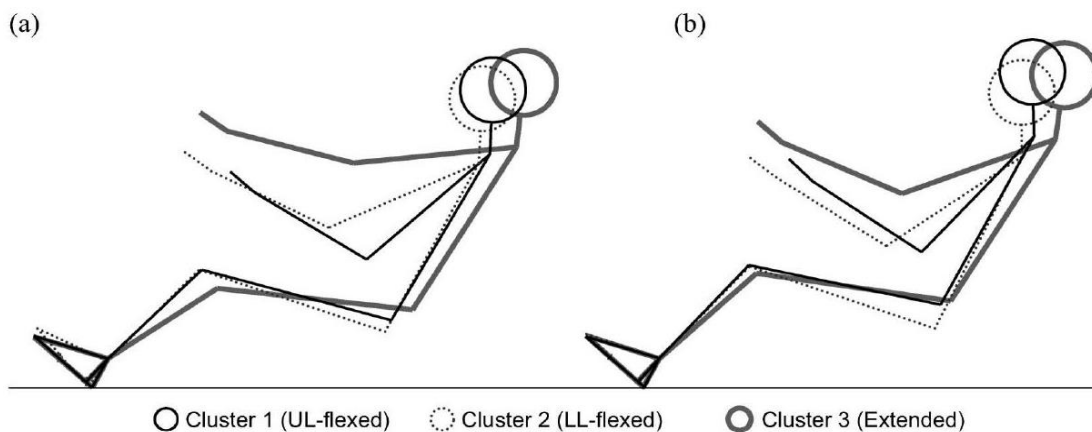


Figure 2.16: Schematic comparison of the postural strategies in a sedan (a) and in a SUV (b), extracted from Kyung et al. (2010, p. 382).

2.6.2 Seated reach

This chapter begins with a description of reaching and grasping (2.6.2.1). Then, the terms movement regularity and variability are explained (2.6.2.2). In 2.6.2.3, hypotheses, influencing factors and corresponding empirical studies are summarized. Hypotheses and studies often address several influence factors of movement patterns at once. Study designs are described because they are very different. Consequently, hypotheses and studies are described one after the other (and not ordered by influence factors). Still, studies which include investigations on the influence of age are presented in chapter 2.6.2.4.

Chapter 2.6.3 lists the influence factors for movement patterns. Conditions which ease reach and are likely to reduce discomfort are described as a conclusion.

2.6.2.1 Reach and grasp

“Reach to grasp” movements are common in daily living and in particular for tool manipulations (Li, 2014; Lee & Jung, 2015). Arm postures in reach to grasp movements are influenced by the orientation of the target. They cannot successfully be explained by the motor control strategies applied to arm postures in reaching movements (Soechting & Flanders, 1993; Tillery, Ebner & Soechting, 1995; Li, 2014).

Reaching to grasp a target combines two independent neural processes: reaching and grasping (Wing, Lederman, Nowak & Hermsdörfer, 2001). Reaching describes moving the hand towards the targets. Grasping refers to shaping the hand according to the object (Wing et al., 2001; Li, 2014). For a stable grasp, the wrist velocity approaches zero when the fingers contact the object. For reach to grasp movements, the arm posture is significantly influenced by the grasp orientation (Li, 2014). Motion analysis shows that the fingers already begin to shape for the grasp while the hand is being moved towards the objects. (Sanctis, Tarantino, Straulino, Begliomini & Castiello, 2013)

The wrist naturally separates the upper limbs in macro- and microstructure. The macro structure encompasses shoulder, arm, elbow, forearm and wrist. These elements are mainly used for reaching. The micro structure is the hand with palm and fingers. Object manipulation can be performed by power grasping or by precise grasping with the hand. During a power grasp, all fingers are flexed around an object and the thumb is flexed in the opposite direction towards the fingers. This enables “forcible press” (Li, 2014, p. 43). The precise grasp describes holding the object with the thumb and maximal three fingers. It allows for accurate manipulations. (Li, 2014)

The handbrake application is performed in the power grasp by moving mainly the macrostructure of the upper limbs and – if necessary – the torso. It has similarity to a guided reach movement with added contribution from a growing external force.

2.6.2.2 Movement regularity and variability

Li (2014, p. 37) differentiates between “regularity” and “variability” in human arm movements: Regularity refers to movements (e.g. for daily-life tasks) with significant similarities within and also across healthy human individuals. Variability occurs when arm movements of each individual differ for the same task. Li (2014) summarizes several motion control strategies including Donders’, Fitt’s and the 2/3 Power law. She concludes that the predictions of postures based on available hypotheses are not fully in

agreement with natural motions of the human arm. The variability of human postures can be used to distinguish skilled from unskilled task execution. (Li, 2014)

In this thesis, regularities of handbrake application movements are investigated. The focus is on the macrostructure of the right upper limb and the trunk with corresponding joint angles.

Neural and sensorimotor control (of object manipulation) is not in focus of this literature overview. It is described in detail for instance by Nowak & Hermsdörfer (2001).

2.6.2.3 Reach movement hypotheses, influence factors and empirical studies

For reach tasks, the initial location of the hand does influence the reach posture. However, it does not completely define it due to the kinematic redundancy of the human body (Zhang & Chaffin, 1997).

Burgess-Limerick, Abernethy & Neal (1993) found that during human movements (symmetric lifting with two hands) multiple joint angles and hand position changes occur almost simultaneously.

The simplest hypothesis on the question “What guides reach postural behavior respectively movements?” is that a body segment will only be moved if a target cannot be reached sufficiently well with all segments located more distal from the pelvis (Delleman, Hin & Tan, 2003). This hypothesis is put forward in some publications (Evershed, 1970; Korein, 1984; Case, Porter & Bonney, 1990). The majority of papers describe cost functions (Delleman et al., 2003). For example, Hsiao & Keyserling (1991) propose that to reach a target a proximal segment has a higher tendency to stay closer to a neutral posture than a more distal segment (to the pelvis). The term “neutral posture” refers to a posture with minimal discomfort at joints and adjacent body segments. (Delleman et al., 2003)

Numerous studies have discussed and support the leading joint hypothesis (Dounskaia, 2010; Ambike & Schmiedeler, 2013). It suggests that multi joint movements are generated by using a muscle moment at one leading joint, which introduces interaction moments to the subordinate respectively trailing joints. Thus, the active control of the leading joint supports “the preference to minimize the active control of the trailing joint” (Dounskaia & Wang, 2014, p. 1050). The active control of the leading joint is suggested to reduce the demands for active coordination of joint motions and thus to minimize the effort to control errors during the movement (Todorov, 2004) and during movement planning (Sternad, Abe, Hu & Müller, 2011).

The simplified joint control pattern hypothesis (Dounskaia & Wang, 2014) is about preferred patterns of joint coordination during arm movements. It suggests that either the shoulder or the elbow is actively moved while the other (trailing) joint is predominantly passively moved via interaction and gravitational moments (Dounskaia & Wang, 2014).

Several publications have shown (Delleman et al., 2003) that the arm posture of a final hand position depends on the starting position of the hand (e.g. Soechting, Buneo, Herrmann & Flanders, 1995; Gielen, Vrijenoek, Flash & Neggers, 1997; Desmurget, Grea & Prablanc, 1998; Hepp, Haslewanter, Straumann, Hepp-Reymond & Henn, 2012).

The knowledge model of movement selection by Rosenbaum et al. (1995) suggests that reaching postures reflect the knowledge subjects gained about postures they have adopted earlier ("stored postures"). The knowledge considers how much the stored postures differ from the new target posture (accuracy costs) and how expensive the move from the start posture to the stored posture will be (travel costs). The travel costs were quantified considering the weight of the body segments, moved by rotating the hip, shoulder or elbow (Fischer, Rosenbaum & Vaughan, 1997). Experiments confirmed some predictions of the model: Fischer, Rosenbaum & Vaughan (1997) observed the least rotation at the joint which moves the largest weight. (Delleman et al., 2003)

Hsiao & Keyserling (1991) investigated seated reach of three subjects for a variety of reach directions and distances. In agreement with their hypothesis (see above), the trunk showed a greater tendency to stay close to its neutral posture than the segments of the upper extremities, Contradictory to their hypothesis, the least neutral tendency was observed for the pelvis. When a location was too far away, subjects rather shifted their pelvis on the seat than flexing or twisting the trunk. (Hsiao & Keyserling, 1991)

When the buttock is fixed (e.g. by a seatbelt), forward reaching positioning of the hand is initially achieved by glenohumeral anteversion. The trunk leans forward at a small rate. When the hand needs to move more and more forwards, the glenohumeral anteversion reaches its maximum and the trunk flexion gradually takes over. (Snyder, Chaffin & Schutz, 1972; Kaminski, Bock & Gentile, 1995; Fischer et al., 1997; Mark et al., 1997; Zhang & Chaffin, 1997; Delleman, 1999; Vaughan, Rosenbaum, Harp, Loukopoulos & Engelbrecht, 1998).

Delleman et al. (2003) studied postural behavior in static sideward reaching. They observed that trunk (chest, pelvis) was not involved for reaches up to 40° - 50° azimuth

angle depending on the reach distance. 0° is straight forward in a horizontal plan with the center at the sternum. For larger azimuth angles, arm, chest and pelvis were involved with similar contribution rates to the total range of motion. Apparently, these segments “share the musculoskeletal load equally” (Delleman et al., 2003, p. 1) which is in agreement with the findings of studies on static gazing postural behavior (Delleman & Hin, 2000; Delleman, Huysmans & Kuijt-Evers, 2001).

A number of studies have been conducted on seated reach postures and movements, factors altering them (Zhang & Chaffin, 1997; Chaffin, Faraway, Zhang & Woolley, 2000; Chevalot & Wang, 2004; Chateauroux & Wang, 2008) and methods to simulate them (Verriest, 1998; Chaffin, Faraway & Zhang, 1999b; Wang & Zhang & Chaffin, 2000; Wang, Chevalot, Monnier & Trasbot, 2006).

Individual's factors (such age, gender and anthropometry) and vehicle related factors (e.g. vehicle segment, vehicle interior geometrical layout and driving venue) have been shown to have an effect on drivers' sitting and reaching postures (Chaffin et al., 2000; Park, Kim, Kim & Lee, 2000; Reed et al., 2000, Hanson, Sperling & Akselsson, 2006; Kyung, 2008).

Zhang & Chaffin (1997) completed a study with 6 participants and 48 reach movements. The movement directions are illustrated in Figure 2.17.

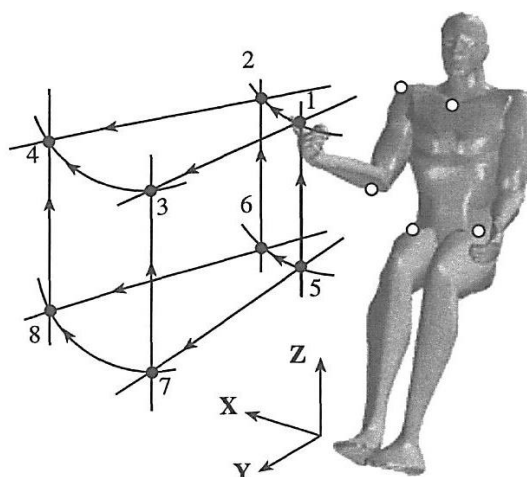


Figure 2.17: Illustration of hand motion trajectories for seated reach tasks, extracted from Zhang & Chaffin (1997, p. 662).

They found r^2 values between 0.86 and 0.99 for the relationship between hand position and five joint angles (torso flexion and lateral bending, shoulder extension and abduction, elbow flexion).

They studied how hand location, motion direction and speed as well as their interactions influence the joint angles:

- Hand motion direction and hand location showed a significant interacting effect on most joint angles (except for elbow flexion).
- Hand motion significantly influenced elbow flexion and shoulder abduction angles.
- Hand location was proved having a main effect on all five angles.
- No significant effect of speed was observed.

Zhang & Chaffin (1997) explained the significant effect of hand motion direction with the direction-dependent body segment mechanical stiffness and inertia, demonstrated by Flash & Mussa-Ivaldi (1990) and Karst & Hasan (1990).

Many investigations have shown that joint angles and hand coordination have a sigmoidal shaped displacement profile and a bell shape for their velocity profiles (Boston, Rudy, Mercer & Kubinski, 1993; Zhang & Chaffin, 1997).

Zhang & Chaffin (1997) made several observations in their experiment on strategic planning of human movement and postural control. They found that for medial-lateral and up-down movements, people mainly relied on arm movements. Minimized torso participation was observed independent from the torso flexion angle.

These findings indicate that the strategy employed for movement control is aimed at saving energy since torso motions requires a high level of energy. (Zhang & Chaffin, 1997)

This is in line with the hypotheses described at the begin of this chapter (2.6.2.3).

When a significant torso movement is required (e.g. in anterior-posterior reaching tasks), the torso motion starts simultaneously with the reach motion. Thus, the body movement is executed as a multi segment movement in a synergetic way (and not moving one segment after the other). This also suggests efficient use of energy. (Nelson, 1983; Marshall, Wood & Jennings, 1986; Zhang & Chaffin, 1997)

Influence of visual demand and head posture on seated reach movement was studied by Kim, Martin, Dukic & Hanson (2006).

2.6.2.4 Influence of age

Chateauroux & Wang (2008) investigated the effect of age, gender and target location on seated arm reach capacity and postures. 38 subjects, divided in four groups of age

and gender, were requested to reach 84 targets. The targets were located in space according to the subjects' anthropometry and reach capacity.

Gender did not cause a difference in maximum reach distance. Elder participants had a shorter maximal reach distance (on average by 4.8 % of upper limb length) compared to the younger participants. Age significantly influenced the reach posture, particularly when interacting with the target azimuth angle. Elder subjects moved their trunk less than the younger ones whenever possible, even for targets with medium reach distances. For targets deviating from the sagittal plane, they used reduced neck and trunk axial rotations, compensating by a greater rotation of the pelvis. This is in agreement with Reed et al. (2003b) and Reed et al. (2004).

The findings by Chateauroux & Wang (2008) are in agreement with the findings by Doriot & Wang (2006) who investigated the effect of age and gender on upper body joint ROMs. They found highest reduction in ROM with increasing age for the neck and trunk. Especially neck extension, lateral flexion and axial rotation as well as trunk lateral flexion and axial rotation were observed to be reduced with aging.

The results in Chateauroux & Wang (2008) are also in line with the study by Chevalot & Wang (2004) on effects of age, gender and target location on perceived discomfort for seated reach movements. As anticipated, elder participants perceive more discomfort. In particular reaching eccentric targets was more difficult for them than for the young.

The interaction of age and azimuth angle of the target has significant effect on the discomfort perception (Chevalot & Wang, 2004). Reasons are the reduction of the balance-limited seated lateral reach capability (Parkinson et al., 2006) and the reduction of trunk ROM (Doriot & Wang, 2006) with increasing age.

Aging has also been shown to decrease the performance of tasks requiring multi-segmental motions (Lawton, 1990). In ball throwing motion analysis, elder subjects did not rotate their trunk and arm as much as the younger (Haywood, Williams & VanSant, 1991). Potential reasons are reduced flexibility in the shoulder girdle, pain or fear of pain – inhibiting torso and shoulder motion approaching the ROM – and the desire to prevent soreness after the exertion (Haywood et al., 1991; Reed, Parkinson & Wagner, 2004). Also in forward reaches when standing, elder participants have shown reduced torso rotation and flexion, which supports the conclusion that the volitional reach capability decreases with age (Cavanaugh et al., 1999).

Muscle strength becomes especially important when a movement approaches the limits of a joint's ROM (Chaffin et al., 2000). As mentioned above, females averagely have

55 % of the shoulder and arm strength of males (Laubach, 1978). On average, age related decrease of force-producing capabilities (including strength) begins at the age of 25 years and is about 5 % to 10 % per decade (Bhise, 2012).

Li & Zhang (2007) have observed a significant effect of dynamic strength on the movement strategy for lifting. Force producing capabilities might also influence reach movements.

Chaffin et al. (2000) describe the effects of stature, age and gender on seated reach motion postures to typical target areas in a vehicle.

Table 2.1: Mean changes in major joint angles for each 10 cm of body height difference for hand reach to the target areas. Extracted from Chaffin et al. (2000, p. 414).

Target Area	Trunk Forward	Trunk Lateral	Trunk Rotation	Shoulder Vertical	Shoulder Horizontal	Right Elbow
Console	<i>ns</i>	-0.5°	<i>ns</i>	- 2.1°	3.0°	- 7.1°
Radio	3.3°	-1.0°	2.0°	- 7.4°	<i>ns</i>	- 4.1°
Overhead	1.1°	-0.4°	1.8°	- 9.9°	<i>ns</i>	-10.3°
Far Right	6.1°	-6.2°	2.9°	-10.0°	3.1°	- 2.0°

Note: *ns* = no significant difference could be found.

In their study with 38 subjects, body height had the largest effect on joint angles (Table 2.1). Age also accounted for differences, the elder participants presented less arm abduction and shoulder forward rotation than younger subjects. Gender had only a marginal effect. (Chaffin et al., 2000)

Reed et al. (2004) studied the torso kinematics of seated reaches. Twelve young subjects reached about 100 target locations while sitting on each of three different seats (industrial, car and truck seat). Pelvis mobility was found to be an important contributor to reach capability, especially for reaches to distant locations, see Figure 2.18.

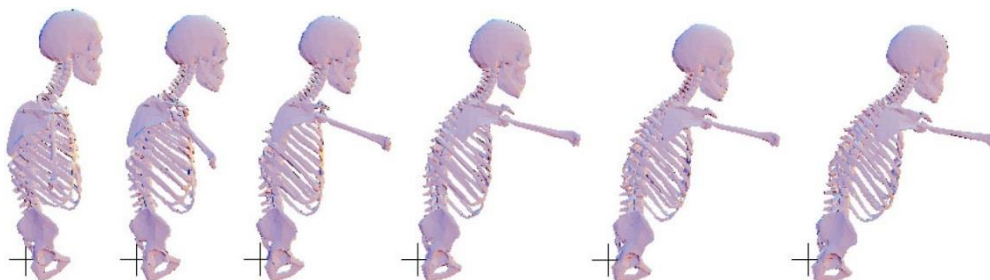


Figure 2.18: Kinematics for a forward reach in a truck seat showing rotation of the pelvis. Crossed lines indicate the seat H-Point. Extracted from Reed et al. (2004, p. 4).

“On padded seats, the pelvis pivots around a moving axis generally located below the pelvis, within the seat cushion. The effective center of rotation is produced by

forward/lateral pelvis rolling and increased penetration into the cushion as the weight of the torso is offloaded from the seat back. “(Reed et al., 2004, p. 6)

Based on different torso kinematics, illustrated and described in Figure 2.19, reach targets were categorized into four zones. (Reed et al., 2004)

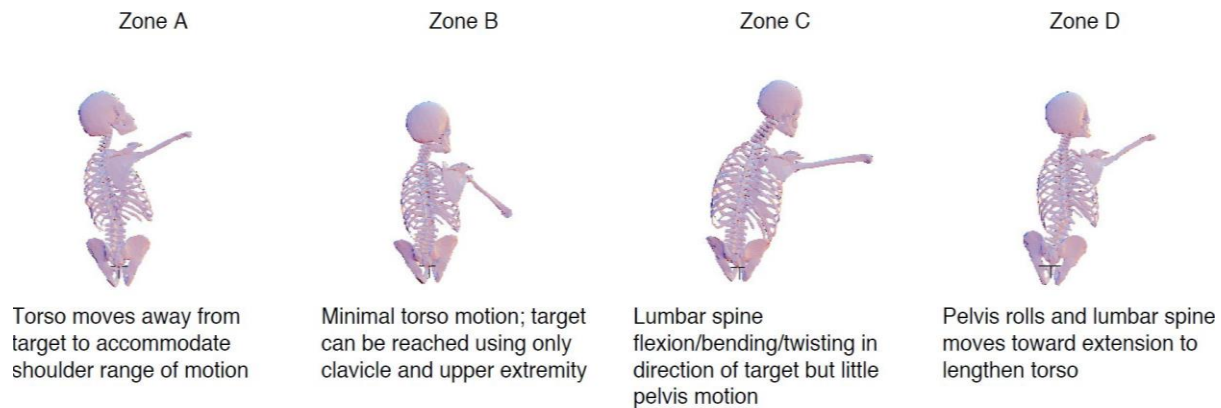


Figure 2.19: Illustration of typical terminal postures for reaches to targets in four zones. Extracted from Reed et al. (2004, p. 6).

The transition from B to C for lateral reaches was found to occur prior to reaching the maximum range of motion of the upper extremities (Delleman et al., 2003).

It can be concluded that for frequently used vehicle controls such as shifter and handbrake, locations within zone B would decrease perceived discomfort. This is in particular relevant for elderly people who in particular aim to move the spine as little as possible (see above).

Balance is a more delimitating factor than ROM for lateral and nearly lateral maximum reaches (Reed et al., 2003a; Reed et al., 2004).

The study conducted by Vandenberghe et al. (2010) shows that kinematics and muscle activity are affected by the target location of a 3D reach target. They found that changes in reach width result mainly in changes of kinematics and muscle activity of the shoulder. Changes in reach height affect additionally kinematics and muscle activity of the elbow. This is in agreement with the simplified joint control pattern hypothesis (Dounskaia & Wang, 2014).

2.6.3 Conclusions

Reach postures in vehicles start from the driving postures. Driving postures are influenced by many factors such as body height, gender, age, vehicle class, seat design and driving venue (Schmidt, Amereller, Franz, Kaiser & Schwartz, 2014). Seat

position/adjustment can vary considerably, even for the same person in the same vehicle (Jonsson et al., 2008).

For reach, several hypotheses on movement patterns with different explanation approaches have been presented. Most of them agree that body segments will only be moved in the case a target cannot be sufficiently well reached by all segments located more distal from the pelvis (Evershed, 1970; Korein, 1984; Case et al., 1990; Delleman et al., 2003).

Influence on reach postures has been shown for the following characteristics:

- Target location (Vandenberghe, Levin, Schutter, Swinnen & Jonkers, 2010) and orientation (Li, 2014).
- Body height (Chaffin et al., 2000).
- Gender: females have a smaller body height and lower muscle strength than males (Laubach, 1978).
- Skilled versus unskilled execution (Rosenbaum, Loukopoulos, Meulenbroek, Vaughan & Engelbrecht, 1995; Li, 2014).
- Individual capabilities such as maximum ROM, strength, balance (see examples with regards to age below).
- Age, which on average:
 - Reduces maximum ROM e.g. for neck, trunk (Haywood et al., 1991; Reed, Parkinson & Klinkenberger; Reed et al. 2004; Cavanaugh et al., 1999; Doriot & Wang, 2006; Chateauroux & Wang, 2008) and shoulder girdle (Cavanaugh et al., 1999; Chaffin et al., 2000; Reed et al. 2004).
 - Reduces balance (Parkinson, Chaffin & Reed, 2006).
 - Reduces muscle strength (Bhise, 2012), which is especially important when a movement approaches the limits of a joint's ROM (Chaffin et al., 2000).
 - Decreases performance to execute tasks requiring multi-segmental motions (Lawton, 1990).
 - Decreases maximum reach distance respectively volitional reach capacity (Reed et al., 2003b; Reed et al., 2004; Chateauroux & Wang, 2008).
 - Increases discomfort, especially for eccentric targets (Chevalot & Wang, 2004).

Effects of several factors on reach and discomfort have been described above. Consequently, previous research suggests that reach can be facilitated respectively perceived discomfort can be reduced for people of all ages (and especially elder people) by:

- Minimizing deviations of joint angles from neutral position (Hsiao & Keyserling, 1991), enabling them to be distant from maximum ROM limits (Zacher & Bubb, 2004).
- Minimizing motion - especially rotation - of body segments proximal to pelvis and moving larger weight, particularly minimizing torso – forward, sideward, rotatory – motion (Haywood et al., 1991; Cavanaugh et al., 1999; Chateauroux & Wang, 2008) and pelvis motion (Reed et al., 2004).
- Allowing postures distant to balance limits (Reed et al., 2003a).
- Minimizing load respectively keeping it away from maximum load limits (Zacher & Bubb, 2004).
- Minimizing number of body segments in use (Lawton, 1990).
- Minimizing energy consumption (Wang, Verriest, Lebreton-Gadegbeku, Tessier & Trasbot, 2000; Wang et al, 2004).

Reaching for the handbrake and grasping the handle are likely to have an influence on discomfort perception of handbrake application. It can be expected that movements and forces during the handbrake application (object manipulation) will also have an important role in the subjective perception. However, they are not sufficiently documented in published research. Influences of age, body height respectively gender are anticipated due to their effect on reach movements and reach discomfort.

Movements and biomechanical parameters can be modeled using DHMs. In the next chapter (2.7), a generic overview of DHMs is provided. RAMSIS, the software used in this thesis for posture prediction, is presented in chapter 2.8. AMS, the software applied in this thesis for biomechanical modeling, is described in chapter 2.9.

2.7 Digital Human Models

There are more than 150 Digital Human Models globally available for workplace and product design, ergonomics and safety evaluation. There is no “absolute” and universally accepted categorization. (Bubb & Fritzsche, 2009)

Marler et al. (2009) categorize in modeling the human shape, predicting posture, predicting dynamic motion, modeling clothing, modeling physiology and modeling muscles. Bubb & Fritzsche (2009) classify in anthropometric models, models for production design, biomechanical models, anatomical models and cognitive models.

Categories are overlapping. There can be cross overs which have features of several categories (Bubb & Fritzsche, 2009) and cannot clearly be assigned to one of the categories.

95 % of the industrial market of ergonomic manikins is dominated by three DHMs:

- JACK (Siemens, Munich, Germany) is applied for animation and visualization in vehicle design and factory planning.
- SAFEWORK (SAFEWORK, Montréal, Canada) is used for workplace and product design as well as factory planning.
- The main field of RAMSIS (Human Solutions, Kaiserslautern, Germany) application is vehicle design. (Bubb & Fritzsche, 2009)

2.7.1 Advantages, limitations and challenges

Competitive pressure demands new products to be developed and produced in a short time. Customers expect high levels of convenience, comfort and safety. So, the capabilities are needed to apply digital humans with defined population characteristics and to connect them with 3D graphic renderings of products respectively work / operational environments. (Zhang & Chaffin, 2005)

The deployment of DHM methods enables “easier and earlier identification of ergonomic problems, and lessens or sometimes even eliminates the need for physical mock-ups and real human subject testing” (Zhang & Chaffin, 2005, p. 1; Badler, Phillips & Webber, 1993; Zhang & Chaffin, 2000). Also, the quality of subjective evaluation studies and therefore of the product can be increased by use of DHMs.

After investing in implementation and training at the beginning of DHM deployment, the application of Digital Human Modeling, digital prototyping and virtual testing methods in ergonomic or computer-aided engineering (CAE) enables to reduce overall development

costs and to shorten process times, see Figure 2.20 and Figure 2.21. (Kiewert & Lindemann, 1998; Chaffin, 2001; Ehrlenspiel, Römer, Pache, Weißhahn, Lindemann & Hacker, 2001; Zhang & Chaffin, 2005, p. 2)

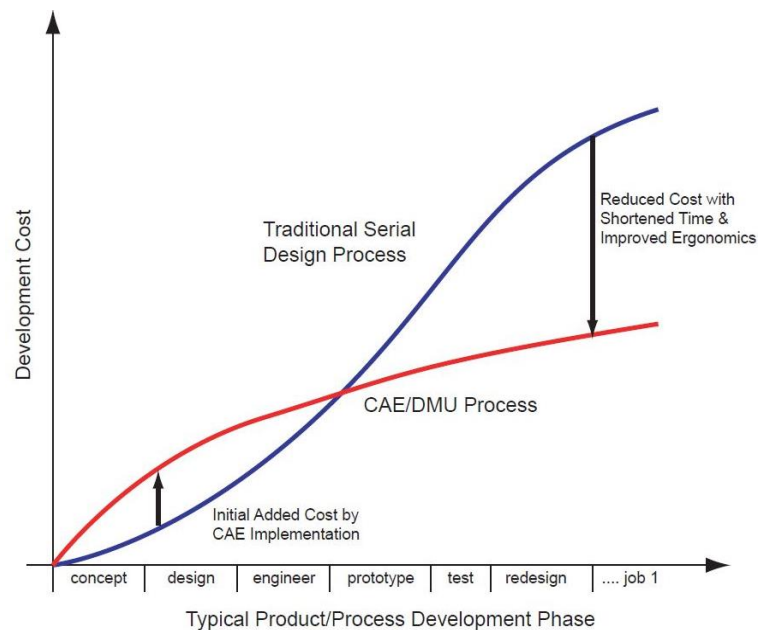


Figure 2.20: Comparison of schematic cost profiles between a traditional ergonomic design process and a CAE ergonomic design process. Extracted from Zhang & Chaffin (2005, p. 2) who adapted from Chaffin (2001).

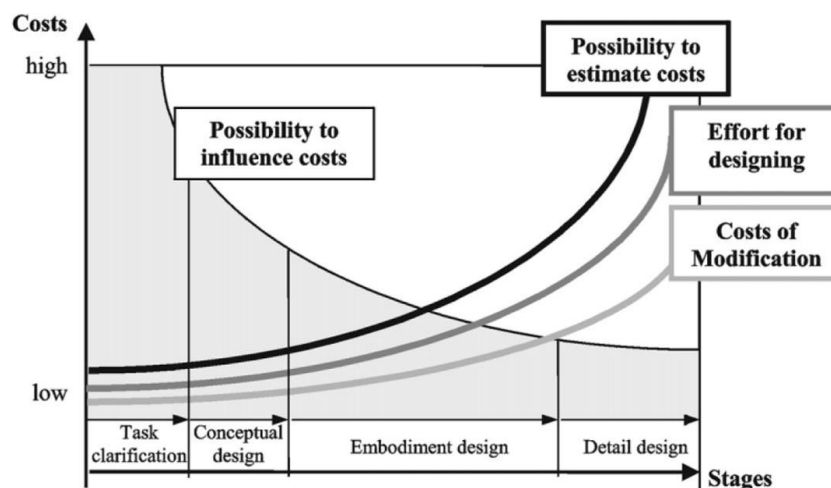


Figure 2.21: Stages and costs of the product development process. Extracted from Römer et al. (2001, p. 476), who translated from Ehrlenspiel et al. (1998).

A lot of literature has been published about functions and features of different human models and how they can be applied for ergonomic evaluation and design of products and processes (Chaffin, 2001; Duffy, 2009).

Case studies about the successful industrial application of DHMs - described in Chaffin (2001) and summarized in Zhang & Chaffin (2006) - highlight the advantages of DHMs: Simulating specific user or customer groups with their characteristics and needs,

recognize potential problems and related risks, allowing staff with limited ergonomic background to assess ergonomic problems and advocating ergonomics as such. The case studies also reveal areas for further research and enhancement. An actual problem was that users were not in position to define how a human model with defined anthropometric and demographic characteristics should be positioned in the virtual environment. Modelling and assessment of dynamic activities respectively movements is even more complicated. It is demanding to predict complex postures and movements in a timely and realistic way. (Chaffin, 2001; Zhang & Chaffin, 2005)

Another challenge is the trade-off between biomechanical realism respectively detailedness and computational efficiency (Zhang, 2001; Zhang & Chaffin, 2005). The creation of high quality experimental data is another main challenge. Motion measurements are a prerequisite for the development and verification of motion prediction models. Estimations of shape and characteristics of the neuro and musculoskeletal system are required to create the models. Data acquisition, which is “in vivo, non-invasive, and subject to minimal artifact and interference” (Zhang & Chaffin, 2005, p. 7), is difficult to conduct with current methods.

The main modeling frameworks are deterministic and do not reflect the full spread of motor variability. They successfully explain average movement characteristics but do not reflect intra- or inter person variability. Many models have numerous DOFs but were built on limited movement variations with not all DOFs activated. (Zhang & Chaffin, 2005)

Dynamic measurements of the skeletal movement and properties of the musculoskeletal systems in vivo are problematic. Considering the motor variability, modeling of repetition and time effects (such as fatigue or tissue) is still a challenge. (Zhang & Chaffin, 2005)

For more detailed descriptions of general capabilities, limitations and future opportunities of DHMs, see Chaffin (2001; 2009) or Zhang & Chaffin (2005).

2.7.2 Development history

The “theory of proportions” described by Vitruv in the first century AD was the basis of the anthropometric studies by Leonardo Da Vinci conducted in the 1480s (Bubb & Fritzsche, 2009).

Harless (1860) conducted one of the earliest detailed investigations about human body segment parameters. He weighted and measured the body parts of two adult male

cadavers. Braune & Fischer (1890) determined body and segmental mass center locations – one of the fundamental studies in research on body segment parameters.

Modern attempts to describe the human body mathematically started in the middle of the 20th century with a model of six cylinders representing arms, legs, head and torso (Kulwicksi, Schlei & Vergamini, 1962). Also Saziorski et al. (1984) suggested models for the human anthropometry. As the time progressed, the human body had become researched in an increasingly detailed way. Increasingly sophisticated mathematical and CAE models of the human and its interaction with the environment have been developed.

For a deeper insight in the history of Digital Human Models and key concepts Bubb & Fritzsche (2009) and Marler et al. (2009) are recommended.

2.7.3 Selected categories of DHMs

In this chapter, anthropometric, biomechanical and posture/motion predictions models are described. For other models (such as cognitive, physiological, clothing models) Duffy (2009) is recommended.

2.7.3.1 Anthropometric models

Visualization and scaling methods (Marler et al., 2009) are often integrated into anthropometric models. They allow representing and scaling the variability of human sizes and proportions (anthropometry). Models usually base on empirical data (e.g. serial measurements of segment length, mass, inertial properties) and mathematical modeling (Saziorski, Aruin & Selujanow, 1984). (Bubb & Fritzsche, 2009)

Anthropometric models are applied to space, clearance, reach and visibility investigations. SAFEWORK, RAMSIS and JACK have established themselves successfully as industry standards. (Bubb & Fritzsche, 2009)

2.7.3.2 Biomechanical models

The calculation of dynamic behavior of the human relies on information on geometrical and mechanical properties of the human body, which are derived by empirical data and mathematical modeling (Saziorski et al., 1984). The human can be modeled as a mechanical system, typically as a multi-body system (MBS) with rigid elements representing bones, which are connected by joints. Spring and damping elements represent muscles and ligaments. (Bubb & Fritzsche, 2009)

MBS systems utilize Newton's law of motion by applying the mechanical principles of D'Alembert or Hamilton. With the mechanic principle of D'Alembert, the "force equilibrium" of static and dynamic forces is determined. The principle of Hamilton is a general integral principle of mechanics leading to Euler-Lagrange differential equations; it is applied in the modeling softwares SIMPACK (Dassault SIMULIA, Gilching, Germany) and Alaska (Institute of Mechantronics, Chemnitz, Germany). (Bubb & Fritzsche, 2009)

There are diverse applications for biomechanical models in ergonomics, sports science and medical applications. Countless specialized models and problem solvers have been developed in addition to the commercially available MBS software packages. (Bubb & Fritzsche, 2009)

One of the commercially available MBS is AMS. It was developed to represent anatomic properties of the skeleton, muscles and tendons. Modeling and analysis are based on inverse dynamics. The musculoskeletal system is represented by a mechanism of rigid elements, which are connected by joints and actuated by Hill-type muscles. (Bubb & Fritzsche, 2009; Rasmussen, Dahlquist, Damsgaard, Zee & Christensen, 2003)

Another type of anatomic models is referred to as "Voxel" (composed of "volumetric" and "pixel") model: It has been developed in the field of medical information technology. Voxels describe type, location and size of body organs. (Bubb & Fritzsche, 2009)

The Finite Element Method (FEM) is a numerical tool. Structures are cut into elements for which the solutions of boundary value problems are approximated. FEM details are described in e.g. Reddy (2016). FEM models of the human body have been described in Pankoke (2003) and Choi et al. (2006). Both models are used in seat development, e.g. to calculate seating pressure distribution.

2.7.3.3 Posture and motion models

The challenge of modeling is closely related to solving the famous "Bernstein's Problem": how the human body handles the huge number of degrees of freedom to guide the hand or foot to a certain target. Since the 1920s, lots of efforts have been made to answer this question by experiments and model development.

In their paper about the control of redundant manipulators, Gielen, van Bolhuis & Theeuwes (1995, p. 504) state: "[...] the problem of biological and kinematic redundancy is not solved yet. Some algorithms have been proposed, which may be suitable for some particular applications, but no general solution is available now". The

authors describe and compare several approaches to overcome the issues related to the redundancy of muscles and joints; this paper is recommended for a deeper insight.

In 1998, Gielen, van Bolhuis & Vrijenoek still describe the progress in understanding the control of the large number of degrees of freedom as disappointing.

Li (2014) describes objective functions respectively criteria for redundancy resolution in detail: maintaining the equilibrium posture, maximizing motion efficiency, minimizing changes in joint angles, minimizing changes in kinetic energy, minimizing the work in joint space.

A biomechanical representation of the human body and algorithms, that configure or drive this representation, are required for human motion or posture (as a special type of motion) prediction. (Zhang & Chaffin, 2005)

A biomechanical model requires a sufficient level of detail for a realistic representation of the human body (e.g. number of degrees of freedom, movement capability) and its postures or motions. Essential reason for this is the validity of biomechanical or ergonomic analysis: "It has been shown that small errors in the posture or motion specification can lead to significant errors in joint loading and muscle force estimation" (Zhang & Chaffin, 2005, p. 1). Another reason is an appealing look of the human models. (Zhang & Chaffin, 2005)

The algorithms need to be time efficient. In addition to simulation efficiency, software usability is another important factor for industrial application of DHMs. (Zhang & Chaffin, 2005)

There are four basic computational approaches for the prediction of motion or posture:

1. **Forward (or direct) kinematics** stands for calculating joint and end-point (e.g. fingertip) location from known joint or segmental angles.
2. With **inverse kinematics**, joint or segmental angles are calculated from known joint or end-point coordinates.
3. **Forward (or direct) dynamics** is the approach of deriving body motion from muscle activity or even neural excitation.
4. **Inverse dynamics** estimates inner forces and moments (e.g. joint reaction forces) from body motions respectively postures. (Zhang & Chaffin, 2005)

The number of joint angles and thus degrees of freedom (DOF) is typically larger than the dimension of end-point locations. The number of muscle segments is also larger than the number of DOFs (which specify the movement). Thus, kinematic redundancy

(inverse dynamics) or muscle redundancy (forward, inverse dynamics) occur. (Zhang & Chaffin, 2005)

These redundancies are fundamental challenge in modeling human motion. As mentioned above, they are often referred to as the “Bernstein’s problem” (Bernstein, 1967).

Optimization is a widely used approach for solving redundancy. Functions (performance criteria, cost functions) are formed for a mathematical representation of optimal strategies. The way how the optimization problem is formulated influences the computational complexity. (Zhang & Chaffin, 2005)

Human simulation or prediction models can be divided into four classes: with and without muscles, each for static and dynamic investigations. Zhang & Chaffin (2005) provide an overview of literature with examples of these four approaches, their advantages, disadvantages and challenges. In this work a selection is presented.

Static optimization and inverse kinematics are used to solve posture definition issues.

Optimization routines can be based on the theory that humans follow an optimal strategy when they control their preferred postures. This strategy is described mathematically as an objective function, which is also referred to as performance criterion or cost function. (Zhang & Chaffin, 2000)

Cost functions can aim for a minimum deviation from a reference posture (neutral posture, optimum posture) (Ryan, 1972) or minimum joint load, discomfort or energy consumption (Park, 1973; Byun, 1991; Dysart & Woldstad, 1996;).

Cost functions typically used in posture prediction models are the biomechanical characteristics joint moment and L5/S1 pressure, the physiological characteristic energy consumption and the psychophysical characteristic joint discomfort. (Jung & Choe, 1996)

There is the hypothesis that the human body control can be modeled by making use of cost functions for each joint. It takes into account the physiological costs to maintain the joint angle(s) (see above). Those costs depend on joint angles and the force (effort) to hold this joint position. So, a posture configuration is chosen by minimizing total cost (minimum discomfort, maximum comfort). (Cruse, Wischmeyer, Brüwer, Brockfeld & Dress, 1990)

Classical approaches in the automotive field have been developed based on “experiments, statistical models and inverse kinematics” (Wirsching & Engstler, 2012, p. 2232; Reed, Manary, Flannagan & Schneider, 2002).

For example, RAMSIS is a DHM which was developed for vehicle design. Various anthropometric databases and functions enable to model a wide range of potential occupants. The posture prediction approach is based on most probable postures derived from experiments (Geuß et al., 1995). Ausejo & Wang (2009) focus on motion capture and human motion reconstruction. Monnier et al. (2009) provide a review of several motion simulation approaches.

The classical automotive approaches show sufficient validity when applied for tasks similar to the experiments they are based upon. However, they have deficiencies for other tasks (Kolling, 1997; Wirsching & Engstler, 2012). Forces, stability and discomfort aspects are important, but often not considered (Wirsching & Engstler, 2012).

There are different approaches for the simulation and calculation of strength, which can also influence postures and movements (Li & Zhang, 2007). One of the approaches is to model the musculoskeletal system in high detail, which is done in AMS. (Damsgaard et al., 2006; Bubb & Fritzsche, 2009)

AMS, a dynamic model with musculature, has been applied and validated for human movement prediction during squat vertical jumping and cycling. Summation of squared muscle activity and summation of muscle metabolic energy expenditure have been applied as cost functions (Farahani, 2014).

Another approach is based on the experimental investigation of the active maximum and passive receding joint moment data for a wide range of postures (Bubb & Fritzsche, 2009). The actual maximum moment, which can be applied in a posture, is described by a 3D volume for each joint (Schwarz, 1997; Schaefer, Rudolph & Schwarz, 2000). Here, the posture prediction is based on the assumption that humans try to minimize the joint load when adopting their postures. The approach is referred to as “Force-Controlled-Posture-Prediction-Model” (FOCOPP). It was aimed for implementation in RAMSIS to calculate postures and discomfort ratings (Seitz, Recluta, Zimmermann & Wirsching, 2005). Seitz et al. (2005) describe this approach in detail.

The initial results were promising although there were some deficiencies and no detailed validation. Wirsching & Engstler (2012) enhanced the model with more realistic boundary conditions by implementing force coupling restrictions between environment and manikin. The validation (closing a car door and lifting a box) showed plausible

posture prediction but partly there were still too large deviations between reality and prediction. The authors trace the deviations back to the generality of the method. Task specific models may provide smaller deviations but are only suitable for the specific applications.

2.7.3.3.1 Modeling reach

No study has been found about modeling handbrake application movements or model validation. However, part of the handbrake application is the reach to the handbrake handle. Modeling seated reach has been in focus of several publications (such as Jung, Choe & Kim, 1994; Jung & Choe, 1996; Wang & Verriest, 1998; Chaffin et al., 1999b; Zhang & Chaffin, 2000; Reed et al., 2004).

Wang & Verriest (1998), Chaffin et al. (1999) as well as Zhang & Chaffin (2000) provide overviews how to overcome redundancy of muscles and joints for seated reach. In a more recent publication, Gielen (2009) quantitatively compared the prediction of various models for the generation of multi joint movements in 3D with experiments. He found no good model to accurately explain the characteristics of complex 3D movement trajectories (Gielen, 2009).

Reed et al. (2004) stress the absence of standardized methods to model seated reach in vehicles. They list the approaches researchers have proposed to predict final reach postures or reach motions:

- Regression equations (Ryan, 1972; Snyder et al., 1972),
functional regression on stretch pivot parameters (Faraway & Julian J., 2003).
- Optimization based inverse kinematics (Wang & Verriest, 1998).
- Analytical inverse kinematics (Jung & Choe, 1996),
optimization based differential inverse kinematics (Zhang & Chaffin, 2000).

Many human models used for ergonomic investigations predict reach postures based on inverse kinematics. Reach motion is derived from interpolation between starting and ending postures. Heuristic and optimization based approaches are used to handle the kinematic redundancy. Reed et al. (2004) found that inverse-kinematic methods based on interpolation tend to generate artificial movement patterns since the interpolation approaches are not derived from human motion data. (Reed et al., 2004)

In e.g. Zhang & Chaffin (2000), the posture prediction relies on human motion data bases. The prediction can still deviate from natural movements respectively postures

since those data bases are limited to the investigated scenarios (including geometrical layout and subject group).

Cost functions (see above) show that a wide range of arm postures can lead to equal total costs, even if the cost functions consider physiological costs such as joint angles and loads. It was observed that the posture at the end of a movement also depends on the posture at the beginning. (Cruse et al., 1990)

The posture prediction model by Jung & Choe (1996) is based on psychophysical discomfort function and considers posture and load. It was developed from an experiment with four healthy male students.

Zhang & Chaffin (2009) developed and validated posture prediction models for simulating in-vehicle seated reach based on motion capturing of ten subjects and optimization based on differential inverse kinematics. The prediction shows mean joint angle errors of 5.2° after exclusion of extreme reaches. (Zhang & Chaffin, 2000)

Reed et al. (2004) state that no model has achieved wide acceptance. They trace this back to several reasons. One of them is that the models, especially the commercially ones, have not been independently validated. Jung & Choe (1996) emphasize that many reach models provide possible postures but lack precision and realism.

Wang & Verriest (1998) developed a geometric algorithm to predict arm reach postures. When discussing the results of their results, they explain: "Simulating human postures is a very difficult and complex problem owing to the redundancy of the human musculoskeletal system" (Wang & Verriest, 1998, p. 41).

In the discussion they stress: "Owing to the limited knowledge of human movement control strategies, the aim of the inverse kinematic algorithm is not to predict the exact postures but to provide a postural manipulation tool for the users of human models" (Wang & Verriest, 1998, p. 43). This is also the aim for the handbrake posture prediction model presented in this thesis (see chapter 7).

2.7.3.4 Models providing discomfort prediction

It is widely recognized that discomfort models for ergonomic workload analysis should encompass the three factors described in a model by Loring et al. (2002): posture, force and time. (Wang, 2009)

A lot has been published on the assessment of postural stressfulness (Kee & Karwowski, 2001b; Wang, 2009).

Several methods have been implemented into DHMs such as RULA (Rapid Upper Limb Assessment, McAtamney & Corlett, 1993) or OWAS (Ovako Working Posture Analysis System, Karhu, Kansu & Kuorinka, 1977). The methods were mainly created for analysis of working postures and the evaluation criteria were based on expert opinions.

More recent studies have involved recording and analysis of subjective perception of discomfort for postures (Kee & Karwowski, 2001a).

Wang (2009, p. 25-3) underlines that “Up to now, most discomfort models are specific and their range of application is limited to experimental conditions”. He differentiates between models based on design parameters and models based on biomechanical parameters.

In models based on design parameters, discomfort ratings are related with design parameters of a product. The advantage of these models is that they can directly be used to assess or to optimize the design of a product. They are independent of modeling humans and their motions. Their disadvantage is that effects of design parameters, which were not captured by the experiment, stay unconsidered. (Wang, 2009)

Biomechanical discomfort models can be based on various parameters such as joint angles, joint load or muscle load. So, biomechanical parameter based models enable to understand contributors to discomfort. They can help to explain perceived discomfort when subjects perform a particular task or use a specific product. (Wang, 2009)

The following subchapters (2.7.3.4.1 and 2.7.3.4.2) provide some examples.

2.7.3.4.1 Task specific discomfort models

The discomfort model for seated arm reaching posture by Jung & Choe (1996), see above, is based on joint angles and load. The model explains 79 % of the variation in the discomfort ratings ($r^2 = 0.79$) and is statistically highly significant ($p < 0.001$). However, there is some multi-collinearity between the factors.

Dickerson et al. (2006) studied the relation between shoulder moment and perception of muscular effort in loaded reaches. They found linear correlations ($r = 0.67 - 0.88$) between individual subject moment profiles and perceived efforts. Overall, the effort perception correlated significantly ($p < 0.05$) and moderately ($r = 0.71$) to the shoulder moment loading.

Wang et al. (2004) and Pannetier & Wang (2014) aimed to identify biomechanical criteria which influence discomfort perception of clutch application. In the investigation

from 2004, it was shown that the work of knee and hip joints for clutch depression had higher relevance for the comfort assessment than the joint moments at the end of clutch depression. This indicates that the discomfort rating for clutch depression may be a result of the perception of the whole process – and not of only a single state of it.

The joint work was calculated as the integral of joint moment over joint angle and has covered both factors over time – so, it contains a high information value. The subjects themselves were a large source of variation regarding comfort ratings and their reproducibility was low. (Wang et al., 2004)

Romain & Xuguang (2012) proposed ankle and knee joint angles as discomfort factors for clutch application. They observed that less constrained movement lead to lower discomfort. Pannetier & Wang (2014) found significant correlation between discomfort ratings and knee and ankle moments at the end of depression.

The examples above refer to models which are very specific to a defined task. So, they cannot be applied them for general discomfort prediction for arbitrary tasks. (Wang, 2009)

2.7.3.4.2 More generic approaches of discomfort models

Several documents have been published on more general approaches of discomfort modeling.

In the European research project REAL MAN (Lestrelin & Trasbot, 2005) an approach for discomfort prediction for the whole body was proposed. It includes discomfort prediction for the joints based on their joint angles (relative to the maximum range of motion) and joint moments (relative to its maximum moments). The approach is based on the assumption that joint angles and joint moments influence the discomfort independently. (Wang, 2009)

Zacher & Bubb (2004) have performed experiments to validate these assumptions and to determine discomfort functions based on joint angles and moments. They found that the discomfort perception correlates to joint angle and moment level. The discomfort perception is also influenced by the moment direction. The correlations are joint specific. Zacher & Bubb (2004) demonstrated that the evaluation of discomfort for a task depends on the maximal discomfort perceived in one region (e.g. joint or segment) of the body. So, discomfort functions are required for each direction of each degree of freedom for every joint. (Zacher & Bubb, 2004)

To determine the static and dynamic discomfort functions for a wide range of postures and motions, a discomfort database for all the different joint angles and moments had to be established. The results of the REAL MAN project are summarized by Lestrelin & Trasbot (2005). One remaining issue is the „Difficulty to validate the discomfort criteria, because of the big variability of the subjective assessment of discomfort” (Lestrelin & Trasbot, 2005, p. 9).

Kee & Karwowski (2001, 2003) proposed joint angle iso-comfort functions as ranking method for joint motion discomfort assessments. Chung et al. (2005) described a similar method for the whole body postural stress prediction based on the postural classification of body parts.

Dufour & Wang (2005) suggested the concept of neutral movement to establish joint discomfort functions. They applied it for the car ingress/egress motion. This concept extends the concept of neutral (or least discomfort) postures to posture discomfort assessments. A person’s neutral movement is that one generating the least discomfort. (Dufour & Wang, 2005)

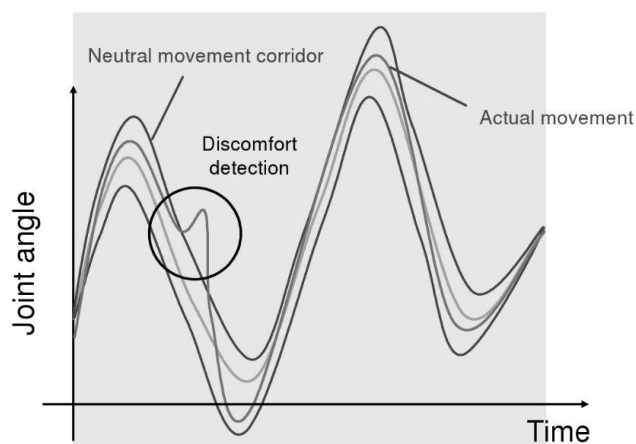


Figure 2.22: Neutral movement concept. Extracted from Wang (2009, p. 25-5).

The approach is to determine a “corridor” for each joint angle to reflect intra and inter individual variations of the neutral movements, see Figure 2.22. Deviations from the neutral movement corridor may indicate discomfort perception. (Wang, 2009)

Monnier et al. (2006) implemented the motion simulation and evaluation tool “RPx”, which is based on the neutral movement concept. It was analyzed for light truck ingress/egress movements and seated lateral reaching (Monnier, Renard, Chameroy, Wang & Trasbot, 2006; Monnier, Wang & Trasbot, 2009).

The concept of neutral movement can be a helpful CAE tool for the design of products. However, the definition of the neutral movement effects the discomfort evaluation strongly. The concept does not explain why certain movements are preferred. The expansion of the concepts to the prediction of discomfort based on joint angles and loads requires the acquisition of large amount of data: joint angles, joint moments (depending on joint angles, external forces and their direction) and discomfort perception. (Wang, 2009)

The FOCOPP approach presented in 2.7.3.3 also encompasses discomfort prediction functionality. There are still deficiencies in the posture prediction (Seitz et al., 2005; Wirsching & Engstler, 2012), so the tool is currently not commercially available.

Li (2009) provides an overview of major commercially available DHM packages (excluding research project and military packages).

Wang (2009 p. 25-6) concludes his chapter on discomfort evaluation and motion measurement: "Until now, discomfort, induced by internal biomechanical constraints that affect the human musculoskeletal system, has not adequately been taken into account in Digital Human Modeling. We believe that discomfort modeling requires a detailed muscular activities simulation."

Very recent research focusses on the combination of DHMs, including DHMs with muscular activation simulation.

2.7.3.5 Combination of DHMs for discomfort prediction

When people perceive and rate discomfort, e.g. as passengers in vehicle, they do not focus on single factors. They simultaneously sense various discomfort aspects (related to joint angles, joint loads, muscle activities, pressure distributions at interfaces) which lead to an overall discomfort perception (Ulherr & Bengler, 2014). They might not be able to distinguish the discomfort facets.

"The feeling of discomfort is rather a combination of relevant parameters than a sum" (Ulherr & Bengler, 2014, p. 3). This is in agreement with Jung & Choe (1996) who developed a discomfort predicting equation based on joint angles and load as parameters. It is also in line with the findings by Zacher and Bubb (2004).

The type of parameters influencing discomfort and their effect on the discomfort perception might differ depending on the task. For instance, discomfort perception has been correlated to posture (Geuß et al., 1995; Jung & Choe, 1996; Kee & Lee, 2012) and muscular load (Jung & Choe, 1996) respectively joint load (Dickerson, Martin &

Chaffin, 2006; Pannetier & Wang, 2014). Furthermore, interface pressure respectively force distribution has been shown to influence seat comfort perception (de Looze et al., 2003; Mergl et al., 2005; Mergl, 2006).

Several DHMs are available for the prediction of individual factors. Commercially available and in automotive industry widely used tools are for example:

- RAMSIS for posture prediction (results are e.g. joint angles and locations).
- AMS for simulation of muscle and joint loads.
- CASIMIR for the mechanical analysis of the occupied seat (e.g. the prediction of the pressure distribution at the contact area between seat and human). (Ulherr & Bengler, 2014)

Holistic ergonomics assessments require the combination of specialized tools (Bonin et al., 2014). Using the output parameters of one tool (e.g. posture) as input for another tool (e.g. for biomechanical analysis or FEM analysis) and vice versa may mutually increase the quality of prediction. (Bonin et al., 2014)

Some approaches have been documented on the combination of DHMs (Bonin et al., 2014; Siefert & Nuber, 2014; Ulherr & Bengler, 2014).

Two examples shall be described: The project UDASim aims to combine RAMSIS, AMS and CASIMIR for a global discomfort assessment. UDASim is the acronym of the German “Umfassende Diskomfortbewertung für Autoinsassen durch Simulation” (English: “Global discomfort assessment for vehicle passengers by simulation”). The project started 2013 and is funded by the German Ministry of Education and Research. See Figure 2.23 for the project sketch and Figure 2.24 for a more detailed description. (Ulherr & Bengler, 2014)

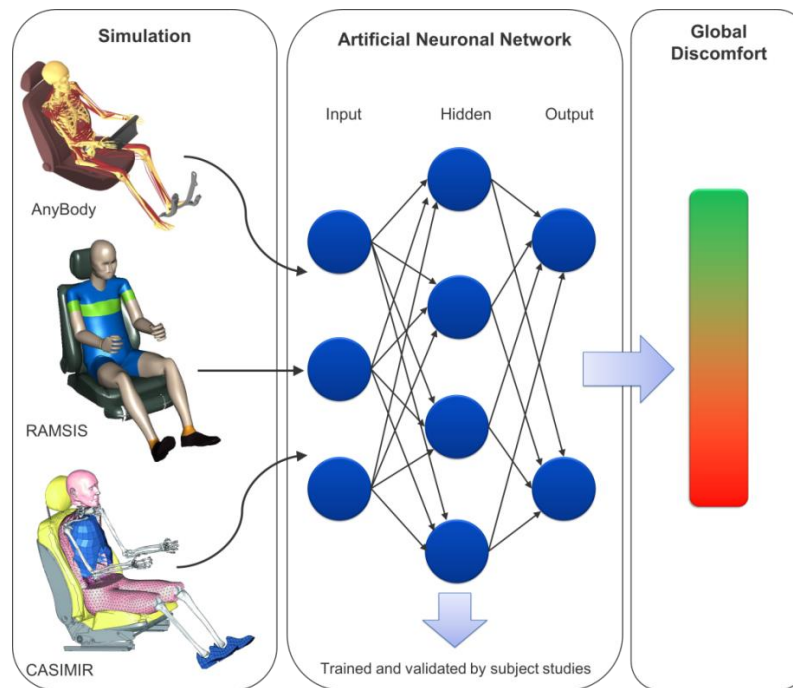


Figure 2.23: Intended procedure of the UDASim project. Extracted from (Ulherr & Bengler, 2014, p. 3).

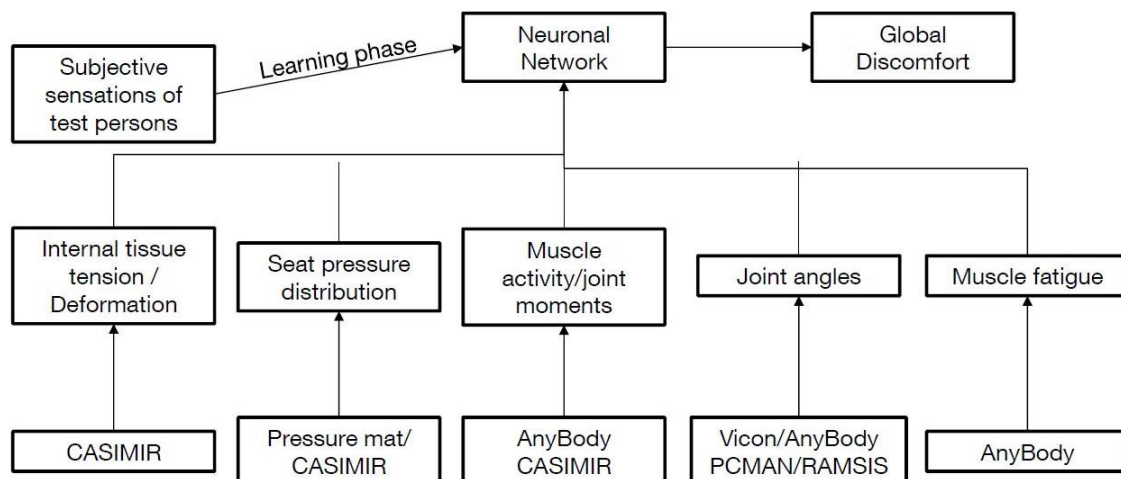


Figure 2.24: The UDASim global discomfort assessment. Extracted from the conference presentation (Ulherr & Bengler, 2014, p.11).

Another example is the combination of AMS and JACK (Paul & Lee, 2011; Bonin et al., 2014). JACK provides the outer body dimensions and can be used for posture simulation. AMS offers the capability of detailed biomechanical analysis.

A different approach was chosen by the ESI Group: “[...] ESI’s Virtual Seat Solution [...] integrates a finite element (FE) and a muscle balance solvers” (Borot, Cabane & Marca, 2014, p. 3). This allows modeling e.g. the influence of the seat on the leg motion when depressing a pedal. The muscle activity and its effects on the mechanical and geometrical properties of the body are considered for the calculation of e.g. H-Point or

pressure distribution at the contact interface between human and seat. (Borot et al., 2014)

Data exchange and compatibility between DHMs is a prerequisite for combining DHMs. Research has been completed on data exchange possibilities between different DHMs and/or motion capturing systems (Barre & Armand, 2014; Bonin et al., 2014). Only individual and customized solutions could be found in literature (Rim, Moon, Kim & Noh, 2008; Paul & Lee, 2011; Jung, Damsgaard, Andersen & Rasmussen, 2013). No commercially available data exchange tool could be identified for major DHMs used in industry.

Combining DHMs is promising to enhance the prediction quality for discomfort by considering a wide range of contributing factors.

It is also an opportunity for product / car manufacturers: Currently different product design aspects are addressed by the application of several tools by different departments, especially when it comes to seat comfort. The knowledge is spread and interdepending aspects of discomfort are assessed independently. Combining DHMs can increase efficiency and communication between different departments. Redundant work might be avoided and a more holistic assessment can be accomplished resulting in a higher product quality. (Siefert & Nuber, 2014)

2.7.4 Conclusions

Human posture/motion prediction models typically do not reflect the richness of motor variability (intra- or inter person), but successfully explain average posture/movement characteristics for specific applications (Zhang & Chaffin, 2005).

On the one hand it is a disadvantage, that studies on movements and discomfort perception are designed for a specific purpose (such as prediction of standing or seated reach movements, ingress / egress movements for the 2nd row of a passenger car or movements during handbrake application) with a specific experimental set up. When extrapolating beyond the boundary conditions established and validated by experimental data, it is difficult to estimate accuracy of the models.

On the other hand, generating a single model for several applications (e.g. press push button, apply gear shifter, pull handbrake) bears the risk that predictions for each of the applications become less accurate. Not even models created for a special purpose will cover all possible variations of the task and customer. In the foundation studies typically

only the influence of most relevant factors is investigated. Studying every potential set up is too time-consuming and expensive.

E.g. in case of the handbrake application, a research set up considering the variety of influencing factors would need to study effects of:

- Handbrake location and lever arm (force application point and pivot point), handle angle, pull angle, force level.
- Type of vehicle (high seater vs. low seater), seat location etc.
- Subject populations differing in anthropometry, age, capabilities etc.

Thorough research of all these factors would be very resource consuming. So, a study design shall be established focusing on the investigation of most relevant factors only. The resulting models for handbrake application movement and discomfort shall represent the average characteristics of typical vehicle drivers and so cover the major customer group. It won't be possible and is not efficient nor economically reasonable to model all drivers with their special needs.

The combination of different Digital Human Models allows considering a wider range of factors influencing discomfort perception and may enhance the prediction accuracy.

2.8 RAMSIS

RAMSIS is used in this work for posture prediction. RAMSIS is the acronym for "Rechnergestütztes Anthropometrisches Mathematisches System zur Insassensimulation" which translates to "computer-aided anthropometric mathematical system for occupant simulation".

RAMSIS development was initiated by the German Forschungsverein für Automobiltechnik (FAT) in the 1980s. It was developed by the Human Solutions GmbH (former Tecmath) who implemented the software based on research conducted by the Technical University of Munich. An Industry Advisory Panel (IAP), consisting of seven vehicle manufacturers and two seat suppliers, consulted the project. Since then, RAMSIS has become the main comprehensive system for occupant packaging and ergonomics. Compared to traditional ergonomic assessments (such as subjective evaluation clinics), the application of RAMSIS can save time and costs as well as increase accuracy. (Seidl, 1995; Van der Meulen & Seidl, 2007)

RAMSIS is applied by more than 75 % of global car manufacturers (Bubb & Fritzsche, 2009).

RAMSIS offers a multitude of functions which are of value for product and production design within different industries such as automotive, aircraft and fashion. Accurate representation of the human body, posture prediction, discomfort analysis, analysis of reach, required space and field of view were functions available from the beginning of RAMSIS development. Over the years, a variety of further functionalities has been added such as integrated SAE standards, analysis of forces, calculation of belt routing, manikin scaling based on body scans, cognitive analysis, analysis of occupant and seat interaction, simulation of ingress/egress. (van der Meulen & Seidl, 2007; Wirsching, 2013; Human Solutions GmbH, 2015;)

2.8.1 Internal and external model

The base for the geometric-kinematic human model of RAMSIS is the human anatomy. RAMSIS contains an internal model for motion simulation and an external model for body contour modeling (Figure 2.25).

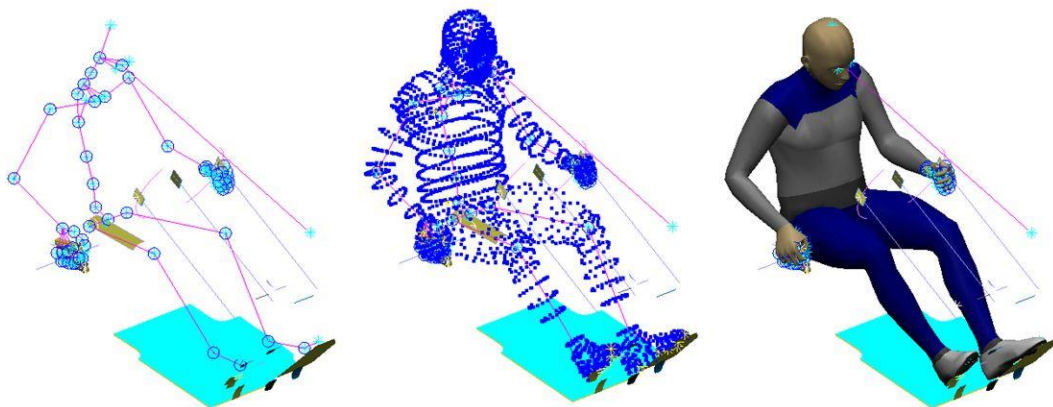


Figure 2.25: Left: inner model (blue circles, purple lines). Middle: inner and outer model. Right: Shaded representation. (RAMSIS NextGen screenshots in V.1.1.001, March, 03, 2015).

The internal model is a simplified skeleton, represented by joints and connecting “sticks”. It is the basis of the kinematic model and therefore for the posture prediction. The centers of rotation between the body segments are simplified models of the human joints. The internal model is a compromise between two conflicting objectives: the “implementation of all essential postural and kinematic characteristics into the model” and “the restriction of the number of joints and their degrees of freedom to a minimum in order to ensure good model performance with regard to the rapid calculation of movements of the man model” (Seidl, p. 4). The human spine consists of 24 vertebral bodies. In RAMSIS, the spine consists of 6 vertebral bodies which still provide flexibility comparable to the human spine. (Geuß, 1995; Seidl, 1995; Seidl, 1997; Seitz, 2003)

The outer model represents the body surface (blue dots in Figure 2.25, middle). The skin is used for the interaction of the manikin and the geometrical environment and defines characteristics of the segments such as mass. It is not modeled with rigid, geometrically simple objects, but by a huge network of anchor points which are connected with the internal model; thus it is posture depending: A surface generator calculates the surface (“skin”) based on anchor points. The connection varies depending on the joint positions. The generator can be modified to enable the required level of refinement. (Geuß, 1995; Seidl, 1997)

Detailed descriptions of the internal and external model and how they were derived are described in Geuß (1995).

2.8.2 RAMSIS platforms

RAMSIS is available as a Windows stand-alone application and integrated in CATIA or Autodesk CAD software. It can also be integrated in virtual reality systems for real time simulation of a product. RAMSIS data can be imported and exported via several data formats (including IGES, SAT, AVI, VDA and JT). (Human Solutions GmbH, 2015)

For this work, RAMSIS NEXTGen V 1.1.001 was applied.

RAMSIS NextGen was launched by Human Solutions in April 2014 and offers multiple advantages and new functionalities for the user:

- Several manikins can be simulated and viewed at once, if required even with different anthropometries and tasks.
- Enhanced body shapes and additional visualization options provide a more realistic representation of the human.
- Previous investigations can be reused and modified.
- The user interface is more user-friendly.
- A modular composition (“plug-in structure”) helps to adjust the software to the users’ needs and work environment.

All in all, RAMSIS NextGen offers increased flexibility, efficiency and a better representation of the regions, a product (e.g. a car) is aimed at. (Human Solutions GmbH, 2014c; Human Solutions GmbH, 2014d; Human Solutions GmbH, 2015)

2.8.3 RAMSIS NextGen plug-ins

This subchapter lists and describes the plug-ins applied in this work:

- The basic plug-in is the Framework consisting of work environment, geometry and general functions.
- The BodyBuilder plug-in offers possibilities to generate individual manikins and systematic test samples of manikins with different anthropometries.
- The Ergonomics plug-in encompasses the functions needed to establish test groups with individual roles to run “collective” posture calculation and analysis.
- The Project Manager allows for file pre-selection for a quick application to manikins, calculation of succeeding tasks and quick changes between geometries. (Human Solutions GmbH, 2014c)

Further plug-ins are available for the application of standards and to enable import and export of external file formats. (Human Solutions GmbH, 2014c)

For each plug-in, Human Solutions provides detailed manuals which assist application of the software and provide background information. On the following pages, most relevant functions and information are summarized. For more detailed description, refer to the manuals cited above.

2.8.3.1 The BodyBuilder plug-in

The BodyBuilder plug-in enables generation of body dimensions based on large population databases (e.g. Germany, Italy, Sweden, North America, South America, India, Japan). The user can choose the gender, age group (e.g. 18-70 or 56-70) and reference year, see Figure 2.26. The reference year is important due the acceleration of body height, which is growing from generation to generation. The mathematical model of the average growth of a population within a given time period is based on anthropometric data of 40 past years and the application of extrapolation techniques (Seidl, 1997).

The key dimensions (body height, sitting height and waist circumference) can be adjusted using values (percentile or mm) or using predefined types:

- Body height: very short, short, medium, tall, very tall.
- Torso sitting height: short, medium, long.
- Waist circumferences: slim, medium, large.

The key dimensions are almost not interdependent and statically characterize the different anthropometries (Wirsching & Premkumar, 2007). In addition, 23 dependent measurements (such as length, width, depth, circumference of the body segments) are automatically calculated. All dimensions can be modified manually. It is also possible to import dimensional data from scanned or measured individuals (Hamfeld, Hansen, Trieb & Seidl, 1999; Van der Meulen, Peter & Seidl, 2007; Human Solutions GmbH, 2014a).

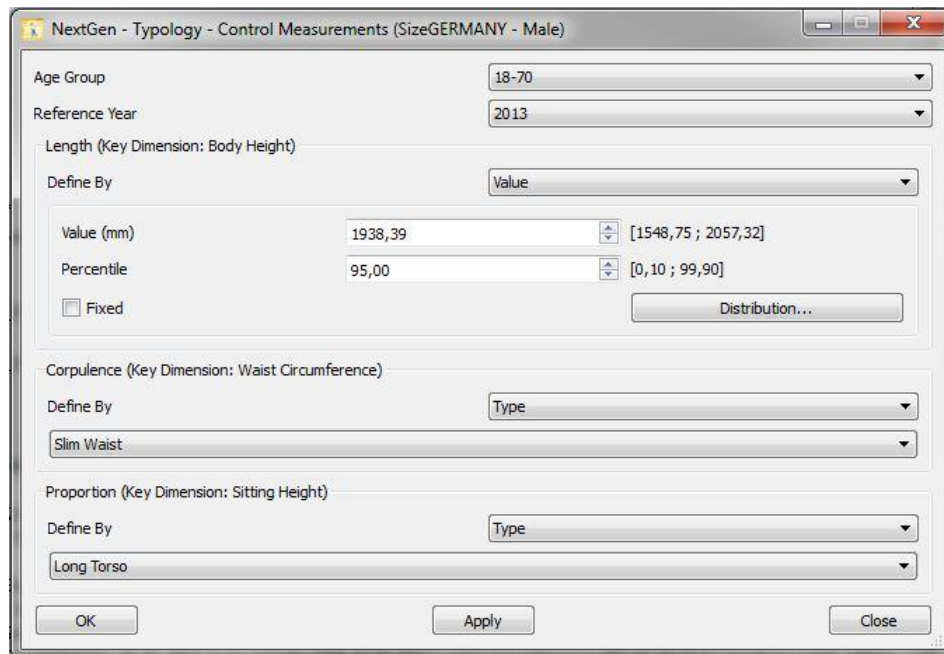


Figure 2.26: Control measurements used for scaling of manikins in RAMSIS (screenshot in NEXTGen, V.1.1.001, March, 10, 2015).

Wirsching & Premkumar (2007) describe the multi-dimensional mathematical function of RAMSIS which generates optimized test samples for specific design and population requirements.

2.8.3.2 The Ergonomics plug-in and posture calculation

The ergonomics plug-in provides role definition and posture calculation. Roles can be defined for the manikins as shown in Figure 2.27.

They enable to choose between different settings for range of motion, H-Point, corpulence adjustment, posture model, prepositioning posture and prepositioning point. (Human Solutions GmbH, 2014b)

The prepositioning posture represents the optimal angles of the posture model (“neutral posture”). Prepositioning is required for a plausible posture calculation due to the underlying calculation routine.

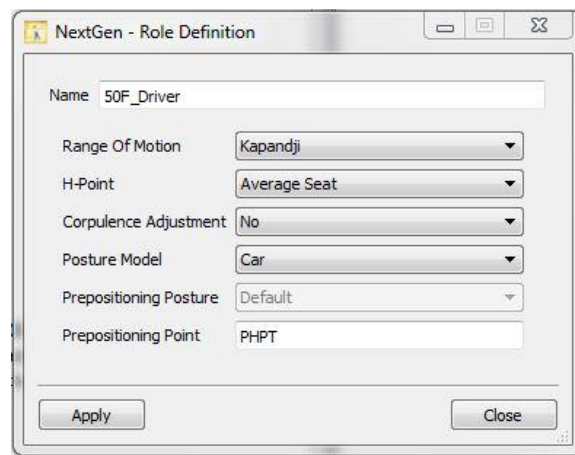


Figure 2.27: Example of role definition menu (screenshot in V.1.1.001, March, 10, 2015).

Figure 2.28 shows examples of available posture models. Each model is licensed individually. It is also possible to create dedicated “User Defined Posture Models” (see 2.8.4.1). (Human Solutions GmbH, 2014b)

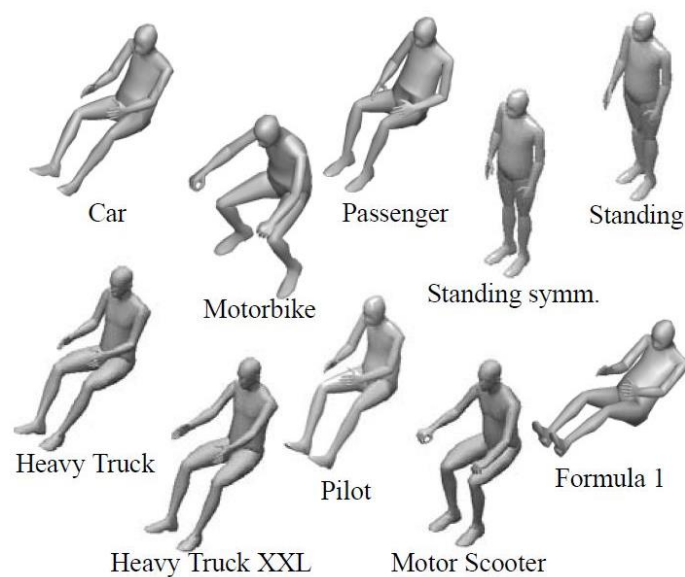


Figure 2.28: Examples of posture models available in RAMSIS (Human Solutions GmbH, 2014b, p. E/P26).

RAMSIS simulation starts with defining the parameters of the manikin or test sample and loading the geometry. The relationship between the manikin, surrounding geometric components and postural details can be defined using twelve types of constraints. Selectable points or skin segments of the manikin (e.g. skin point, joint points, eye-points, shoe sole) can be connected or restricted to geometric elements of the vehicle.

All (active) constraints applied to a manikin or test sample represent a task. E.g. the task of driving can be defined by placing the hands on the steering wheel, the right foot

on the slightly depressed accelerator pedal, the left foot on the carpet and the H-Point in seat adjustment field (Geuss, 1998).

In the software itself, the word “restrictions” is used instead of “constraints”, see Figure 2.29.

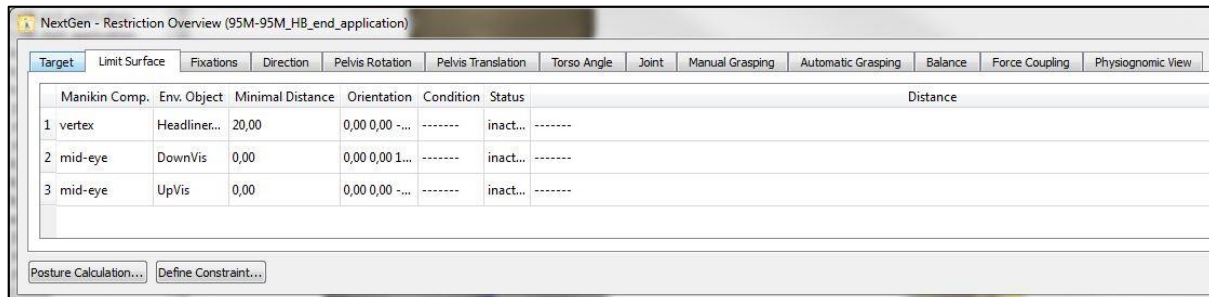


Figure 2.29: Exemplary screenshot of restriction types in RAMSIS (screenshot in V.1.1.001, March, 10, 2015).

For detailed description of all types of constraints, see the manual (Human Solutions GmbH, 2014b).

For reference, the constraints “target” and “limit surface” will be explained: “Target” defines contact conditions between the manikin “and objects of the geometric environment, optionally with tangency condition”. “Limit surface” separates “allowable and forbidden regions of the environment for body points, skin surfaces or body elements”. (Human Solutions GmbH, 2014b, p. E63)

There are two types of posture prediction implemented in RAMSIS, the probability controlled posture prediction model (PROCOPP) and the force controlled posture prediction model (FOCOPP).

For the PROCOPP model, multi-dimensional probability distributions of joint angles were derived from experiments. Based on them, RAMSIS predicts the most probable posture (Seidl, 1995; Bulle, Dominioni, Wang & Compigne, 2013). The Car Driver Posture Model is a PROCOPP model. Several validation studies have shown a valuable prediction quality (see 2.8.4) and Ford has successfully applied this model for many years in combination with a large number of anthropometric databases available in RAMSIS.

The FOCOPP model (see 2.7.3.3) incorporates geometrical constraints and external forces. It is based on minimizing the joint strain and discomfort. Validation studies of the FOCOPP model have shown deviations between prediction and reality and thus the need for further development (Seitz et al., 2005; Wirsching & Engstler, 2012). Therefore it was decided to base this work on the Car Driver Model, which is a PROCOPP model.

2.8.4 The Car Driver Model (CDM)

2.8.4.1 Posture prediction

In this study, the Car Driver Model is applied to predict the driver posture. As a preview of chapter 7: The prediction of handbrake application postures was achieved with a user defined model, developed from the Car Driver Model and analysis of motion capturing data (Raiber, 2015). Therefore, it is important to understand the function and background data of the Car Driver Model.

The car driver posture prediction model is based on experimental observations from several laboratory studies by Seidl (1995). Altogether 99 subjects took part in four studies conducted on two test rigs. Static postures related to driving, viewing (looking in different directions), reaching to controls (e.g. pedals, buttons) and corresponding H-Points were investigated. 615 body postures were captured and analyzed using a photographic analysis system. The driving postures were recorded in package configurations representing a sport car, a sedan and a minivan.

From the experimental postures, multidimensional probability distributions of joint angles were calculated. Based on them, the most probable posture can be calculated for a given set of geometrical constraints (Seidl, 1995; Bulle et al., 2013). In the following sections this is explained in more details.

The joint angles were analyzed from the captured body postures. The distribution curve is very tight and sharp for some joint angles. This indicates that different subjects adopted mostly the same angle basically independent from the task. This was observed e.g. for the hip joint angles. For other joint angles, the subjects showed variations of the angles depending on the task. The distribution curve was wide and flat. They did not prefer a certain angle and wide ranges of angles were perceived comfortable.

Consequently, different joint angles receive different weightings in the calculation routine. Joint angles with a narrow and high probability function get higher priority and will deviate less from the peak value than those with a wide and flat probability function.

It was observed that for different tasks the distributions of joint angles were shaped differently but did have similar mean values. For this reason, the Car Driver Posture Model is based on the combined data of the four experiments. (Bubb, 2013; Seidl, 1995)

The measurement results were transformed in continuously differentiable equations so that probability “pots” are generated for each joint, which is illustrated in Figure 2.30. By application of an optimization process the software searches for the lowest point with

the multi-dimensional mountains of angle probabilities. In this routine each joint angle is optimized. In this way, the system calculates the most probable posture a person would adopt within physiological limits of motion for the given task, represented by a set of constraints. (Seidl, 1995; Bubb, 2013)

Using the neutral posture (all joint angles of the manikin equal to the optimal angle of the posture model) for prepositioning the manikin at the start of the posture calculation is an “indispensable precondition for the calculation of plausible postures” (Human Solutions GmbH, 2014b, p. E/P27) and helps to decrease calculation time.

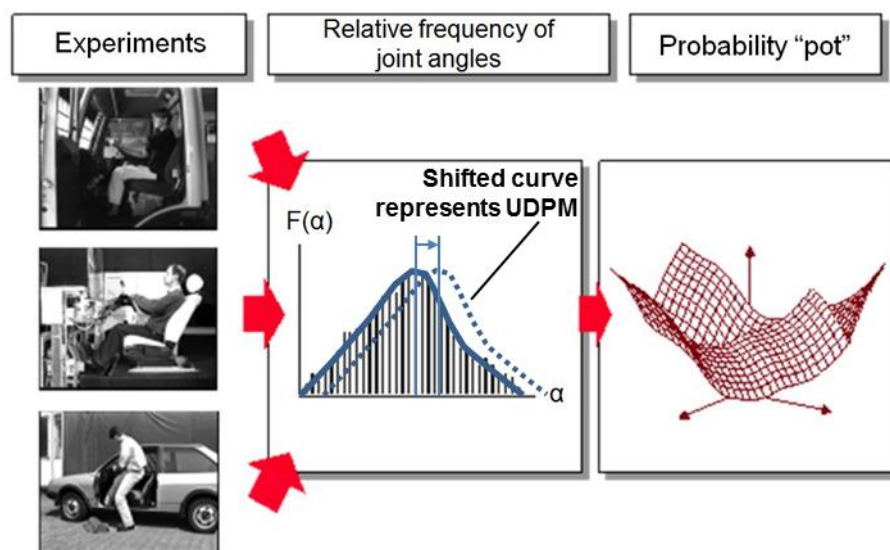


Figure 2.30: Procedure to define the probability “pot” of joints (example shoulder joint).
 Modified from Bubb (2013, p. 14).

2.8.4.1.1 User Defined Posture Models

User Defined Postures Models (UDPMs) can be derived from an existing posture model by modification of the “optimal” angles as illustrated in Figure 2.30.

However, the probability distribution (curve shape) of the angles cannot be modified. For this reason it is important to choose an appropriate base posture model. (Human Solutions GmbH, 2014b)

2.8.4.1.2 Validation of posture prediction

The Car Driver Posture Model has been validated extensively for driving postures (Kolling, 1997; Alexander & Conradi, 2001; Loczi, Dietz & Nielson; Park, Jung, Chang, Kwon & You, 2011; Bulle et al., 2013). In general, the RAMSIS predictions are close to experimental observations. Especially the mean differences between predicted points (such as eye point or SGRP) and observed coordinates are small.

Differences for singles subjects and vehicle configurations can be larger. There are several reasons including intra-individual variability in driving postures due to e.g. personal preferences and habits as well as experiences (e.g. the habituation to the primary vehicle people are driving). Bulle et al. (2013, p.5) propose to introduce “different sets of constraints and/or different posture models [...] according to stature group and vehicle”.

A lot has been published on the application of RAMSIS for the prediction of the driving posture. However, no useful information could be found on joint angles for handbrake application, on their prediction with RAMSIS or on corresponding validation studies. (Raiber, 2015)

In Ford-internal studies it was found that the postures of handbrake application created with the standard Car Driver Model did not predict reliable and realistic postures. Therefore, a User Defined Posture Model for handbrake application was developed based on the Car Driver Posture Model. (Raiber, 2015)

2.8.4.2 Discomfort prediction

During the posture investigations, conducted to develop the Car Driver Posture Model (Seidl, 1995), the subjects' comfort respectively discomfort perceptions were determined by using psychophysical measurement methods (Krist, 1993). The subjects were requested to assess their perception using several scales. Hardening of body regions, fatigue and the comfort and discomfort of the seating posture were rated. The ratings were correlated to the joint angles from the experiments.

Additionally, orthopedic aspects of the seating postures were assessed to enable mitigation of the discrepancy between healthy and comfortable sitting. These assessments were based on investigations about spine contours (Heidinger, 1990).

All in all, several discomfort aspects (“discomfort profile”, see Figure 2.31) of the calculated posture are estimated by RAMSIS based on multiple regression equations. The discomfort profile is intended to allow for a relative comparison of several designs and corresponding postures. It does not enable absolute assessments. (Krist, 1993)

The predictions of the regression model are better for unfavorable postures than for favorable postures. According to Krist (1993), the main reasons are: Uncomfortable states and their causes can be perceived better. For comfortable states a higher variability of ratings was observed which worsens the prediction accuracy. (Krist, 1993)

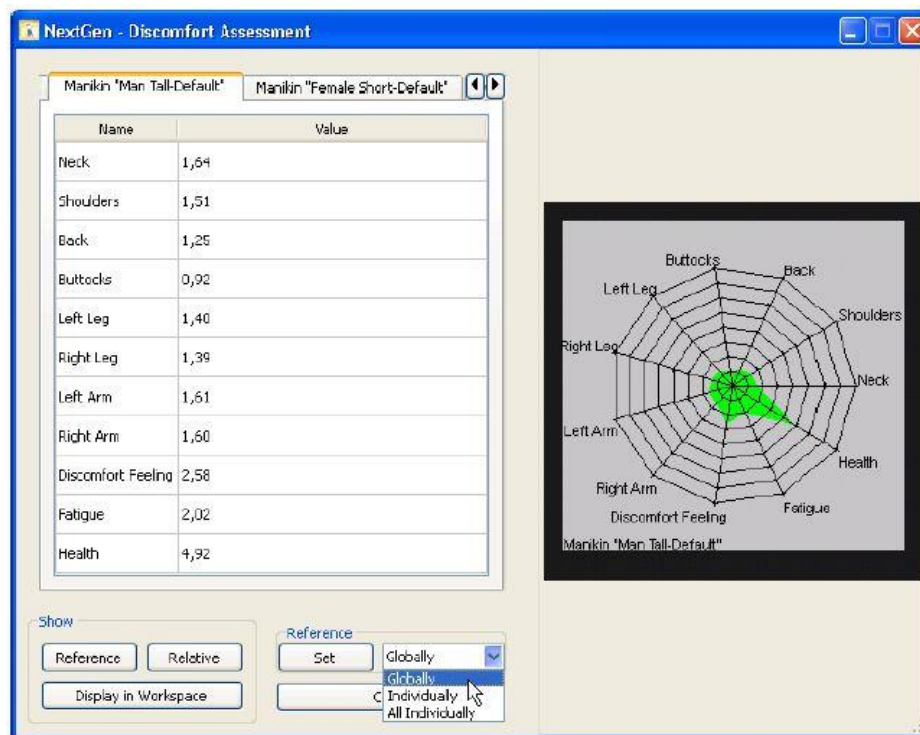


Figure 2.31: Discomfort assessment values and diagram (Human Solutions GmbH, 2014b, p. E104).

2.8.4.2.1 Validation of discomfort prediction

Validation has shown that the RAMSIS discomfort prediction model is beneficial for a qualitative comparison between different designs (design B is more comfortable than design A) of the driving workplace. However, it should not be used for an absolute/quantitative assessment (design A is twice as comfortable as design B). Krist (1993).

The tendencies of the RAMSIS ratings in a comparison of two driving postures corresponded with the subjects' ratings in only 50 % to 60 % of the studied cases. This underlines the importance to use a group of manikins with different anthropometries for discomfort prediction to assess different designs (Nilsson, 1999).

Loczi et al. (1999) have used the RAMSIS comfort module to optimize the location of a car handbrake. However, there is no detailed information and no comparison between RAMSIS postures and corresponding discomfort predictions to experimental data.

Nam et al. (2013) found that RAMSIS discomfort predictions (overall, shoulder, right arm) often had similar tendencies as the subjects' ratings for nine shifter designs.

A disadvantage of RAMSIS discomfort prediction model is that the interdependency of joint angles and related body part discomfort is not directly accounted for (Krist, 1993). Another limitation is that the discomfort rating does not consider forces (e.g. external,

joint or muscle loads), which can significantly influence discomfort perception (Zacher & Bubb, 2004).

2.8.5 Conclusions

For developing the Car Driver Model, data of four experiments covering different driving tasks were combined (Seidl, 1995; Bubb, 2013). The prediction model has been successfully validated for driving postures. There is still the risk that postures of other driving related tasks (such as handbrake application) – which have not yet been validated – might be predicted less accurately.

The proposal by Bulle et al. (2013, p. 5) to introduce “different sets of constraints and/or different posture models [...] according to stature group and vehicle” is likely to enhance prediction accuracy. However, too many different sets of constraints and posture models may be contrary to the needs of development engineers for tools to be applied quickly and easily. This thesis aims for a good balance of prediction quality and process efficiency.

Due to the above mentioned limitations of the RAMSIS discomfort prediction model, another human model, AnyBody Modeling System (AMS), is used additionally.

AMS allows calculating loads within the human body, which is a prerequisite for a more holistic discomfort metric.

2.9 The AnyBody Modeling System (AMS)

The AnyBody Modeling System (AMS) was developed at Aalborg University in Denmark which led to the foundation of AnyBody Technology A/S (ABT), Aalborg, Denmark. ABT sells AMS licenses and develops AMS further.

Chapter 2.9 is mainly based on the ABT website including tutorials (AnyBody Technology A/S, 2015b), AMS Wiki (AnyBody Technology A/S, 2014) and a review of AMS by Damsgaard et al. (2006). Other references are indicated in the course of the text. The structure of this chapter partly follows the descriptions in the master theses by Majid (2011) and Koch (2013).

In AMS, the human body, the environment and their interaction can be simulated to calculate biomechanical parameters such as muscle forces and activation, joint reaction forces and moments. The musculoskeletal system is modeled as a rigid-body system so that standard methods of multibody dynamics can be applied.

A body models is a generic model of the human body. To apply a task to it, it needs to be put in the right context which is achieved with an application model. An application model typically contains a body or body part model, an environment model and a model of the activity in scope. So-called drivers are used to animate the human model. They enable time depending postures, e.g. based on kinematic measurements. External loads (e.g. forces or moments, gravity) can be modeled and also modified time-dependent with regards to their direction, magnitude and point of application.

Based on given motions and external loads, AMS applies inverse dynamics routines to calculate internal forces and moments (e.g. for muscles and joints), muscle activities etc. From computing perspective, this is much more efficient than forward dynamics which calculates motion based on given muscular activation.

The human body models consist of several segments (bones) which are connected by joints, ligaments and muscle-tendon units.

It is very time-consuming and complex to build a human model with:

- The above mentioned elements.
- Realistic mechanical properties.
- Realistic geometrical proportions (e.g. locations of muscle origin and insertion).
- And its applications (e.g. cycling or driving a car).

Thus, there is a database of body models, body part models and application models. This database is AnyBody Managed Model Repository (AMMR). It was developed by scientists and experienced users and is maintained by ABT. The purpose of the AMMR is that users can apply the body models and connect them with different types of applications.

Every AMS user can access AMMR, download and modify the models. Most users will find appropriate models for their purposes which only need little modifications. It is also possible to build a new model from scratch.

The required realistic representation of the muscle geometry is complex: “muscles consist of soft tissue and they wrap about each other and the bones, ligaments, and other anatomical elements in a complicated fashion” (Damsgaard et al., 2006, p. 1100). Sufficiently realistic modeling of the muscle recruitment is another challenge. There are much more muscles than degrees of freedom, resulting in multiple alternatives of activated muscles and their degree of activation for each step of a task.

Human muscles are controlled by the central nervous system (CNS) by mechanisms which are not sufficiently understood. For realistic modeling, optimization methods (muscle recruitment models) are applied to overcome the problem of redundancy and recruit muscles.

In the following chapters the model set up (choice of body and muscle models, scaling, application) and analysis (kinematic analyses, inverse dynamics, calculated parameters) are described. At the end, validation results and limitations are summarized.

2.9.1 User Interface

AnyScript is the model definition language and was developed especially for AMS. It is an object-oriented programming language similar to C++ or Java. AnyScript offers a lot of predefined classes to define bones, joints, muscle, movements, constraints, external forces etc.

The user interface provides several windows such as an editor, a model tree and a model view window. A screenshot of the interface is shown in Figure 2.32

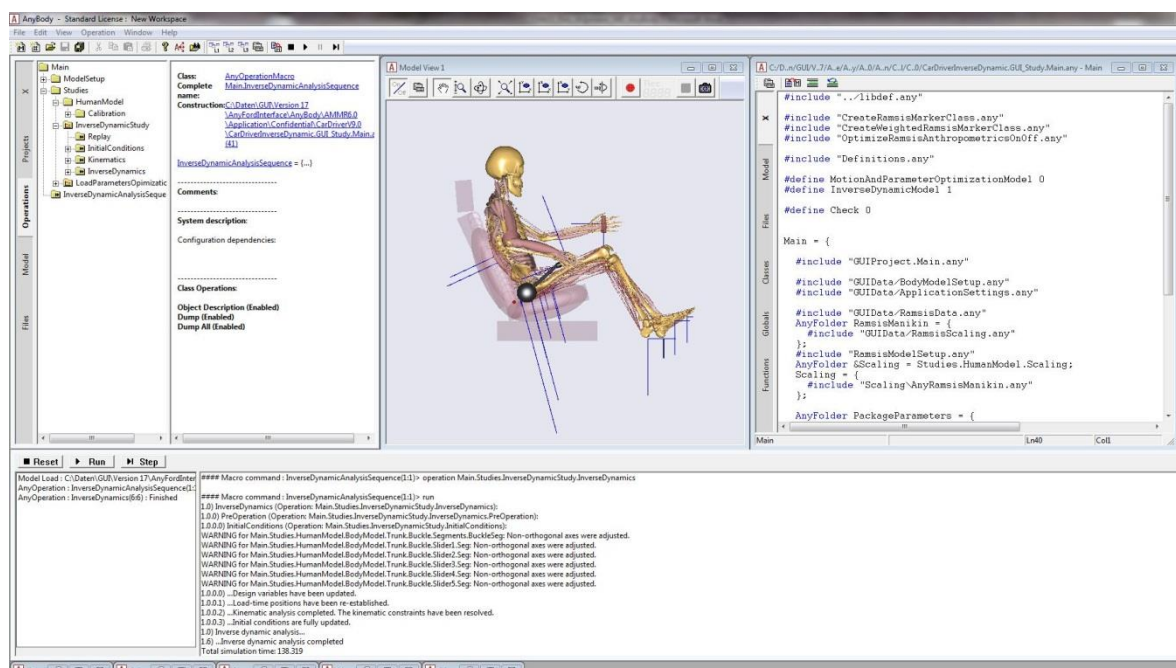


Figure 2.32: Screenshot of AMS (version 5.3.0.3365) user interface, April, 23, 2015.

It is also possible to run AMS as a console application, so that it can be controlled by software. Ford has developed a proprietary graphical user interface which enables to run AMS without programming skills for several automotive related applications (Rausch & Upmann, 2015a).

2.9.2 Applications

Numerous applications can be chosen from AMMR. They often contain predefined scaled models for the body parts or the whole body. There are muscle models as well as application/environment models (e.g. support geometry with predefined connection to the body, external loads and movements).

There are e.g. gait, orthopedic and rehabilitation, sports, daily activity, automotive and aerospace applications available. Additional models, which show how the AMMR content was validated in comparison to in vivo measured data, are provided, too. The automotive applications include a seated human, two pedal models and an egress model. AMS allows the model kinematics to follow motion capturing data. (AnyBody Technology A/S, 2015b)

Ford and ABT have developed a set of additional automotive applications which include a scalable human model, a model of the vehicle interior, specification of constraints between the manikin and vehicle and typical movements of vehicle occupants. (Siebertz et al., 2004; Rausch, 2005; Siebertz & Rausch, 2006)

The handbrake application includes models of the handbrake, seat, floor, footrest, brake pedal, clutch pedal and steering wheel (Siebertz & Rausch, 2006).

2.9.3 Body Models

The Body models are described on the ABT website in AMS tutorials and the AMS Wiki (AnyBody Technology A/S, 2014, 2015b). There, the joints and muscle models are characterised in detail with references. This chapter provides an overview.

The AAUHuman full body model was developed at the Aalborg University (AAU), Denmark. It consists of body parts which were developed by or based upon data from third parties. The full body model comprises a shoulder/arm model as well as different leg, trunk and foot models, which can be used in multiple combinations.

2.9.3.1 Arm and shoulder model

The model of arm and shoulders was derived from two cadavers. Included bones and joints are illustrated in Figure 2.33 and Figure 2.34. The model contains the spherical SternoClavicular (SC), AcromioClavicular (AC) and Glenohumeral (GH) joints. Humero-Ulnar (FE) and Ulna-Radial (PS) joints are modeled as revolute joints. The wrist joint consists of two revolute joints with non-coincident axis of rotations so that two DOFs are

provided. There is the Scapulo-Thoracic gliding plane (ST) between thorax and scapula. The hand is modeled rigid. (Siebertz et al., 2004; AnyBody Technology A/S, 2015b)

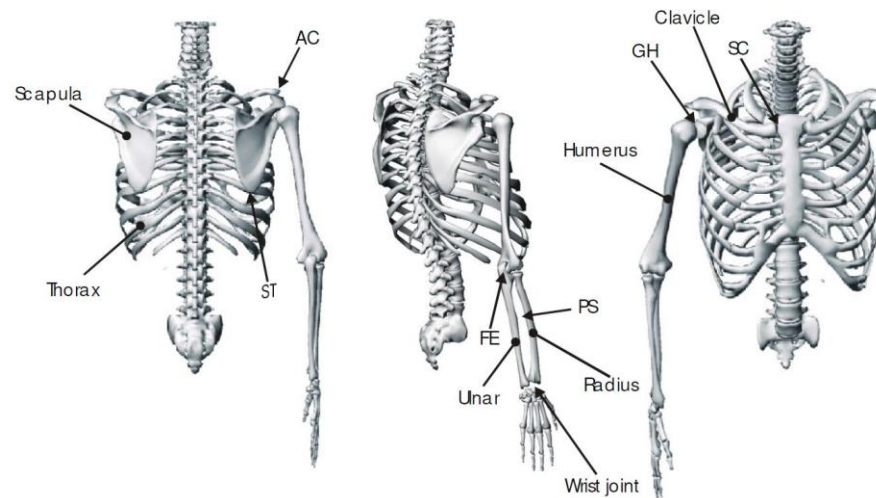


Figure 2.33: Bones and joints of the arm and shoulder model (Siebertz et al., 2004, p. 20).

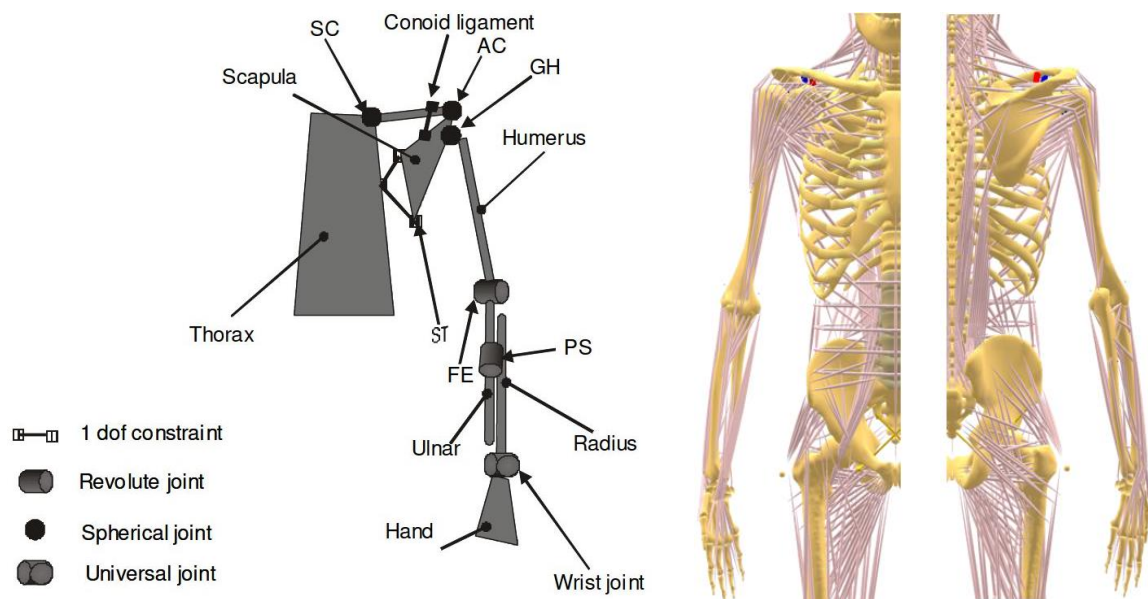


Figure 2.34: Arm and Shoulder model:

Left: Illustration of segments and connecting joints (Siebertz et al., 2004, p. 20).

Middle: Illustration of muscles (front view), Right: Illustration of muscles (rear view) (AnyBody Technology A/S, 2015b).

The arm and shoulder model encompasses 118 muscles (see Figure 2.34) for each side of the body, which partly reflect wrapping mechanisms. Some larger muscles, e.g. in the shoulder, have been divided into groups of muscles to better reflect the geometry and the force paths.

2.9.3.2 Trunk model

The trunk model comprises the spine (including cervical, thoracic and lumbar vertebrae and the sacrum), pelvis, thorax and skull (Figure 2.35). The lumbar spine model and the cervical spine model are highly detailed. The lumbar spine model consists of five vertebrae with three DOF spherical joints in between, 188 muscle elements and intra-abdominal pressure simulation. The cervical spine model consists of seven vertebrae with three DOF spherical joints from T1 to C2, a one DOF joint between C2 and skull and 136 muscle elements. (Siebertz et al., 2004; Zee, Hansen, Wong, Rasmussen & Simonsen, 2007; AnyBody Technology A/S, 2015b)

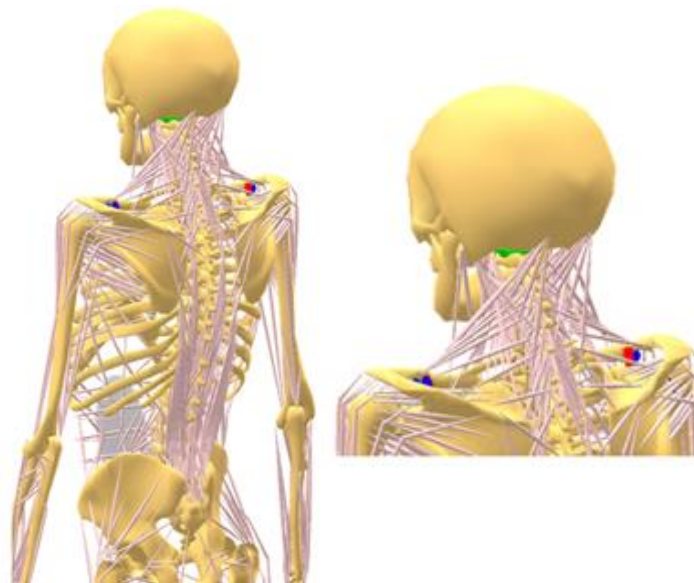


Figure 2.35: Illustration of the trunk model (AnyBody Technology A/S, 2015b).

2.9.3.3 Leg and foot models

At the beginning of the AMS development, there was only one leg model available with a low degree of details. The LegTLEM (Leg Twente Lower Extremity Model) provides more details. It consists of 159 muscle elements and has seven joint degrees of freedom per leg, see Figure 2.36.

Additionally, two complex foot models have been developed for which the validation is still ongoing. They were not utilized in this study as for handbrake application trunk and upper extremities are essential.

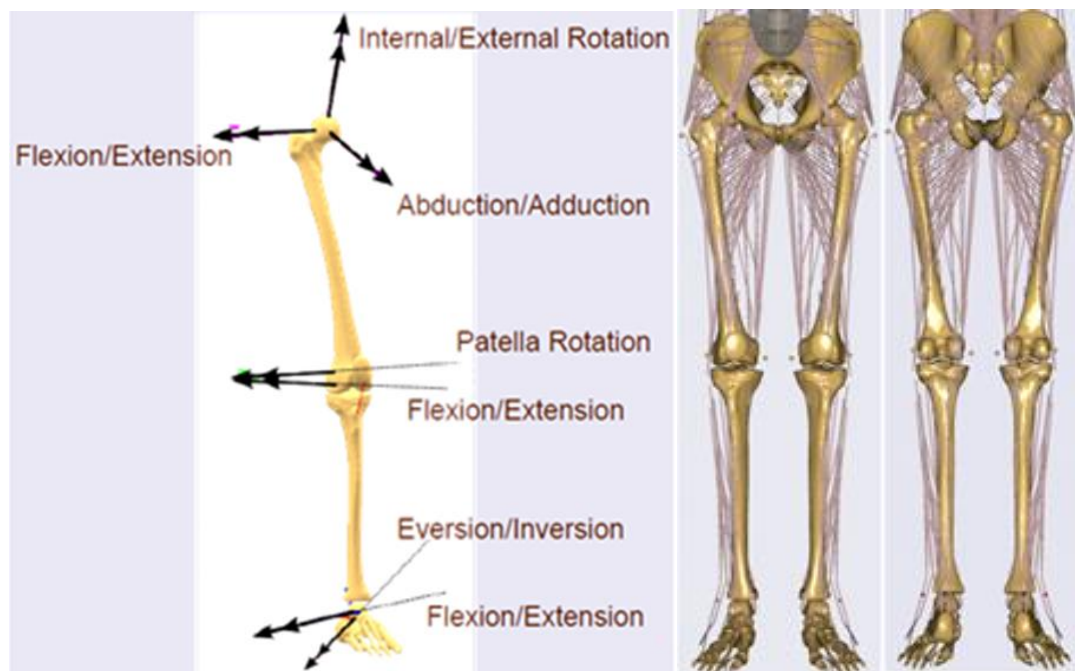


Figure 2.36: Illustration of the LegTLEM model: Joint degrees of freedom and muscle modeling (AnyBody Technology A/S, 2015b).

2.9.4 Muscle modeling

In AMS, there are different muscle types and models.

2.9.4.1 Muscle types

The path from the origin to the insertion of a muscle can be described by two of the three available muscle model types. AnyViaPointMuscles run from origin over segment related key points to the insertion point.

For a more sophisticated wrapping (to find the shortest path around “obstacles”) from origin to insertion, AnyShortestPathMuscle can be used. The course of the muscle is defined by elements (e.g. cylinders) so that the muscle describes the shortest path from origin to insertion while spanning the objects. This type requires computation time and accurate adjustments.

The third muscle type is the AnyGeneralMuscle. It does not work using a defined path but can be attached to kinematic measures. So it can introduce either a moment around a joint (without a certain path) or a force between two points. AnyGeneralMuscle is used to model external force or moment constraints.

2.9.4.2 Muscle models

Muscle models have to represent the properties of muscles in different operating conditions. There are two general approaches.

The first one is to model the microscopic physical phenomena of muscle contraction. It traces back to Huxley (1980) and requires differential equations and therefore significant computing capacity.

The other, numerically very efficient and in AMS implemented approach is a phenomenological model. It reproduces many muscle properties although it does not directly reflect the microscopic mechanisms of muscle contraction. This model is based on the fundamental publications of A. V. Hill, which are summarized and referenced in Bassett (2002),

AMS offers the choice between three muscle models which represent different degree of complexity regarding their physiological behavior.

- The AnyMuscleModel is a very simple muscle model. The only input is the strength of the muscle at optimum length. In contrast to reality, the strength is independent from the actual length and contraction velocity of the muscle (compare 2.1.1.1.2).
- The AnyMuscleModel2Elin simulates the muscle strength proportional to its actual length and contraction velocity. This model consists of a contractile element (the muscle) and a linearly elastic tendon which is modeled as serial-elastic element.
- The AnyMuscleModel3E is the most complex muscle model in AMS and represents the Hill-model.

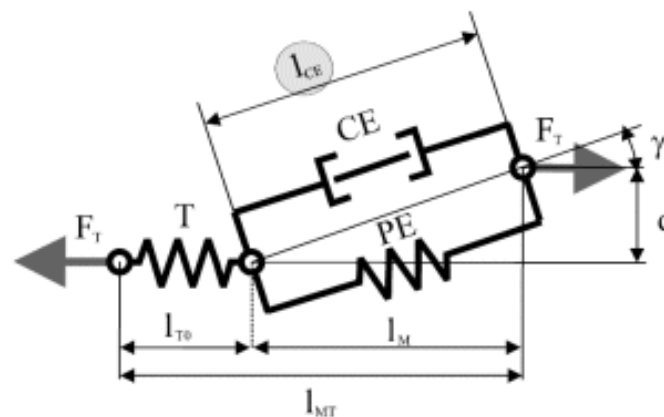


Figure 2.37: Schematic representation of the AnyMuscleModel3E muscle model including tendon (AnyBody Technology A/S, 2015b).

The AnyMuscleModel3E consists of three elements as illustrated in Figure 2.37:

1. The contractile element (CE) represents the active properties of the muscle fibers.
2. The parallel-elastic element (PE) represents the passive stiffness of the muscle fibers.
3. The serial-elastic (T) element represents the elasticity of the tendon.

This muscle model takes the velocity strength and length strength relations into account. Pennation angle and other properties can also be considered. However, this complex model requires multiple physiological parameters. These parameters can be difficult to determine or estimate, e.g. the definition of postures in which each muscle has its optimum length. This is a novel and challenging field of research. (Koch, 2013)

The upper extremities involve complex joints in the region of the shoulder girdle including scapula and clavicle, so that the movement of the joints and the corresponding muscle paths are complex to model in AMS. Additionally, necessary input parameters for the AnyMuscleModel3E are difficult to determine.

Koch (2010) compared the results of isometric strength measurements of the upper extremities of 30 subjects with AMS AnyMuscleModel and AnyMuscleModel3E calculations.

The AnyMuscleModel tended to overestimate the isometric strength which can be reduced significantly by adjusting reference forces in AMS.

The AnyMuscleModel3E overestimated the strength of muscles for some postures. These implausible results might be caused by non-optimal muscle strength-length calibration of the arm muscles or muscles unrealistically sliding over a joint and consequently have an unrealistic length. Hence, the AnyMuscleModel3E of the upper extremities needs further enhancements.

As the AnyMuscleModel led to more robust results in Koch (2010), it was applied in this study. Typical handbrake application corresponds to relatively low speed and non-extreme muscle lengths, which supports this decision.

2.9.5 Scaling methods

The purpose of scaling is to modify the anthropometry of the human model according to a reference configuration with known values. There are two types of scaling: Scaling of geometrical properties and scaling of muscle strength.

2.9.5.1 Geometrical scaling

Geometrical scaling applies to the overall and segment geometry as well as to more sophisticated characteristics such as muscle insertion points, wrapping surfaces and additional muscle parameters. So, scaling influences e.g. the path and the lever arms of the muscles. In AMS, body segments have defined masses and nodes which follow the moving segment. The inertial properties of a segment are defined by its mass and

moments of inertia. Each segment has a local coordinate system with its origin in the center of gravity of the segment. Nodes are used for joint centers, muscle origin and insertion points. They are defined relative to the local coordinate system (LCS) of the segments. (Rasmussen et al., 2005; Annegarn, 2006; Koch, 2013)

Linear scaling is performed by application of the following equations:

$$s = S \cdot p + t \quad (2.1)$$

$$S = \begin{pmatrix} S_{11} & 0 & 0 \\ 0 & S_{22} & 0 \\ 0 & 0 & S_{33} \end{pmatrix} \quad (2.2)$$

The position vector of the node in the LCS of the scaled segment is calculated with the S 3x3 scaling matrix S, the translation vector t and the original node location p as shown in (2.1) and (2.2). S_{11} defines the scaling in x, S_{22} the scaling in y and S_{33} the scaling in z direction. (Rasmussen et al., 2005; Annegarn, 2006; Koch, 2013)

There are two types of geometrical scaling available in AMS, isometric and non-isometric scaling.

2.9.5.1.1 Isometric scaling

In this method, the segments are scaled by the same scaling factor K_L for all three axes. K_L is the quotient of the scaled length L_1 and the original length L_0 .

$$S_{11} = S_{22} = S_{33} = K_L = \frac{L_1}{L_0} \quad (2.3)$$

This scaling method is a very rough method and does not reflect biology (Annegarn, 2006). For this reason it will not be applied in this study.

2.9.5.1.2 Non-isometric scaling

In non-isometric scaling considers segment length and mass.

Length scaling is described in (2.4).

$$S_{22} = K_L = \frac{L_1}{L_0} \quad (2.4)$$

The cross-sectional dimensions are scaled by application of the following equations.

$$K_M = \frac{M_1}{M_0} \quad (2.5)$$

$$S_{11} = S_{33} = \sqrt{\frac{K_M}{K_L}} \quad (2.6)$$

The mass ratio K_M is the quotient of the scaled segment mass M_1 and the original segment mass M_0 . Assuming that the mass density is constant, the scaling factor for the cross-sectional area is K_M/K_L . Therefore, the cross sectional directions are square rooted. This method reflects that the cross section scaling of the bone depends on its length and mass. Non-isometric scaling is significantly more realistic than isometric scaling. (Rasmussen et al., 2005; Annegarn, 2006; Koch, 2013; AnyBody Technology A/S, 2015b)

Therefore, non-isometric scaling is applied in this study as geometrical scaling method.

2.9.5.2 Muscle strength scaling

There are three major methods of strength scaling which are based on

1. Body mass
2. Body mass and composition
3. Body mass, composition, gender, age and further body measures (segment lengths and weights). (AnyBody Technology A/S, 2015b)

2.9.5.2.1 Body mass scaling

The body mass scaling method is based on the assumption that muscle strength and mass correlate because muscle strength depends on the cross-sectional area of the muscle which correlates to the mass. As heavy people are usually stronger than light ones, it makes sense to utilize the body mass for muscle strength scaling.

The volume has a cubical proportion to linear length dimensions. The cross sectional area has a quadratic proportion to them. So, the scaled force F is calculated by multiplication of the reference force and the mass quotient with an exponent of $2/3$ which is shown in (2.7). (Annegarn, 2006; Koch, 2013; AnyBody Technology A/S, 2015b)

$$F = F_0 \cdot K_M^{\frac{2}{3}} \quad (2.7)$$

This scaling method has been applied in this study, as subjects with normal weight were chosen and corresponding manikins were modeled in RAMSIS and AMS. Still, other more detailed scaling laws are briefly described below.

2.9.5.2.2 Body mass and composition scaling

The assumption that a higher body mass is caused by a higher muscle mass is not always correct. A higher body mass can also be the consequence of a higher mass of fat. Thus, there is a scaling method, shown in (2.8), which estimates the scaled muscle force F based on the mass percentage of the muscles in the body, $R_{muscle,1}$, and in the reference body, $R_{muscle,0}$.

$$F = F_0 \cdot \frac{K_M}{K_L} \cdot \frac{R_{muscle,1}}{R_{muscle,0}} = F_0 \cdot \frac{K_M}{K_L} \cdot \frac{(1 - R_{other} - R_{fat,1})}{(1 - R_{other} - R_{fat,2})} \quad (2.8)$$

R_{muscle} is the whole body mass percentage (1 =100 %) minus the fat mass percentage, R_{fat} , and the mass percentage of other components (such as blood and bones), R_{other} . There are several methods to determine R_{fat} and R_{other} .

The scaling law is based on the assumption that the mass density of a segment is constant. To take length and mass into account, the scaling factor of the cross-sectional area is K_M/K_L (compare 2.9.5.1.2). (Annegarn, 2006; AnyBody Technology A/S, 2015b; Koch, 2013)

2.9.5.2.3 Scaling law by Annegarn

In the above mentioned scaling laws, the effects of age, gender and segment circumferences are not taken into account. Annegarn (2006) has developed more complex scaling laws for lower and upper extremities which include these details. Annegarn's scaling laws are not based on theoretical considerations (like the scaling laws mentioned above), but on experiments with subjects and resulting regression models. (Annegarn, 2006; Koch, 2013)

2.9.6 Kinematic analysis

For the calculation of biomechanical parameters, the body model, its posture or motions and external forces need to be preset. Motions can be defined by defining postures for discrete points in time.

The body model consists of rigid segments (bones), which can move in up to three translation and up to three rotation directions (DOFs), if there are no constraints. If the model consists of n segments, this results in $6n$ DOFs.

Segments can be constraint by the definition of joints and drivers. To determine the positions of all segments at all times, $6n$ pieces of information about the positions are required to resolve the $6n$ degrees of freedom. So, kinematic analysis is about solving

6n equations with the help of 6n unknowns by the application of mathematics. The outcomes are equilibrium conditions for the segments at each given point of time.

The kinematic outputs include positions, orientations, velocities and accelerations of all segments and joints; joint angles; length and contraction velocities for all muscles. So, the kinematic analysis describes the body model motion based on the given conditions. Forces and moments are not involved in these calculations. (Rausch, 2005; Majid, 2011; Koch, 2013; AnyBody Technology A/S, 2015b)

2.9.7 Inverse dynamics

Inverse dynamic calculates biomechanical parameters such as muscle forces based on known motions and external forces. The calculation of forces is done by resolving equilibrium equations. If there are fewer equilibrium equations available than forces to be calculated, the system is statically indeterminate.

Key demands to inverse dynamics solvers are to handle statically indeterminate problems and unilateral force elements because muscles can only pull and not push. (Koch, 2013; Majid, 2011)

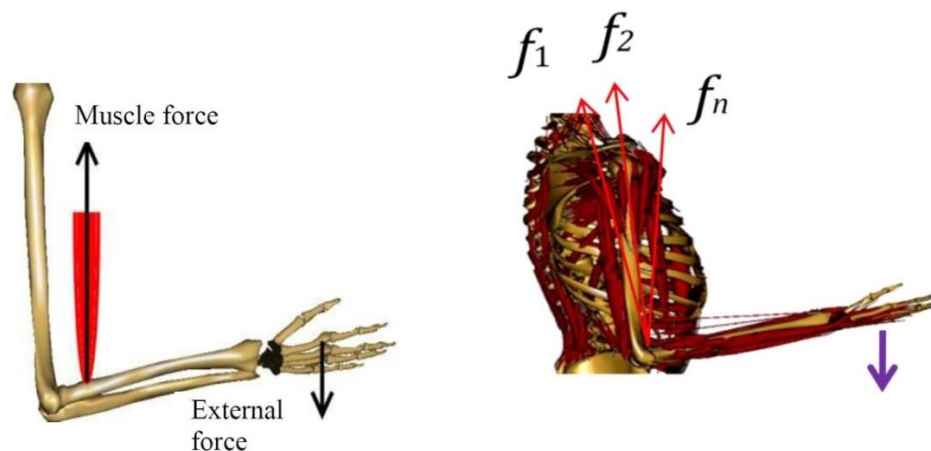


Figure 2.38: Muscle recruitment for isometric contraction. Simple model (left) and complex model (right) (AnyBody Technology A/S, 2015b).

Figure 2.38 (left) illustrates the principle of inverse dynamics. If the magnitude of the external force, the length of the forearm and the insertion point of the biceps muscle on the forearm are known, the muscle force can be calculated from the moment equilibrium about the elbow. With a more detailed model, complications occur. One of them is that the body has many more muscles than necessary to counterbalance the degrees of freedom (Figure 2.38, right). So there are numerous possible ways how the body can recruit its muscles to perform a task. (Majid, 2011; Koch, 2013)

2.9.7.1 Muscle recruitment

Muscle recruitment describes the choice which muscles to use (and to which activation level) to perform a movement or maintain a posture.

In a real human, the CNS chooses the arrangement of muscles to perform a task. As human can reproduce movements with good precision, the assumption is made that muscles are recruited based on an optimality criterion, e.g. so that the load on muscles and the body in general is reduced. The different implemented optimization criteria are all based on assumptions of the optimal function of the CNS. (Damsgaard et al., 2006; Rasmussen et al., 2003)

For more detailed descriptions refer to Rasmussen, Damsgaard & Voigt (2001), Damsgaard et al. (2006) or the ABT website (AnyBody Technology A/S, 2015b). These references provide mathematical descriptions and comparisons of implemented recruitment optimization options. They describe advantages and disadvantages of the three objective function types and several power values (see below). They also provide references, which partly describe comparisons to EMG measurements.

In order to solve the muscle recruitment problem by an inverse dynamics approach, the optimization problem is described with (2.9) which is subject to (2.10) and (2.11).

$$\text{Minimize } G(f^{(M)}) \quad (2.9)$$

$$C \cdot f = d \quad (2.10)$$

$$0 \leq f_i^{(M)} \leq N_i, \quad i \in \{1, \dots, n^{(M)}\} \quad (2.11)$$

G is the objective function describing the selected criterion of the muscle recruitment strategy of the CNS. G is minimized for all unknown forces which can include muscle forces $f^{(M)}$ and joint reactions $f^{(R)}$. (2.10) describes the dynamic equilibrium equations constraining the optimization. C is the coefficient matrix for the unknown forces. d contains given applied loads and inertia forces.

N_i is the normalized muscle force – often referred to as muscle activity. (2.11) describes that the strength of the muscles N_i is positive because muscles can only pull. (2.11) also specifies that N_i is limited by force capability $n^{(M)}$. Depending on the chosen muscle model the force capability $n^{(M)}$ can also take the working condition of the muscle (length, velocity of contraction) into account.

(2.12) to (2.14) describe major forms of objective functions. The most popular form of objective function is the polynomial criterion shown in (2.12).

$$G(f^{(M)}) = \sum_{i=1}^{n^{(M)}} \left(\frac{f_i^{(M)}}{N_i} \right)^p \quad (2.12)$$

The soft saturation criterion is described in (2.13). It eliminates the need to define additional constraints to avoid overloaded muscles which is required for (2.12).

$$G(f^{(M)}) = - \sum_{i=1}^{n^{(M)}} \sqrt[p]{\left(1 - \frac{f_i^{(M)}}{N_i} \right)^p} \quad (2.13)$$

Both – the polynomial and the soft saturation criterion – have a variable power, p . The higher the power, the quicker muscles are activated and deactivated. It is generally agreed that $p=1$ leads to physiologically not reasonable results as the stronger muscles do all the work but real muscle are known to share load. Higher powers lead to a better reflection of human muscle recruitment but are less numerical attractive. Too high power values can lead to speeds of activation/deactivation which are not physiologically possible. They can cause numerical instabilities and may be less robust.

Very large powers in the polynomial criterion (2.12) lead to numerically equivalent solutions to the so called min-max criterion (2.14).

$$G(f^{(M)}) = \max \left(\frac{f_i^{(M)}}{N_i} \right) \quad (2.14)$$

This is not only numerically attractive, but also physiologically. Under the assumption that muscle fatigue and activity are proportional, this criterion delays fatigue as much as possible. It can be referred to as a minimum fatigue criterion. A disadvantage of this criterion is that it switches muscles on and off very abruptly which may be faster than physiologically possible. Another disadvantage is that muscles with a marginal contribution will still be applied to the full potential, too. This may lead to too much muscle synergism: muscles with very poor working conditions (small moment arms) are exploited to a questionable degree. These disadvantages do not apply for lower order polynomial criteria.

Crowninshield & Brand (1981) chose – for muscle force and activation prediction during elbow isometric contraction and gait – the polynomial criterion with the power of three ($p=3$). It appeared to represent the consensus of values reported in literature and the predicted muscle activity was comparable to EMG measures. Also Arjmand & Shirazi-Adl (2006) found that muscle activities predicted with the polynomial criterion with the power of three qualitatively matched measured EMG data.

So, in this study it was decided to use the polynomial criterion with the power of three. It combines the advantages to sufficiently reflect physiological muscle recruitment and to be mathematically robust.

2.9.7.2 Mechanical model

Applying a mathematical model of the mechanical system, equations in the form of (2.10) are generated. A general multibody system dynamics approach is adapted with Cartesian coordinates for each segment. The segments are models as rigid bodies; wobbly masses of soft tissues are not taken into account. The coordinates $q_i = [r_i^T p_i^T]^T$ describe the position of the i^{th} segment. r_i is the global position vector of the center of mass. p_i is a vector of four Euler parameters. $v_i = [\dot{r}_i^T w_i'^T]^T$ defines the velocity of the body. The vector w_i' is the angular velocity of the segment in the segment fixed reference frame.

The kinematic analysis is performed in Cartesian coordinates by the resolution of kinematic constraints in (2.15).

$$\Phi(q, t) = 0 \quad (2.15)$$

$q = [q_1^T \dots q_n^T]^T$ is the coordinate vector for all n segments. The time t indicates that some constraints are kinematic drivers in addition to normal holonomic constraints which result from the joints. For inverse dynamic analyses the constraints must describe the motion. So a full set of equations is required in (2.15). (Damsgaard et al., 2006)

For further details refer to Damsgaard et al. (2006).

2.9.8 Simulation results

Application of the inverse dynamics calculation – by minimizing muscle load as defined by the muscle recruiting criterion (2.9) – results in numerous calculated “outputs”. The units are always the SI units (AnyBody Technology A/S, 2014). In the next paragraphs, AMS output parameters are described including their anticipated relevance for this study (compare 2.2 to 2.5).

2.9.8.1 Metabolic power consumption and total metabolic energy

Discomfort can be related to energy consumption during a task (Wang et al., 2004). A relationship between work and discomfort has been shown e.g. for clutch pedal operation (Wang et al., 2004). Hence, metabolic power consumptions and total

metabolic energy are expected to be closely connected to the discomfort perception for the operation of vehicle controls, which are not operated permanently.

They are measures indicating the effort for the whole body respectively whole handbrake application process embracing information on posture, load and time. So, it is expected to be beneficial to analyze the metabolic power consumption and total metabolic energy for body regions respectively the complete body.

In AMS, the metabolic power consumption P_{met} is a crude estimate of the metabolism in the muscle. It takes different efficiencies for concentric and eccentric work into account, but not the metabolism of isometric force (AnyBody Technology A/S, 2015b). The metabolic energy of a single muscle consumed during a task is calculated by integrating its power over the duration of the task. The total metabolic energy E_{met} is the sum of the metabolic energy of all muscles.

2.9.8.2 Muscle activity

Muscle activity can influence the discomfort perception. E.g. it has been shown that too high muscle efforts result in discomfort (Jung & Choe, 1996; Rausch & Upmann, 2015b). EMG values are typically used to assess muscle fatigue (de Luca, 1997; Senner, 2001) which is related to discomfort (Zhang et al., 1996). Measuring EMG values requires clinics with subjects and is mostly limited to muscles underneath the skin. It is error-prone and simulation of muscle activity can be at advantage. Wang (2009) states that a detailed muscular activities simulation has not been considered adequately in research of discomfort modeling. A literature review in 2015 confirmed this. Scarce documentation has been found on discomfort prediction based on muscle activity modeling (Kim & Lee, 2009). As AMS muscle activity prediction has been validated successfully (2.9.9), it can be assumed that AMS muscle activity prediction is relevant to predict discomfort.

Depending on the muscle type, AMS provides up to 23 calculated parameters for each of the more than 500 muscle units. The muscle activity describes the muscle activation level in comparison to its maximum voluntary contraction (AnyBody Technology A/S, 2015b). For AnyMuscleModel3E also the muscle length and contraction speed are considered in the calculation.

In AMS, muscles are often modeled as a group of muscle bundles with differing load paths, e.g. the deltoid muscle is modeled out of 6 scapular parts and 6 clavicular parts. For muscles, which are implemented as a group of muscles, maximum and mean

muscle activity for the group can be calculated. Also, maximum and mean muscle activities for all muscles in a body region such as trunk, left and right lower and upper extremities can be computed.

2.9.8.3 Joint reactions and joint moment measure

The contribution of joint forces and moments to the discomfort perception has been extensively documented (Wang et al., 2004; Zacher & Bubb, 2004; Dickerson et al., 2006; Romain & Xuguang, 2012; Pannetier & Wang, 2014). So, joint reactions and joint moment measures (Figure 2.39) are expected to be relevant for discomfort perception in this study, too. Discomfort can be caused by too high muscle effort (Rausch, 2015a) which is particularly well reflected by the joint moment measure (see below).

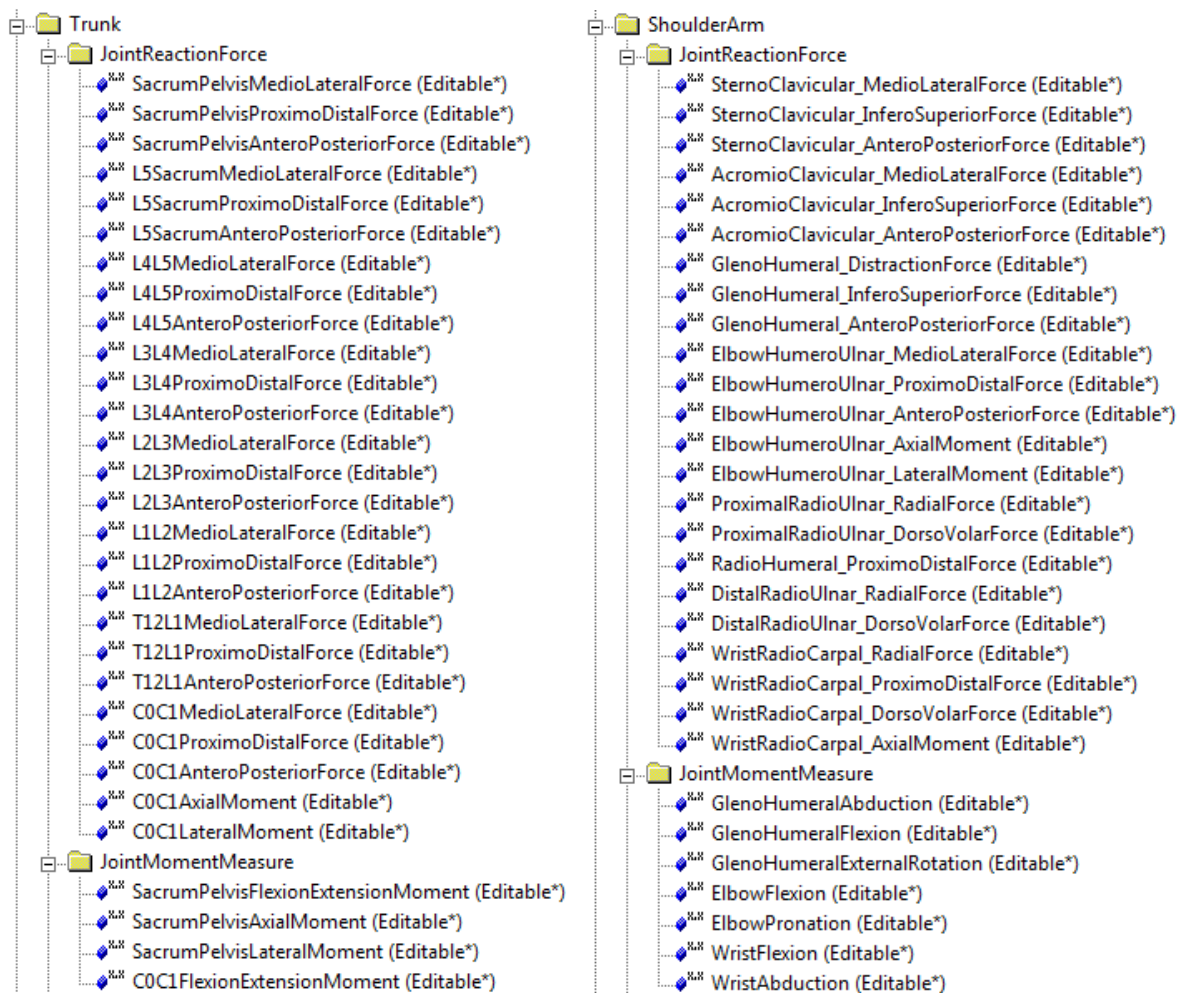


Figure 2.39: Screenshot of AMS showing joint reactions and joint moment measures of trunk and shoulder/arm. Forces/moments in the folder “JointReactionForce” are calculated considering muscle and external loads. Moments in the “JointMomentMeasure” folder are calculated only from muscle loads.

Joint reactions (forces and moments) are calculated in AMS based on muscle and external loads including gravity (AnyBody Technology A/S, 2014) because both loads result in strain in the joints.

A joint moment measure includes only the moments, resulting from the muscles spanning the joint, but not the moments from reactions between the human model and its environment. “The resulting force and moment are equal to the total moment and force which are supplied by the muscles” (AnyBody Technology A/S, 2015a). So, the joint moment measures provide good information about muscle strain. (Rausch, 2015b)

2.9.8.4 Joint angles

Joint angles as a measure of the postural load have widely been shown to contribute to discomfort perception (Krist, 1993; Kee & Karwowski, 2001b; Zacher & Bubb, 2004; Romain & Xuguang, 2012). Joint angles are calculated via the kinematic analysis in AMS.

2.9.9 Validation

Research for one “true” and general muscle recruitment criterion is ongoing, but the task may never be accomplished. As mentioned above, muscle recruitment criteria are based on assumptions about the optimal function of the CNS. This optimality approach fulfils basic demands (i.e. dynamic equilibrium) and the better criteria do provide physiologically reasonable results.

Validation of AMS is complex as muscle forces cannot be measured directly and EMG measurements can only indicate muscle activity of muscles underneath the skin. On the other hand this underlines the need for biomechanical models because in many cases they are the only possibility to provide essential information, such as body internal forces or moments. (Damsgaard et al., 2006)

Damsgaard et al. (2006) provide multiple references in which results of inverse dynamics are compared to experimental results. The ABT website (AnyBody Technology A/S, 2015b) lists 101 publications on AMS validation (May, 15, 2016).

In general it can be stated that AMS allows for a reasonably accurate prediction which muscles are activated for which time periods, see the exemplary illustration in Figure 2.40.

The magnitude of muscle activity (calculated by AMS) and the magnitude of the EMG value (measured in an experiment) can differ for a number of reasons including:

- Inadequacies of the model.
- There is no well-established relationship between EMG signals and real muscle force (Damsgaard et al., 2006).
- EMG measurements are prone for measuring inaccuracies (De Luca, 1997).

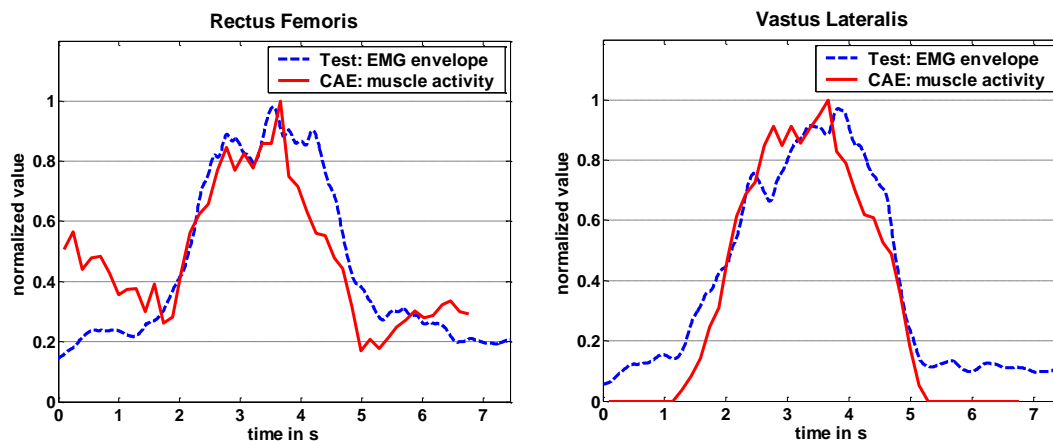


Figure 2.40: Validation results for brake pedal application. Extracted from Rausch (2015a, p. 11).

At Ford, several validation studies including brake pedal application and steering have been completed (Rausch, 2010; Rausch, 2015a). As anticipated, activation periods of muscles correspond well with the experimental EMG data whereas the magnitude of the activation partly differs due to the above mentioned reasons.

Laursen, Jensen, Németh & Sjøgaard (1998) measured EMG values of shoulder muscles while the subjects were performing isometric tasks. Siebertz et al. (2004) simulated the experimental set up in AMS. The calculated muscle activities correspond well with the EMG measurements.

Also validation of strength scaling has shown good correlations between subjects' strength and AMS simulation (Rausch, 2010).

2.9.10 Limitations

The optimality assumption of the muscle recruitment criteria and the application of inverse dynamics result in several restrictions for the application.

Muscle activity dynamics is neglected and optimality is assumed. So, the methodology has to be restricted to relatively slow and familiar movements the human is used to

perform, e.g. daily activities such as gait. It is not clear if the same degree of optimality can be assumed for less familiar tasks. (Damsgaard et al., 2006)

For enduring static postures (e.g. seating in a car and keeping the accelerator pedal depressed for driving a constant speed) changes in the activation patterns of synergetic muscles have been observed. More fatigued muscle get weaker and less fatigued muscle take over higher loads (Rausch, Siebertz, Christensen & Rasmussen, 2006). This has not been implemented yet in AMS.

Simulation of control tasks – such as engaging the clutch – involves interaction of synergistic and antagonistic muscles. Modeling with an optimality approach is not recommended for this condition.

These limitations are no counter-arguments for the simulation of handbrake application because it is a relatively slow movement and the subjects are familiar with it.

2.9.11 Conclusions

Muscle activity (Jung & Choe, 1996; Rausch & Upmann, 2015b), power and energy (Wang et al., 2004), joint reactions (Wang et al., 2004; Zacher & Bubb, 2004; Dickerson et al., 2006; Romain & Xuguang, 2012; Pannetier & Wang, 2014) and joint angles (Krist, 1993; Kee & Karwowski, 2001b; Zacher & Bubb, 2004; Romain & Xuguang, 2012) have been shown to contribute to discomfort. While some of these parameters can be measured in studies with subjects (e.g. joint angles), others can hardly, with several limitations or not at all be measured.

AMS allows for calculation of such parameters. It is well validated (AnyBody Technology A/S, 2015b) and in use by several automotive companies. Therefore; it is used in this study.

2.10 The handbrake

2.10.1 Brake systems

Brake systems are essential for the roadworthiness and safe operation of motor vehicles. Thus, they are subject to legal requirements. Their four main component groups are actuation device, energy supply system, force transmission system and (wheel) brakes.

Vehicle brake systems can be classified in the following types:

1. The **primary brake system (service brake)** has the functions to slow down the vehicle, keep its speed constant on a descent or to get it completely to a halt. The driver can vary the braking effect with a foot operated pedal. Commercial vehicles are additionally equipped with a continuous operation braking system which enables the driver to keep the vehicle at a constant speed on long descents.
2. The **auxiliary brake system** takes over the functions of the service brake system in case of failure.
3. The **parking brake system** prevents the stopped or parked vehicle from moving. In most vehicles, the parking brake system also fulfills the tasks of the auxiliary brake system. Main mechanical actuation devices are hand operated levers and foot operated pedals. An EBP (electronic park brake) is activated by a hand operated electrical switches. (Wallentowitz, 2005; Reif, 2014)

This study is about the ergonomic respectively discomfort evaluation of the hand lever operated park brake. Hand operated mechanical park brakes are referred to as handbrakes. Details of other types of brakes, their components and functions are described in e.g. Wallentowitz (2005) or Reif (2014).

2.10.2 Legal requirements

Vehicles sold in particular markets have to comply with the local legal requirements. In this chapter the ergonomic aspects of the legal requirements relating to handbrakes are described. Vehicles sold in Europe have to fulfill ECE (Economic Commission for Europe) requirements. Vehicles sold in USA have to comply with FMVSS (Federal Motor Vehicle Safety Standards) requirements. Most other regions have adopted ECE or FMVSS requirements.

The legal requirement ECE 13 – H (2014) dictates that the driver has to be able to activate the handbrake from the driving seat and that the system shall hold the loaded vehicle stationary on a 20 % grade (up or down). The regulation restricts the application force to a maximum of 400 N for passenger vehicles with up to nine seats. For vehicles with more seats and vehicles used for transportation of goods (commercial vehicles) the maximum application force is limited to 600 N in ECE 13 –11 Supp. 11 (2014). In the United States a handbrake application force of up to 400N is allowed for light vehicles

(FMVSS 135, 2012). Up to 125 pounds (556 N) of handbrake application force are allowed for commercial vehicles (FMVSS 105, 2012).

The legal requirements define the default conditions for automotive manufacturers. However, they do not provide sufficient information to design handbrakes compatible to the majority of the target population regarding ergonomics including handbrake location and application forces. E.g. smaller people, especially elder females, will have difficulties or will not even be able to apply the maximum specified forces. Also the location (reach) is not clearly specified which might impede parts of the target population from having good reach. Accessibility and reach clearances are not defined at all.

2.10.3 Automotive standards and key indicator method

Based on studies on anthropometry, muscular strength and endurance as well as on range of motion, ergonomic guidelines for workplaces and products (chapter 2.10.3) have been established to support reducing discomfort. They are applied in the development of products and workplaces (Grandjean, 1988; Schmidtke, 1993).

The intention of this subchapter is to provide relevant examples of standards respectively guidelines with regards to automotive development and workplace design. Also their usefulness for handbrake ergonomics is addressed.

For more insight into automotive ergonomics, refer to Bhise (2012) or Gkikas (2013). Steinberg et al. (2007) is recommended for an overview of key indicator methods for manual handling operations.

2.10.3.1 Automotive standards and guidelines

Vehicles are usually designed for the occupants' range of 90 % to 95 % of the target population. Occupant package aims for a layout of relevant vehicle interior components by considering the occupant's characteristics (i.e. anthropometry, reach, strength, vision) and vehicle attributes (e.g. space, size of components, crash safety, aesthetical styling). The Society of Automotive Engineers (SAE) has issued numerous standards which recommend practices for occupant packaging. Selected examples are shown in Figure 2.41. (Kyung, 2008; Macey & Wardle, 2009)

For this study, the SAE standards on the vehicle coordinate system, the seating reference point (SGRP), the seat adjustment field and driver hand control reach are referenced. SAE J1100 (2009) describes measurements and standard procedures for

vehicles dimensions. It also defines a vehicle coordinate system which is applied in this study and illustrated in Figure 2.42.

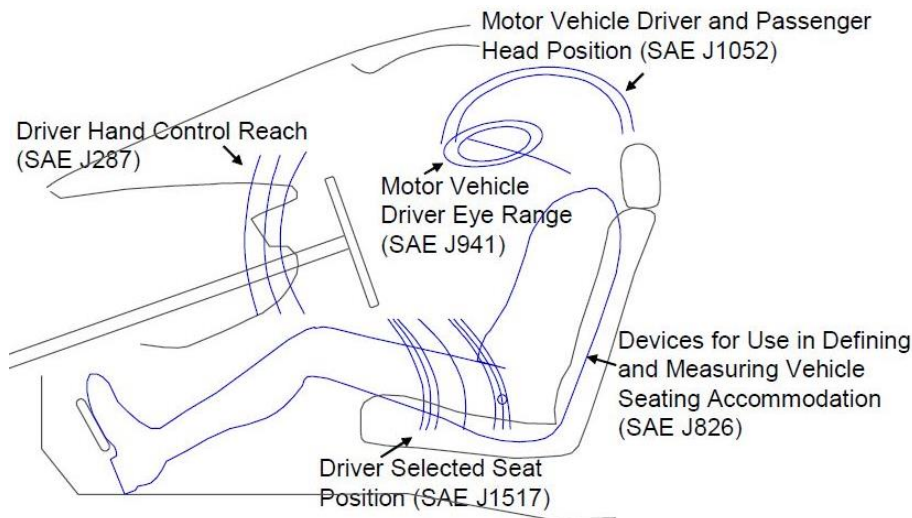


Figure 2.41: Examples of SAE accommodation design tools and recommended practices, extracted from Kyung (2008, p. 29) who modified from Peacock & Karwowski (1993).

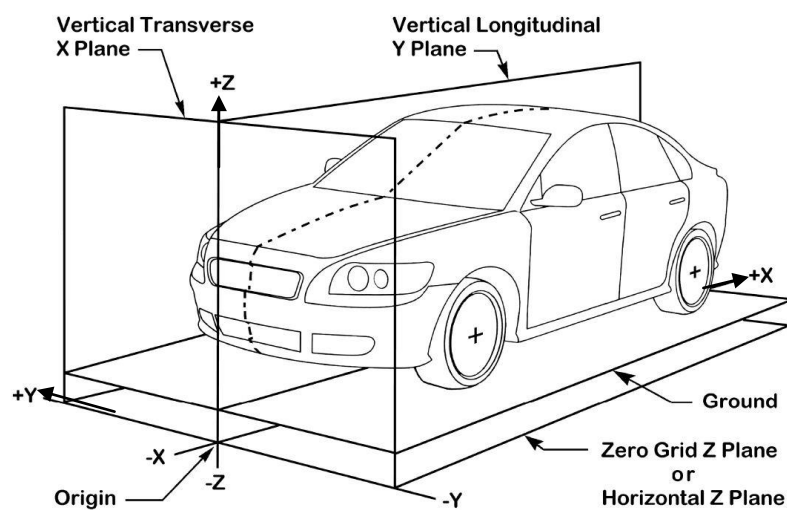


Figure 2.42: The three dimensional vehicle reference system as defined in Society of Automotive Engineers, Inc. J1100 (2009, p. 31).

Figure 2.43 highlights important principles in vehicle interior design. The H-Point Machine (HPM), representing a 95 percentile SAE manikin, is applied according to SAE J826 (2008) to define the seating reference point (SGRP). The SGRP corresponds to the hip-point of the HPM. The SGRP is relevant for almost all driver related elements of the vehicle interior package as it is used as an anchorage point to define required space and locate controls (Macey & Wardle, 2009).

The seat adjustment field (SAF, also called H-Point travel range/path) can be defined by the H-Points of the HPM when the seat is moved in its extreme positions (SAE J1100, 2009). The rearmost lowest available H-Point location is called RLP, see Figure 2.43.

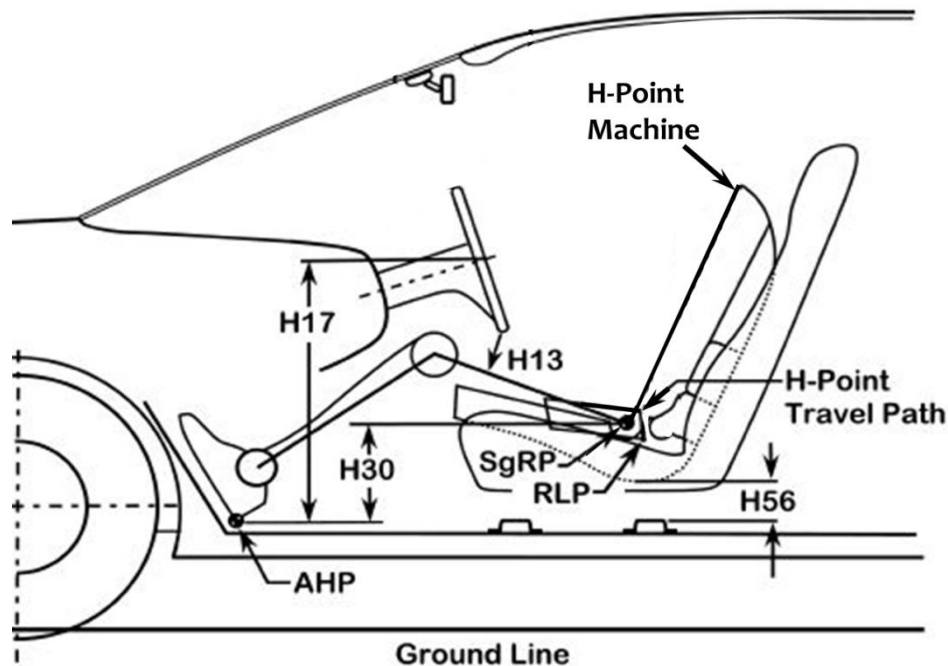


Figure 2.43: H-Point machine, SGRP, H-Point travel path and selected interior dimensions as defined in Society of Automotive Engineers, Inc. J1100 (2009, p. 85), illustration is slightly modified.

To describe a subject's seating position, it is common practice at Ford to record the corresponding coordinates of the HPM for the subject's seat adjustment. The anatomic hip-coordinate of the subject is typically not measured.

Thus, subject specific anatomical properties (e.g. amount of tissue underneath the hip joint) are neglected. Still, this procedure allows reproducibly comparing seat adjustments of subjects. After measuring the SGRP and the boundaries of the SAF in a physical vehicle, scales are designed accordingly and applied to the vehicle to enable easy and quick determination of the seat adjustment.

Starting from the SGRP, clearances, roominess and vision targets can be defined (Macey & Wardle, 2009). Related methods are described e.g. in SAE J1100 (2009) and SAE J287 (2007). SAE J287 (2007) describes hand reach envelopes for 3 finger, extended finger and full hand grasp of controls. The boundaries represent the reach of 95 % of US drivers.

The application of legal requirements and SAE standards helps to fulfil only the basic needs of the occupants.

As example, SAE J287 (2007) does not describe how exertive an attainable reach will be, so there is no guidance how to optimize the control location within the reach zone (Reed et al., 2003a) to minimize reach discomfort. Reed et al. (2003a) present an approach for modeling reach capability and difficulty for push button reaches. In this study effects of the location of the target (push button) on the level of reach difficulty were documented. The model cannot directly be transferred to handbrake design due to the differences between handbrake application and pushing buttons.

Modern vehicles have a high standard of occupant package. Comfort is recognized as a major selling argument and an important factor in product buying decisions (de Looze et al., 2003). Vehicle manufacturers aiming to develop vehicles positively outstanding from competitors regarding the use of controls, require a deeper understanding how to minimize discomfort and maximize comfort.

To design car controls which can be used comfortably by the majority of the target customer group and to minimize discomfort, a deeper understanding and analysis of the control task is required. The effect of the following factors on the discomfort perception needs to be understood:

- Control location.
- Target population.
- Button/handle execution.
- Application forces.
- Resulting movement.
- Other influencing factors.

In the development of the control, it might be possible to refer to some literature for some of the influencing factors. However, often (expensive) subjective evaluation studies and/or application of Digital Human Models are required to allow for data driven decisions to pursue optimized ergonomics.

This chapter (2.10.3.1) focused on standards and guidelines of vehicle package including reach to controls. In the next chapter (2.10.3.2) guidelines for the evaluation of working processes are presented.

2.10.3.2 Key indicator methods for manual handling operations

Discomfort is influenced by the physical characteristics of the task (de Looze et al., 2003). To prevent injuries and disorders in workplace design, the physical characteristics of tasks need to be assessed regarding the risk of physical overload and for the discomfort they might cause (Steinberg, Caffier, Schultz, Jakob & Behrendt, 2007).

In occupational science, there are many key indicator methods for risk assessment. They can be applied to describe job demands and strains to assess the risk of physical overload. Examples are the Job Strain Index and the Occupational Repetitive Actions-Risk Index. (Steinberg et al., 2007)

According to Steinberg et al. (2007, p. 6) typical indicators are:

- *“Duration of task per working day*
- *Action forces, manner, level, frequency/duration of application*
- *Posture and movement of head, trunk, legs*
- *Posture and movement of finger, hand, arm, and shoulder*
- *Organisational requirements as timing, breaks, and work flow*
- *Work environment with reference to strain on upper extremities, as coldness.”*

Steinberg et al. (2007) state that publications about the risk assessment for repetitive hand-arm movements are in agreement that biomechanical, physiological-metabolic and tolerability criteria are relevant. So, duration, frequency, weight of external loads, postures and movements define the strains. Regarding the assessment methods, Steinberg et al. (2007) underline that a consensus is hardly to recognize. There is a large range of indicators used across the 37 key indicator methods they studied.

Cause and effect structures of the methods and models are often not specified (Steinberg et al., 2007). The main aim of these methods is to prevent disorders (rather than to prevent discomfort). Thus, it will be difficult to apply them in product design to prevent discomfort. However, criteria which have an influence on the prevention of disorders are assumed to have an influence on the discomfort perception as well.

Similarly, there are a lot of indicators which can be used for evaluating discomfort of a product. An additionally complicating detail is that the potential user groups of many products have a wider spread of characteristics (e.g. age) than typically existing in working populations.

2.10.4 Handbrake lever design

This chapter is about handbrake design and terminology.

Figure 2.44 illustrates where the handbrake application force F is measured. FAP is the force application point. Its location is defined by dimension a (40 mm) in FMVSS 135 (2012).

In plan view, the handbrake is typically parallel to the longitudinal axis of the vehicle or close to it. α describes the side view orientation of the lever in the fully released location. The geometry of the handbrake lever is not regulated. So, manufacturers can define the location of the handbrake in the vehicle (within the legally specified space, see 2.10.2) and the geometrical dimensions of the handbrake lever and grip area (handle).

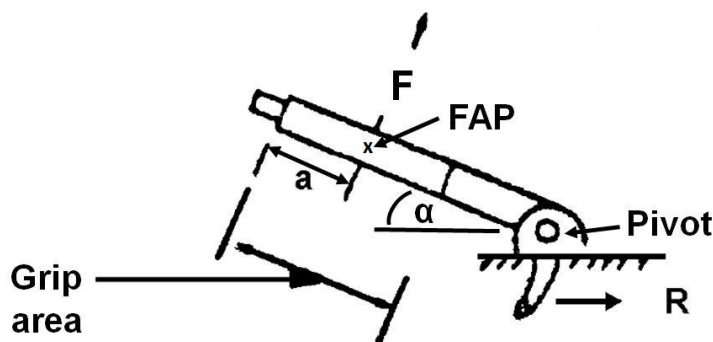


Figure 2.44: Illustration of the handbrake lever centerline y-section. Modified from FMVSS 135 (2012, p. 27).

When a handbrake is applied, the application force increases with the travel (also named application angle) as shown in Figure 2.45.

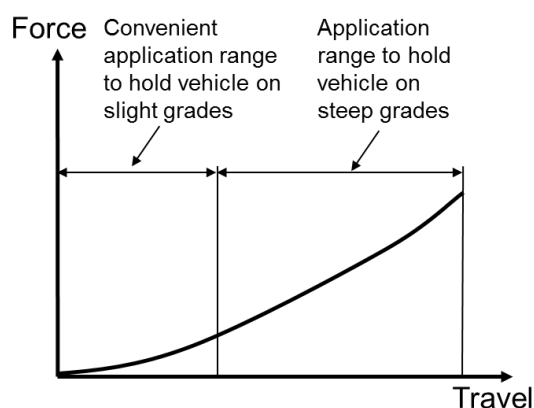


Figure 2.45: Illustration of handbrake application force versus handbrake travel.

The convenient application range covers so-called daily use: to hold the car on a slight grade. The shape of curve is not regulated, so the manufacturers can define it.

The legal requirements only roughly define the location of the handbrake (it has to be operable from driving seat) and the maximum application force (to hold the vehicle on 20 % gradient). So, vehicle manufacturers can define a wide range of details such as handbrake location, geometry (lever length, handle length, installation angle) and force travel curve. Thereby, they can influence the handbrake ergonomics and discomfort perception.

2.10.5 Relevance of the handbrake design

In this chapter the background is explained why handbrakes (hand operated park brake levers) are still important in this day and age with the availability of the Electronic Park Brake (EPB, hand operated electrical switch to activate the park brake). Furthermore, the reasons are provided why it is worthwhile for the car manufactures to optimize handbrake ergonomics and minimize discomfort although it is not legally prescribed.

Some customers do not like EPBs as they appreciate the feedback (tactile and aural) by a lever. EPBs are more expensive than levers. This is especially important for the continued existence of handbrake levers because an increasingly large number of cars is sold in emerging markets where customers mainly choose low-cost vehicles. Still, most vehicles have hand operated mechanical park brakes.

In different regions of the world, people have different habits when to apply the park brake. So, in UK learner drivers are trained to apply the park brake anytime when they have stopped the vehicle at intersections or traffic lights, even on plane ground.

During the development of a vehicle, handbrake location and geometrical design are often in focus of discussions. They are contributed by:

- The design and layout of different elements in the center console (shifter, armrest, cup holders, air ducts etc.)
- Ergonomic respectively discomfort considerations (e.g. reach, clearance, accessibility of handbrake and surrounding controls such as the shifter)
- Numerous attributes (e.g. styling/aesthetics, roominess perception).

Beyond, manufacturing and cost aspects have to be considered.

So, trade-offs between several elements and attributes are common. Therefore, it is essential to understand how much the customer discomfort perception of the handbrake application will change depending on handbrake design and location.

Compliance to all applicable legal requirements (2.10.2) is a prerequisite to sell the vehicle but not sufficient to reduce discomfort of handbrake application. Thus, SAE standards, e.g. for hand control reach SAE J287 (2007), anthropometric tables and ergonomic guidelines – e.g. for application forces (DIN 33411-4, 1987; Schmidtke, 1993) – help to meet basic needs of vehicle occupants.

In the development process, alternative handbrake lever locations and/or geometrical designs have to be assessed regarding their discomfort. The alternatives often differ only slightly, e.g. for location, lever length, installation angle. The above mentioned regulations, standards and guidelines usually do not allow assessing the effect of these variations on discomfort perception of the target customers or subgroups of them (e.g. 5th percentile females or 95th percentile males).

Studies with subjects – to evaluate alternative handbrake designs – are resource consuming. They may lack of reproducibility and objectivity. Also physical prototypes are hardly available at early stages of vehicle development.

Assessments with Digital Human Models don't have these disadvantages. They enable fast, efficient, reproducible and objective evaluations, assessments at early stage of development and comparisons of several variants. (Upmann & Raiber, 2014)

2.10.6 Discomfort perception of handbrake application

Figure 2.9 (p. 16) illustrates in the model of comfort and discomfort by Vink & Hallbeck (2012). According to this model the following factors

1. The human (person),
2. The product,
3. Product usage characteristics and
4. Further characteristics, e.g. the environment

can influence the perception of discomfort and lead to musculoskeletal complaints.

Figure 2.46 shows those characteristics with regards to the discomfort of the handbrake application.

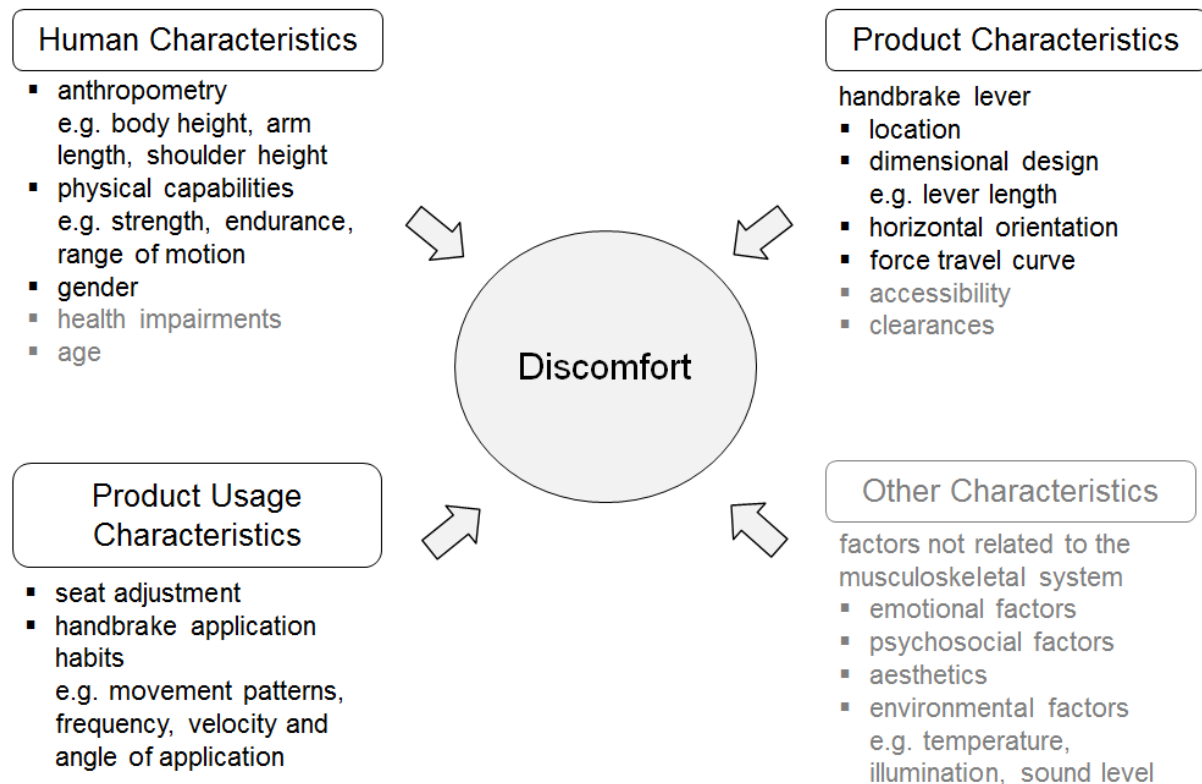


Figure 2.46: Characteristics influencing discomfort perception of handbrake application.

Items shown in grey letters are not in focus of this study. This investigation focuses on the analysis of the musculoskeletal load during handbrake application and its correlation to subjective perception of discomfort. The musculoskeletal load is influenced by kinematics (posture, motion; simulated with RAMSIS) and kinetics (external forces leading to internal load; simulated with AMS).

2.10.7 Conclusions

While a discomfort assessment of the handbrake application with DHMs early in the development process would be highly beneficial, no procedure or metric has been documented so far.

3 RESEARCH PROBLEM AND OBJECTIVE OF THE THESIS

3.1 Research problem

Comfort is recognized as a major selling argument and an important factor in product purchasing decisions (Hartung, 2006). So, manufacturers, aiming to develop vehicles positively exceeding competitors by maximizing comfort and minimizing discomfort in the use of controls, need a deeper understanding how to do so.

In the past mainly subjective evaluation studies were conducted to assure an ergonomic design of vehicles. Meanwhile the number and use of Digital Human Models (DHMs) has increased. Thus, the number of resource intensive subjective evaluations is reduced. DHMs allow for objective, efficient and fast evaluations as well as for assessments and comparisons of several variants at early stage of development (Geuß, 1995; Naumann & Rötting, 2007; Upmann & Raiber, 2014).

Several papers have shown that discomfort is linked to biomechanical parameters and the musculoskeletal system (Zhang et al., 1996; Helander & Zhang, 1997; Kyung, 2008). Consequently, the evaluation with DHMs has to include the analysis of the musculoskeletal load which is influenced by kinematics (posture, motion) and kinetics (external forces leading to internal load) (Chaffin et al., 1999a).

A lot has been published on biomechanical parameters influencing reach posture and reach discomfort as well as their prediction with DHMs, e.g. Jung & Choe (1996).

However, little has been documented about handbrake operation – although the handbrake is an essential and safety relevant control in vehicles. Available requirements and standards are not sufficient to minimize discomfort of handbrake application.

For handbrake application, there is no useful information available one

1. The movement strategies of drivers applying the handbrake,
2. The simulation/prediction of these movements,
3. The factors influencing the perception of discomfort when applying the handbrake and their effects,
4. The prediction of discomfort for handbrake application via DHMs and/or mathematical modeling.

3.2 Objective of the thesis

The aim of this thesis is to remedy these deficiencies by the development and validation of a Computer Aided Engineering (CAE) procedure for handbrake discomfort assessment. A flowchart of such a procedure is illustrated by Figure 3.1.

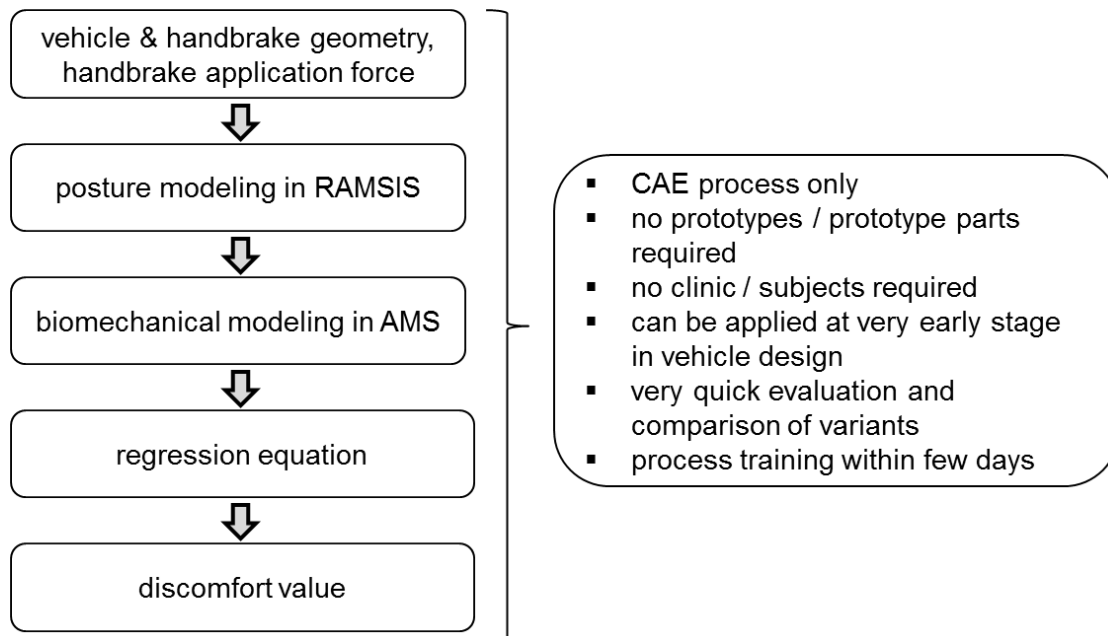


Figure 3.1: CAE procedure to be developed in the course of this work.

The procedure is intended to consist of the following steps:

- For a given vehicle and handbrake geometrical design, the handbrake application postures of key manikins are modeled in RAMSIS.
- In AMS, the postures are combined to a movement, force characteristics are added and the resulting biomechanical parameters are calculated.
- Based on them and a regression equation, a discomfort value can be calculated for the user group and key users.

Such a procedure can only be established if the working hypotheses (stated in chapter 3.3) are tested and confirmed by a multi-step approach (described in chapter 4).

3.3 Hypotheses

To divide the overall task into several steps, subordinate objectives and corresponding working hypotheses are derived from the objective of the thesis.

The overall objective can only be achieved, if all five working hypotheses are tested and confirmed:

1. **Discomfort Feel:** subjects feel different levels of discomfort when applying handbrakes sufficiently different for location and they are able to rate discomfort reproducibly.
2. **Movement patterns:** handbrake application movements follow one or more patterns.
3. **Movement simulation:** handbrake application movement pattern(s) can be simulated using key postures in RAMSIS.
4. **Discomfort correlations:** there are correlations between biomechanical parameters calculated with AMS (based on RAMSIS postures) and the discomfort ratings derived from a corresponding subjective evaluation study.
5. **Discomfort prediction:** combination of selected biomechanical parameters allows predicting discomfort for the target customer population and key subgroups.

4 DESIGN OF THE STUDY

To test and confirm the working hypotheses and develop the described procedure, it is required to run a multi-step investigation, see

Figure 4.1. After each step, related hypotheses are checked and in case of confirmation the next step can follow.

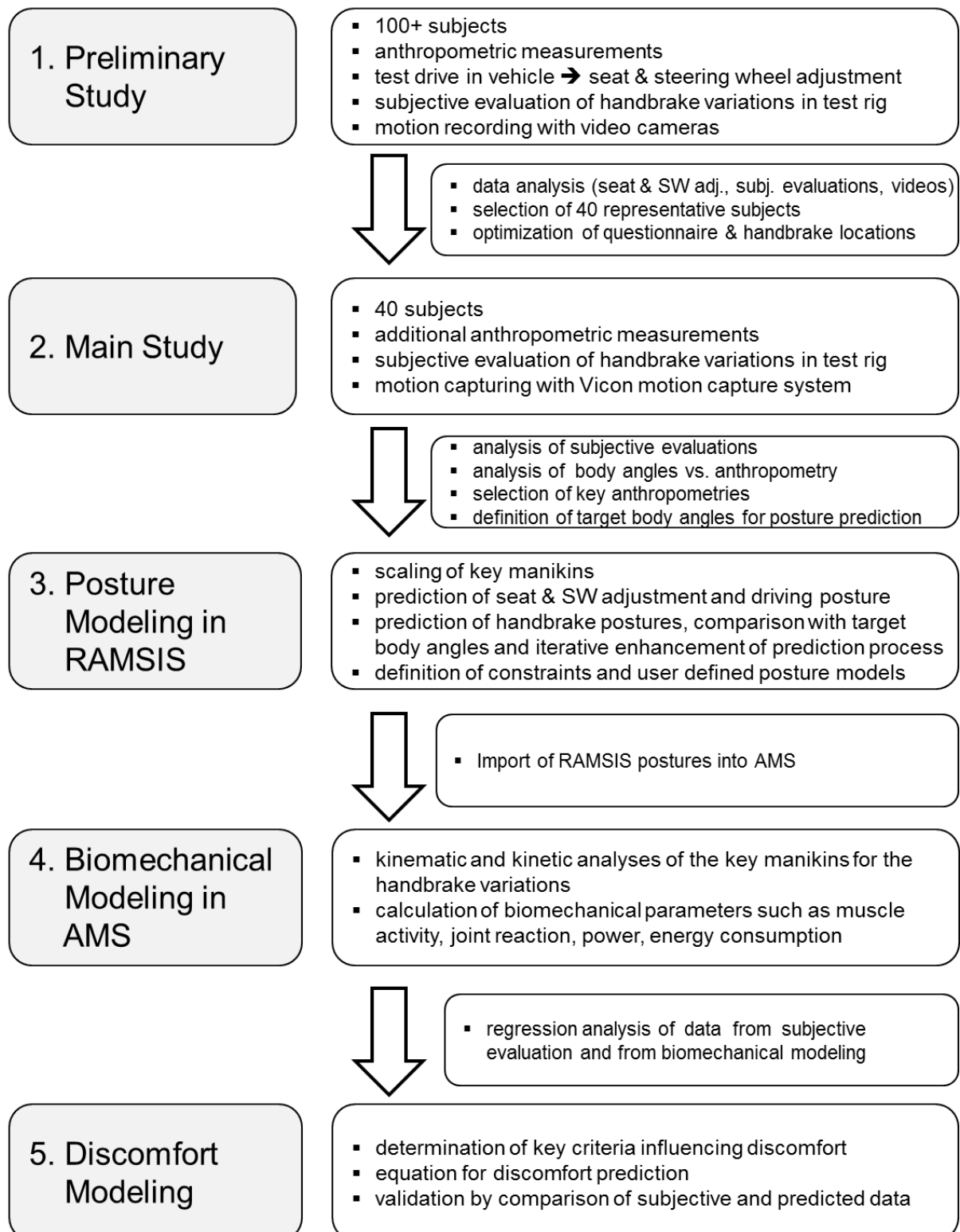


Figure 4.1: Process to reach the objective of this dissertation.

With the preliminary study (step 1), the working hypotheses 1 (discomfort feel) and 2 (movement patterns) are tested by having a large group of subjects evaluating different handbrake variations while their motion is recorded with video cameras. To create different handbrake variations, the location of the handbrake lever is altered. The varying handbrake locations lead to different postures respectively movements so that the biomechanical load changes. This is assumed to be reflected in the subjects' discomfort ratings (Zhang et al., 1996).

If both hypotheses are confirmed, a smaller number of representative subjects assess different handbrake locations in the main study (step 2). Their motion is recorded more accurately with Vicon cameras. Hypotheses 1 and 2 are checked again.

In case of confirmation, RAMSIS is applied to simulate the movement by calculating key postures (step 3). Hypothesis 3 (movement simulation) is checked.

If hypothesis 3 is confirmed, AMS is applied to calculate biomechanical parameters which subsequently are correlated to the subjective ratings (step 4). Hypothesis 4 (discomfort correlation) is checked.

In case of confirmation, mathematical modeling is applied (step 5) and hypothesis 5 (discomfort prediction) is tested. If this hypothesis is also confirmed, a CAE procedure for handbrake discomfort assessment can be proposed and the aim of this thesis is achieved.

The following chapters describe each of the steps.

5 PRELIMINARY STUDY

In the preliminary study, a large number of subjects (5.1.5) evaluated 7 different handbrake locations in a test rig referred to as ErgoBuck (5.1.3). The ratings were analyzed. Participant's postures for particular key frames were studied for the handbrake at mid location.

Prior to the evaluation in the ErgoBuck the subjects performed a test drive in a passenger vehicle (5.1.2) to record preferred seat and steering wheel adjustment and transfer them to the ErgoBuck.

The four main aims of the preliminary study were:

1. To test if the subjects feel different levels of discomfort for the varying handbrake locations and if they are able to rate reproducibly (hypothesis 1).
2. To determine if the handbrake application movements follow patterns (hypothesis 2).
3. To select subjects – representative for movements patterns and capable to rate reproducibly – for the main study.
4. To evaluate the questionnaire and experimental setup to allow for enhancements for the main study.

The preliminary study was conducted with support of the Institute of Biomechanics and Orthopaedics (IBO), German Sport University Cologne, Germany.

This chapter is based on the reports and master theses completed in the context of this project (Lietmeyer, 2013; Heinrich et al., 2014; Rausch & Upmann, 2015b; Rzepka, 2015).

In the following, at first the study design (5.1.1), test vehicle (5.1.2) and ErgoBuck (5.1.3) are described and the handbrake locations are provided (5.1.4). Then the selection of the subjects is explained (5.1.5). After describing the procedure of the experiment (5.1.6), the statistical analysis (5.1.7) and results (5.2) are summarized. A discussion of the preliminary study (5.3) concludes this chapter.

5.1 Methods

5.1.1 Study design

A cross-sectional experimental design was used with randomized order of the trials.

In the factorial design, the independent variables were:

- Handbrake location in x (fore-aft respectively anterior-posterior direction).
- Handbrake location in y (left-right respectively medial-lateral direction).
- Handbrake location in z (height respectively inferior-superior direction).

For each variation of the independent variables, the following dependent variable was determined for each subject:

- Discomfort rating.

A 2² factorial design with center point repetition (Backhaus, Erichson, Plinke & Weiber, 2006) was used for handbrake location in x and z. Two more handbrake locations resulted from shifting the center point in y in medial and in lateral direction (for details see 5.1.4).

For the center point handbrake location, additionally the joint angles/position of the subjects for start and end of handbrake location were determined to enable clustering the subjects into groups of movement patterns.

Subject characteristics which can also have an effect on the discomfort ratings and joint angles/positions are described in 5.1.5.

5.1.2 Test vehicle

Drivers' seating position (including seat adjustment) is the consequence of the selected driving posture and defines the relative position of a person to the handbrake. Accordingly, it will influence the movement and discomfort assessment for the handbrake operation. Also, the steering wheel adjustment/position reflects the driving posture. To determine the individually selected driving posture respectively corresponding seat and steering wheel adjustments/positions, it is required that the subjects drive a vehicle in a typical environment.

For that purpose, a passenger vehicle with electronic park brake (EPB) was equipped with scales to measure the seat and steering wheel adjustment. By consciously choosing a vehicle with EPB, any potential effect of handbrake lever and its location on the individual seat and steering wheel adjustments/positions was avoided.

5.1.3 Testrig ErgoBuck

The Ford-owned ErgoBuck (Sendler & Kirchner, 2012) was chosen as test rig as it provides an adjustable package allowing for the required range of adjustments (Figure 5.1).



Figure 5.1: ErgoBuck adjusted to the test vehicle main package dimensions.

Location, motion ranges and application force characteristics of the controls (e.g. steering wheel, pedals and handbrake) can be adjusted and recorded.

State-of-the-art hardware and software enable to log time, forces and motion of operating elements and additional data such as motion recording. Trigger signals are used to synchronize the measurements. For details refer to Sendler & Kirchner (2012).

The ErgoBuck was adjusted to represent the test vehicle including the same seat and steering wheel adjustment scales. So the participants' seat and steering wheel adjustments/positions in the test vehicle could be transferred easily and accurately to the ErgoBuck. Figure 5.2 shows the scales for longitudinal and vertical seat adjustment.



Figure 5.2: ErgoBuck seat adjustment scale for longitudinal and vertical direction.

The handbrake unit of the ErgoBuck can be adjusted in x, y and z directions by spindles as illustrated in Figure 5.3. For quick adjustment, a power tool can be used.

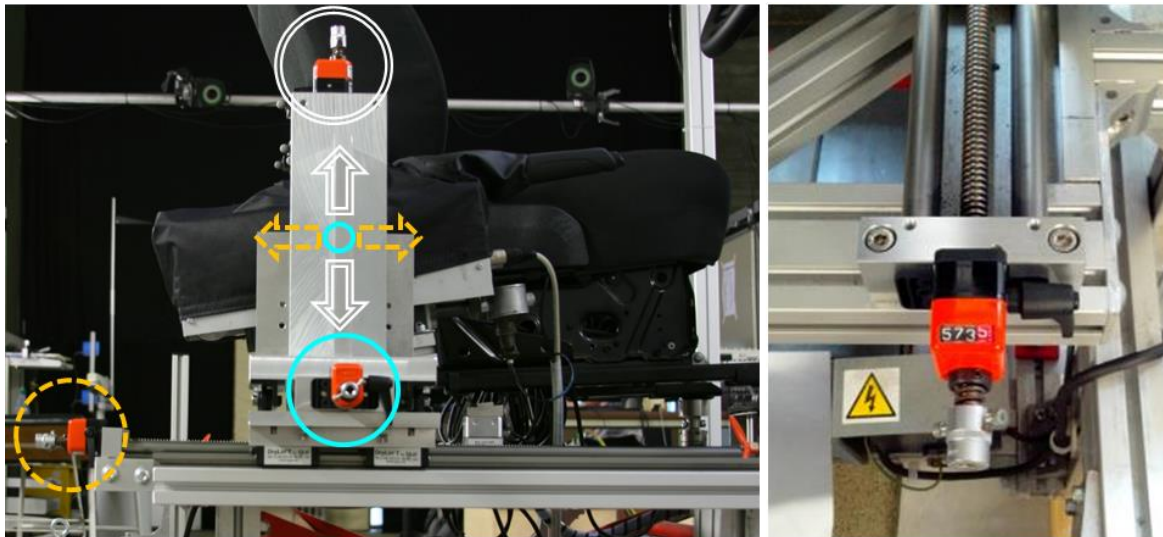


Figure 5.3: Handbrake adjustment unit based on three spindles. Longitudinal (x) direction shown in dashed orange line, transverse (y) in blue line, vertical (z) in double white line.

Force sensors inside the handbrake mechanism allow for measuring the application forces in all three axes. A potentiometer enables measuring the application angle and corresponding travel of the lever. The force travel curve of the handbrake lever can be modified with different spring assemblies inside the handbrake unit. In this investigation, a Ford typical characteristic was used. The geometrical design of the utilized handbrake lever is also typical for Ford vehicles.

5.1.4 Handbrake locations

Each handbrake location is defined by the coordinates of the force application point (FAP, Figure 2.44 on p. 106) in released state of the handbrake. In the preliminary study, the handbrake application was rated for seven handbrake locations which are illustrated in Figure 5.4 and listed in Table 5.1. The locations were selected based on a study conducted by Ford GmbH (Yilmaz et al., 2012). The midpoint (location 1) is used as the origin of the FAP coordinate system. The directions of x, y and z are defined by the vehicle coordinate system as shown in Figure 2.42, p. 102 (Society of Automotive Engineers, Inc. J1100, 2009).

Five of the seven locations are in the $y = 0$ plane and form the corners of a rectangular range (locations 2, 3, 4, 5) and its midpoint (location 1, 8). This experimental design is called 2^2 factorial design with center point: two factors (x and z locations) are varied at two levels (Backhaus, Erichson, Plinke & Weiber, 2006).

Two more locations resulted from shifting the center point in y direction by 25 mm. Location 6 is closer to the occupant; location 7 is farther away from the occupant.

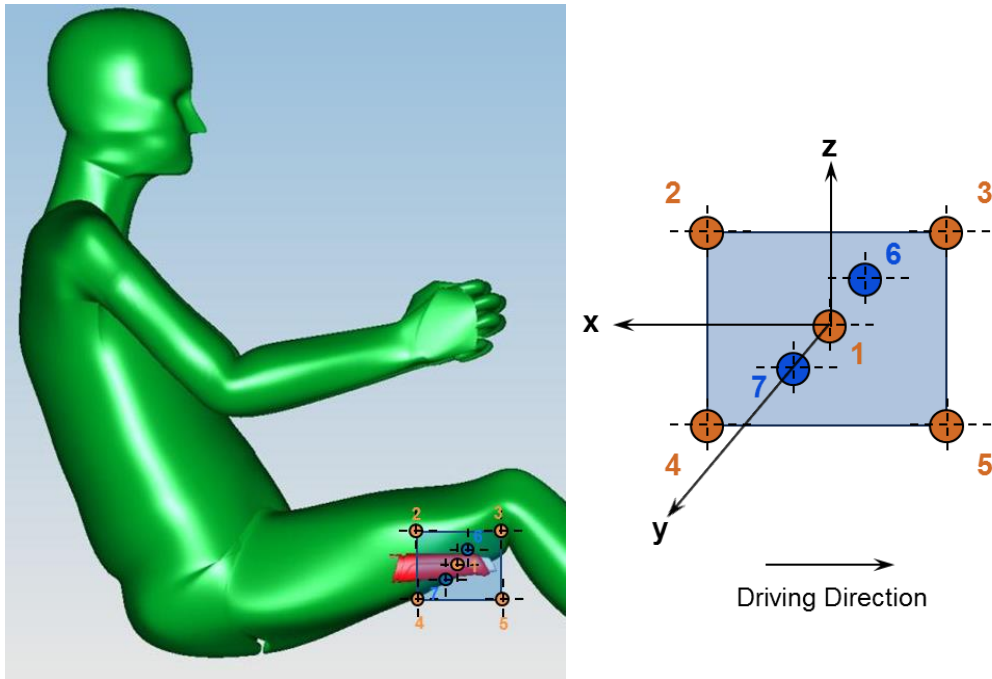


Figure 5.4: Illustration of the investigated handbrake FAP locations in the preliminary study.

Table 5.1: Coordinates of the investigated FAP locations.

FAP coordinates [mm]			
Location	x	y	z
1 (8)	0	0	0
2	46.5	0	40
3	-46.5	0	40
4	46.5	0	-40
5	-46.5	0	-40
6	0	-25	0
7	0	25	0

The handbrake adjusted to the center point was assessed twice (as location 1 and 8 in a randomized order) without the subjects being aware, to check repeatability of their ratings. At least two other locations were evaluated between both center point location assessments.

The order of all handbrake location assessments was randomized to minimize effects of order.

5.1.5 Subjects

Online, newspaper and public announcements were published to recruit subjects. 117 subjects were included from more than 400 responses based on defined criteria surveyed in phone interviews.

Preconditions to participate were:

- Body height for females between 1.50 m and 1.78 m.
- Body height for men between 1.67 m and 1.99 m.
- Possession of a valid driving license plus a minimum driving experience of twelve months.
- Age between 19 and 80 years.
- BMI < 30.
- No acute issues with the musculoskeletal system, no acute pain.
- No injuries/surgeries of the musculoskeletal system for the last twelve months.
- Sufficient German language knowledge.

The body height ranges were based on the SizeGERMANY (2012) database to represent the range of driving population. Particular attention was paid to recruit a sufficient number of subjects in the perimeter areas of body height range (small females and tall men).

Subjects between 19 and 80 years were invited to cover the main healthy driver population. Older drivers were excluded as the variability of physical and mental abilities increases with age. Volunteers with a BMI larger 30 were excluded to avoid in-accuracy in the motion capturing applied in the main study.

The subjects were divided into six groups based on their gender and body height. Even distributions of body height were targeted within the groups. Similar distributions regarding BMI, age and physical activities between the groups were intended. However, the average age of groups with subjects of smaller stature was higher because younger people are usually taller than elderly ones, see Table 5.2.

Sport and other physical activities (e.g. gardening, domestic work and job related physical activities) were documented. It was intended to have a mix of more and less physically active people in each group to represent typical driving population.

Sufficient German language skills were a precondition as the study was conducted in German language.

Table 5.2 shows the characteristics of the subject groups (52 female and 59 male subjects in total) without the six subjects which were excluded from the analysis at a later point in time due their strongly different movement patterns (see 5.2.2.1).

Further characteristics were recorded by questionnaires and anthropometric measurements in each, the preliminary study and the main study.

Table 5.2: Characteristics of the subject groups.

Group		1	2	3	4	5	6
Description		Small females	Medium females	Tall females	Small males	Medium males	Tall males
# Subjects		20	16	16	19	20	20
Body height [m]	Min.	1.50	1.59	1.67	1.67	1.79	1.88
	Max.	1.58	1.66	1.78	1.77	1.87	1.99
	Mean	1.54	1.62	1.72	1.72	1.83	1.91
	SD	0.03	0.02	0.03	0.03	0.03	0.04
BMI [kg/m ²]	Mean	23	23	24	26	26	24
	SD	3	3	3	2	2	2
Age [years]	Mean	51	45	39	57	51	45
	SD	14	15	15	13	12	15
Activity [hours/week]	Mean	16	21	14	19	17	15
	SD	12	14	6	13	10	9

5.1.6 Procedure

The subjects were selected as described above. Each of them was invited for an appointment of 1.5 to 2 hours to an Institute of Biomechanics and Orthopaedics (IBO) laboratory where the ErgoBuck was installed. They received information about the procedure of the study and were explained that they could abort the investigation at any time. They gave their consent in written form.

The subjects filled in a pre-questionnaire (5.1.6.1). In a test drive, their seat and steering wheel adjustments/positions were recorded (5.1.6.2) to be transferred to the ErgoBuck. Anthropometry and other characteristics were measured (5.1.6.3). Then, the evaluation of the different handbrake locations took place in the ErgoBuck while the subjects' motion was recorded with video cameras (5.1.6.4). Finally, the subjects filled out a post-questionnaire.

5.1.6.1 Pre-questionnaire

With the pre-questionnaire, the subjects provided information on their demographics (gender, age), anthropometry (body height, weight), occupation, health and physical activities. It was reconfirmed that the preconditions for participation in the study – which initially had been checked in phone interviews – were still fulfilled. The pre-questionnaire is shown in the appendix (14.2.1).

5.1.6.2 Test drive

The test drive took place in Cologne with a Ford passenger vehicle (see 5.1.2) to record the individual's seat and steering wheel adjustment/positions. In the ErgoBuck,

important references such as the hood, pillars or roof are missing. Visibility conditions have an impact on the adjustments. Therefore, it was considered important to expose the subjects to driving in a real vehicle and to everyday driving scenarios.

The drive included streets with different speed limits, intersections and roundabouts as well as parking. It took 15 to 20 minutes. The subject was accompanied by the study leader.

The route was the same for all subjects, the traffic situation could differ. During the drive, subjects were offered multiple opportunities to readjust the seat and steering wheel. At the end of the drive the adjustments/positions were recorded by the study leader.

5.1.6.3 Anthropometric measurements

For statistical purposes, several anthropometric measures were taken: body weight, body height, shoulder height seated, sitting height, upper arm length, forearm length with hand, hand length and forward reachability. Additionally, the body composition was measured using the bioelectrical impedance analysis method. Details are described in the project reports (Heinrich et al., 2014; Rausch & Upmann, 2015b).

5.1.6.4 Handbrake application

5.1.6.4.1 Procedure

In the laboratory with the ErgoBuck, the boundary conditions (e.g. light, temperature, noise conditions) were kept constant to avoid affecting the subjective perception ratings. Prior to each subject's handbrake evaluations, the seat and steering wheel adjustment/position from the test drive vehicle was transferred to the ErgoBuck.

The subjects sat down on the ErgoBuck seat. They were instructed to adopt a posture as if they had just stopped the car with the right feet on the brake pedal, the left foot on the footrest and both hands on the steering wheel. Starting from this original posture they were instructed to pull the handbrake as if they park the vehicle on a slight grade. An acoustic signal was used to inform the subjects when the corresponding level of handbrake application was reached. After pulling the handbrake, the subjects were instructed to return their hands back to the steering wheel.

For each of the handbrake locations (see 5.1.4) the subjects had to reach the target application level three times. They had a maximum number of 6 trials. If required, the study leader informed the subject how much more or less than required they had pulled.

Prior to the actual subjective evaluations, the subjects conducted test trials (location 1, see Figure 5.4) to familiarize themselves with the required application level.

For each handbrake location, the subjects documented their ratings.

As described above, the order of the eight handbrake assessments (7 locations plus the repetition of the center point) was randomized. The first and the second assessment of the center point were timely separated by the evaluation of at least two other handbrake locations. The handbrake location changes were done so that the subjects could not see direction(s) of the change.

5.1.6.4.2 Subjective evaluation questionnaire

For each handbrake location the subjects were asked five questions (listed in Table 5.3) to rate the handbrake application. They indicated their perception by a mark on a continuous scale shown in Figure 5.5 (for evaluation of visual analog scale see 2.4.1).

Table 5.3: Overview of questions, original wording in German is italic.

Question	Left anchor	Mid anchor	Right anchor
Q1 How do you like the handbrake application? <i>Wie finden Sie die Betätigung der Handbremse?</i>	very good <i>sehr gut</i>	neutral <i>neutral</i>	very poor <i>sehr schlecht</i>
Q2 How would you rate your physical load during the application of the handbrake? <i>Wie bewerten Sie die körperliche Belastung bei der Betätigung der Handbremse?</i>	no load <i>keine Belastung</i>	medium load <i>mittlere Belastung</i>	maximum load <i>maximale Belastung</i>
Q3 How do you rate the above mentioned load in relation to your expectations? <i>Wie beurteilen Sie die o.g. Belastung im Vergleich zu Ihren Erwartungen?</i>	considerably less <i>deutlich geringer</i>	neutral <i>neutral</i>	considerably higher <i>deutlich höher</i>
Q4 How do you perceive the physical load? <i>Wie empfinden Sie die Belastung?</i>	very pleasant <i>sehr angenehm</i>	neutral <i>neutral</i>	very unpleasant <i>sehr unangenehm</i>
Q5 How do you rate the application of the handbrake wrt to perceived discomfort? <i>Wie beurteilen Sie die Betätigung der Handbremse hinsichtlich des empfundenen Diskomforts?</i>	no discomfort <i>kein Diskomfort</i>	medium discomfort <i>mittlerer Diskomfort</i>	maximum discomfort <i>maximaler Diskomfort</i>

This scale enables a continuous mapping of the subjects' perception and has already been extensively applied for comfort and discomfort evaluation of chairs and seats (Shen & Parsons, 1997; de Looze et al., 2003). This type of scale was also applied in Krist (1993) as the foundation of the RAMSIS discomfort assessment.

The scales had three anchor points, the mid was marked as neutral, the ends were labelled with corresponding descriptors. The scales for all locations were shown on the same page (see Figure 5.5) so that the subjects could refer to their previous ratings.

1. How do you like the handbrake application?

neutral

01	very good	_____	very poor
02	very good	_____	very poor
03	very good	_____	very poor
04	very good	_____	very poor
05	very good	_____	very poor
06	very good	_____	very poor
07	very good	_____	very poor
08	very good	_____	very poor

Figure 5.5: Question Q1 with rating scales for all handbrake locations.

For the statistical analysis the marks on the scales were converted into numbers. For this purpose, the distance from the mark to the left anchor was divided by the total length of the scale. The result was rounded to an integer. The left anchor point is equivalent to the value 0 and indicating low discomfort (best rating). A mark coincident with the right anchor point is equivalent to a 100 and indicating high discomfort (worst rating).

5.1.6.4.3 Analysis of joint locations and angles from videos

Three synchronized video cameras (side view, front view and top view) were used to record the handbrake application movements. Subsequent analysis of relevant joint locations and angles was completed based on the first valid trial of the center handbrake location for released (key frame “start”) and pulled (key frame “end”) state. Details are provided in Rzepka (2015).

The following joint angles/positions were analyzed:

- Shoulder: abduction and anteversion/retroversion of the arm; vertical and dorsal-ventral position
- Elbow: flexion, abduction; vertical, dorsal-ventral, medio-lateral position
- Wrist: abduction.

These movement variables are described in more detail in appendix 14.2.2, p. 238 ff.

Movement strategies were identified based on them. Six subjects were excluded from further analysis because their movement patterns were significantly different from all other subjects.

5.1.6.5 Maximal force measurement and post-questionnaire

An isometric maximum arm force (F_{\max}) measurement was completed as the only measure performed after the subjective evaluation of the handbrake application. The measurement is described in the project reports in detail (Heinrich et al., 2014; Rausch & Upmann, 2015b).

In a post-questionnaire each subject provided information on his/her personal vehicle and its park brake, driving experience and handbrake application habits. The questionnaire is presented in appendix 14.2.3., p. 244.

5.1.7 Data analysis

The statistical analysis was completed with Matlab (2011b), Excel (2010), SPSS (21) and Minitab (15) using conventional methods (Backhaus et al., 2006; Rumsey, 2008; Montgomery, 2013).

As the discomfort ratings of the 2^2 factorial design with repeated center point were not normally distributed, a major precondition for analysis of variance (ANOVA) was not fulfilled (Backhaus et al., 2006). Consequently, the non-parametric Kruskal-Wallis test (Montgomery, 2013; Minitab, 2015) was used to analyze if the discomfort ratings (medians) for different handbrake locations differ significantly. The Kruskal-Wallis test allows comparing two or more samples at once.

The cluster analysis method is described briefly below. It was used to determine how the subjects were grouped into movement strategy clusters based on the movement variables. The cluster analysis of this project is described in detail in Heinrich et al. (2014) and Rzepka (2015).

5.1.7.1 Cluster analysis

Cluster analysis is a statistical method to classify similar objects into groups. From a heterogeneous entirety of objects more homogeneous subsets are identified (Gutfleisch, 2008).

Several parameters describing the postures (see 14.2.2, p. 238 ff.) of the 117 subjects for the central handbrake locations at the start and end of handbrake application were utilized in the cluster analysis. Aim was to divide the subjects in an appropriate number of clusters so that each cluster contains subjects with similar movement patterns, which can be characterized.

The cluster analysis, described in Backhaus et al. (2006), was applied in two work steps: In the first work step, the single linkage method was applied to identify outliers.

Additionally, different cluster methods were executed to determine the most appropriate type of cluster analysis and select the relevant variables. In the second work step, the selected cluster analysis type was applied and subjects were grouped into clusters of movement patterns.

Hierarchical agglomerative merging algorithms were applied. These algorithms begin with the smallest partitions which are further summarized step by step. (Backhaus et al., 2006)

Each step consists of:

1. Determination of similarities: values of the variables are compared between two subjects at a time. Differences and conformities are described by proximity values in the so-called "distance matrix".
2. Selection of the merging algorithm: the merging algorithms group the subjects based on the proximity values until all of them are in one group.
3. Determination of the number of clusters: a compromise between ease of handling (low number of clusters) and the demand for homogeneity (high number of clusters) is the aim. (Backhaus et al., 2006)

5.2 Results

5.2.1 Subjective evaluation

The subjects rated by a mark on continuous scale. As the mark on the line is converted to a scale with 100 increments, the data is considered as continuous. The ratings for each question and most data subsets for the handbrake locations are not normally distributed because the Anderson-Darling normality test results in p-values smaller than 0.05 (Table 14.3 and Table 14.4, p. 245). So, it is important to include the median in analyzing effects e.g. of the handbrake locations and of the wording of the questions. The median is more robust to outliers than the mean.

In the following the subjective data will be analyzed to:

1. Determine which of the five questions corresponds to the best differentiation between the ratings for the different handbrake locations.
2. Analyze the influence of the locations on the perceived discomfort to decide if the range of locations is sufficient and hypothesis 1 is fulfilled (i.e. the subjects feel different level of discomfort and are able to rate it reproducibly).

For the analysis of the influence of the questionnaire wording, medians and means were compared. Medians and means were calculated for all questions and locations to

determine their standard deviations (SD) and range (see Table 14.5 Table 14.6, p. 246 and p. 247). Not all means respectively medians are normally distributed (Anderson-Darling-Normality-Tests, Table 14.6, p. 246). Figure 5.6 provides subjective evaluation medians and means for all handbrake locations and questions for the 111 subjects.

Median with 95 % CI and Mean of the Ratings

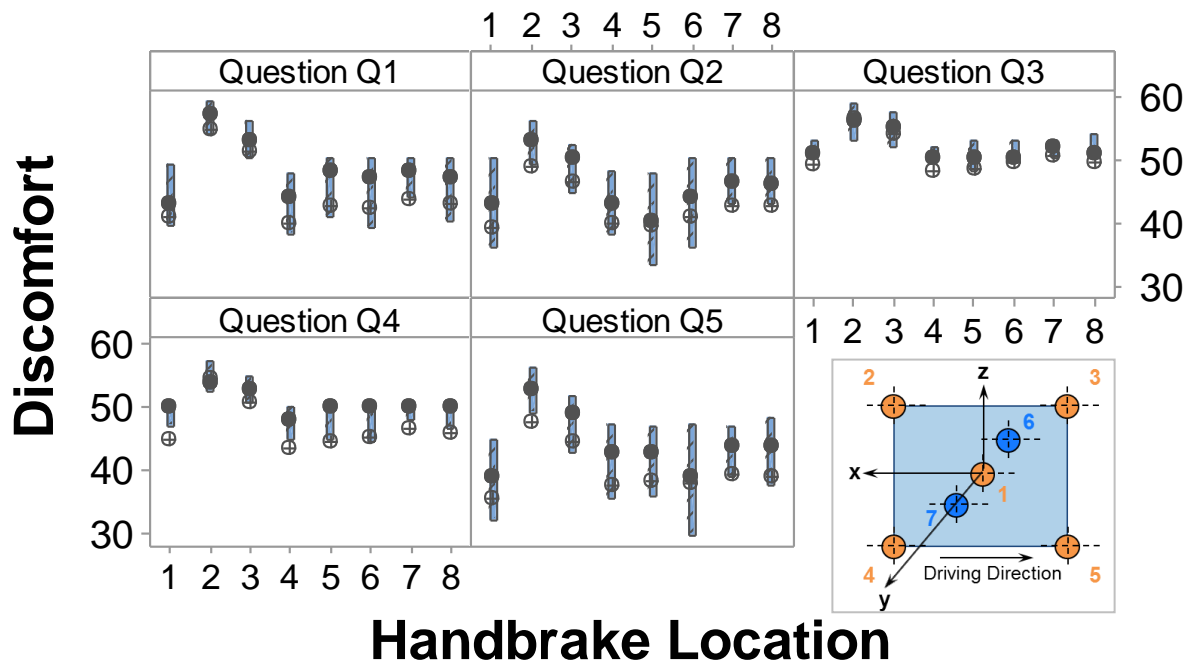


Figure 5.6: Subjective ratings of the preliminary study for all questions. Increasing number indicates increasing discomfort. Right lower corner shows overview of locations (locations 1 and 8 are identical). Filled dot represents median, unfilled to represents mean. Bars represent 95 % confidence interval of median.

The mean is represented by a cross. The median is indicated by a black dot, the bar indicates its 95 % confidence interval for the population median calculated using the 1-Sample Sign command (Minitab, 2015).

Location 1 and 8 are identical and were rated similar. Locations 1, 4, 5, 6, 7 and 8 do not show significant differences as their confidence intervals for the medians overlap. This is also the case for the confidence intervals of the means (Figure 14.15, p. 246).

The chart for question Q1 shows that location 2 and 3 are rated worse than locations 1 (respectively 8), 4, 5, 6 and 7. The confidence intervals for the medians of location 2 and 3 do not overlap with the other confidence intervals. This is only partly the case for question Q2 and Q5.

For question Q1, the data subsets for 5 of the 8 locations are normally distributed. For all other questions, the data subsets of only 0 to 2 locations from 8 are normally distributed (Table 14.4, p. 245).

Questions Q3 and Q4 result in narrower confidence intervals than the other questions. The confidence intervals for the higher locations (2 and 3) and the other locations do not overlap. But both questions result in a high amount of outliers (Figure 14.14, p. 245).

Consequently, question Q1 produces the most meaningful ratings. It has the largest SD and range of median and mean between different locations. So it allows best differentiation of the ratings for the locations.

As not all medians respectively means are normally distributed, Pearson and Spearman's correlations coefficients were calculated to assess the correlations between the ratings of all questions. The correlation coefficients show predominantly strong correlations ($r \geq 0.84$, $p \geq 0.65$) between the ratings of all questions (Table 14.7 and Table 14.8, p. 247).

Based on the visual and statistical analysis, the ratings for question Q1 were utilized for further analysis.

Table 5.4 shows descriptive statistics for question Q1 and each handbrake location. The standard deviations are large for all locations because the subjects rated very differently. As noted above, the medians and means of most ratings for the different locations are very close together. Only locations 2 and 3 show higher perceived discomfort for handbrake application.

Table 5.4: Descriptive statistics for question Q1.

Handbrake Location	Mean	SD	Median	Mode	N for Mode
1	40.95	18.69	43	40	7
2	54.68	19.36	57	54, 62	7
3	51.13	18.74	53	53	7
4	39.57	19.97	44	10	6
5	42.55	19.99	48	48, 52	6
6	42.23	18.87	47	53	7
7	43.67	19.53	48	50	13
8	42.72	19.55	47	50, 54	6

The findings of the visual analysis of Figure 5.6 for Question Q1 were confirmed by the results of Kruskal-Wallis tests:

- There is no significant difference between the ratings for location 2 and 3 (Kruskal-Wallis test A: locations 2 and 3).
- There is no significant difference between the ratings for location 1 (respectively 8), 4, 5, 6 and 7 (Kruskal-Wallis test B: locations 1, 4, 5, 6, 7, 8).

- The ratings for the higher locations (2 and 3) differ significantly from the ratings for all other locations (1, 4, 5, 6, 7 and 8).

For this conclusion, the results of two Kruskal-Wallis tests (test C for locations 1, 4, 5, 6, 7, 8 and 2, test D for locations 1, 4, 5, 6, 7, 8 and 3) were compared to test B.

Consequently, it was decided to increase the range of locations in the main study. Effects of body height on the discomfort ratings for each handbrake location are analyzed in the main study.

5.2.1.1 Reproducibility

To assess the reproducibility, the subject's ratings for location 1 and 8 were compared. The absolute difference between both ratings was calculated for each subject. 6 % of the subjects rated both locations exactly the same, 8 % with a difference of 1 and 5 % with a difference of 2, see Table 14.9 on p. 248. As shown in Table 5.5, 37 % of subjects rated differently by up to 5 and 23 % by 6 to 10. Note: The range of ratings is from 0 to 100 (compare 5.1.6.4.2, p. 125 ff.)

Table 5.5: Difference between the ratings for location 1 and 8.

Absolute difference	Percentage of subjects	Cumulative percentage of subjects
0 to 5	37	37
6 to 10	23	60
11 to 15	17	77
16 to 20	5	82
≥ 21	18	100

5.2.2 Movement patterns

The classification of subjects into clusters of movement patterns was completed by a multi-step approach, which is documented in a project report (Heinrich et al., 2014) and as a master thesis (Rzepka, 2015). It is summarized in the following subchapters.

5.2.2.1 Identification of outliers

Based on the distance matrix, the single linkage method was applied to identify and exclude outliers. Outliers have extreme values in comparison to the sample. They influence the merging and can deteriorate identification of relationships. Therefore they were determined and excluded prior to grouping the subjects into clusters. Six outliers were identified, which is illustrated in the dendrogram in Figure 14.16 on p. 249. In a dendrogram, similar elements are joined by a knot. The more similar the elements are, the closer the knot is placed to them.

Those outliers were excluded from the following steps of cluster analysis and also from the evaluation of subjective evaluation data.

5.2.2.2 Selection of relevant variables

For the selection of relevant movement variables, three merging algorithms were applied: Ward, Complete Linkage and TwoStep. For each of them, solutions with two to four clusters were compared and F-values calculated for the variables. F-values for selected variables are listed in Table 5.6).

Table 5.6: F-values of the Ward method with three clusters for selected movement variables (Heinrich et al., 2014, p. 75).

Cluster	AntRet_A	HG_A	SGv_A	Abd_A	SGh_A	AntRet_E
1	0.32	1.42	1.12	0.26	1.48	0.24
2	0.63	1.18	0.92	0.77	1.09	0.74
3	0.17	0.00	1.13	0.28	0.00	0.20

F-values describe the homogeneity within the cluster. The smaller the F-value, the more homogenous the cluster is regarding a variable. An F-value smaller than one indicates that the variance of the variable in the cluster is smaller than the variance of the complete sample.

The anteversion/retroversion of the upper arm at the start and end (AntRet_A, AntRet_E), the glenohumeral abduction at the start and end and their delta (Abd_A, Abd_E, dAbd) and the vertical movement of the elbow (dESz) lead to homogenous clusters (F-value < 1; highlighted grey in Table 5.6). These variables were selected for the subsequent cluster analysis.

5.2.2.3 Selection of cluster merging algorithm

Table 5.7 shows the averages of the F-values for the selected variables, three merging algorithms and two to four clusters. This range of clusters was expected to balance homogeneity and ease of handling. The Ward method leads to the smallest F-values and consequently to more homogenous clusters than both other methods. Therefore, it was chosen as merging algorithm for the following cluster analysis.

Table 5.7: Averages of F-values for the selected variables (Heinrich et al., 2014, p. 76).

Merging algorithm	Number of clusters		
	4	3	2
Ward	0.38	0.44	0.54
Complete-Linkage	0.47	0.59	0.59
TwoStep	0.53	0.54	0.60

5.2.2.4 Classification of subjects in clusters

The number of movement pattern clusters had to be determined prior to populating them with subjects. Therefore, the Elbow-criterion (Backhaus et al., 2006; Heinrich et al., 2014) was applied and the dendrogram (created with the Ward method, see Figure 14.17 on p. 250) was analyzed. Three clusters were classified.

The values of the variables and the composition of subject characteristics (e.g. anthropometry such as body height) within the clusters as well as the analysis of the t-values (Heinrich et al., 2014) confirmed that three clusters are plausible and meaningful. T-values characterize the representation of variables in the clusters (Backhaus et al., 2006).

5.2.2.5 Analysis of cluster variables

Cluster 1 is characterized by anteversion/retroversion of the upper arm. The abduction of the upper arm and the vertical movement of the elbow are main attributes of cluster 3. The variable values of cluster 1 and cluster 3 strongly differ, whereas cluster 2 variables have values between those of cluster 1 and 3 and are close to the mean of all clusters (see Table 5.8).

Table 5.8: Mean values of variables for the clusters and absolute range of means (Heinrich et al., 2014, p. 84).

Cluster	AntRet_A [°]	AntRet_E [°]	Abd_A [°]	Abd_E [°]	dAbd [°]	dESz [1, 0, -1]
1	11.5	-7.92	20.76	23.17	2.42	-0.04
2	1.14	-16.6	24.06	29	4.94	0.37
3	-6.96	-28.21	33.84	42.11	8.28	0.92
Mean	0.89	-18.46	26.6	32.07	5.47	0.46
Absolute range (max. - min. value)	18.46	20.29	13.08	18.94	5.86	0.96

Subjects in cluster 1 show an anteversion of the upper arm at the start of the handbrake application, whereas those in cluster 3 show retroversion. Accordingly, at the end of handbrake application, subjects in cluster 1 show a smaller retroversion than those from

cluster 3. Subjects from cluster 3 show a higher abduction at the start and end of handbrake application and a higher range of abduction during the handbrake application. They move the elbow to a higher location during the application, whereas on average the vertical elbow location of subjects from cluster 1 does almost not change. The values of the variables selected in the cluster analysis (5.2.2.2) correlate well to the clusters ($|r| > 0.6$ and $|p| > 0.6$), see Table 14.7 and Table 14.8, p. 247.

5.2.2.6 Analysis of the cluster composition

The characteristics of the subjects and their cluster groups were analyzed for correlations (see Table 5.9). Among the anthropometric characteristics, the body height shows the strongest correlation ($r = -0.672$) to the clusters.

The body height strongly correlates ($|r| > 0.8$) to the factors shown in italic in Table 5.9, including body segment lengths and seat adjustment in x, which strongly correlates to the clusters ($r = 0.772$, $p = 0.779$). The body height weakly correlates to F_{\max} , gender and seat adjustment in z, see Table 14.11.

Consequently, the body height can be considered as the major factor for influencing the movement patterns. Age and activity level show no significant correlation to the clusters.

Table 5.9: Correlation between subject characteristics and cluster affiliation.

Correlation to movements strategy	Pearson correlation coefficient r	p-value	Spearman's rang correlation coefficient p
<i>Seat adjustment in x</i>	-0.772	< 0.001	-0.779
Body height	-0.672	< 0.001	-0.677
<i>Body height group</i>	-0.66	< 0.001	-0.664
<i>Shoulder height seating</i>	-0.65	< 0.001	-0.682
<i>Seating height</i>	-0.646	< 0.001	-0.682
<i>Grip width</i>	-0.641	< 0.001	-0.642
<i>Forearm with hand length</i>	-0.625	< 0.001	-0.63
<i>Upper arm length</i>	-0.612	< 0.001	-0.634
Gender	0.567	< 0.001	0.578
<i>Hand length</i>	-0.52	< 0.001	-0.522
F_{\max}	-0.517	< 0.001	-0.520
Seat adjustment in z	0.423	< 0.001	0.458
BMI	-0.227	0.016	-0.236
Steering Wheel Adj. x	-0.255	0.009	-0.223
Steering Wheel Adj. z	-0.195	0.041	-0.163
Activity level	0.084	0.379	0.061
Age	0.058	0.543	0.048

Cluster 1 mainly consists of taller subjects and cluster 3 mainly of smaller subjects. In cluster 2, there are subjects from all body height groups (Table 5.10), but mostly medium height subjects.

Table 5.10: Composition of clusters.

	Females			Males			Cluster composition			Body height [m]	
Group number	1	2	3	4	5	6	number of				
Body height [m]	1.50-1.58	1.59-1.66	1.67-1.78	1.67-1.77	1.79-1.87	1.88-1.99	females	males	all	mean	SD
Cluster 1	0	0	5	5	7	10	5	22	27	1.83	0.09
Cluster 2	3	3	7	11	12	10	13	33	46	1.77	0.11
Cluster 3	17	13	4	3	1	0	34	4	38	1.61	0.08

5.2.3 Inclusion criteria of subjects for the main study

Three inclusion criteria were applied to determine subjects for the main study:

1. Reliable repeatability of the subjects' ratings.
2. Conformity of their individual movement pattern in comparison to the average of their cluster.
3. Achieving most even distribution of body height, so that the change of joint angles depending on body height can be investigated.

The application of these criteria and resulting selection of subjects are described below.

5.2.3.1 Repeatability of subjective ratings

As described in 5.3.1, the subjects used the rating scales differently. Still, the ratings can be used to assess the capabilities of the individual subjects to rate reliably.

For this purpose the difference of the ratings for location 1 and 8 (which are identical) was calculated for each question Q_i according to equation (5.1).

$$\Delta_{Q_i} = \text{abs}(\text{Rating}_{1_{Q_i}} - \text{Rating}_{8_{Q_i}}) \quad (5.1)$$

Some subjects used only a small portion of the scale and others almost the whole range. Thus, the difference of the ratings was divided by the range – the difference between the best and the worst rating – and by the SD of the subject's ratings for all locations. The index for each of the five questions was determined as described in (5.2).

$$\text{Index}_{Q_i} = \left(\frac{\Delta_{Q_i}}{\text{Std}_{Q_i}} + 2 \times \frac{\Delta_{Q_i}}{\text{Range}_{Q_i}} \right) \quad (5.2)$$

As final index the mean of the five indexes was calculated, shown in equation (5.3).

$$\text{Index} = \sum_{i=1}^5 \frac{\text{Index}_{Q_i}}{5} \quad (5.3)$$

The smaller the index, the better are the evaluation capabilities of the subject. Subjects with an index smaller than two were considered for the main study.

5.2.3.2 Conformity with cluster means of movement variables

Table 5.8 (p. 133) lists the means of the movement variables (AntRet_A, AntRet_E, Abd_A, Abd_E, dAbd and dESz) for each individual cluster and for the whole sample.

For the selection of subjects, representative for a cluster, first the absolute difference $absDiff_i$ between each movement variable (i) of a subject and the mean of this variable for the cluster was calculated (5.4).

$$absDiff_i = \left| \left(\frac{1}{n} \sum_{i=1}^n Variable_i \right) - Variable_i \right| \quad (5.4)$$

Then, the maximum absolute difference $absDiff_{i \max}$ was calculated for each movement variable. This is the maximum difference of the variable for all subjects of the cluster and the mean of this variable for the cluster. The relative difference $relDiff_i$ is calculated by dividing the absolute difference by the maximum absolute difference (5.5)

$$relDiff_i = \frac{absDiff_i}{absDiff_{i \max}} \quad (5.5)$$

So, a relative difference of 0 corresponds to conformity of a subject's movement variable with the cluster average. A relative difference of 100 characterizes maximum deviation from the cluster average.

The sum of the relative differences of all 6 variables was calculated for each subject as described in (5.6). The smaller the SumRelDiff for a subject is, the more congruent is his/her movement with the cluster average.

$$SumRelDiff = \sum_{i=1}^6 \frac{absDiff_i}{absDiff_{i \max}} \quad (5.6)$$

5.2.3.3 Ranking list and selection

For each cluster, a subject ranking list was established. The subjects were invited in the sequence of the ranks. Overall 40 subjects were invited: 14 were selected from cluster 2 and 13 subjects from each, cluster 1 and 3.

To establish the ranking lists for the clusters, first subjects with a low repeatability (index ≥ 2) were excluded. The remaining subjects were ordered by SumRelDiff in increasing order. The last subjects for each cluster often had very similar SumRelDiff-values. In these cases the body height was used as an additional selection criterion aiming for an even body height distribution. The dot plot (Figure 5.7) shows the

selected subjects ordered by cluster and body height. Table 5.11 lists mean and standard deviations of the body height for the selected subjects.

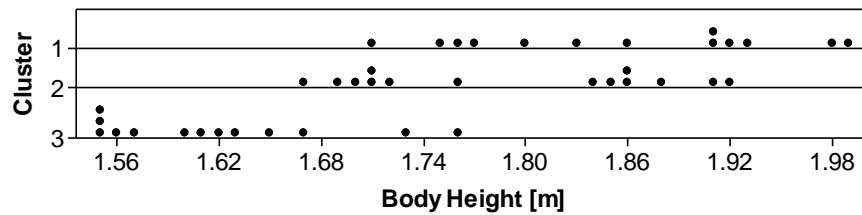


Figure 5.7: Body height of subjects selected for the main study ordered by cluster.

Table 5.11: Mean and standard deviation of body height for selected subjects.

Cluster	Body height [m]	
	Mean	SD
1	1.85	0.09
2	1.79	0.09
3	1.62	0.07

5.3 Discussion and conclusions

5.3.1 Subjective evaluation

The comparison of each subject's rating for the identical locations 1 and 8 has shown that the major portion of the subjects is able to rate reproducibly.

The higher locations (2 and 3) are rated significantly different (worse) for handbrake application than the other locations (1, 4, 5, 6, 7 and 8).

So, hypothesis 1 (compare 3.3, p. 113) was generally confirmed: The subjects perceive different levels of discomfort (when applying handbrake sufficiently different for location) and they are able to reproducibly rate discomfort.

The reasons for higher discomfort ratings for the higher location (2 and 3) match the findings in the literature cited in 2.5 and 2.6: E.g. increased discomfort in case the targets are too close and too far away (Wang & Trasbot, 2011) or when the trunk/pelvis needs to move additionally to the hand and arm (Cavanaugh et al., 1999; Chateauroux & Wang, 2008, Reed & al., 2004).

The rear up location (2) is rated worst. A corresponding handbrake location has shown low force production capability (Chateauroux & Wang, 2012). This location results in a so-called "chicken wing" posture (retroversion and abduction of the upper arm, elbow flexed). The posture becomes even more adverse for smaller subjects who tend to sit more forward. A chicken wing posture itself is perceived awkward in general. This

perception is reinforced by the handbrake application movement (which worsens the posture even further) and force.

The fore up location (3) is rated second worst. Bringing the hand to this location is probably sensed exertive. The resulting movement during handbrake application is adversely effected by applying force, especially for subjects with a more rearward seating position (straight elbow, in adverse case torso leaned forward) and low shoulder position (large anteversion of arm).

The mean ratings for the handbrake application for the other locations (1, 4, 5, 6, 7 and 8) differ only slightly and not significantly due to the large standard deviations which are probably caused by two main reasons:

Firstly, different subjects perceive even the same handbrake location differently due to e.g. differences in anthropometry, seat adjustment, physical capabilities and expectations.

Secondly, the subjects may use the rating scale differently; some subjects tend to rate in the middle range of the scale whereas others tend to use the complete range.

To minimize effects of different scale usage, the evaluation scale was modified for the main study.

The differences between the ratings of locations 1, 4, 5, 6, 7 and 8 mainly remained insignificant no matter how the data was divided into groups (e.g. the six groups, in which the subjects were recruited, see 5.1.5) or what normalization methods were applied. Additionally, it was neither possible to find a good correlation between the ratings and any of potential predictors such as anthropometry, seat adjustment or data from the pre- and post-questionnaire (Lietmeyer, 2013).

To develop a CAE procedure for the prediction of ratings, it is required to derive it from an experimental setup which results in a wide range of different ratings. Therefore, in the main study the range of handbrake locations was expanded.

The mean ratings for all handbrake locations differ most for question Q1 (highest SD of location means in Table 14.6, p. 247) and the mean ratings for the different questions are highly correlated (Table 14.7 and Table 14.8, p. 247). Thus, it was decided to focus on the question Q1 in the main study.

5.3.2 Movement patterns

The application movements of the handbrake at the mid location (1 respectively 8) were analyzed resulting in three clusters of movement patterns. This confirms hypothesis 2

(compare 3.3). The three clusters of movement patterns were found to be mainly influenced by the subjects' body height, which correlates to several body segment lengths and the fore/aft seat adjustment. This is in line with and further complements literature on driving and reach posture: Body height has been shown to influence seat adjustment (Parkin et al., 1995; Fröhmel, 2010), driving posture (Kyung & Nussbaum, 2009) and reach posture (Chaffin et al., 2000). The likely conclusion that body height also influences the handbrake application posture was confirmed.

In the following text the movement patterns and the effect of body height is described for the three clusters.

Cluster 3 shows the smallest average body height of all three clusters. This cluster is characterized by:

1. Retroversion of the upper arm during the handbrake application: smaller subjects tend to sit more forward, so the retroversion of the upper arm is required to reach and apply the handbrake.
2. Larger abduction and range of abduction of the upper arm during handbrake application: a smaller shoulder width requires a larger abduction to bypass the seat with the elbow (arm).
3. Elevation of the elbow during handbrake application: due to the retroversion, the application of the handbrake requires to lift the elbow.

Cluster 1 shows the largest average body height of all three clusters. It is characterized by:

1. Anteversion of the upper arm at the start of handbrake application and slight retroversion at the end. Due to a more rearward seat adjustment, the handbrake is reached by anteversion of the arm, which changes to retroversion during handbrake application.
2. Smaller abduction and range of abduction during handbrake application: a larger shoulder width requires less glenohumeral abduction for the elbow to bypass the seat and avoid hitting it.
3. Maintaining same height of the elbow during handbrake application: during application of the handbrake the elbow is moved rearward which is enabled by the anteversion of the upper arm at the start of the handbrake application.

Cluster 2 is between cluster 1 and cluster 3 with regards to body height and variables characterizing the movement.

The result that the clusters respectively movement patterns mainly depend on the body height and resulting seat adjustment was considered for the choice of subjects for the main study. It was also used for the data analysis in the main study, i.e. the analysis how joint angles and ratings change depending on body height.

The analysis of joint angles with videos is not as accurate as motion capturing with markers and a larger number of cameras. Still it served the purpose to analyze and compare the movements and minimized the time the subjects spent in the experiments.

5.3.3 Inclusion criteria of subjects for the main study

The application of inclusion criteria for the main study participation enabled to recruit subjects:

- With good repeatability of the ratings.
- Representative for the movement pattern of the three clusters.
- With an even distribution of different body heights, including very small and very tall subjects.

6 MAIN STUDY

In the main study, 40 subjects evaluated the handbrake application for different handbrake locations in the ErgoBuck. Their movements were recorded using Vicon cameras. Handbrake force and angle were also recorded. Based on the results of the preliminary study, the handbrake location range was extended and the questionnaire was enhanced.

Aims of the main study were to analyze the movements and subjective evaluations to retest both hypotheses (hypotheses 1 and 2) in more detail than in the preliminary study. The detailed analysis and confirmation of both hypotheses is the precondition to determine target joint angle values for the posture prediction with RAMSIS and also for the discomfort prediction based on RAMSIS, AMS and subsequent mathematical modeling. Since the results of the preliminary study suggested, that the influence of body height on the movement and respectively discomfort assessments should be studied, this aspect was included.

The main study was conducted with support of the IBO. This chapter is largely based on the project reports and master theses accomplished in the context of this project (Heinrich et al., 2014; Rausch & Upmann, 2015b; Rzepka, 2015).

In the following, at first the study design (6.1.1) is explained. Motion analyses (6.1.2) and handbrake locations (6.1.3) are described. After a short presentation of the subject group (6.1.4), the procedure of the experiment (6.1.5), the statistical analysis (6.1.6) and results (6.2) are summarized. A discussion of the study (6.3) concludes this chapter.

6.1 Methods

6.1.1 Study design

In the main study, a similar study design as in the preliminary study was used.

Again, a cross-sectional experimental design with randomized order of the trials was used.

In the factorial design, the independent variables were:

- Handbrake location in x (fore-aft respectively anterior-posterior direction).
- Handbrake location in y (left-right respectively medial-lateral direction).
- Handbrake location in z (height respectively inferior-superior direction).

For each variation of the independent variables, the following dependent variables were determined:

- Discomfort ratings (for subjects and for key percentiles of body height).
- Joint angles (for several time steps of the handbrake application, for subjects and for key percentiles of body height).
- Metabolic power consumption and total metabolic energy (for key percentiles of body height).
- Muscle activities (for key percentiles of body height).
- Joint reactions (for key percentiles of body height).
- Joint moment measures (for key percentiles of body height).

The reason why some of the independent variables were calculated for key percentiles of body height is described in chapter 6.2.

A 2² factorial design with center point repetition (Backhaus, Erichson, Plinke & Weiber, 2006) was used for handbrake location in x and z. Another handbrake location resulted from shifting the center point in y in lateral direction (representation of non-handed handbrake design, see 6.1.3). Yet another handbrake location was added: the center point of the preliminary study which was used as origin of coordinates again (for details see 6.1.3).

An even distribution of body height was a criterion for inclusion of subjects to enable the analysis of the relationship between body height and discomfort ratings respectively joint angles for the different handbrake locations.

6.1.2 Motion analysis

For this thesis, photogrammetric reconstruction (also referred to as optical or camera based motion capturing) has been chosen for being a contactless and accurate method. Since optical motion capturing is contactless, it impairs the movements of the subjects in many cases only marginally (Senner, 2001).

Camera based motion analysis systems record the 3D locations of markers which are fitted to subjects or objects. The markers have to be continuously visible by at least two cameras. The 3D position of each marker at each point in time can be calculated with appropriate software. (Rausch & Upmann, 2015b)

By attaching markers to the human body, the movement of the skeletal system can be traced. The markers are fitted to bony landmarks or close to a joint with the intention to reduce skin artifacts. Small errors cannot be avoided since the marker can usually not

be attached directly to the bones. Thus, there is some movement of the markers relative to the joints. However, motion capturing is still the most accurate non-invasive method available to trace human motion. (Rausch & Upmann, 2015b)

In this study, 10 infrared cameras (Vicon MX F40) and Vicon Nexus motion capture software (Version 1.8.2, Vicon, Los Angeles, USA) were used. Recording frequency was 150 Hz. The spring force of the handbrake, the application angle and the 3D tension forces in the handbrake handle were sampled at 1500 Hz. By using this data and the anthropometric data of the subjects, the individuals can be modeled in RAMSIS and AMS to determine joint angles, reaction forces, joint loads, muscle activity etc. (Heinrich et al., 2014)

The cameras were positioned to ensure visibility of all markers any time by at least two cameras. The arrangement is illustrated in Figure 6.1 (left figure). (Heinrich et al., 2014)

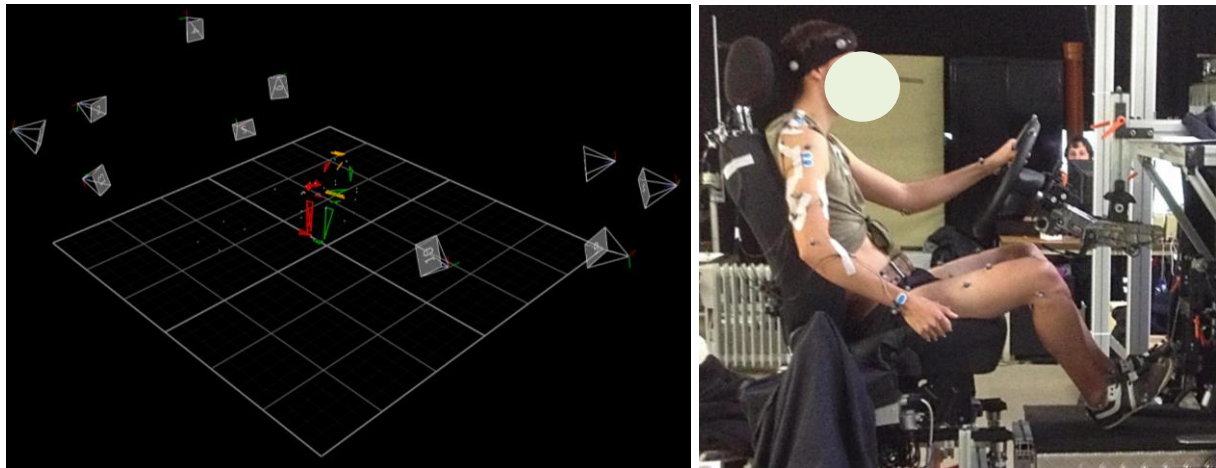


Figure 6.1: Left: Arrangement of the Vicon cameras (Heinrich et al., 2014, p. 120).
Right: Subject equipped with markers is applying the handbrake.

The markers were placed on the subjects as indicated by Figure 6.1 (right picture) and Figure 6.2. The detailed marker set up is described in appendix 14.3.1, p. 252 ff.

As the subjects were seating in a car seat during the study, it was not possible to attach markers on the back side of their hip and trunk. Markers positioned on the front of the hip bone cause issues when the subjects are seated due to skin artefacts or markers hidden in skin folds. Thus, a belt with markers was used to track the hip motion.

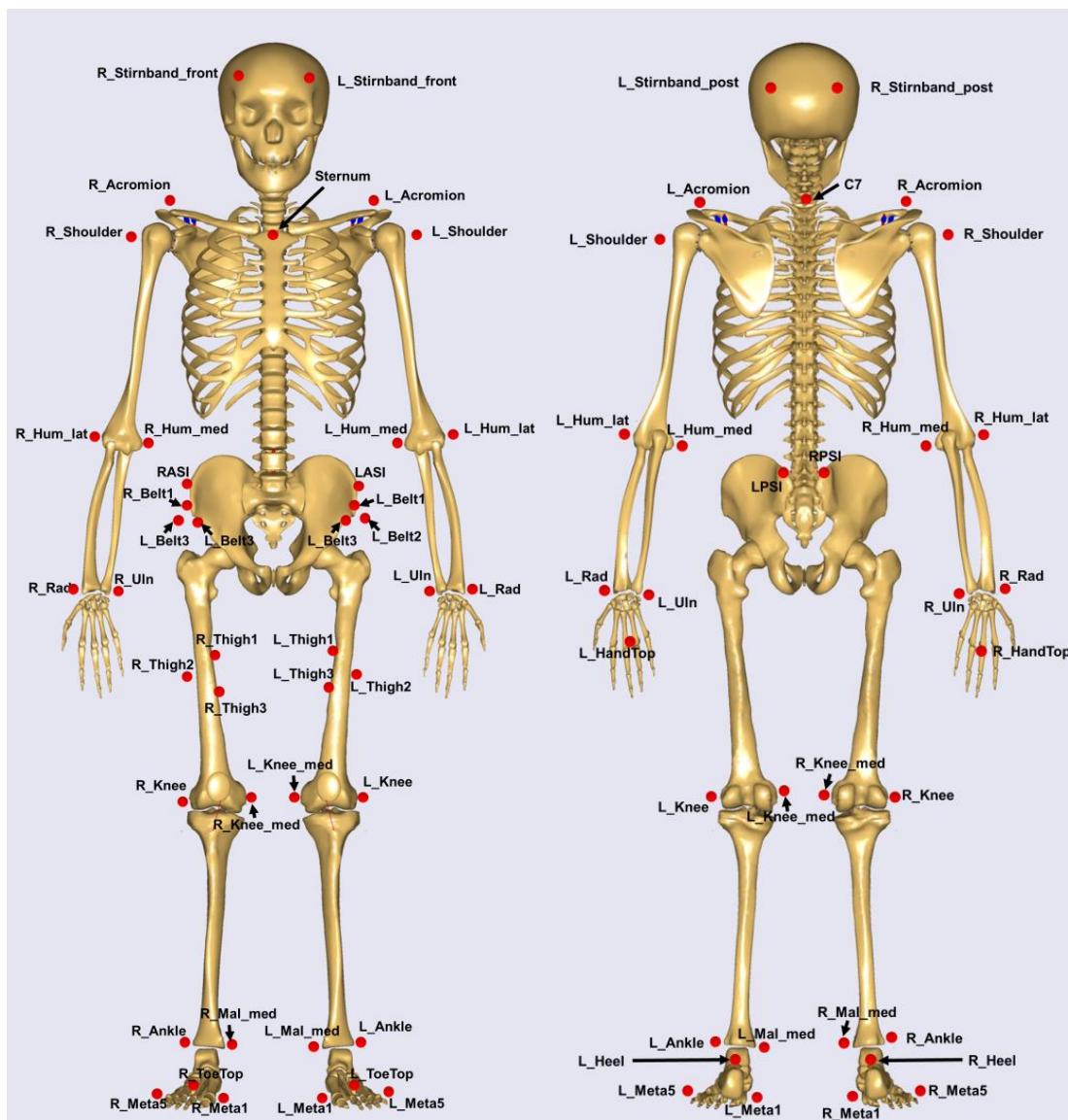


Figure 6.2: Front view (left) and rear view (right) of the marker setup (Rausch & Upmann, 2015b, pp. 24-25.).

First, the subjects were equipped with a complete set of markers including additional markers on the hip and on the spine. Standing in front of the ErgoBuck they were instructed to do calibration movements which is moving each limb separately and taking a bow. These calibration movements allowed the motion tracking system to locate markers with respect to joint centers and to scale the segments. After the calibration motions, the additional markers (C7 on the spine, RASI, RPSI, LASI, LPSI on the hip, see Table 14.15) were removed.

The subjects sat down in the ErgoBuck and applied the handbrake while their motion was recorded. Handbrake forces and application travel were also included in c3d files. The motion of the subjects and the handbrake characteristics were reconstructed in AMS. (Rausch & Upmann, 2015b)

6.1.3 Handbrake locations

The major aim of this project is to establish a correlation to predict subjective discomfort ratings for handbrake application based on biomechanical parameters derived from simulation. To establish such a correlation it is essential that in the subjective evaluation study the handbrake variations are significant to get sufficiently differing ratings. (Rausch & Upmann, 2015b)

In the preliminary study, the mean subjective ratings for most locations (1, 4, 5, 6, 7 and 8) did not differ significantly. Consequently, for the main study a larger range of handbrake locations was defined. It is shown in Figure 6.3 and Table 6.1. (Upmann, 2014)

Table 6.1: Coordinates of the investigated FAP locations.

Location	FAP coordinates [mm]		
	x	y	z
1/6	26.5	0	-20
2	106.5	0	40
3	-53.5	0	40
4	106.5	0	-80
5	-53.5	0	-80
6/1	26.5	0	-20
7	26.5	55	-20
8 (center point in preliminary study)	0	0	0

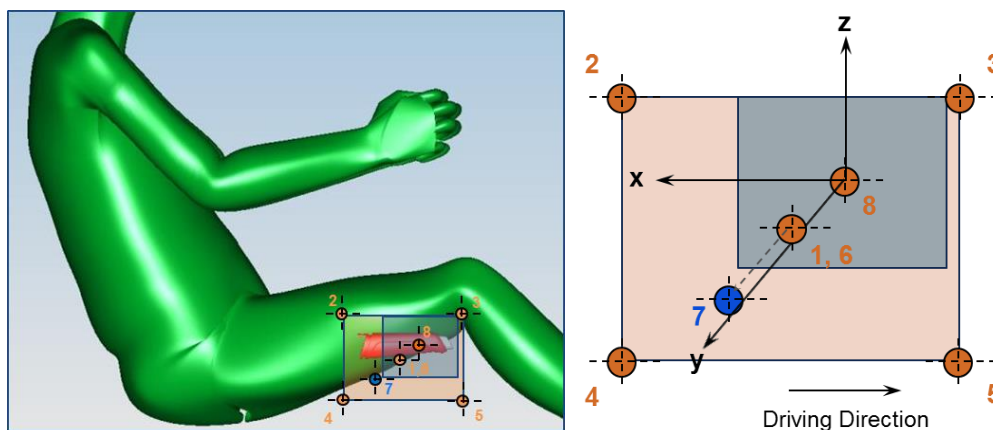


Figure 6.3: Illustration of the investigated handbrake FAP locations in the main study.

To define the new range a market analysis was completed. The handbrake locations of 65 different vehicles across all passenger vehicle segments were measured and analyzed. (Upmann, 2014)

To represent most of the automotive market and to drive for more different ratings (compared to the preliminary study), the x-range of handbrake locations was mainly extended rearwards and the z-range was extended downwards. (Upmann, 2014)

The y range covered in the preliminary study was found to be representative for most of the market. This includes vehicles with the handbrake at the centerline of the vehicle and vehicles with a “handed” handbrake (handbrake location subject to driver seat side). In the preliminary study, the variation in y had not resulted in significantly different ratings. Thus, for the main study it was decided to keep y at 0 mm and modify only x and z location. This y = 0 location is within 5 mm of the mean location of all measured vehicles. (Upmann, 2014)

There are also non-handed handbrakes on the market. This means that left hand drive and right hand drive vehicles (driver seat on the left respectively on the right) have the same y-location of the handbrake. To represent a typical location of a non-handed handbrake it was decided to introduce a single y = 55 mm position for the mid x and z location. (Upmann, 2014)

The midpoint of the new x and z range (location 1 = location 6) was chosen to be assessed two times with the purpose to perform a repeatability check. The center location of the preliminary study was included as location 8. Again, this location was utilized as the origin of the coordinate system for the handbrake location.

6.1.4 Subjects

16 female and 24 male subjects participated in the main study. Inclusion criteria and body height distribution are described in 0. It was anticipated that the motion reconstruction may not be possible for all subjects and all trials. To protect for sufficient yield of motion data (minimum 10 data sets per movement cluster), 13 to 14 subjects representing each movement cluster were invited.

6.1.5 Procedure

The main study subjects were included as described above. Each of them was invited for an appointment of approximately 2 hours of duration at a laboratory of the IBO where the ErgoBuck was located. There they received the instructions. Again, they were explained that they could abort the study any time. They were asked for their statement of consent in written form.

The subjects filled out a pre-questionnaire (6.1.5.1). Their anthropometry was measured (6.1.5.2) and they got prepared for motion capturing (6.1.5.3). During the subsequent evaluation of the handbrake at all different locations, their motion was recorded with Vicon cameras (6.1.5.4). At the end, the subjects completed a post-questionnaire (6.1.5.4.3).

6.1.5.1 Pre-questionnaire

In the pre-questionnaire, the subjects replied to questions about their general driving habits and their health and emotional status. The pre-questionnaire can be found in the appendix 14.3.2, p. 255.

6.1.5.2 Anthropometric measurements

In addition to the anthropometric measurements in the preliminary study, several other measurements were taken (Heinrich et al., 2014; Rausch & Upmann, 2015b) to allow for potential future application of AMS scaling law by Annegarn (see 2.9.5.2.3, p. 90).

6.1.5.3 Preparation of the subjects

The subjects were equipped with markers as described in 6.1.2 and asked to perform the calibration movements.

6.1.5.4 Handbrake application

6.1.5.4.1 Procedure

The same procedure as in the preliminary study (5.1.6.4.1, p. 124) was applied using the revised handbrake locations (6.1.3, p. 145) and a modified questionnaire which is described below.

6.1.5.4.2 Subjective evaluation questionnaire

In the preliminary study, the first question was the least specific but resulted in the largest differences in mean ratings for the different handbrake locations. All questions resulted in highly correlated ratings. So, in the main study it was decided to use only one question similarly unspecific as the first question of the preliminary study.

To improve the scale usage, the original scale was replaced based on the findings of Shen & Parsons (1997) who evaluated the validity and reliability of rating scales frequently used to assess comfort and discomfort. The scale which showed highest

validity and reliability was the Category Partitioning Scale (see 2.4.1). It was used for the main study with five major classifications (very good, good, neutral, poor, very poor) and ten sub-classifications as shown in Figure 6.4. The subjects were asked to first select the major classification and then the sub-classification. The ratings for all eight handbrake locations were recorded on the same sheet so that each subject could see his/her previous ratings.

For the statistical analysis, the ratings e ($1 \leq e \leq 50$) were transformed into the perceived discomfort ratings d ($0 \leq d \leq 100$) to cover the same range as in the preliminary study, see equation (6.1). The range of 100 is expected to ease application and interpretation in an engineering environment.

$$d = 100 - 2 \cdot e \quad (6.1)$$

With this, a 50 on the scale was converted into the value 0 (no discomfort, best rating). A 0 on the scale was converted into a 100 (high discomfort, worst rating) for the further analysis.

Subject-ID: _____

How do you rate the application of the handbrake?

Handbrake No.	1	2	3	4	5	6	7	8		
very good	50	<input type="checkbox"/>	<input type="checkbox"/>	<input type="checkbox"/>	<input type="checkbox"/>	<input type="checkbox"/>	<input type="checkbox"/>	<input type="checkbox"/>	<input type="checkbox"/>	better ↑
	49	<input type="checkbox"/>	<input type="checkbox"/>	<input type="checkbox"/>	<input type="checkbox"/>	<input type="checkbox"/>	<input type="checkbox"/>	<input type="checkbox"/>	<input type="checkbox"/>	
	48	<input type="checkbox"/>	<input type="checkbox"/>	<input type="checkbox"/>	<input type="checkbox"/>	<input type="checkbox"/>	<input type="checkbox"/>	<input type="checkbox"/>	<input type="checkbox"/>	
	47	<input type="checkbox"/>	<input type="checkbox"/>	<input type="checkbox"/>	<input type="checkbox"/>	<input type="checkbox"/>	<input type="checkbox"/>	<input type="checkbox"/>	<input type="checkbox"/>	
	46	<input type="checkbox"/>	<input type="checkbox"/>	<input type="checkbox"/>	<input type="checkbox"/>	<input type="checkbox"/>	<input type="checkbox"/>	<input type="checkbox"/>	<input type="checkbox"/>	
	worse ↓	45	<input type="checkbox"/>	<input type="checkbox"/>	<input type="checkbox"/>	<input type="checkbox"/>	<input type="checkbox"/>	<input type="checkbox"/>	<input type="checkbox"/>	<input type="checkbox"/>
		44	<input type="checkbox"/>	<input type="checkbox"/>	<input type="checkbox"/>	<input type="checkbox"/>	<input type="checkbox"/>	<input type="checkbox"/>	<input type="checkbox"/>	<input type="checkbox"/>
		43	<input type="checkbox"/>	<input type="checkbox"/>	<input type="checkbox"/>	<input type="checkbox"/>	<input type="checkbox"/>	<input type="checkbox"/>	<input type="checkbox"/>	<input type="checkbox"/>
		42	<input type="checkbox"/>	<input type="checkbox"/>	<input type="checkbox"/>	<input type="checkbox"/>	<input type="checkbox"/>	<input type="checkbox"/>	<input type="checkbox"/>	<input type="checkbox"/>
		41	<input type="checkbox"/>	<input type="checkbox"/>	<input type="checkbox"/>	<input type="checkbox"/>	<input type="checkbox"/>	<input type="checkbox"/>	<input type="checkbox"/>	<input type="checkbox"/>
good	40	<input type="checkbox"/>	<input type="checkbox"/>	<input type="checkbox"/>	<input type="checkbox"/>	<input type="checkbox"/>	<input type="checkbox"/>	<input type="checkbox"/>	<input type="checkbox"/>	better ↑
	39	<input type="checkbox"/>	<input type="checkbox"/>	<input type="checkbox"/>	<input type="checkbox"/>	<input type="checkbox"/>	<input type="checkbox"/>	<input type="checkbox"/>	<input type="checkbox"/>	
	38	<input type="checkbox"/>	<input type="checkbox"/>	<input type="checkbox"/>	<input type="checkbox"/>	<input type="checkbox"/>	<input type="checkbox"/>	<input type="checkbox"/>	<input type="checkbox"/>	
	37	<input type="checkbox"/>	<input type="checkbox"/>	<input type="checkbox"/>	<input type="checkbox"/>	<input type="checkbox"/>	<input type="checkbox"/>	<input type="checkbox"/>	<input type="checkbox"/>	
	36	<input type="checkbox"/>	<input type="checkbox"/>	<input type="checkbox"/>	<input type="checkbox"/>	<input type="checkbox"/>	<input type="checkbox"/>	<input type="checkbox"/>	<input type="checkbox"/>	
	worse ↓	35	<input type="checkbox"/>	<input type="checkbox"/>	<input type="checkbox"/>	<input type="checkbox"/>	<input type="checkbox"/>	<input type="checkbox"/>	<input type="checkbox"/>	<input type="checkbox"/>
		34	<input type="checkbox"/>	<input type="checkbox"/>	<input type="checkbox"/>	<input type="checkbox"/>	<input type="checkbox"/>	<input type="checkbox"/>	<input type="checkbox"/>	<input type="checkbox"/>
		33	<input type="checkbox"/>	<input type="checkbox"/>	<input type="checkbox"/>	<input type="checkbox"/>	<input type="checkbox"/>	<input type="checkbox"/>	<input type="checkbox"/>	<input type="checkbox"/>
		32	<input type="checkbox"/>	<input type="checkbox"/>	<input type="checkbox"/>	<input type="checkbox"/>	<input type="checkbox"/>	<input type="checkbox"/>	<input type="checkbox"/>	<input type="checkbox"/>
		31	<input type="checkbox"/>	<input type="checkbox"/>	<input type="checkbox"/>	<input type="checkbox"/>	<input type="checkbox"/>	<input type="checkbox"/>	<input type="checkbox"/>	<input type="checkbox"/>
neutral	30	<input type="checkbox"/>	<input type="checkbox"/>	<input type="checkbox"/>	<input type="checkbox"/>	<input type="checkbox"/>	<input type="checkbox"/>	<input type="checkbox"/>	<input type="checkbox"/>	better ↑
	29	<input type="checkbox"/>	<input type="checkbox"/>	<input type="checkbox"/>	<input type="checkbox"/>	<input type="checkbox"/>	<input type="checkbox"/>	<input type="checkbox"/>	<input type="checkbox"/>	
	28	<input type="checkbox"/>	<input type="checkbox"/>	<input type="checkbox"/>	<input type="checkbox"/>	<input type="checkbox"/>	<input type="checkbox"/>	<input type="checkbox"/>	<input type="checkbox"/>	
	27	<input type="checkbox"/>	<input type="checkbox"/>	<input type="checkbox"/>	<input type="checkbox"/>	<input type="checkbox"/>	<input type="checkbox"/>	<input type="checkbox"/>	<input type="checkbox"/>	
	26	<input type="checkbox"/>	<input type="checkbox"/>	<input type="checkbox"/>	<input type="checkbox"/>	<input type="checkbox"/>	<input type="checkbox"/>	<input type="checkbox"/>	<input type="checkbox"/>	
	worse ↓	25	<input type="checkbox"/>	<input type="checkbox"/>	<input type="checkbox"/>	<input type="checkbox"/>	<input type="checkbox"/>	<input type="checkbox"/>	<input type="checkbox"/>	<input type="checkbox"/>
		24	<input type="checkbox"/>	<input type="checkbox"/>	<input type="checkbox"/>	<input type="checkbox"/>	<input type="checkbox"/>	<input type="checkbox"/>	<input type="checkbox"/>	<input type="checkbox"/>
		23	<input type="checkbox"/>	<input type="checkbox"/>	<input type="checkbox"/>	<input type="checkbox"/>	<input type="checkbox"/>	<input type="checkbox"/>	<input type="checkbox"/>	<input type="checkbox"/>
		22	<input type="checkbox"/>	<input type="checkbox"/>	<input type="checkbox"/>	<input type="checkbox"/>	<input type="checkbox"/>	<input type="checkbox"/>	<input type="checkbox"/>	<input type="checkbox"/>
		21	<input type="checkbox"/>	<input type="checkbox"/>	<input type="checkbox"/>	<input type="checkbox"/>	<input type="checkbox"/>	<input type="checkbox"/>	<input type="checkbox"/>	<input type="checkbox"/>
poor	20	<input type="checkbox"/>	<input type="checkbox"/>	<input type="checkbox"/>	<input type="checkbox"/>	<input type="checkbox"/>	<input type="checkbox"/>	<input type="checkbox"/>	<input type="checkbox"/>	better ↑
	19	<input type="checkbox"/>	<input type="checkbox"/>	<input type="checkbox"/>	<input type="checkbox"/>	<input type="checkbox"/>	<input type="checkbox"/>	<input type="checkbox"/>	<input type="checkbox"/>	
	18	<input type="checkbox"/>	<input type="checkbox"/>	<input type="checkbox"/>	<input type="checkbox"/>	<input type="checkbox"/>	<input type="checkbox"/>	<input type="checkbox"/>	<input type="checkbox"/>	
	17	<input type="checkbox"/>	<input type="checkbox"/>	<input type="checkbox"/>	<input type="checkbox"/>	<input type="checkbox"/>	<input type="checkbox"/>	<input type="checkbox"/>	<input type="checkbox"/>	
	16	<input type="checkbox"/>	<input type="checkbox"/>	<input type="checkbox"/>	<input type="checkbox"/>	<input type="checkbox"/>	<input type="checkbox"/>	<input type="checkbox"/>	<input type="checkbox"/>	
	worse ↓	15	<input type="checkbox"/>	<input type="checkbox"/>	<input type="checkbox"/>	<input type="checkbox"/>	<input type="checkbox"/>	<input type="checkbox"/>	<input type="checkbox"/>	<input type="checkbox"/>
		14	<input type="checkbox"/>	<input type="checkbox"/>	<input type="checkbox"/>	<input type="checkbox"/>	<input type="checkbox"/>	<input type="checkbox"/>	<input type="checkbox"/>	<input type="checkbox"/>
		13	<input type="checkbox"/>	<input type="checkbox"/>	<input type="checkbox"/>	<input type="checkbox"/>	<input type="checkbox"/>	<input type="checkbox"/>	<input type="checkbox"/>	<input type="checkbox"/>
		12	<input type="checkbox"/>	<input type="checkbox"/>	<input type="checkbox"/>	<input type="checkbox"/>	<input type="checkbox"/>	<input type="checkbox"/>	<input type="checkbox"/>	<input type="checkbox"/>
		11	<input type="checkbox"/>	<input type="checkbox"/>	<input type="checkbox"/>	<input type="checkbox"/>	<input type="checkbox"/>	<input type="checkbox"/>	<input type="checkbox"/>	<input type="checkbox"/>
very poor	10	<input type="checkbox"/>	<input type="checkbox"/>	<input type="checkbox"/>	<input type="checkbox"/>	<input type="checkbox"/>	<input type="checkbox"/>	<input type="checkbox"/>	<input type="checkbox"/>	better ↑
	9	<input type="checkbox"/>	<input type="checkbox"/>	<input type="checkbox"/>	<input type="checkbox"/>	<input type="checkbox"/>	<input type="checkbox"/>	<input type="checkbox"/>	<input type="checkbox"/>	
	8	<input type="checkbox"/>	<input type="checkbox"/>	<input type="checkbox"/>	<input type="checkbox"/>	<input type="checkbox"/>	<input type="checkbox"/>	<input type="checkbox"/>	<input type="checkbox"/>	
	7	<input type="checkbox"/>	<input type="checkbox"/>	<input type="checkbox"/>	<input type="checkbox"/>	<input type="checkbox"/>	<input type="checkbox"/>	<input type="checkbox"/>	<input type="checkbox"/>	
	6	<input type="checkbox"/>	<input type="checkbox"/>	<input type="checkbox"/>	<input type="checkbox"/>	<input type="checkbox"/>	<input type="checkbox"/>	<input type="checkbox"/>	<input type="checkbox"/>	
	worse ↓	5	<input type="checkbox"/>	<input type="checkbox"/>	<input type="checkbox"/>	<input type="checkbox"/>	<input type="checkbox"/>	<input type="checkbox"/>	<input type="checkbox"/>	<input type="checkbox"/>
		4	<input type="checkbox"/>	<input type="checkbox"/>	<input type="checkbox"/>	<input type="checkbox"/>	<input type="checkbox"/>	<input type="checkbox"/>	<input type="checkbox"/>	<input type="checkbox"/>
		3	<input type="checkbox"/>	<input type="checkbox"/>	<input type="checkbox"/>	<input type="checkbox"/>	<input type="checkbox"/>	<input type="checkbox"/>	<input type="checkbox"/>	<input type="checkbox"/>
		2	<input type="checkbox"/>	<input type="checkbox"/>	<input type="checkbox"/>	<input type="checkbox"/>	<input type="checkbox"/>	<input type="checkbox"/>	<input type="checkbox"/>	<input type="checkbox"/>
		1	<input type="checkbox"/>	<input type="checkbox"/>	<input type="checkbox"/>	<input type="checkbox"/>	<input type="checkbox"/>	<input type="checkbox"/>	<input type="checkbox"/>	<input type="checkbox"/>

Figure 6.4: Questionnaire for the handbrake evaluation used in the main study.

6.1.5.4.3 Measurement data acquisition

The motion of the subjects was captured during the handbrake application as described in 6.1.2. By using trigger signals it was synchronized with the recordings of the handbrake force and application angle.

6.1.5.5 Post-questionnaire

After the handbrake applications the subjects filled out the post-questionnaire which is presented in appendix 14.3.3, p. 256. It comprises information about the evaluation of the handbrake applications, about the subjects' feelings and about the study as a whole.

6.1.5.6 Measurement data processing

The recorded motion data were processed with Vicon Nexus to assign the markers to the appropriate anatomic landmarks. Data sets were saved as C3D-files (Heinrich et al., 2014). The motion of the subjects was reconstructed (Rausch, Popovic & Upmann, 2014). As anticipated and protected for by the number of invited subjects, in some cases motion reconstruction with Vicon Nexus and AMS was not possible. These motion data sets were excluded from further analyses. For each subject, each handbrake location and each joint angle the values of the trials were checked for consistency with a Matlab routine (Rausch et al., 2014). If one of the trials was strongly differing from the rest, it was considered as an outlier and excluded from further analysis.

The joint angles reconstructed with AMS were analyzed in Matlab for the start of handbrake application and for reaching the target application angle (Rausch et al., 2014).

The joint angles were analyzed to retest hypothesis 2 and – if positive – to develop and validate handbrake posture prediction with RAMSIS.

Detailed analysis was completed for the clavicle, shoulder, elbow and wrist joint angles of the right body side and the spine ("pelvis thorax angles"). Those joint angles are referred to as key joint angles below. They are described in appendix 14.4 (p. 259 ff.).

The key joint angles were analyzed depending on handbrake location and body height because the body height was shown to be the major factor influencing movement patterns in the preliminary study. (Raiber, 2015)

Other joint angles, e.g. of the legs and left arm, were not analyzed. The reasons are that they were considered not relevant for handbrake application and that the prediction of driving postures with RAMSIS was already extensively validated (Raiber, 2015), see 2.8.4.1.2., p. 76.

6.1.6 Data analysis

Data analysis was done in Matlab (2011b), Excel (2010), SPSS (21) and Minitab (15) using conventional statistical methods (Backhaus et al., 2006; Rumsey, 2008). A brief explanation of the terms r , r^2 , r^2_{adj} , p etc. is provided in 8.1.5, p. 178 ff.

Since the discomfort ratings of the 2^2 factorial design with repeated center point were not normally distributed, a major precondition for analysis of variance (ANOVA) was not fulfilled (Backhaus et al., 2006). Consequently, non-parametric pairwise Mann-Whitney tests (Costich-Sicker et al., 2002; Minitab, 2015) were used to analyze if the discomfort ratings (medians) for different handbrake locations differ significantly.

Correlation and regression analysis were applied to investigate the relationship between body height and discomfort ratings respectively joint angles.

6.2 Results

6.2.1 Subjective evaluation

6.2.1.1 Reproducibility

To assess the reproducibility, subject's discomfort ratings d for the mid location (labeled 1 and 6) were compared. This is the rating on a 0 to 100 scale, see 6.1.5.4.2, p. 147. The absolute difference between both ratings was calculated for each subject. As shown in Table 6.2, 20 % of subjects had a shift of up to 5 on the scale and 20 % had a shift between 6 and 10. These subjects rate quite reproducibly while 30 % of the subjects showed a shift larger than 20.

The reproducibility was lower than in the preliminary study (compare 5.2.1.1, p. 131).

Table 6.2: Difference between the ratings for location 1 and 6.

Absolute difference	Percentage of subjects	Cumulative percentage of subjects
0 to 5	20	20
6 to 10	20	40
11 to 15	10	50
16 to 20	20	70
≥ 21	30	100

6.2.1.2 Handbrake locations

The ratings for some handbrake locations (2, 4, 5, 6 and 8) are normally distributed, whereas the ratings for locations 1, 3 and 7 are not normally distributed (see Table

14.17, p. 257). Therefore, medians with confidence intervals (CIs) are shown in Figure 6.5. Means with CIs are illustrated in Figure 14.20, p. 257.

Table 6.3 and Figure 6.5 show that in comparison to the preliminary study, a larger range of the scale has been used and several locations are rated significantly different from each other.

Table 6.3: Descriptive statistics of the discomfort ratings.

Location	Mean	SD	Median	Mode	N for Mode
1	28.85	15.97	24	20	7
2	64.80	17.46	63	60	5
3	46.10	18.23	43	30	5
4	34.25	20.38	29	22,28	4
5	55.65	23.58	56	80	5
6	32.70	15.46	31	20	5
7	48.40	18.88	50	50	5
8	33.00	15.06	34	28	4
1 and 6	30.78	12.53	28	20	12

Discomfort: Median with 90% CI and Mean of Discomfort Ratings

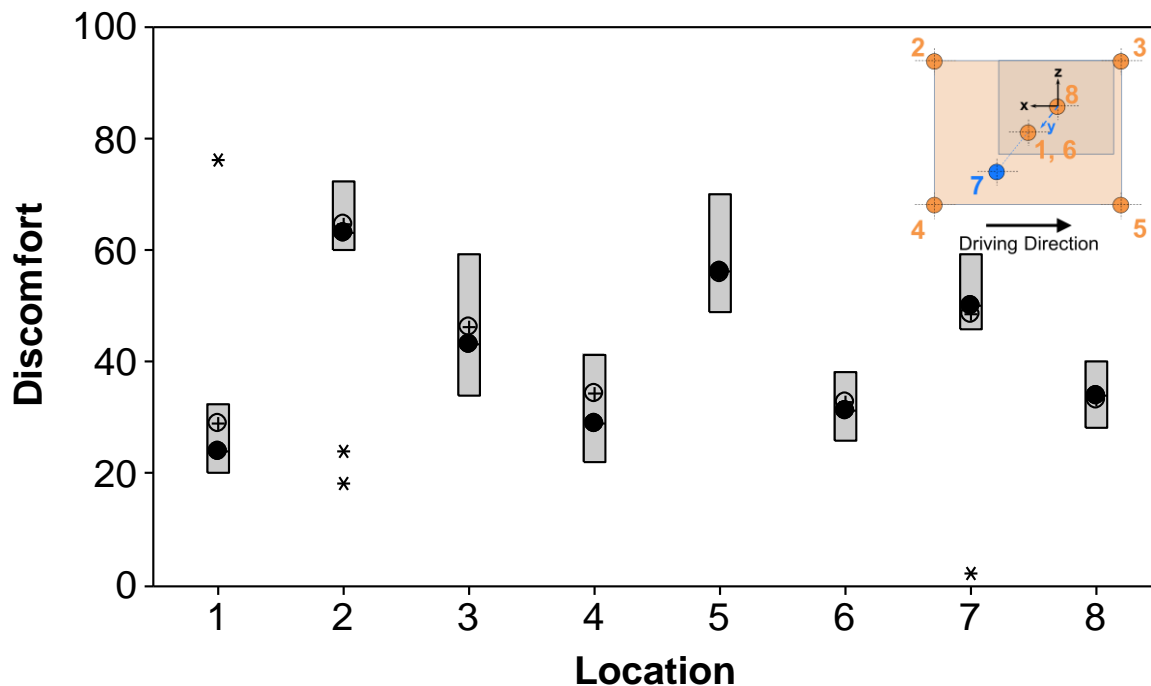


Figure 6.5: Subjective ratings of the main study. Increasing number indicates increasing discomfort. Filled dot represents median, unfilled one represents mean. Bars represent 90 % confidence interval of median.

Pairwise Mann-Whitney tests show that there are statistically different medians between several of the locations (Table 14.18, p. 257). The discomfort ratings between location 1 and 6 (same location) do not statistically differ ($p = 0.19$), which confirms the capability

of the subject group to rate consistently. Location 7 gets significantly higher discomfort ratings than locations 1 and 6. Thus, the large shift in y does cause higher discomfort. Locations 2 (rear up), 3 (fore up) and 5 (fore down) result in higher discomfort than the more central locations (1, 6 and 8) and the rear down location (4).

In the preliminary study, the body height was shown to have a major influence on the motion pattern. This indicates that the body height may also have an influence on the discomfort ratings which is discussed below. Table 14.19 (p. 258) lists statistical parameters describing the relationship between the discomfort ratings for the locations and the subjects' body height. Location 4 and 5 show the highest correlation coefficients (r , ρ) and p -values < 0.05 . So, for these locations the discomfort ratings are significantly influenced by the body height.

The perceived discomfort decreases with increasing body height for location 4 which is the rear down location (Figure 6.6, left). The perceived discomfort increases with body height for location 5 which is the fore down location (Figure 6.6, right).

Figure 6.6 shows that the variation of ratings by people of similar body height is larger than the mean change in discomfort between small and large body heights which is expressed by the discomfort difference of the regression line over body height.

For the development of mass production vehicles, it is common to apply average ratings of key customer percentiles.

So, it is not beneficial to use the discomfort ratings of single subjects as targets for the discomfort predictions. It is also neither desired nor possible to predict a single person's discomfort rating.

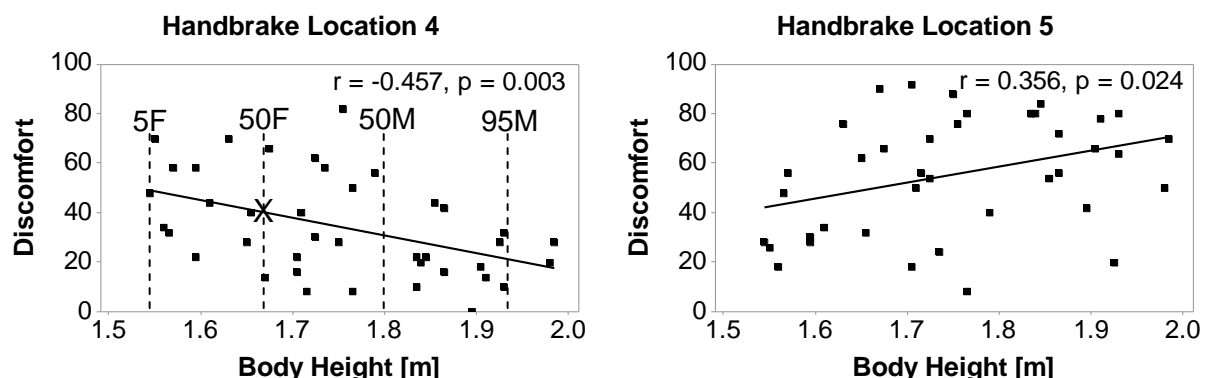


Figure 6.6: Discomfort ratings versus body height for location 4 (left) and 5 (right).

The following key percentiles are typically used in automotive development:

- 5th percentile body height female (5F).
- 50th percentile body height female (50F).
- 50th percentile body height male (50M).
- 95th percentile body height male (95M).

They are used in this study because they reflect the most relevant range of customer body heights. The body height of the four key percentiles was determined with SizeGERMANY (2012) for the year 2013 (in which the study was conducted) and is indicated in Figure 6.6 by vertical lines.

To determine average discomfort ratings for the key customer percentiles, linear regression equations were calculated for discomfort versus the body height. This was done for each handbrake location.

The value of the regression equation for a body height corresponding to the key percentile was used as the target discomfort value for the discomfort prediction (see chapter 9). For instance, the target discomfort for handbrake location 4 and 50F is marked by a cross in Figure 6.6.

The large variation of ratings by people of similar body height also occurs for those locations for which there is no significant effect of body height. The scatterplot of location 8 is shown as an example in Figure 6.7. The scatterplots for all other locations are provided in the appendix 14.3.4.

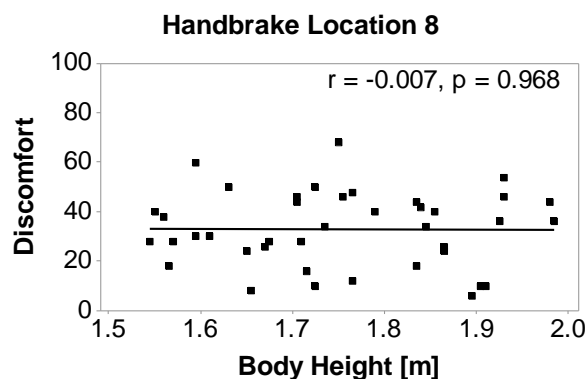


Figure 6.7: Discomfort ratings versus body height for location 8.

6.2.2 Joint angles

The joint angle analysis was completed in the master thesis by Raiber (2015). It was found that the movement results in a linear change of the key joint angles. Therefore the further analysis of the joint angles focused on two key frames indicating the start and

end of handbrake application (Rausch et al., 2014; Rausch & Upmann, 2015b). These body posture key frames reflect the maximum joint angle change during handbrake application and are exemplarily shown in Figure 6.8. This choice of key frames also reflects the primacy and recency effect and the peak-end rule (compare 2.3.3.3, p. 26), The start key frame is determined as the moment in which the handbrake angle starts to change. The end key frame is the state when the handbrake reaches the target application angle.

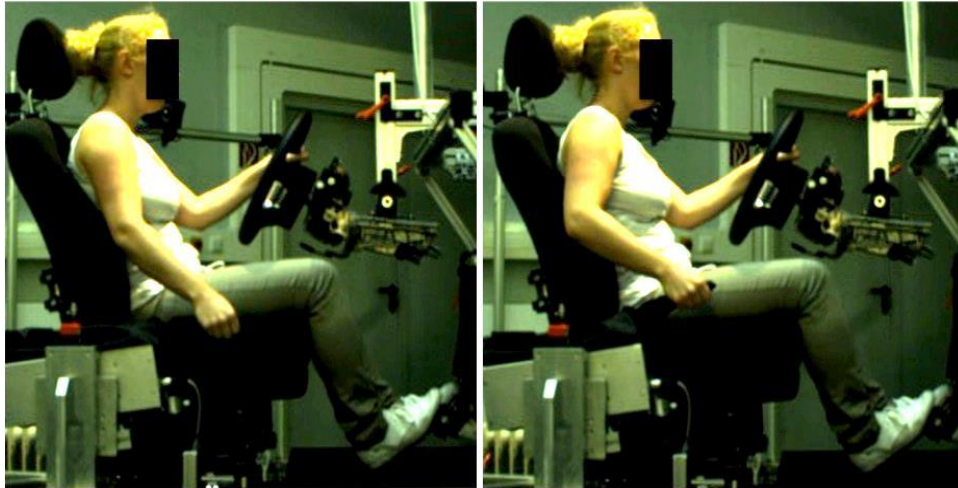


Figure 6.8: The two postures chosen to describe the handbrake application movement are determined with the start (left) and end (right) key frames. Extracted from Raiber (2015, p. 55).

The relationship between key joint angles and body height was analyzed for both key frames of all handbrake locations as illustrated exemplary in Figure 6.9.

The scatter plot shows the elbow flexion of the subjects for the start and end of handbrake application for location 1. Additionally there are corresponding lines of regression and regression plus/minus one standard deviation.

The example shows that even for similar body heights the right elbow flexion can differ more than the regression line discomfort changes over the complete range of body height.

For the development of mass production vehicles, it is common to simulate average postures of key customer percentiles. So it is not beneficial to use the joint angles of single subjects as targets for the RAMSIS posture predictions. It is also neither desired nor possible to predict a single person's joint angles.

To determine average postures respectively joint angles for the key customer percentiles, linear regression equations were calculated for each joint angle versus the

body height. This was done for the start and end of handbrake application of each handbrake location.

The value of the regression equation for a body height corresponding to the key percentile was used as the target joint angle for the RAMSIS simulation. For instance, the target elbow flexion angle for the start of handbrake application for 50F is marked by a cross in Figure 6.9.

In the following the target angles are also referred to as “study angles” since they were derived from the main study. All target angles are listed in Raiber (2015).

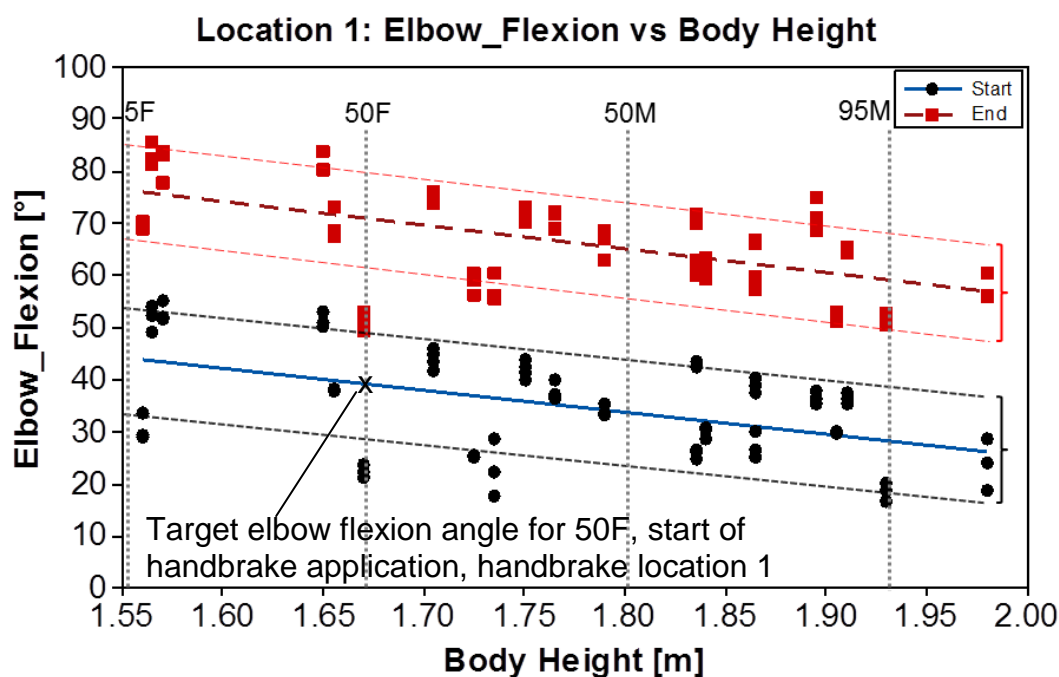


Figure 6.9: Scatter plot of the elbow flexion for the right arm for handbrake location 1 at start (black dot, solid line) and end (red rectangle, dotted regression line). The dashed lines above and below regression lines as well as the brackets on the right indicate plus/minus one standard deviation.

In general, the start respectively end joint angles for the different handbrake locations show large differences between the four key percentiles for glenohumeral anteversion and abduction, elbow and wrist flexion, sternoclavicular protraction and pelvis thorax (spine) extension. In contrast, differences in pelvis thorax rotation and lateral flexion, wrist abduction and sternoclavicular elevation are small. (Raiber, 2015)

Additionally to the joint angles at the start and end of handbrake application, their deltas (the change of joint angles during the handbrake application) were calculated (Table 14.20, p. 263). The angular differences are illustrated in a boxplot, Figure 6.10. The larger the change of a joint angle between start and end of handbrake application is, the more this joint angle contributes to the movement. Elbow flexion, glenohumeral

anteversion, wrist flexion and glenohumeral abduction show highest changes during the movement. The joint angle changes between start and end of handbrake application show major differences between the four key percentiles for glenohumeral abduction and wrist flexion. The more the start respectively end joint angles and their delta differ between the percentiles for a joint angle, the more this joint angle explains the movement differences between the percentiles.

Similarly to the joint angles, the adjustments/positions of the seat depending on the body height were calculated (Raiber, 2015). They have an effect on the hip location of the subjects and therefor on the other joint angles during handbrake application. Further details are described in the master thesis by Raiber (2015).

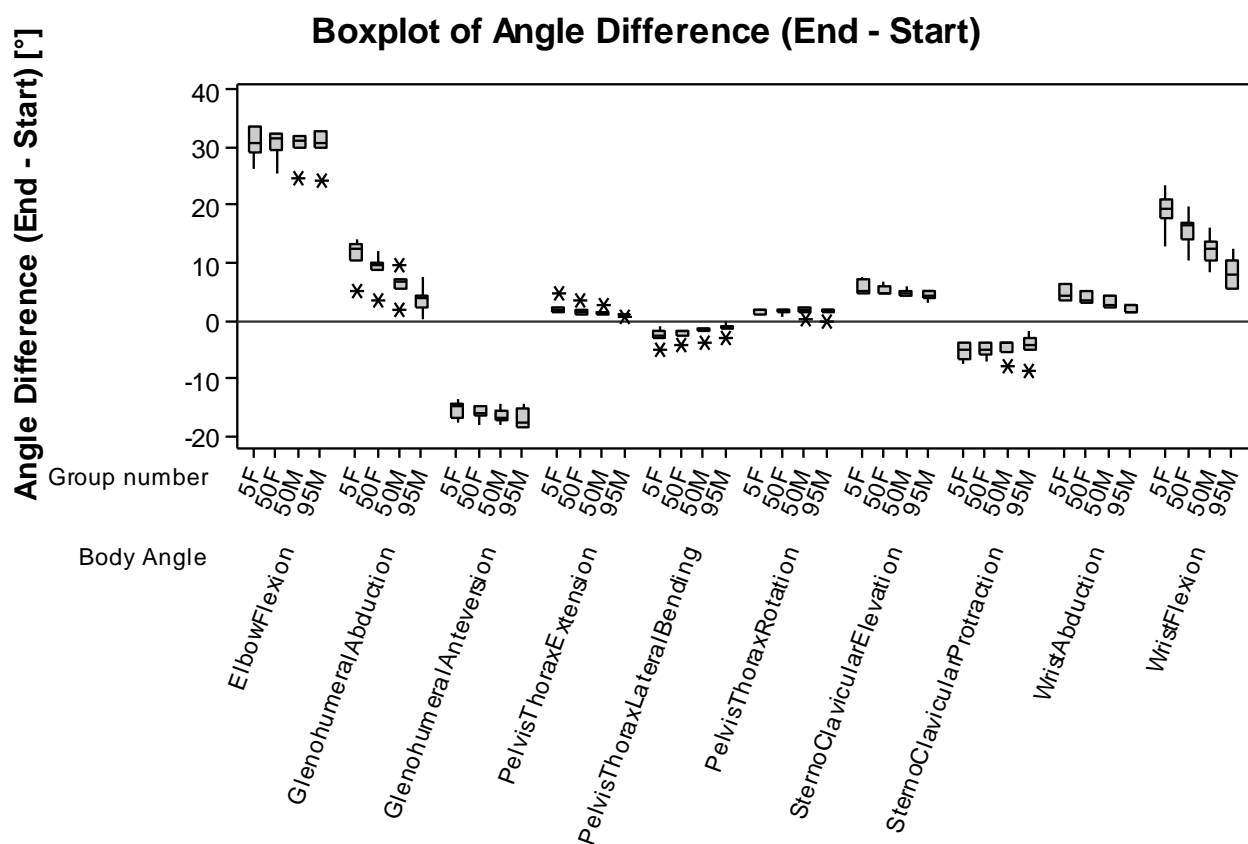


Figure 6.10: Boxplot of joint angle differences between start and end of the handbrake application.

6.3 Discussion and conclusions

6.3.1 Subjective evaluation

In the main study, the subjects used a wider range of the scale compared to the preliminary study. This is probably a result of the increased spread of handbrake locations and the enhanced rating scale.

The ratings of the complete subject group do not significantly differ for the identical locations 1 and 6. However, the individual reproducibility was different for each subject: With a discomfort range from 0 to 100, 20 % of the subjects rated the same location within 0 to 5 points difference. Further 20 % rated within a 6 to 10 point difference. This 40 % have a very good respectively good reproducibility. 30 % of the subjects rated with a more than 20 point difference, their reproducibility is poor.

Although reproducibility was one criterion of the subject selection for the main study, the reproducibility in the main study was lower than in the preliminary study. The reason is not obvious as the enhanced scale was assumed to enhance reproducibility. The reproducibility of individuals may vary over time and depending on the task. Subject dependent reproducibility and rather fair reproducibility within a complete subject group have been documented in reach discomfort literature (Chevalot & Wang, 2004; Wang & Trasbot, 2011).

The central locations 1, 6 and 8 and the rear down location 4 receive lowest mean discomfort ratings. These locations probably allow the majority of the subjects to apply the handbrake in rather comfortable postures, i.e. not leaning forward the torso, no high level of elbow flexion, upper arm anteversion, retroversion or abduction. These handbrake locations respectively body postures support good force generation capabilities (Chateauroux & Wang, 2012) and most subjects are likely to have similar handbrake locations in their vehicles.

The finding that target distance, azimuth angle and elevation (compare Figure 2.15, p. 34) have a quadratic effect on the perceived discomfort of target reach (Wang & Trasbot, 2011) is qualitatively transferable to the effect of handbrake location on perceived discomfort of handbrake application.

Location 7 results in higher discomfort than location 1 and 6. This can be explained by a larger glenohumeral abduction required for location 7 since it is further away in y direction (lateral direction) from the subject. The larger abduction leads to a higher lever arm of the external force and according higher load on affected muscles and joints.

Location 2 (rear up) suggests a “chicken wing” posture and thus low force generation capabilities (Chateauroux & Wang, 2012) which explains the higher perceived discomfort (compare 5.3.1, p. 137 ff.).

Location 3 (fore up) leads to an uncomfortable start and end posture (for larger subjects anteversion of the arm, eventually leaning forward with the torso, smaller subjects require large upper arm abduction) and is also unfavorable for force generation (compare 5.3.1).

The perceived discomfort shows a significant correlation to body height for location 5 (fore down, $r = 0.36$, $p < 0.05$) and 4 (rear down, $r = -0.457$, $p < 0.05$). However, the variation in the data is large. Further measures assessing the relation of discomfort ratings and body height are listed in Table 14.19: (p. 258) for all the handbrake locations.

Location 5 (fore down) results for taller subjects in higher discomfort than for smaller ones. Taller subjects sit more rearward so that applying the handbrake in the fore low location requires them to have a higher anteversion of the upper arm and eventually leaning forward with the torso. So, additionally to the force of the handbrake, an even higher amount of body weight need to be hold leading to higher joint and muscle load. Some subject may get closer to their physical limits to keep their body in balance.

For the rear down handbrake location (4), the perceived discomfort decreases with the body height. Smaller subjects (with shorter legs) perceive a higher discomfort as they sit more forward which leads to a retroversion (chicken wing posture) which is rather an uncomfortable posture and more adverse to apply force.

For all handbrake locations, the ratings show a high variation even for a small range of body height. For location 4 and 5, the variation of ratings for subjects of similar body height is larger than the mean discomfort difference between the smallest and tallest body height. The high variation in discomfort ratings, even for subjects with similar body heights, is assumed to be caused by numerous reasons (see 2.2 and 2.3), i.e. differences in body segment lengths, joint angles, physical capabilities, expectations (e.g. influenced by the handbrake in their own vehicles), usage of the rating scale and a different level of reproducibility between subjects. Also psychosocial and emotional components may have affected the subjects' ratings, which actually should have assessed the physical discomfort. High variations of discomfort and comfort ratings between subjects have also been reported in literature (Lestrelin & Trasbot, 2005) and were suggested as a reason that discomfort models explained only about 50 % of the

variability in discomfort ratings (Wang et al., 2004, p. 219; Wang & Trasbot, 2011). “It should be noted that a big source of variation of comfort ratings is the subject his(her)self “(Wang et al., 2004, p. 219).

All in all, the trends of the discomfort values are comprehensible and can be explained with the posture and resulting load in the body. They are also in agreement with findings from literature (compare 2.5 and 2.6). For discomfort prediction, trends alone are insufficient and quantification is essential. Thus, modeling with AMS and RAMSIS is needed.

Due to the large variation in subjects' ratings and subject depending reproducibility, it is neither useful nor possible to predict the discomfort of each subject. As mentioned above, in the automotive industry it is common to model key percentiles of the customer group. This is expected to be a useful and efficient approach for the discomfort prediction, too. Therefore the aim of this thesis is set to predict the discomfort value of the regression line for selected key body heights, referred to as target discomfort respectively study discomfort. As key percentiles the 5th and 50th percentile female (5F and 50F) and 50th and 95th percentile male (50M and 95M) are chosen to represent the major population of drivers. Exemplarily, the target discomfort for 50F for handbrake location 4 is marked by a cross in Figure 6.6 (left, p. 153).

The subjective evaluation analysis has reconfirmed hypothesis 1. Subjects perceive different levels of discomfort and the major portion of them are able to rate it reproducibly.

6.3.2 Joint angles

The different handbrake locations influence the joint angles in an expected way. E.g. a smaller distance in z (height) between shoulder and handbrake (location 2) results in a larger elbow flexion, glenohumeral abduction and sternoclavicular elevation (Raiber, 2015). Most of the motion capturing data could be reconstructed successfully in Vicon Nexus and AMS. If this was not the case, data sets were excluded from the study. In general motion capturing fulfilled the aim to analyze and compare the movements of the subjects. Still, minor errors may have occurred such as imperfect marker placement or a shifting of the hip belt during the trial.

When plotting the joint angles against the body height, the regression lines show changes over the body height for most of the joint angles. For example, at the end of handbrake application, glenohumeral abduction, elbow flexion and sternoclavicular

elevation decrease over increasing body height, whereas glenohumeral anteversion increases with increasing body height.

This confirms the anticipations based on empirical knowledge on seating position dependency on body height (Parkin et al., 1995; de Leonardis et al., 1998; Welsh, Clift, Morris, Cook & Watson, 2003; Jonsson et al., 2008; Fröhmel, 2010). It is in line with the findings of the preliminary study that the movement patterns mainly depend on body height (5.2.2.6). Average changes of joint angles over body height have also been documented for seated reach posture (Chaffin et al., 2000).

The joint angle analysis confirms that joint angles differ most between the movement strategy groups respectively subjects of different body heights (e.g. glenohumeral anteversion and abduction, see 5.2.2.5). So, the macro movement patterns depend on body height and according segment lengths and seat adjustment.

Figure 6.9, p. 156, shows that even for similar body heights the right elbow flexion can differ more than the average elbow flexion change over the complete range of body height. This observation is also valid for the other investigated joint angles. These different movement patterns for subjects of similar body height can be named micro movement patterns. They are a consequence of the musculoskeletal system redundancy (see 2.6). They are hard to analysis as fluent transitions can appear which make classifications difficult. Large numbers of individuals are required to study them in detail. It makes matters even more complicated that the movement of the same person for a given task (e.g. handbrake application for same handbrake) can differ between trials (Raiber, 2015). Individual effects may depend on the handbrake in the personal car of the subjects, their physical capabilities and limitations, habits and preferences.

For seated reach postures – in addition to the average change of joint angles over body heights – the 95 % confidence intervals were plotted by Chaffin et al. (2000). They indicate that – also for reach – subject depending variation occurred on top of the stature depending variation. So, the findings on handbrake application are in qualitative alignment with research on reach.

Due to the high variation of joint angles, it appears neither useful nor is possible to predict the discomfort of each individual. In the automotive industry it is common to model key percentiles which are representative for the customer group. This is expected to be a useful and efficient approach for the prediction of joint angles, too. Therefore the aim is set to predict the joint angle values of the regression line (named target angles) for a given body height with RAMSIS. Key percentiles – the 5th and 50th percentile

female (5F and 50F) and 50th and 95th percentile male (50M and 95M) – are chosen to represent the major population of drivers.

So, the joint angle regression values for the four percentiles were chosen as the target values (study values) for the posture prediction with RAMSIS which is described in the next chapter.

The joint angle analysis has shown body height depending movement patterns which confirms hypothesis 2 (Handbrake application movements follow one or more patterns).

7 POSTURE MODELING

Aim of the posture modeling was to develop a RAMSIS procedure for the four key percentiles. It shall deliver reliable posture prediction for both key frames of the handbrake application and all seven handbrake locations. It is assumed that if the prediction for each of the studied handbrake location succeeds, it is also applicable for the whole location range surrounded by studied handbrake locations.

This procedure needs to meet two major requirements. Firstly, the predicted postures need to deliver joint angles sufficiently close to the target angles derived from motion capturing (6.2.2), so that hypothesis 3 (handbrake application movement pattern(s) can be simulated by predicting key postures with RAMSIS) is corroborated. Secondly, the procedure needs to be user friendly, efficient and reliable to be applied in vehicle development. User friendliness shall be achieved by introducing the minimum number of constraints and posture models for all locations and key percentiles.

The procedure was developed in a master thesis (Raiber, 2015) which is summarized in this chapter.

The development of the procedure comprised three major steps which are illustrated in Figure 7.1. On the right side, details – including specific challenges and their resolutions – are listed.

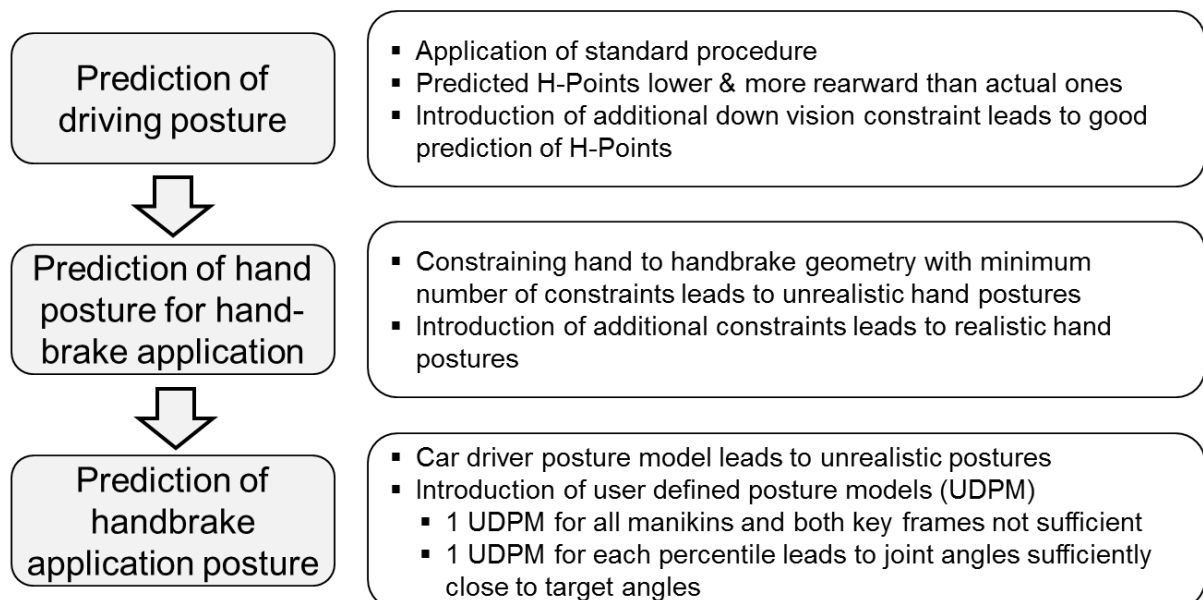


Figure 7.1: Major steps of developing the procedure for handbrake application posture prediction with RAMSIS.

In the following, preliminary considerations and the three steps are described. For each step, methods, results and discussion are summarized.

7.1 Preliminary considerations

For doing the comparison between study and RAMSIS joint angles some characteristics of the motion capturing system and RAMSIS have to be considered.

With motion capturing, changes in angles between body segments are easier to determine than rotational movements. The calculation of the human and RAMSIS manikin segmental rotation is not consistent as reference points differ. E.g. two markers are attached on the wrist of the subjects to capture the rotational movement. This is not the case in RAMSIS because a single joint point represents the RAMSIS wrist. So, the external rotation of the glenohumeral joint and the pronation of the radioulnar joint as measured with the motion capturing system are not comparable with the corresponding upper extremity posture of the RAMSIS manikins. Thus, the affected joint angles were not considered for the posture comparison between RAMSIS and the motion capturing data.

In addition, in RAMSIS the hand needs to be constrained to the handbrake, which limits the wrist movement (flexion/extension and abduction/adduction). Thus, the joint angles of the wrist were lower weighted for the posture comparison.

7.2 Prediction of driving posture

It is common in automotive industry to focus on key percentiles representing the range of the customers. Manikins for the four most commonly used body height percentiles (key percentiles) were created based on the anthropometric database SizeGERMANY (2012) for the year 2013 in which the study was conducted. A 5th percentile body height (5F) and a 50th percentile body height (50F) female and two males of the 50th respectively 95th percentile body height (50M and 95M) were generated. Besides the chosen body heights, all other body proportions (e.g. seating height) were selected to be on average of the corresponding population.

When calculating the driving posture, the seat and steering wheel adjustments/positions are calculated, too. The seat position and H-Point are very important for the handbrake application postures as they influence the relative position of the subject respectively RAMSIS manikin and the handbrake.

The CAD geometry of the test vehicle respectively ErgoBuck was used for predicting the driving posture using standard constraints as described in 2.8.3.2 on p. 72 ff. (Geuss, 1998). The resulting H-Points (representing the seat adjustment) and steering wheel

adjustments/positions were compared to the participants' chosen adjustments/positions in the test drive of the preliminary study. For the seat and steering wheel positions, regression lines over the body height were generated. The values for the key percentiles were calculated and used as target values for the prediction (same procedure as for the ratings and joint angles).

The predicted postures suggested more rearward and lower H-Points than actual H-Points were. The constraints probably did not represent the visibility demands of the drivers sufficiently. So, an additional down vision constraint was added. This sight constraint assures a good driver's field of view through the wind shield and over the hood. The resulting H-Points and steering wheel positions were in line with the values derived from the preliminary study. The difference between the "actual" and simulated H-Point was lowest for the 5F manikin (delta less than 3 mm in x and z) and highest for the 95M manikin (delta less than 5mm in x respectively 7.5mm in z).

Those differences indicate a good prediction quality, especially when considering the typically low interpersonal repeatability of seat adjustment – e.g. 49 mm for length adjustment (Jonsson et al., 2008) – and the large variation of seating positions between subjects of same body height (Fröhmel, 2010).

The accurate prediction of the H-Points and steering wheel adjustments/positions was taken as the basis of further investigations focusing on the handbrake application.

For the prediction of the hand posture and complete body posture of handbrake application, the H-Point was fixed to the value predicted by the simulation of the driving posture. Likewise, the left hand was fixed to the steering wheel correspondingly adjusted to its simulated location. The right foot was placed on the brake pedal, the left one was constrained to the footrest.

7.3 Prediction of hand posture for handbrake application

In this context, hand posture refers to the grasping posture of the hand including fingers and wrist.

RAMSIS offers a grasping database with 29 hand postures to save the users from defining constraints for the numerous joints of the hand. When a hand posture is applied, all hand angles are adjusted at once according to the selected grasp type. The grasping database includes grasping, pressing, pulling, touching, gripping and surrounding postures. (Human Solutions GmbH, 2014b)

To predict realistic hand postures for all handbrake locations and manikins, an appropriate hand grasping posture type has to be chosen. Furthermore, the hand needs to be appropriately constrained to the handle.

The comparison of the predicted wrist and hand angles to those derived from motion capturing was not done by comparing joint angles in AMS joint and segment coordinate system. The reason is: In RAMSIS the wrist is represented by only one point. When the RAMSIS posture is transferred into AMS, the calculation of radioulnar pronation and glenohumeral rotation is impeded. Consequently, the videos of the preliminary study trials were analyzed visually to get an understanding of natural hand postures during the handbrake application.

To simulate the postures for handbrake application, the right hand has to be constrained to the handbrake so that the hand of the manikin is realistically placed on the handle of the handbrake. The pre-defined grasp types in RAMSIS define the hand posture, which needs to be aligned to the geometry. However, all attempts to constrain the hand with the minimum number of constraints and without introducing some kind of auxiliary geometry resulted in interferences and inappropriate hand postures as shown in Figure 7.2.

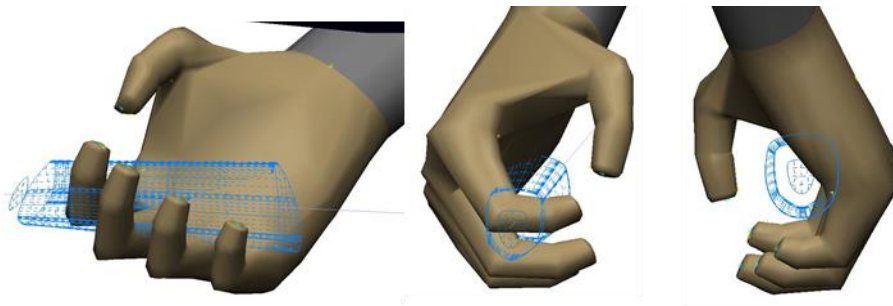


Figure 7.2: Interferences of the hand and handle (Upmann & Raiber, 2014, p. 12).

By choosing the most adequate grasp type and introducing auxiliary geometry with corresponding constraints, the predicted hand postures provided a good alignment of the hand and the handle and looked sufficiently realistic for all handbrake locations and percentiles. This is exemplarily illustrated in Figure 7.3. Since the hand is modeled rigid in AMS (see 8), it is perfectly acceptable that the diameter the fingers embrace is larger than the actual grip.



Figure 7.3: Grasp of the handbrake handle (Upmann & Raiber, 2014, p. 12).

During the development of the procedure for simulating the hand grasping posture it was observed that the hand placement has a large influence on the body posture prediction. So, the consistent application of the identified hand constraints is crucial for the next step.

7.4 Prediction of the handbrake application posture

The right hand was constrained to the handbrake as defined in 7.3. The other constraints were kept as described at the end of 7.2. With this set of constraints, an attempt was made to predict the posture of the key percentiles for start and end of the handbrake application for the different handbrake locations. Initially, the standard RAMSIS Car Driver Model (CDM, see 2.8.4) was used.

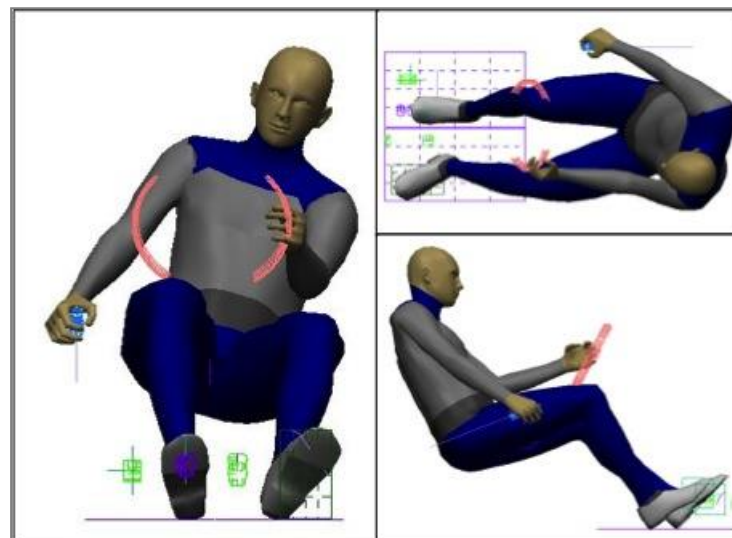


Figure 7.4: Typical predicted handbrake posture when using the RAMSIS Car Driver Posture Model (Raiber, 2015, p. 77).

First, the predicted postures were visually compared to the subjects' postures. Major differences occurred. The subjects tended to distinctly flex their elbows to pull the

handbrake while the RAMSIS manikins had straight arms, leaned the upper body to the left and lifted the right shoulder (Figure 7.4).

In the Car Driver Model (CDM), there is a target and a probability curve for each joint angle. They were derived based on combining the results of several foundation studies mainly focusing on driving and reach postures (see 2.8.4.1). RAMSIS calculates the most probable respectively least uncomfortable posture considering all joint angles (Seidl, 1995).

For the wrist angles, it was observed that the RAMSIS CDM predicts them typically straight, unless there are constraints forcing wrist adduction or abduction and/or palmar flexion or extension. So, in the RAMSIS CDM any non-straight wrist posture seems to be considered unfavorable respectively unlikely.

The constraints, which were applied to restrict the manikin's hand to the handbrake lever, demanded non-straight wrist postures. These strongly influence the other joint angles, which offset the uncomfortable wrist angles. Thus, the whole posture becomes unnatural. (Divivier & Wirsching, 2015; Raiber, 2015)

This led to the conclusion that the Car Driver Model is not capable to reliably predict realistic handbrake application postures without adaptation. The original foundation data, it was based on, does not sufficiently account for handbrake application.

Actions were necessary to improve the posture prediction accuracy for the handbrake application while keeping the procedure user friendly. In the literature, there are suggestions to improve driving posture prediction performance for different vehicle types and body heights by using "different sets of constraints and/or different posture models [...] according to stature group and vehicle" (Bulle et al., 2013, p. 1).

This approach was adapted for the handbrake application. It was decided to keep the constraints as before and to modify the CDM target posture by developing User Defined Posture Models (UDPM, see 2.8.4.1.1, p. 76). The minimum number of UDPM had to be found to assure both, a reliable posture prediction and a user friendly procedure.

To assess the quality of the posture prediction, joint angles of the predicted postures were compared to the joint angles derived from the analysis of the motion capturing data. These joint angles were available in AMS segment coordinate and joint angle systems, which are defined very differently from those in RAMSIS. Therefore, the RAMSIS predicted postures were imported into AMS. After a kinematic analysis in AMS,

the joint angles could be compared to the study joint angles in the AMS joint angle system.

For each percentile, handbrake location and joint angle, the predicted joint angle values were compared to the study (target) values. The acceptable range was defined as the target angle plus/minus one standard deviation (compare Figure 6.9).

The CDM was used as basis for the UDPM. In an iterative process, the target values for selected joint angles were modified. The RAMSIS user interface does not allow modifying the probability functions, thus they could not be changed.

The attempt to use a single UDPM for all four key percentiles did not facilitate good alignment of prediction and target. So, for each key percentile one dedicated UDPM was developed, which was used for the start and end posture. The calculated joint angles were compared to the study joint angles for the start and the end of the handbrake application for all percentiles and handbrake locations. The UDPMs were optimized by iterative steps which are described in detail by Raiber (2015).

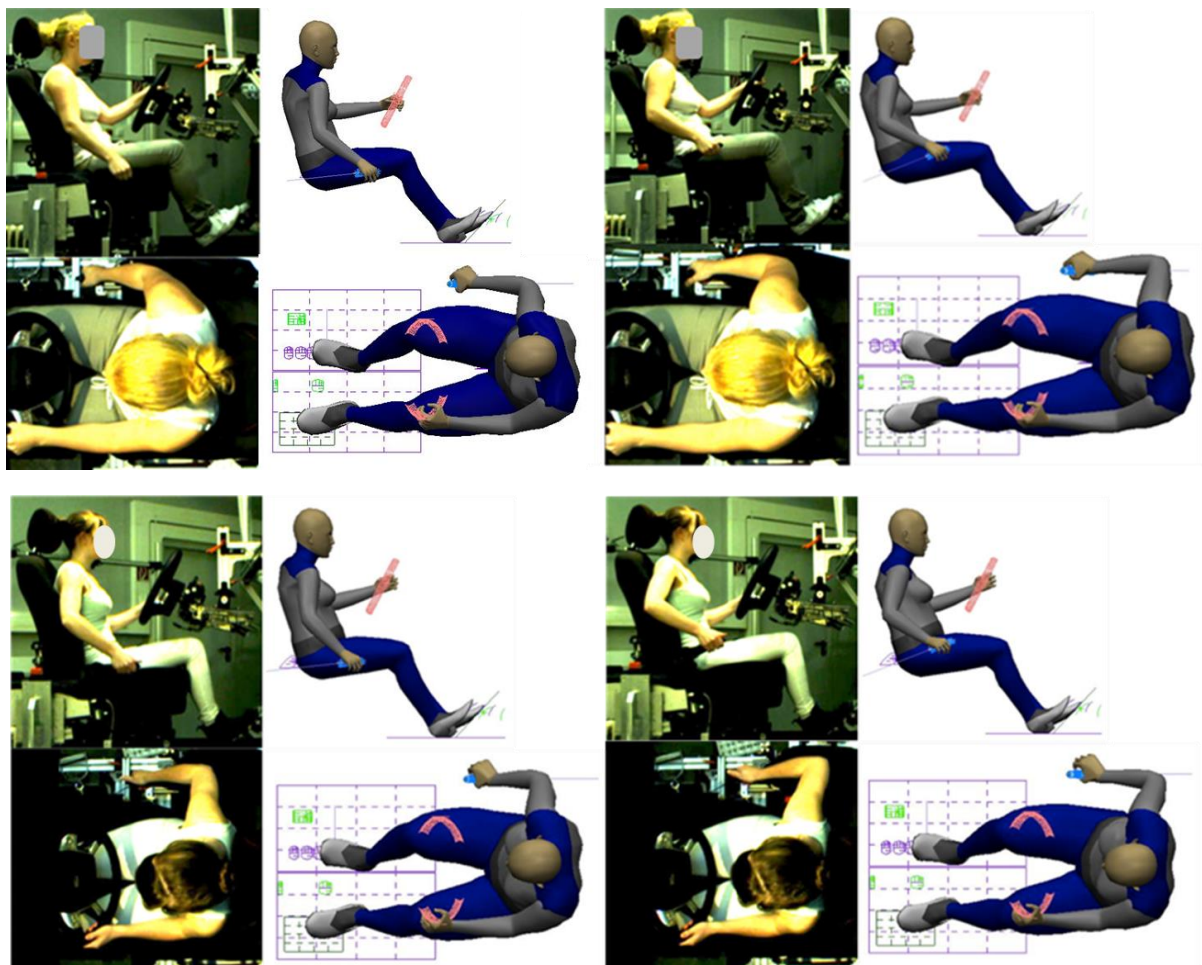


Figure 7.5: Predicted RAMSIS postures compared to corresponding participants in start (left) and end (right) position from side (up) and top (down) view (Raiber, 2015, p. 85 and 88).

The application of the four resulting UDPMs provides reliable posture prediction as exemplary shown in Figure 7.5 . Only few deviations of joint angles from the target values occur. They mainly happen for the wrist angles – as mentioned above – and for the extremer scenarios (rear down location for 5F, fore down location for 95M). Potential reasons include:

- The wrist was rigidly constrained to the handbrake handle.
- The simplified wrist joint in RAMSIS (see 7.1, p. 164) may contribute.
- For UDPMs only the UDPM target angles could be modified and not their probability distributions (see 2.8.4.1.1, p. 76).
- There was only a single UDPM for start and end posture for each percentile.

The joint angles do change between start and end of handbrake application. The changes of the predicted and study derived target values were compared to understand and assess the effect of using a single UDPM for predicting the start and end posture of the handbrake application for each key percentile.

Table 7.1 shows the change of the joint angles during the handbrake application exemplarily for 50M and handbrake location 1. This example shows that on average the change of the predicted joint angles is smaller than the change of the target angles derived from motion capturing. The predicted amount of motion is smaller than the average motion of the subjects. This is also valid for the other percentiles and the other handbrake locations.

Table 7.1: Comparison of changes in joint angles during handbrake application (between start and end) between the target and prediction values for the 50M and location 1. R is the abbreviation for right hand side.

Joint angle difference (end - start)	Target [°]	Prediction[°]	Delta [°] (target - prediction)
RGlenohumeral_Anteversion	-17.4	-12.9	-4.5
RGlenohumeral_Abduction	6.9	3.3	3.6
RElbow_Flexion	31.3	27.5	3.8
RWrist_Flexion	12.7	0.2	12.5
RWrist_Abduction	2.4	-1.3	3.7
RSternoClavicular_Protraction	-4.1	-6.5	2.4
RSternoClavicular_Elevation	4.2	-1.8	6
PelvisThorax_Extension	0.9	0.0	0.9
PelvisThorax_LateralBending	-1.4	-0.7	-0.7
PelvisThorax_Rotation	1.5	-0.6	2.1

The reason is that for each percentile one and the same UDPM is used for start and end posture prediction which has target values between start and end posture. It influences both the start and the end postures into the direction of the in-between posture.

The application of the four UDPMs does lead to predicted postures within the target range for most of the joint angles. Adding more UDPMs would decrease user-friendliness of the procedure. Thus, it was consciously decided not to increase the number of UDPMs.

Consequently, hypotheses 3 (handbrake application movement pattern(s) can be simulated via RAMSIS key postures) was confirmed.

The developed posture prediction procedure is considered applicable for similar handbrake designs within the handbrake location range investigated in this study. For significantly differing handbrake designs and/or handbrake locations, further studies are recommended.

The developed procedure can be used to predict the handbrake application posture e.g. for visualization purposes and clearance checks in vehicle development. In this project, it will be used as input for biomechanical analysis and discomfort prediction. This is described in the following chapters.

8 BIOMECHANICAL MODELING AND CORRELATION TO DISCOMFORT

In this chapter, the analysis of the handbrake application in AMS, resulting biomechanical values and their correlation to the discomfort ratings are described. The aim was to test hypothesis 4 (there are correlations between biomechanical parameters calculated with AMS, based on RAMSIS postures, and the discomfort ratings derived from a corresponding subjective evaluation study).

8.1 Methods

8.1.1 AMS setup

AMS version 5.3.0.3365 and an additional Ford proprietary user interface, the AnyFord Interface (AFI) version 17.2, were applied. The AFI enables the user e.g. to import postures and anthropometric data from RAMSIS to simplify scaling and biomechanical analysis based on RAMSIS simulations (Siebertz & Rausch, 2006).

The applied AMS model of handbrake application was one of several AMS automotive applications developed by Ford and ABT (compare 2.9.2, p. 82).

The list of selected body, muscle, scaling and muscle recruitment models is shown in Table 8.1. The third column references the chapter where the models and the details of the selection process are described. The corresponding page is referenced in the fourth column.

Table 8.1: AMS setup.

Model	Selection	Chapter	Page
Body model	AAUHuman full body model including	2.9.3	82
	Arm and shoulder model	2.9.3.1	82
	Trunk model (neck Modeled rigid)	2.9.3.2	84
	LegTLEM model	2.9.3.3	84
Muscle model	AnyMuscleModel	2.9.4.2	85
Geometrical scaling	Non-isometric scaling	2.9.5.1.2	88
Muscle strength scaling	Body mass scaling	2.9.5.1.2	89
Muscle recruitment	Polynomial criterion with the power of three	2.9.7.1	92

The geometrical set up of the test vehicle respectively ErgoBuck with all seven different handbrake locations was reproduced in AMS software. Optimum support forces were assumed between the manikin's left hand and the steering wheel, the left foot and the footrest, the right foot and the brake pedal as well as between the seat and thigh, buttock and back.

The force between the hand and the handbrake was modeled as a function of pulling direction and handbrake application angle, which were modeled as a function of time (Rausch et al., 2014).

The motion of handbrake application was divided in several steps shown in Table 8.2.

Table 8.2: Modelling steps in AMS.

Step no.	Step name	Description	Handbrake appl. angle	Force transfer between handle and hand	RAMSIS posture
1	start	grasp without force transfer at handle	0	no force transfer	start posture
2	force	start of handbrake application	0	ideal support, no additional handbrake appl. force	start posture
3	application movement	application of handbrake	increasing angle	according to force angle function	none, AMS interpolates
4	end	end of handbrake application	target angle	according to force angle function	end posture

For step 1 (“*start*”), the RAMSIS start posture is modeled with no force transfer between the hand and the handle. This represents the diver’s posture reaching out to grasp the handbrake. The hand is not supported by the handbrake. The body has to maintain balance holding the weight of the right arm and hand with no support for the right arm and hand. This grasp posture without force transfer may have an influence on the discomfort perception. Therefore it is modeled and considered in the analyses additional to the application of the handbrake.

Step 2 (“*force*”) is also based on the RAMSIS start posture and differs from step one by the force transfer between the hand and the handbrake handle. The handle is modeled as a support of the hand allowing for force transfer. So, the handle can hold parts of the right upper extremity weight supporting maintaining balance.

Step 3 (“*application movement*”) is the actual application of the handbrake. For a given number of interim time steps, AMS interpolates between RAMSIS start and RAMSIS end postures while the corresponding values for handbrake application angle and force are considered. The higher the number of interim steps, the longer the calculation process takes in AMS. It was decided to have four interim steps between start and end of handbrake application to be able to check the course of the biomechanical values during the handbrake application.

Step 4 (“*end*”) marks the end of the handbrake application and is based on the RAMSIS end posture, the respective target application angle and the corresponding handbrake application force. All in all, seven time steps were analyzed.

8.1.2 Modeled handbrake applications

Four AMS manikins (5F, 50F, 50M, 95M) were modeled based on the anthropometric data (such as segment length and masses) of the RAMSIS manikins described in chapter 7.2, p. 164. For each of the manikins and for all handbrake locations (6.1.3, p. 145 ff.), the handbrake application was modeled. Location 1 and 6 are identical. All in all, 28 handbrake applications - 4 manikins times 7 handbrake locations - were simulated as described in 8.1.1. Figure 8.1 shows an example.

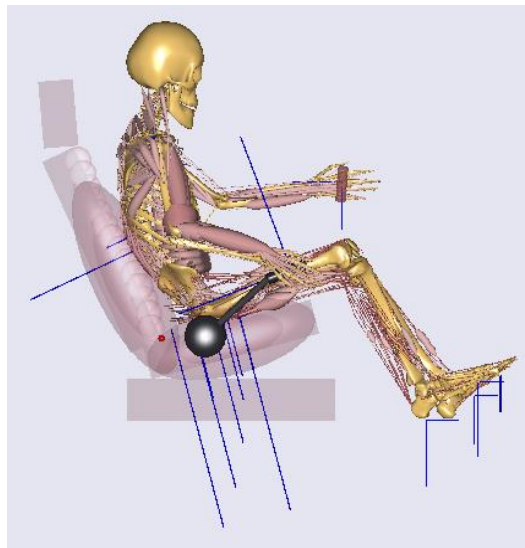


Figure 8.1: Inverse dynamics results for step 4 of the handbrake application for 50M and handbrake location 8.

8.1.3 Analyzed biomechanical parameters calculated with AMS

As described in chapters 2.2 to 2.5, several biomechanical parameters may influence the discomfort perception. AMS calculates a very large number of biomechanical parameters. It is the aim of this work to identify those factors with a major impact on the discomfort perception and to quantify their influence. To address this task efficiently, a pre-selection of parameters, anticipated to influence the discomfort perception, was done based on the literature research. The four selected parameters are described in the literature chapter 2.9.8, p. 94 ff. The details of the analysis are described in the following subchapters, 8.1.3.1 to 8.1.3.4. They were calculated for all 7 simulation steps (Table 8.2).

For the detailed analysis, the values from the time steps *start* (suffix _S), *force* (suffix _F) and *end* (suffix _E), compare Table 8.2, were selected for two reasons. Firstly, a pre-analysis had shown the steps in between (*application movement*) would not enhance the correlations of the biomechanical parameters and discomfort. Secondly, this choice

accounts for the essential steps with regards to the primacy and recency effects (Atkinson & Shiffrin, 1968) and the peak-end rule (Redelmeier & Kahneman, 1996), compare chapter 2.3.3.

8.1.3.1 Metabolic power consumption and energy

The metabolic power consumption (P_{met}) was calculated for all body regions: trunk (suffix $_Trunk$), right and left leg ($_RLeg$, $_LLeg$), right and left arm and shoulder ($_RArm$, $_LArm$) for the discrete points in time. The prefixes R and L abbreviate right and left (for all AMS outputs). Additionally the total metabolic energy (E_{met}) is calculated which is the energy consumption up to the given point in time. So, six factors related to power and energy were calculated for the given points in time.

8.1.3.2 Muscle activity

The maximum muscle activity ($MaMAct$) and mean muscle activity ($MeMAct$) of 42 shoulder and arm muscles as well as of 19 trunk muscles were analyzed. They are listed – with their abbreviations – in appendix 14.5. Additionally, the maximum and mean muscle activities for all muscles of the above mentioned body regions ($MAct$) were considered in the analysis. Muscle activities are shown as decimal values, e.g. a muscle activity of 0.02 corresponds to 2 %.

8.1.3.3 Joint reaction forces and moment measures

Values of 49 joint reactions and 11 joint moment measures were calculated for the given points in time. They are shown in Figure 2.39 (p. 96) and are listed with their abbreviations, effective directions and sign conventions in appendix 14.5.3 (p. 270 ff.).

8.1.3.4 Joint angles

16 joint angles of trunk and right arm were analyzed. They are illustrated in 14.4 (p. 259 ff.) and listed with their abbreviations in Table 14.30 (p. 275).

8.1.4 Relation of biomechanical parameters and discomfort perception

The principle of minimum work (Wang et al., 2004; Wang et al., 2000) suggests that lower values of power, energy, muscle activity, joint reactions and moment measures should result in lower discomfort.

This may not be correct for all use cases since ratings for subjective perceptions such as discomfort strongly depend on the individual expectations. The subject's discomfort

ratings might not perfectly reflect only the level of actual physical discomfort as subjects may not be able to keep their sensations apart.

So, reducing physical discomfort does not necessarily lead to lower perceived discomfort. E.g. very low handbrake application force reduces the joint loads but is likely to be perceived as a defective handbrake.

The relationship to discomfort will be investigated for the predictor groups: metabolic power consumption and total metabolic energy, muscle activity, joint reactions and moment measures as well as joint angles.

Body height and gender will additionally be considered as they might influence the expectations and thus the perception of the discomfort:

E.g. a smaller person may experience higher muscle activity than a larger person with the same task. As the smaller person is used to this and has no different expectation, the discomfort rating may be lower (better) than when a tall person experiences the same muscle activity but is not used to it (and expects lower muscle activity). Also, the energy consumption of a taller person's handbrake application may be larger since body segments of higher weight needs to be moved. The taller person may perceive lower discomfort due to a better relationship of levers, a higher muscle strength and thereby lower muscle activity. Consequently, which of the effects is more crucial depends on numerous different factors.

As described in 6.3.1 (p. 158 ff.), for all the handbrake locations the discomfort target values are determined by calculating the discomfort value with the regression equation for the body height of the key percentiles. Location 1 and 6 are identical and the ratings of the subject group do not differ significantly. So the mean of their target values was considered as a target value for this common location. The target values are shown in Table 8.3.

Table 8.3: Discomfort target values for the handbrake locations and percentiles. The mean discomfort of location 1 and 6 is taken for the analysis.

Location	5F	50F	50M	95M
1	27.38	27.65	27.95	28.24
2	72.39	69.01	65.42	61.78
3	44.43	44.85	45.31	45.77
4	48.09	38.71	28.74	18.61
5	41.68	51.78	62.53	73.44
6	30.90	32.65	34.51	36.40
7	49.24	49.06	48.88	48.69
8	32.54	32.07	31.56	31.05
Mean 1 & 6	29.14	30.15	31.23	32.32

8.1.5 Mathematical procedure

One aim of this thesis was to understand and quantify the correlation of discomfort and the investigated parameters. The analysis was completed in Minitab (Minitab, 2015). Prior to explaining the procedure, selected mathematical terms will be explained.

The 50 level rating scale, which was converted into discomfort ratings from 0 to 100, was considered as interval scale (Bühner, 2004, p. 70). The Pearson correlation coefficient r was applied as a measure of the linear association between the predictors and the discomfort rating. The association is better, the closer the absolute value of r is to 1 (Costich-Sicker et al., 2002; Minitab, 2015). In this study, absolute r values in the range of 0.5 are interpreted as moderate relations. Absolute r values larger than 0.7 are interpreted as indication for good relations.

In multiple regression analysis, r^2 is the coefficient of determination. It is a measure of variation explained by the model. r^2 of 1 indicates that the model explains the variation in the data in full. r^2_{adj} is a modified r^2 which accounts for the number of predictors and data points. r^2_{adj} should ideally be very close to r^2 (Costich-Sicker et al., 2002; Minitab, 2015).

p is a measure indicating the statistical significance of a factor or the complete regression model. Typically, p -values ≤ 0.05 are considered as significant (Costich-Sicker et al., 2002; Minitab, 2015). In this study, p -values ≤ 0.06 are considered as significant. This conscious decision was based on the visual analysis of the biomechanical parameters and discomfort scatterplots. p -values ≤ 0.01 are considered highly significant.

The selection of variables and the procedure to develop a prediction equation is explained below.

For the biomechanical parameters, the values time steps S, F, E were considered (compare Table 8.2). As for the joint angles the values for S and F are the same, there are only the time steps S and E.

In literature, mainly linear (Jung & Choe, 1996; Zacher & Bubb, 2004; Dickerson et al., 2006; Romain & Xuguang, 2012) and quadratic (Kee & Karwowski, 2001b) correlations of discomfort to biomechanical parameters were documented. The visual analysis of the biomechanical parameters and discomfort scatterplots reconfirmed those types of correlations.

So, as described in 8.2, this led to the selection of the variables and their squared values for further analysis.

To screen for variables which correlate sufficiently and significantly to discomfort, Pearson correlation coefficient r and p -values were calculated for the variables and squared variables. If the p -value was smaller than or equal to 0.06 and the Pearson correlation coefficient larger than 0.35, the variable or squared variable was considered for further analyses. All in all, 1252 correlations were studied as shown in Table 8.4.

Table 8.4: Overview of analyzed factors and correlations. Relation types takes in consideration that the association between discomfort and the factor as well as the squared factor were analyzed.

Factor group	Number of factors analyzed	Number of time steps analyzed	Time steps	Number of relation types	Total number of investigated correlations
Metabolic power consumption and energy	6	3	S, F, E	2	36
Mean and max. muscle activity for body parts	10	3	S, F, E	2	60
Max. muscle activity right of shoulder and arm	42	3	S, F, E	2	252
Mean muscle activity right of shoulder and arm	42	3	S, F, E	2	252
Max. muscle activity of trunk	19	3	S, F, E	2	114
Mean muscle activity of trunk	19	3	S, F, E	2	114
Joint reactions (forces and moments)	49	3	S, F, E	2	294
Joint moment measures (caused purely by muscles)	11	3	S, F, E	2	66
Joint angles	16	2	S, E	2	64
Sum	214				1252

8.2 Results and discussion

The correlations of variables and squared variables to discomfort were analyzed. Figure 8.2 and Figure 8.3 show examples of good linear relationships between the variable and discomfort. For the inferior superior force of sternoclavicular joint at the end of handbrake application, discomfort increases when the direction changes from inferior to superior and with increasing magnitude of the superior force (Figure 8.2, left). Highest discomfort values are reached for handbrake locations 5 (fore down) and 2 (rear up).

For the humeroulnar axial moment at the end of handbrake application (Figure 8.3), the values are negative which indicates external direction of the moment acting on the ulna. The larger the absolute value of external moment is, the lower is the perceived discomfort.

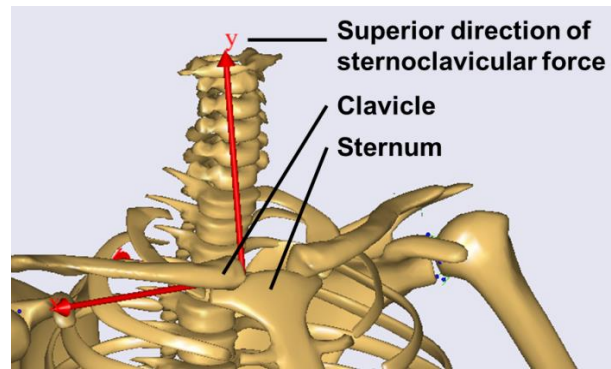
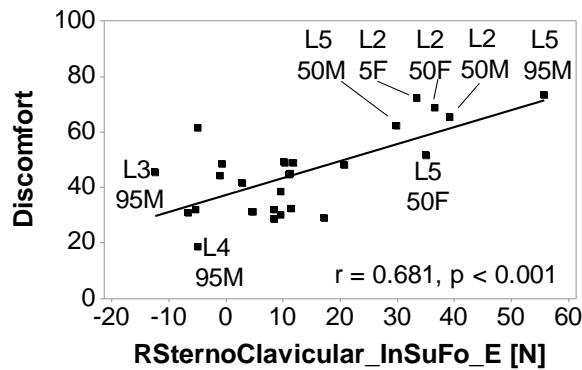


Figure 8.2: Left: Inferior superior force of sternoclavicular joint at the end. Force acts from thorax on clavicle. Positive sign indicates superior force direction.

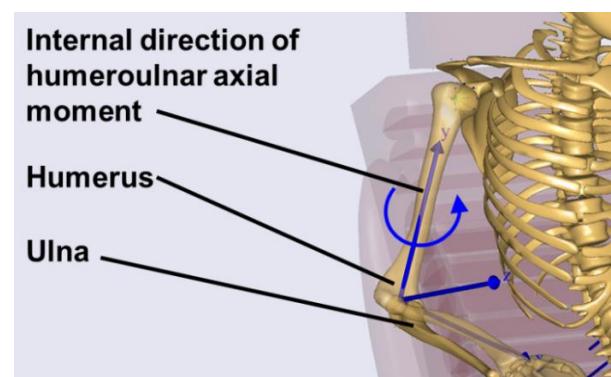
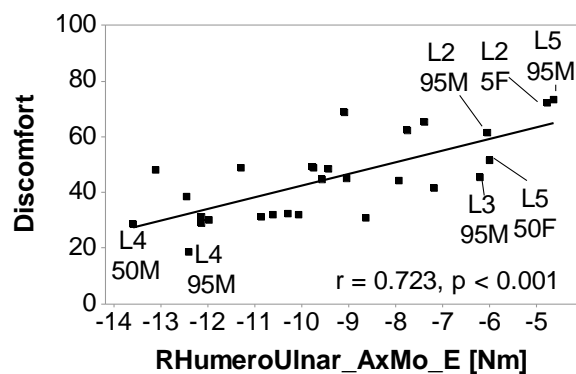


Figure 8.3: Right: Humeral ulnar axial moment at the end of handbrake application. The moment acts from humerus on ulna. Internal direction is positive. So, the negative sign indicates external direction of the moment acting on the ulna.

Figure 8.4: shows an example of a correlation between discomfort and a squared variable, the pelvis axial rotation.

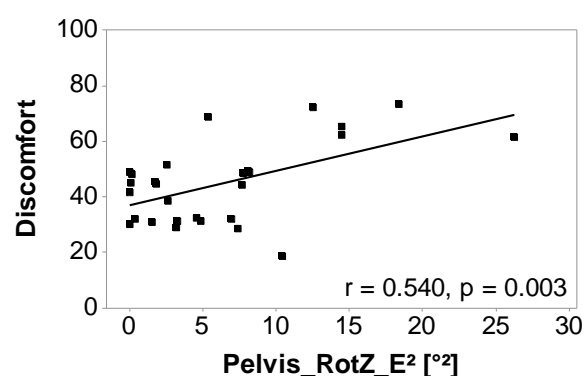
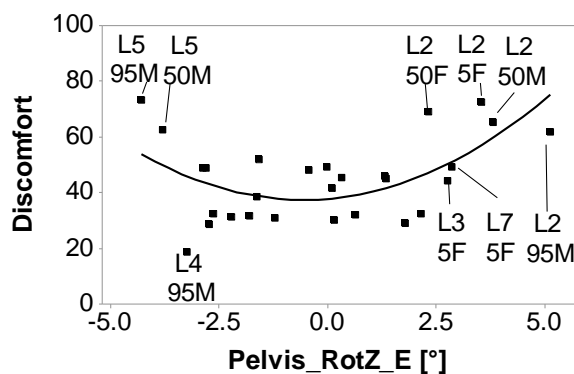


Figure 8.4 Discomfort versus the pelvis axial rotation to the left (positive) and to the right (negative). Rotations in both directions increase discomfort.

Quadratic relations are expected in particular for joint angles. The optimum joint angle (respectively optimum joint angle range) is likely to lead to minimal discomfort values.

An increase or decrease from the optimum is likely to result in discomfort. As described in 8.1.5, all of the 1252 p and r values were calculated to investigate the relation between discomfort and the factors respectively squared factors for the described points in time. For each of the factor groups (such as joint angles or joint reactions), the number of correlations with $p \leq 0.06$ (significant) and $p \leq 0.01$ (highly significant) was determined, see Table 8.5.

Table 8.5: Overview of factors and their correlation to discomfort.

Factor group	Number of correlations analyzed	Number of correlations with $p \leq 0.06$	Percentage of correl. with $p \leq 0.06$	Number of correlations with $p \leq 0.01$	Percentage of correl. with $p \leq 0.01$
Metabolic power consumption and energy	36	20	56	6	17
Mean and max muscle activity for body parts	60	8	13	2	3
Max muscle activity right shoulder and arm	252	52	21	8	3
Mean muscle activity right shoulder and arm	252	56	22	8	3
Max muscle activity trunk	114	23	20	6	5
Mean muscle activity trunk	114	21	18	6	5
Joint reactions (forces and moments)	294	30	10	17	6
Joint moments (caused purely by muscles)	66	6	9	5	8
Joint angles	64	7	11	3	5
All in all	1252	223	18	61	5

Metabolic power consumption and energy showed highest percentages of significant and highly significant correlations. A potential explanation is the high information content of those values.

Table 8.6 shows the factor with highest absolute r value for each factor group. The r values are between 0.54 and 0.723 which indicates moderate respectively good correlations. The p-values (smaller than or equal to 0.003) suggest high significance. These are first indications that it may be possible to predict discomfort based on AMS output.

Highest absolute r values are obtained for the axial moment of the right humeroulnar joint at the end and the mean muscle activity of the right rhomboid muscle at the end.

Table 8.6: Best correlating factors in each factor group.

Factor group	Best correlating factor	p-value	r
Joint reactions (forces and moments)	RElbowHumeroUlnar_AxialMoment_E	< 0.001	0.723
Mean muscle activity right shoulder and arm	MeMAct_RRhomboides_E	< 0.001	-0.698
Joint moments (caused purely by muscles)	RGlenoHumeral_ExternalRotation Moment_E ²	< 0.001	0.637
Mean and max muscle activity for body parts	MeMAct_LArm_F	0.001	0.613
Max muscle activity right shoulder and arm	MaMAct_RPronatorQuadratus_F	0.002	0.559
Mean muscle activity trunk	MeMAct_RErectorSpinae_F	0.002	0.556
Joint angles	RGlenohumeral_Abduction_S	0.002	0.550
Max muscle activity trunk	MaMAct_RObliquusInternus_F ²	0.003	0.548
Metabolic power consumption and energy	Pmet_Trunk_S	0.003	0.540

In the following, correlating factors with $p \leq 0.06$ are listed for each of the factor groups. From a large number of factors with significant correlations, factors were selected to be described to fulfill the main purpose to illustrate:

1. The correlation quality.
2. Patterns which are representative for a number of factors.
3. Patterns with interesting phenomena.
4. Factors which are part of the regression model (covered in chapter 9).

It was found that there are factors and squared factors which correlate well with discomfort over their complete bandwidth (e.g. as in Figure 8.3), while others correlate well only within certain ranges of bandwidth, often toward the higher values of the factor (as in Figure 8.8).

8.2.1 Metabolic power consumption (Pmet) and total metabolic energy (Emet)

Table 8.7 shows the factors with $p \leq 0.06$ and their r values, ordered by decreasing value of r . Factors highlighted in body print are mentioned in the text. Their values for percentiles and handbrake locations are listed in Table 14.31.

Table 8.7: Pmet and Emet factors with correlations to discomfort with p-values ≤ 0.06 . Factors shown in bold are mentioned in the text.

Factor	r	p
Pmet_Trunk_S	0.540	0.003
Pmet_LArm_F	0.516	0.005
Pmet_RLeg_F ²	0.509	0.006
Pmet_LArm_F ²	0.505	0.006
Pmet_Trunk_S ²	0.484	0.009
Pmet_RArm_S ²	0.483	0.009
Pmet_RLeg_E ²	0.472	0.011
Pmet_LLeg_F²	0.467	0.012
Pmet_RLeg_F	0.450	0.016
Emet_F ²	0.446	0.017
Pmet_RArm_S	0.435	0.021
Pmet_LLeg_E ²	0.422	0.025
Pmet_LLeg_F	0.401	0.034
Emet_total_F	0.401	0.034
Pmet_LLeg_E	0.398	0.036
Pmet_RLeg_E	0.397	0.037
Pmet_Trunk_F	0.396	0.037
Pmet_RArm_E	-0.386	0.043
Pmet_Trunk_F ²	0.380	0.046
Pmet_RArm_E ²	-0.372	0.052

The metabolic power consumed at the start (when the handbrake is grasped but there is no force transfer yet, Pmet_Trunk_S, see Figure 8.5 on the left) is the best correlating factor within this group of factors.

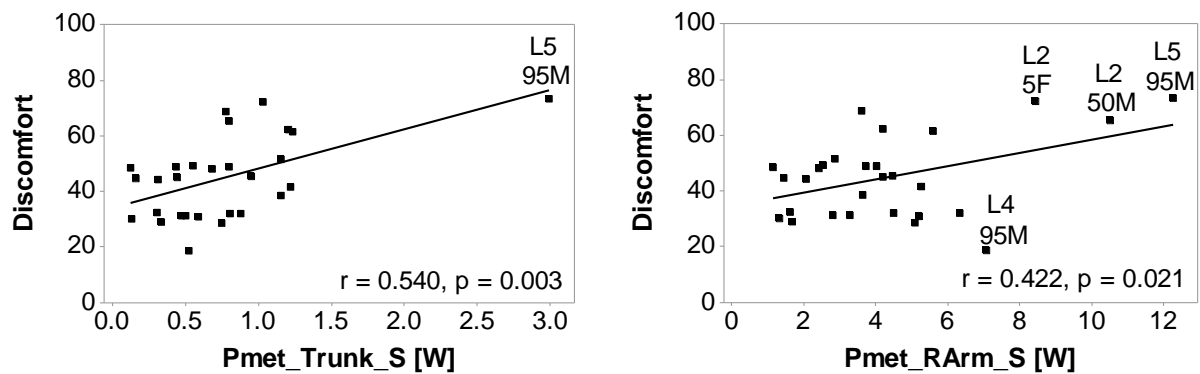


Figure 8.5: Discomfort versus metabolic power of the trunk (left) and right shoulder and arm (right) at the start time step.

Higher metabolic power values and higher discomfort occur especially for location 5 (fore down, large anteversion of arm, forward leaning of trunk, exertion of muscles to stabilize posture, highest value for 95M) and location 2 (rear up, exertion of trunk and arm muscles to stabilize for chicken-wing posture of shoulder and arm).

Pmet_RArm_S (the metabolic power consumed the right arm at the start) in is part of the regression model (chapter 9). It correlates to Pmet_Trunk_S ($r = 0.725$, $p < 0.001$). As shown in Figure 8.5 (right), again the 95M reaches the highest value (location 5) and location 2 results in high values for 5F and 50M.

Pmet_LLeg_F² (the squared metabolic power of the left leg at the time when the handbrake is used as support) is also part of the regression model. It grows when a high support of the leg is used to balance respectively stabilize the posture. Highest values are reached for 5F for location 2 (rear up) and 4 (rear down) and for 95M for location 5 (fore down) and 7 (large lateral distance), see Figure 8.6 (left figure). These are unfavorable concurrences of body height (with corresponding seat position) and handbrake location. For low values of Pmet_LLeg_F², there is a high variation of discomfort ratings. This indicates that for those handbrake locations and percentiles other contributors have larger effects on the discomfort perception.

Pmet_Trunk_S (Figure 8.5 on the left), Pmet_RArm_S (Figure 8.5 on the right) Pmet_LLeg_F² (Figure 8.6 on the left) have two patterns in common:

1. Most of the data points are at lower Pmet values. Lower Pmet_LLeg_F² values also lead to a high variation of discomfort ratings.
2. There are few “outliers” for higher Pmet values and higher discomfort ratings. For Pmet_Trunk_S there is even only one outlier.

These patterns can indicate a spurious relationship. However, a causal relationship (dependency) between each of the three Pmet values and discomfort makes sense. It can be concluded that for the handbrake locations and percentiles which lead to smaller Pmet values (Pmet_Trunk_S, Pmet_RArm_S, Pmet_LLeg_F²) other factors have a higher contribution to the discomfort rating. However, for higher values of Pmet_Trunk_S, Pmet_RArm_S, Pmet_LLeg_F², these factors gain influence on the discomfort rating.

When the perceived discomfort increases with higher consumed power or energy, r is positive. This is mainly the case. However, for the metabolic power at the end of handbrake application r is negative (-0.386) which is illustrated in Figure 8.6 (left).

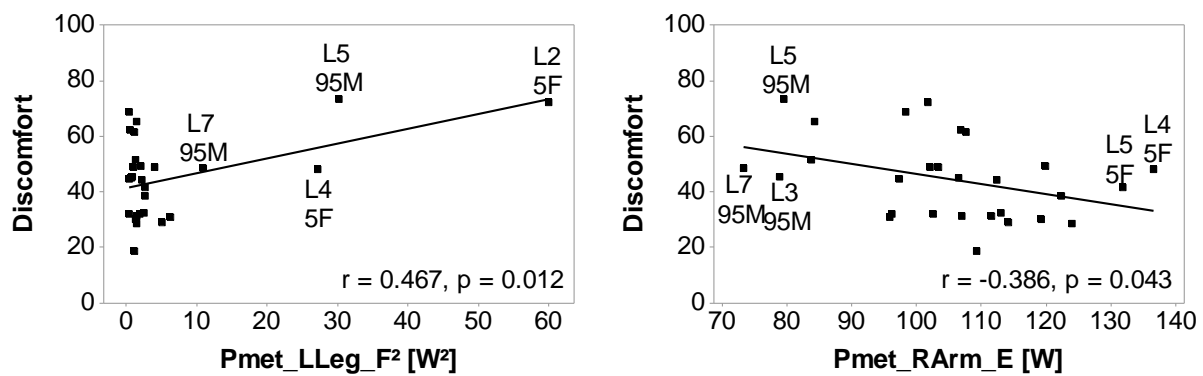


Figure 8.6: Left: Discomfort versus squared metabolic power at the force time step, right: discomfort versus metabolic power of the right shoulder and arm at the end.

Several reasons may contribute to a different extent (depending on percentile and handbrake location) such as expectations, seat position, muscle mass and lever arms of upper extremities. Other biomechanical values may partly have a larger influence on the discomfort perception. E.g. smaller females are at a disadvantage for muscle volume and lever arms of their upper extremities. They are used to high efforts when pulling the handbrake and unfavorable handbrake locations relative to the typical seat position (fore up). So, “low” expectations might be a reason that high metabolic power values lead to rather moderate discomfort ratings (see Figure 8.6).

Drivers expect to consume more energy towards the end of the handbrake application. This is in contrast to the start of the handbrake application, when lower power consumption is likely (the handbrake application force is small). A poor starting posture can also increase discomfort even if the final posture seems ergonomically acceptable (i.e. when towards the end of handbrake application relatively low energy is consumed in comparison to other percentiles or handbrake locations). E.g. this is the case for the 95M who rates the fore down location (5) poor (discomfort rating is 73) but has one of the lowest Pmet_RArm_S values.

All in all, it can be concluded that metabolic power and energy consumption factors at the start and force time steps correlate moderately (r up to 0.54) but highly significant (p close to 0) to discomfort. They enable to differentiate between poor and good ergonomic conditions for the start posture, which has a significant impact on the overall discomfort rating. It seems not to be useful to base discomfort prediction on the metabolic energy of the right arm at the end for the reasons mentioned above.

8.2.2 Muscle activity

8.2.2.1 Maximum and mean muscle activity for body regions

Maximum and mean muscle activities of body regions with significant correlations to discomfort ($p \leq 0.06$) are shown in Table 8.8. All of them are related to the trunk, left and right shoulder and arm muscular activities at the force time step (the handle is not yet pulled but there is force transfer between right hand and handle). The factors reflect the muscular load required to hold the trunk and arm in the posture to begin with handbrake application. Still, none of them is part of the final prediction equation. However, this load is reflected in the regression equation (chapter 9) by metabolic power values and by muscle activities of the pectoralis major and the trapezius muscle.

Table 8.8: Mean and max muscle activity of body regions with correlations to discomfort with p-values ≤ 0.06 .

Factor	r	p
MeMAct_LShArm_F	0.613	0.001
MeMAct_LShArm_F ²	0.564	0.002
MaMAct_Trunk_F	0.430	0.022
MaMAct_RShArm_F	0.416	0.028
MaMAct_RShArm_F ²	0.412	0.029
MaMAct_Trunk_F ²	0.410	0.030
MeMAct_Trunk_F ²	0.393	0.039
MeMAct_Trunk_F	0.385	0.043

8.2.2.2 Maximum and mean muscle activity for the trunk

Table 8.9 lists the trunk muscles for which the maximum (left column) respectively mean (right column) muscle activities correlate to discomfort with p-values ≤ 0.06 . Both columns are ordered by decreasing value of r. The muscles interact for rotation, lateral flexion and flexion/extension of the trunk. The force time step is predominant, so the trunk muscle activity indicates the portion of discomfort caused when force transfer between hand and handbrake starts.

Table 8.9: Trunk muscles for which maximum and mean muscle activities show correlations to discomfort with p-values ≤ 0.06 . Factors shown in bold are mentioned in the text.

Max. muscle activity of muscle	r	p	Mean muscle activity of muscle	r	p
RObliquusInternus_F²	0.548	0.003	RErectorSpinae_F ²	0.565	0.002
RObliquusIntern_F	0.522	0.004	RErectorSpinae_F	0.556	0.002
Transversus_F	0.517	0.005	LSemispinalis_F	0.539	0.003
RSemispinalis_F	0.510	0.006	LSemispinalis_F ²	0.536	0.003
RectusAbdominis_S ²	0.510	0.022	Transversus_F	0.517	0.005
Transversus_F ²	0.502	0.006	Transversus_F ²	0.502	0.006
RSemispinalis_F ²	0.492	0.008	LThoracicMultif_F ²	0.447	0.017
LThoracicMultifidi_F	0.450	0.016	RQuadratusLumborum_E ²	0.446	0.017
LThoracicMultif_F ²	0.450	0.016	LThoracicMultifidi_F	0.437	0.020
LMultifidi_F	0.446	0.017	LMultifidi_F	0.436	0.021
RErectorSpinae_F	0.440	0.019	RectusAbdominis_S ²	0.433	0.022
RErectorSpinae_F ²	0.431	0.022	RSemispinalis_F ²	0.416	0.028
LMultifidi_F ²	0.426	0.024	RSemispinalis_F	0.402	0.034
RThoracicMultifidi_F ²	0.417	0.027	RQuadratusLumborum_E	0.392	0.039
RThoracicMultifidi_F	0.410	0.030	LMultifidi_F ²	0.390	0.040
LErectorSpinae_F ²	0.393	0.039	RThoracicMultifidi_F ²	0.386	0.043
LSemispinalisL_F ²	0.391	0.040	RectusAbdominisS	0.372	0.051
LErectorSpinae_F	0.388	0.042	RThoracicMultif_F	0.367	0.055
LSemispinalis_F	0.377	0.048	LErectorSpinae_F ²	0.366	0.055
RQuadratusLumborum_E ²	0.374	0.050	RObliquusExternus_S	0.361	0.059
RectusAbdominis_S	0.372	0.051	LThoracic_Multifidi_E ²	0.359	0.060
RMultifidi_F	0.360	0.060			
RMultifidi_F ²	0.360	0.060			

Most of the muscles appear in the left and in the right column of Table 8.9. Both, their maximum and mean values correlate significantly to discomfort. In most cases maximum and mean muscular activity of a muscle are highly correlated and show similar or same r and p values when correlated to discomfort (e.g. Transversus_F). However, there are also cases in which the r and p values differ when comparing the correlation of maximum and mean muscle activity to discomfort (e.g. RErectorSpinae_F). So, both, maximum and mean muscular activity of trunk muscles, were kept in the dataset for the generation of a regression model.

Figure 8.7 (left) shows the association of discomfort with the maximum muscle activity of the right internal oblique muscle (illustrated in Figure 14.28) which is involved in trunk rotation, lateral bending and flexion/extension. The relationship between the mean muscle activity of right erector spinae muscle (erects the spine, Figure 14.29) at the force time step is shown in Figure 8.7 (right).

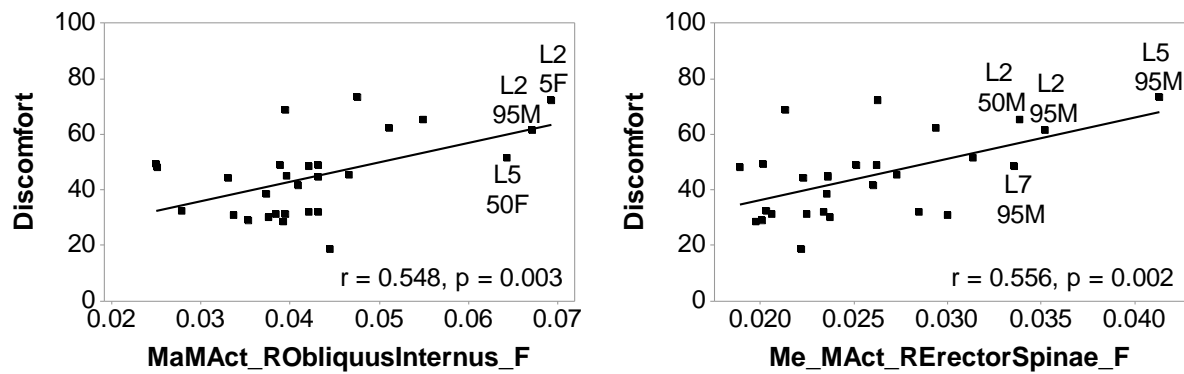


Figure 8.7: Left: Discomfort versus maximum muscle activity of right internal oblique muscle at the force time step versus discomfort. Right: Discomfort versus mean muscle activity of right erector spinae muscle at the force time step.

None of the trunk muscle activities was part of the regression model. Probably other factors cover the information content with regards to discomfort perception. Still, the r values of up to 0.57 and the p -values close to 0 indicate that trunk muscles are valuable indicators of discomfort, especially its share experienced during the force time step.

8.2.2.3 Maximum and mean muscle activity for right shoulder and arm muscles

Table 8.10 shows the right shoulder and arm muscles for which the maximum (left column) respectively mean (right column) muscle activities show correlations to discomfort with p -values ≤ 0.06 . Values in both columns are sorted by decreasing value of r . All three time steps are represented, the best correlations are related to the end and force time step.

Most of the muscles appear in the left and in the right column of Table 8.10, so their maximum and mean values correlate significantly to discomfort. In most cases maximum and mean muscular activity of a muscle are highly correlated and show similar or same r and p -values when correlated to discomfort (e.g. RTricepsMedialHead_S²).

Table 8.10: Right shoulder and arm muscles for which maximum and mean muscle activities show correlations to discomfort with p-values ≤ 0.06 . Factors shown in bold are mentioned in the text.

Max. muscle activity of muscle	r	p	Mean muscle activity of muscle	r	p
RPronatorQuadratus_F	0.559	0.002	RRhomboideus_E	-0.698	< 0.001
RRhomboideus_E	-0.528	0.004	RRhomboideus_E ²	-0.603	0.001
RBicepsBrachiiCaput_F ²	0.508	0.006	RPronatorQuadratus_F	0.533	0.002
RSubscapularis_F ²	0.484	0.009	RDeltoidesScapularPart_F ²	0.533	0.003
RInfraspinatus_E ²	0.481	0.010	RDeltoidesScapularPart_F	0.529	0.004
RTricepsMedialHead_S ²	0.480	0.010	RTrapeziusScapularPart_E²	0.522	0.004
RTricepsLateralHead_S ²	0.478	0.010	RTricepsMedialHead_S ²	0.480	0.010
RTrapeziusScapularPart_E ²	0.477	0.010	RTricepsLateralHead_S ²	0.478	0.010
RBrachioradialis_F ²	0.469	0.012	RAnconeus_S ²	0.467	0.012
RAnconeus_S ²	0.465	0.013	RSternocleidomastoid_F ²	0.465	0.013
RSternocleidomastoid_F ²	0.465	0.013	RExtensor_DigitiMinimi_S ²	-0.465	0.013
RExtensor_DigitiMinimi_S ²	-0.465	0.013	RBrachioradialis_F ²	0.463	0.013
RSubscapularis_F	0.462	0.013	RAnconeus_S	0.454	0.015
RPectoralisMajorClavicularPart_E	0.459	0.014	RBrachialis_F ²	0.453	0.016
RTricepsMedialHead_S	0.453	0.015	RDeltoidesClavicularPart_E	0.452	0.016
RRhomboideus_E ²	-0.452	0.016	RTricepsMedialHead_S	0.452	0.016
RBrachialis_F ²	0.450	0.016	RTricepsLateralHead_S	0.448	0.017
RTricepsLateralHead_S	0.448	0.017	RDeltoidesClavicularPart_E ²	0.444	0.018
RAnconeus_S	0.445	0.018	RPronatorTeresHumeralHead_E	-0.442	0.018
RInfraspinatus_E	0.445	0.018	RExtensor_DigitiMinimi_S	-0.439	0.019
RPronatorTeresCaputHumeral	-0.442	0.018	RInfraspinatus_E ²	0.438	0.020
RExtensorDigitiMinimi_S	-0.439	0.019	RSubscapularis_S ²	0.436	0.020
RBicepsBrachii_F	0.435	0.021	RFlexorPollicis_S ²	0.429	0.023
RSerratusAnterior_F	0.435	0.021	RPectoralisMinor_F ²	0.425	0.024
RFlexorPollicis_S ²	0.429	0.023	RPectoralisMajorThoracicPart_E	0.424	0.024
RPronatorQuadratus_F ²	0.426	0.024	RPectoralisMajorClavicularPart_E	0.423	0.024
RDeltoidesClavicularPart_E	0.423	0.024	RPectoralisMajorThoracicPart_E ²	0.417	0.041
RPectoralisMajorClavicularPart_E ²	0.422	0.025	RPronatorTeresHumeralHead_E ²	-0.409	0.031
RSerratusAnterior_F ²	0.420	0.026	RSerratusAnterior_F ²	0.408	0.031
RPectoralisMinor_F ²	0.420	0.026	RPectoralisMinor_F	0.408	0.031
RDeltoidesClavicularPart_E ²	0.419	0.025	RFlexorPollicis_S	0.407	0.031
RPectoralisMajorThoracicPart_E	0.417	0.027	RSternocleidomastoid_E ²	0.405	0.032
RPronatorTeresHumeralHead_E ²	-0.409	0.031	RTrapeziusScapularPart_F ²	0.404	0.016
RFlexorPollicis_S	0.407	0.031	RTrapeziusScapularPart_E	0.404	0.033
RSternocleidomastoid_E ²	0.405	0.032	RTrapeziusClavicularPart_F ²	0.404	0.033
RPectoralisMajorThoracicPart_E ²	0.402	0.034	RSupraspinatus_E ²	0.399	0.035
RPectoralisMinor_F	0.400	0.035	RLatissimusDorsi_E	-0.398	0.036
RPronatorTeresHumeralHead_F ²	0.400	0.035	RCoracobrachialis_E	0.394	0.038
RCoracobrachialis_E	0.395	0.038	RTeresMajor_E	-0.394	0.038
RTricepsLateralHead_S ²	0.394	0.038	RExtensorCarpiRadialis_E ²	0.390	0.040
RTrapeziusScapularPart_F²	0.391	0.040	RCoracobrachialis_E ²	0.388	0.041
RCoracobrachialis_E ²	0.386	0.042	RPectoralisMajorClavicularPart_E ²	0.388	0.041
RSupinatorUlnarPart_F ²	0.386	0.043	RSupinatorUlnarPart_F ²	0.386	0.043
RPronatorTeresUlnarHead_F	0.376	0.049	RSerratusAnterior_F	0.385	0.043
RTeresMajor_E	-0.376	0.049	RPronatorTeresHumeralHead_F ²	0.385	0.043
RSubscapularis_S ²	0.374	0.050	RPronatorTeresUlnarHead_F	0.376	0.049
RSupinatorHumeralPart_F ²	0.374	0.050	RTricepsLongHead_S ²	0.374	0.050
RAbductorPollicis_E ²	0.369	0.053	RSubscapularis_S	0.371	0.052
RSerratusAnterior_E ²	0.369	0.053	RPronatorTeresHumeralHead_F	0.370	0.053
RBrachioradialis_F	0.367	0.055	RAbductorPollicis_E ²	-0.369	0.053
RExtensorPollicis_E ²	0.365	0.056	RExtensor_Pollicis_E ²	0.365	0.056
RTrapeziusScapularPart_E	0.362	0.058	RInfraspinatus_E	0.364	0.057
			RPronatorQuadratus_F ²	0.363	0.057
			RPectoralisMajorClavicularPart_F²	0.362	0.058
			RSubscapularis_F ²	0.361	0.059
			RTrapeziusScapularPart_F	0.359	0.060

For the maximum muscle activity with the highest r value, this phenomenon reoccurs similarly. The association of discomfort and the maximum muscle activity of the right pronator quadratus muscle at the force time step and discomfort is shown in Figure 8.9 (left). This muscle, which pronates the forearm (Platzer et al., 2003), is shown in Figure 14.31 (p. 269). It is eye-catching again that the discomfort has a high variation when this muscle is not activated as other factors determine the discomfort perception. The phenomenon of a high variation of discomfort for a very low muscular activity of a specific muscle occurs also for other muscles. The reason is that for some of the percentiles and handbrake locations other sources of discomfort occur, which overlay and determine the discomfort perception.

Both muscle activities in Figure 8.8 show patterns which may indicate spurious relationships (compare Figure 8.5 and Figure 8.6) and therefore have to be interpreted with caution. Reasons for the patterns have been described above.

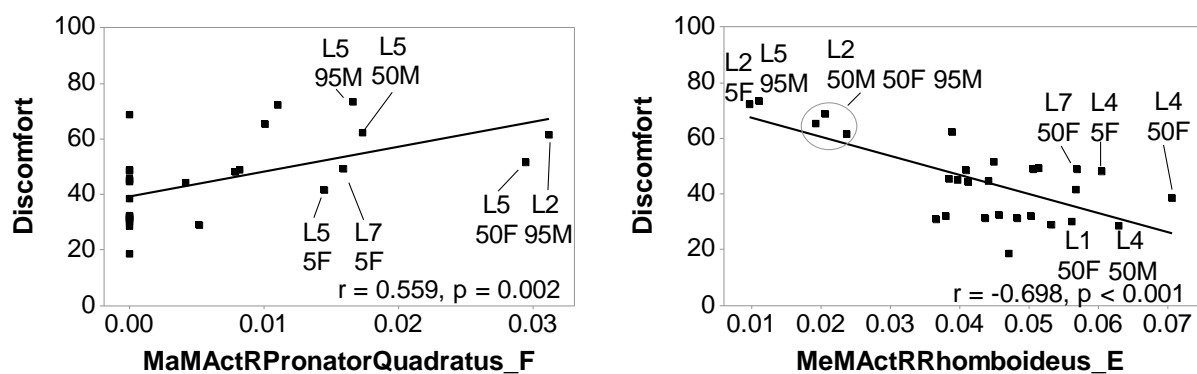


Figure 8.9: Left: Discomfort versus maximum muscle activity of the right pronator quadratus muscle at the force time step. Right: Discomfort versus mean muscle activity of the right rhomboid muscle at the end time step.

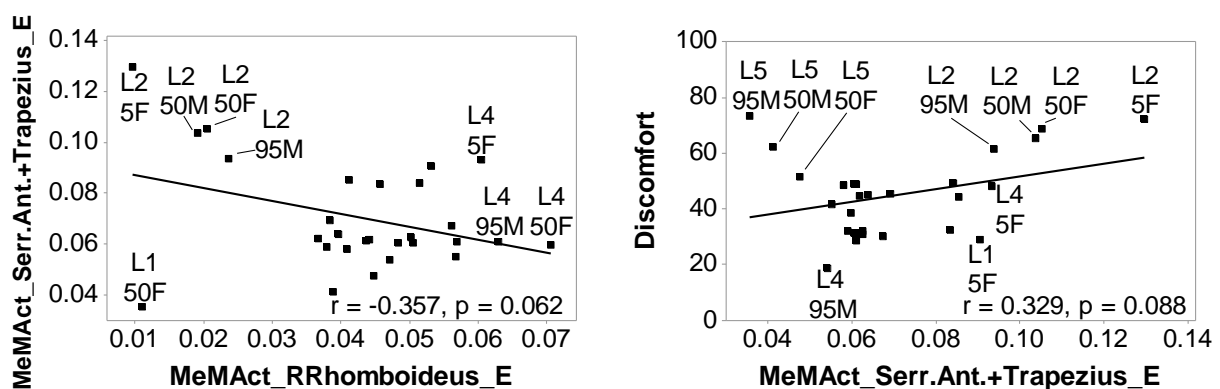


Figure 8.10: Left: Scatterplot of the mean muscle activity of the right rhomboid muscle at the end time step versus the mean muscle activity of right serratus anterior and both parts of the trapezius muscle. Right: Discomfort versus the sum of mean muscle activities of right serratus anterior and both parts of the trapezius muscle.

Also Figure 8.9 and Figure 8.10 partly show patterns common for spurious relationships, so need to be analyzed with caution, too.

Figure 8.9 (right) shows another interesting phenomenon: The discomfort decreases with increasing muscle activity of the right rhomboid muscle at the end time step. The rhomboid muscle fixates the scapula to the ribcage. Contracting it pulls the scapular towards the thorax and towards the spine in upward (cranial) and medial direction (Platzer et al., 2003). It is illustrated in Figure 14.29 (p. 267).

This phenomenon (discomfort decrease with increasing muscle activity of the right rhomboid muscle) can be explained with the mean muscle activity of its antagonists, serratus anterior and trapezius muscle, which increases when the activity of the rhomboid muscle decreases (Figure 8.10). The antagonists allow for increasing anteversion and elevation of the arm and elevation of the shoulder: Growing muscle activity of the antagonists increases discomfort (Figure 8.10, right). The serratus anterior muscle is illustrated in Figure 14.28 (p. 266) and Figure 14.29 (p. 267). One of its functions is to pull the scapular forwards, which is a precondition for the anteversion of the arm. It also rotates the scapular outwards which enables elevation of the arm (Platzer et al., 2003). The trapezius muscle - which is illustrated in Figure 14.29 - supports the serratus anterior muscle to in enabling elevation of the shoulder (Platzer et al., 2003).

Absolute values for r of up to 0.7 and for p close to 0 indicate that maximum and mean muscle activities can be used as valuable indicators of discomfort during handbrake application. However, some of the figures presenting muscle activities versus discomfort show patterns indicating spurious relationships and have to be interpreted carefully.

A direct comparison of r and p -values to literature is not possible as the experimental set up, rating scales and calculation routines strongly differ from the ones in this thesis. Still, a similar high correlation level as in this work was shown for the correlation of the sum of normalized EMG values of 8 muscles and the normalized reach discomfort perception with $r = 0.73$ (Jung & Choe, 1996).

8.2.3 Joint reactions

Joint reaction forces and moments are calculated based on muscle and exterior forces. Table 8.11 lists the joint reactions, which show correlations to discomfort with p -values ≤ 0.06 , ordered by decreasing value of r .

Most of them and in particular those with the highest absolute r values belong to shoulder and arm joints at the end time step. The r of up to 0.723 and p -values close to 0 indicate that the joint reactions are a very valuable indicator of discomfort, especially its portion caused during the end time step. There are also significant correlations of discomfort and vertebrae reactions, mainly for the force time step.

Table 8.11: Joints reactions which show correlations to discomfort with p -values ≤ 0.06 . Factors shown in bold are mentioned in the text.

Joint reaction	r	p
RElbowHumeroUlnar_AxialMoment_E	0.723	< 0.001
RSternoClavicular_InferoSuperiorForce_E ²	0.715	< 0.001
RElbowHumeroUlnar_AxialMoment_E ²	-0.700	< 0.001
RSternoClavicular_InferoSuperiorForce_E	0.681	< 0.001
RAcromioClavicular_InferoSuperiorForce_E²	0.622	< 0.001
C0C1_AnteroPosteriorForce_F	-0.588	0.001
C0C1_AnteroPosteriorForce_F ²	0.563	0.002
RDistalRadioUlnar_RadialForce_E²	0.561	0.002
RSternoClavicular_AnteroPosteriorForce_E ²	0.545	0.003
RGlenoHumeral_InferoSuperiorForce_E	0.523	0.004
RWristRadioCarpal_ProximoDistalForce_E ²	0.522	0.004
RWristRadioCarpal_ProximoDistalForce_E	-0.505	0.006
RGlenoHumeral_InferoSuperiorForce_F²	0.498	0.007
RAcromioClavicular_InferoSuperiorForce_E	-0.493	0.008
RDistalRadioUlnar_DorsoVolarForce_F ²	0.492	0.008
C0C1_MedioLateralForce_E	0.490	0.008
RSternoClavicular_MedioLateralForce_F	0.479	0.010
RElbowHumeroUlnar_MedioLateralForce_E	-0.468	0.012
RElbowHumeroUlnar_MedioLateralForce_E ²	-0.463	0.013
RDistalRadioUlnar_DorsoVolarForce_E	0.460	0.014
RElbowHumeroUlnar_AnteroPosteriorForce_S ²	0.458	0.014
RSternoClavicular_MedioLateralForce_F ²	0.458	0.014
RDistalRadioUlnar_DorsoVolarForce_E ²	-0.454	0.015
RDistalRadioUlnar_DorsoVolarForce_F	-0.436	0.020
RElbowHumeroUlnar_LateralMoment_E ²	0.424	0.025
L2L3_MedioLateralForce_F ²	0.402	0.034
RWristRadioCarpal_DorsoVolarForce_E	0.402	0.034
L1L2_MedioLateralForce_F ²	0.396	0.037
C0C1_LateralMoment_F ²	0.377	0.048
C0C1_ProximoDistalForce_E ²	0.375	0.049

Figure 8.2 (p. 180) shows the scatterplot of the inferior superior force of the sternoclavicular joint versus discomfort. Figure 8.3 (p. 180) displays the scatterplot of the axial moment of the humeral ulnar joint versus the discomfort. Both graphs show strong good correlations between the joint reaction and discomfort with little scattering (respectively outliers) which is also reflected by the low p -value and high value of r .

Those characteristics are representative for many other significant correlations between a joint reaction and discomfort, especially for the end time step.

Some correlations show quadratic characteristics, e.g. the right distal radio ulnar radial force at the end (Figure 8.11) or the right glenohumeral inferior superior force at the force time step (Figure 8.12). In this case, the discomfort is lowest for a value (respectively range of values) of the joint reaction (typically in proximity to zero) and increases when the value diverges from it either in one or the other direction.

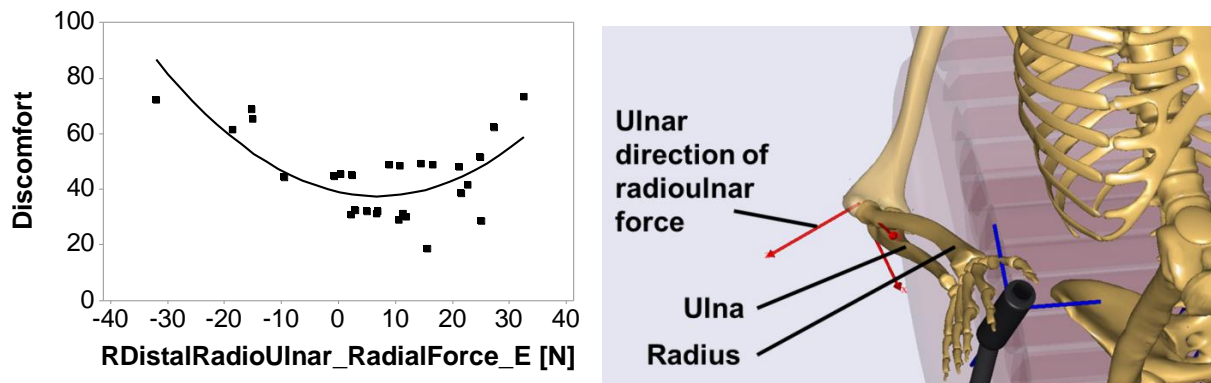


Figure 8.11: Right distal radio ulnar radial force at the end versus discomfort, squared value correlates to discomfort with $r = 0.561$ and $p = 0.002$. Force acts from ulna on radius. Ulnar direction is positive.

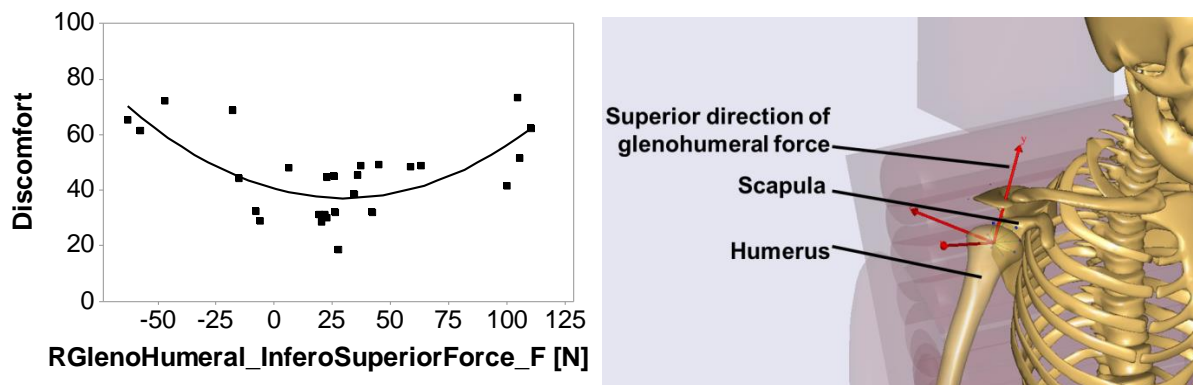


Figure 8.12: Right glenohumeral inferior superior force at the force time step, squared value correlates to discomfort with $r = 0.498$ and $p = 0.007$. Force acts from scapula on humerus. Superior direction is positive.

For the end time step, the axial moment of the right humeral ulnar joint (Figure 8.3, p. 180) and the squared inferior superior force of the right acromio clavicular joint (Figure 8.13 and Figure 8.14) are the predictors with major contribution to the prediction quality of the regression model (chapter 9).

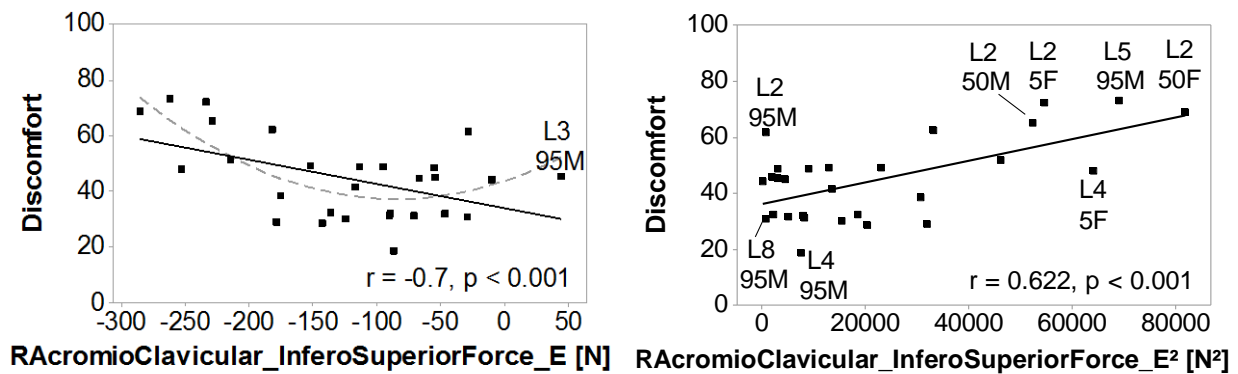


Figure 8.13: Inferior superior force of the right acromio clavicular joint at the end (left) and squared value (right) versus discomfort. Force acts from clavicle on scapula. Superior direction is positive.

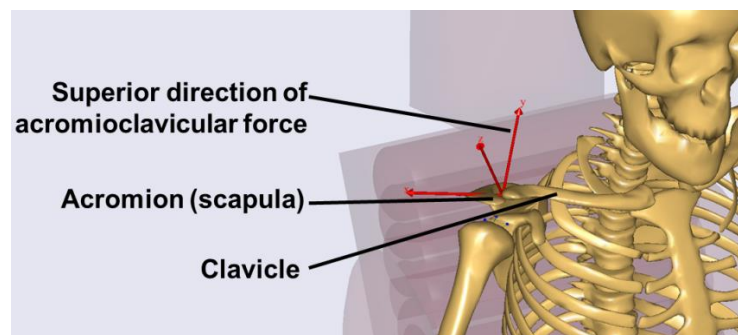


Figure 8.14: Superior force direction of the right acromioclavicular joint. Force acts from clavicle on scapula. Superior direction is positive.

In comparison to the other factor groups, the joint reactions show the best correlations to discomfort. They appear to be more robust and more comprehensive predictors of discomfort than the muscle activity. The values of the regression lines of the discomfort of the variable / squared variable typically deviate from the discomfort values derived from the study (for each key percentile and location) to a similar extent over the complete range of data points. For muscle activity, there are many cases in which for no respectively low muscle activity the variation of discomfort values is very large. Other parameters obviously have a higher contribution to discomfort for some of the percentiles and handbrake locations.

The joint reactions were calculated based on external forces and the muscle forces acting on the joint. Therefore, they contain more comprehensive information than a single muscle.

8.2.4 Joint moment measures

The joint moment measures reflect the moments created purely by muscles. Table 8.12 shows those which correlate to discomfort with p-values ≤ 0.06 . They are sorted by decreasing value of r .

Table 8.12: Joint moment measures which show correlations to discomfort with p-value ≤ 0.06 . Factors shown in bold are mentioned in the text.

Joint moment measure	r	p
RGlenoHumeral_ExternalRotationMoment_E²	0.637	< 0.001
RElbow_FlexionMoment_F ²	0.533	0.003
RWrist_AbductionMoment_E	0.482	0.009
RWrist_AbductionMoment_E ²	0.481	0.009
RGlenoHumeral_FlexionMoment_E	0.48	0.01
RGlenoHumeral_AbductionMoment_E	0.397	0.037

Most of them relate to the end time step, only the squared right elbow flexion moment is from the force time step. They all refer to the moments of the right glenohumeral, elbow and wrist joint. The r values of up to 0.637 and p-values close to 0 indicate that the joint moment measures are a very valuable indicator of discomfort, and especially its portion accumulating during the end time step.

As an example, Figure 8.15 shows the right glenohumeral external rotation moment at the end time step (left chart) and its squared value (right chart) versus discomfort. A decent quadratic relationship can clearly be recognized. Figure 8.16 illustrates the rotational moment.

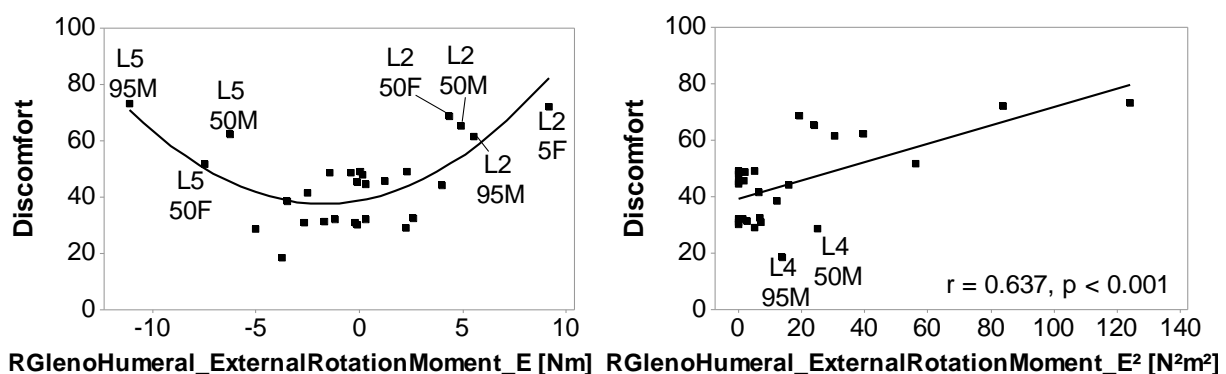


Figure 8.15: Right glenohumeral external rotation moment at the end time step (left) and its squared value (right) versus discomfort.

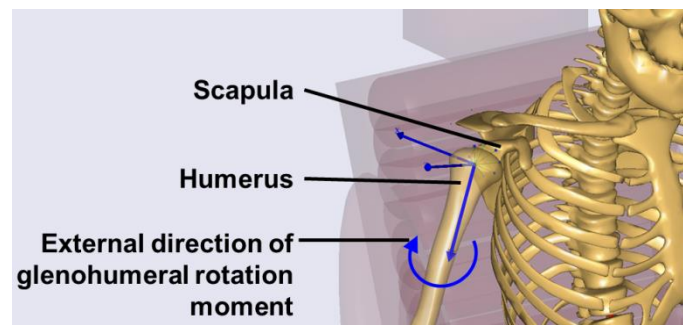


Figure 8.16: External glenohumeral rotation moment.

An example for a linear relationship is shown in Figure 8.17. The depicted wrist abduction moment at the end time step is part of the prediction equation (see chapter 9)

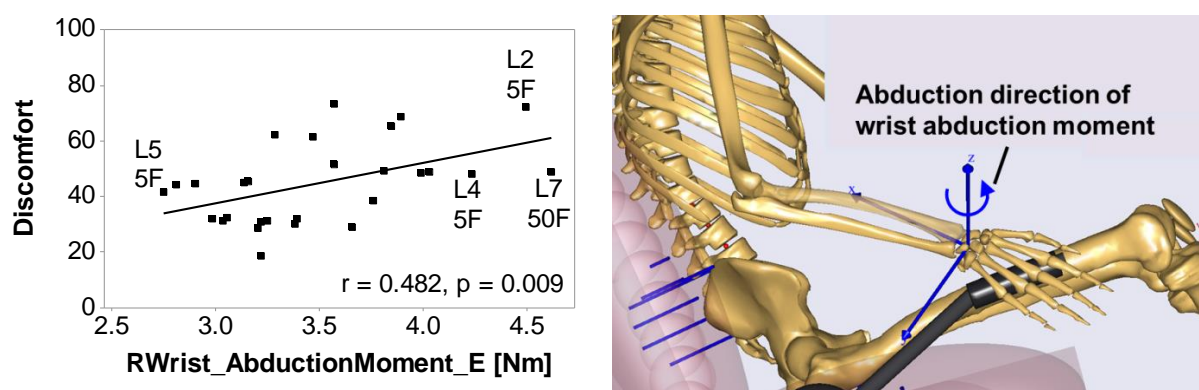


Figure 8.17: Right wrist abduction moment at the end time step versus discomfort.

Similar to the joint reactions (refer to the end of 8.2.3), the joint moment measures generally seem to be more robust and more comprehensive predictors of discomfort than the muscle activities.

Correlations between discomfort and joint reactions respectively joint moment measures reach r values up to 0.72 and $p < 0.001$. Once again, a direct comparison to published studies is not possible as experimental set up, rating scales and calculation routines differ strongly from this study. However, Dickerson et al. (2006) found a similar quality of correlation ($r = 0.71$ and $p < 0.05$) for the perceived muscular effort and normalized shoulder torque.

8.2.5 Joint angles

Table 8.13 shows the joint angles which have correlations to discomfort with $p \leq 0.06$. The r values of up to 0.56 and p -values close to 0 indicate that the joint reactions are a meaningful indicator of discomfort.

Glenohumeral, sternoclavicular and pelvis angles are contained for both (start and end) time steps: The right glenohumeral abduction angle at the start time step (see Figure

8.18, left, and Figure 14.24), the squared pelvis axial rotation angle at the start and end (Figure 8.4, p. 180), the right glenohumeral external rotation angle (Figure 8.19, Figure 14.24 on p. 260), the right glenohumeral anteversion angle (also called flexion, see Figure 14.24, p. 260) and the sternoclavicular elevation angle at the end (Figure 8.18 right and Figure 14.23, p. 259) significantly correlate to discomfort.

Table 8.13: Joint angles with correlations to discomfort with p-values ≤ 0.06 . Factors shown in bold are mentioned in the text.

Joint angle	r	p
RGlenoHumeral_Abduction_S²	0.566	0.002
RGlenoHumeral_Abduction_S	0.55	0.002
Pelvis_AxialRotation_E ²	0.54	0.003
RGlenoHumeral_ExternalRotation_E²	0.435	0.021
RGlenoHumeral_Flexion_E ²	0.404	0.033
RSternoClavicular_Elevation_E²	0.367	0.055
Pelvis_AxialRotation_S ²	0.365	0.056

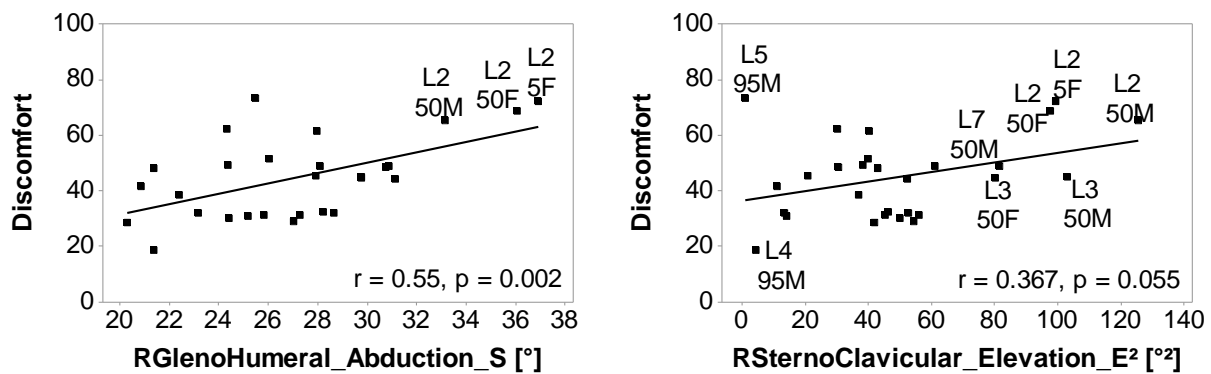


Figure 8.18: Left: Right glenohumeral abduction at the start versus discomfort. Right: right squared sternoclavicular elevation at the end versus discomfort. Sternoclavicular elevation is positive for all percentiles and manikins.

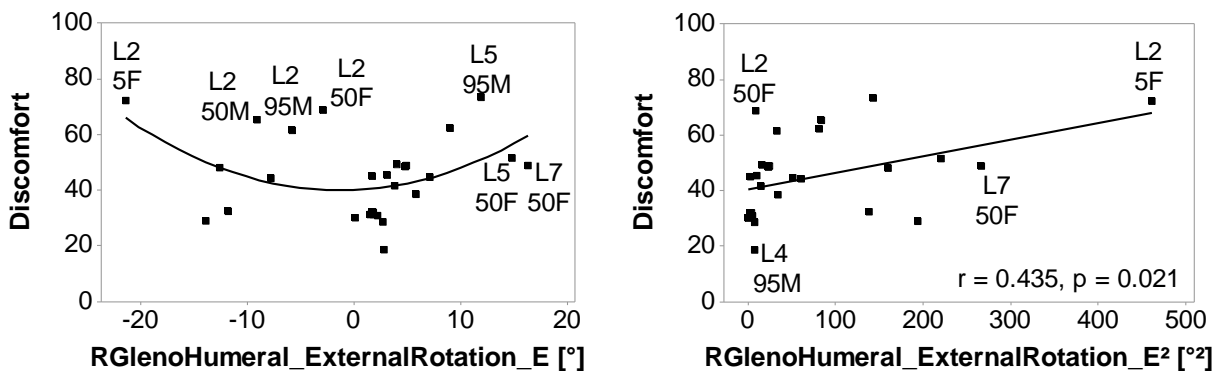


Figure 8.19: Right glenohumeral external rotation at the end (left) and squared value (right) versus discomfort.

All these angles are zero in neutral standing posture. Deviations from zero in either direction lead to increases in discomfort. This is in line with anticipations and explains why for joint angles squared values correlate better to discomfort than the values themselves (not squared). Compare also Figure 8.4 (p. 180, pelvis axial rotation angle at the end time step versus discomfort). As glenohumeral abduction has positive values only, the correlation quality of the factor and squared factor is very similar (Table 8.13).

The squared right glenohumeral external rotation at the end (Figure 8.19, right) and the squared sternoclavicular elevation at the end (Figure 8.18, right) are part of the regression equation to predict discomfort (chapter 9). Similar to some muscle activities (e.g. in Figure 8.8), there are larger variations especially for angles close to zero. In these cases other factors have higher contribution to the discomfort perception.

The right glenohumeral abduction angle at the start and squared pelvis rotation angle at the end correlate to discomfort with high significance ($p < 0.01$). However, they do not appear in the prediction equation (chapter 9). They were obviously excluded in the stepwise regression process for inter-correlating to other factors. Thus, they would not significantly improve the prediction quality of the model. E.g. glenohumeral abduction angle is associated with the metabolic energy of the right arm at the start.

In literature, one study was found with even better correlations to glenohumeral and elbow angles: In this study (Kee, 2002), the perceived discomfort was rated for operating different controls with predefined joint angles. Four levels of each glenohumeral flexion, glenohumeral abduction and elbow flexion were studied. Quadratic regression equations were derived to calculate normalized discomfort based on each of the joint angles. R^2 varied between 0.86 (glenohumeral abduction) and 0.99 (glenohumeral flexion, elbow flexion). Regression equations based on the three joint angles and handedness resulted in r^2 values between 0.76 and 0.96) for the four different types of controls (Kee, 2002). In another study (Jung & Choe, 1996), the reach discomfort regression equation based on external load and joint angles (including glenohumeral flexion, abduction and rotation, elbow flexion) achieved an r^2 value of 0.79. For both cited studies, the study setup and scale are not directly comparable to this study. Still, in both cited studies and in this study, the glenohumeral joint angles are the joint angles with best correlations to discomfort.

8.2.6 Body height and gender

The anthropometric respectively demographic measures – body height and gender – and their squared values do not significantly correlate to discomfort. Absolute r values are smaller than 0.023 and the p -values are larger than 0.91. Originally, these potential predictors were included into the starting basis of most relevant predictors as their contribution to reach discomfort perception has been demonstrated (Chevalot & Wang, 2004; Wang & Trasbot, 2011). At the end, these factors did not appear in the prediction equation.

8.3 Conclusions

In each of the biomechanical factor groups, there were one or more factors correlating to discomfort with $r \geq 0.54$ and $p \leq 0.01$. Joint moment measures, mean muscle activity of right shoulder/arm and mean/maximum muscle activity for body parts achieved r values between 0.6 and 0.7. The best correlating joint reaction achieved $r = 0.723$. All biomechanical factor groups (joint reactions, joint moment measures, muscle activities, joint angles and metabolic power/energy) have relevance for the discomfort perception.

Hypothesis 4 (there are biomechanical parameters calculated with AMS based on the RAMSIS key postures which correlate to discomfort ratings derived from a subjective evaluation study) was confirmed.

9 DISCOMFORT MODELING

In the previous chapter, it has been shown that numerous biomechanical values significantly correlate to discomfort.

Aim of this chapter is to test hypothesis 5 (combining selected biomechanical parameters allows predicting discomfort for the customer target population respectively key subgroups). If this hypothesis is confirmed like all others hypothesis before, the aim of the doctoral thesis (develop a CAE procedure to predict handbrake application discomfort) is fulfilled.

In this chapter, it is described how hypothesis 5 was confirmed by developing an appropriate prediction equation.

9.1 Methods

Statistical regression is typically utilized to form subgroups of factors which are useful for predicting a dependent variable. It is also a common mathematical procedure to establish a prediction evaluation.

There are three types of statistical regression:

1. Forward selection.
2. Backward deletion.
3. Stepwise regression.

Stepwise regression is applied in this thesis. It is a combination of forward selection and backward deletion. As in forward selection, first the variable with the highest r value is selected. For inclusion in the model, other variables are added one at a time, so that the prediction potential of the regression equation (r^2) is increased most. The process is continued until it meets a predefined statistical criterion. As in backward deletion, variables are being deleted at any step if they no longer significantly contribute to the regression model. (Bortz, 1999; Tabachnick & Fidell, 2007)

In this study, variable were added in case their probability to increase the prediction quality of the regression model was more than 90 % (corresponding to $\alpha_{\text{enter}} = 0.1$ in Minitab). Variables with a probability of more than 90 % not to increase the prediction potential were removed ($\alpha_{\text{remove}} = 0.1$).

For each step, the regression equation, coefficients for a constant and the predictors and their p-values are calculated. Each regression equation is characterized with r^2 , r^2_{adj}

and S . S is the standard error of the regression and represents standard distance of the predicted values from the values derived from the subjective evaluation study. The analysis was conducted in Minitab (2015).

9.2 Results and discussion

9.2.1 Stepwise regression

The biomechanical parameters described in chapter 8 were considered for the regression analysis if they correlated to discomfort with $p \leq 0.06$ and $|r| \geq 0.35$. This preselection enables inclusion of potential predictors with most significant correlation to discomfort and results into a number of predictors which is processible in Minitab.

Factors with values smaller than 10^{-11} for all percentiles and handbrake locations were considered negligible and sorted out. So, the regression analysis was conducted with a dataset containing discomfort and 201 potential predictors for all 7 handbrake locations and all 4 key percentiles.

The results of the stepwise regressions are summarized in Table 9.1. The details are in Table 14.32, p. 277.

Table 9.1: Stepwise regression of discomfort versus predictors
($\alpha_{\text{enter}} = 0.1$, $\alpha_{\text{remove}} = 0.1$).

Step	1	2	3	4	5	6	7	8	9
S	10.3	7.51	6.59	6.03	5.36	4.75	4.03	3.76	3.5
r²	52.3	75.62	82	85.57	89.09	91.83	94.38	95.35	96.18
r²_{adj}	50.47	73.67	79.75	83.06	86.6	89.5	92.42	93.39	94.27

By adding factors, r^2_{adj} is enhanced and S is reduced. With 9 predictors r^2_{adj} is 94.27 and S is 3.5. Equation (9.1) shows the prediction equation with these 9 predictors.

$$\begin{aligned}
 \text{Predicted Discomfort} = \text{Discomfort index} = & \quad (9.1) \\
 = & 34.305 + 3.671 \text{RElbowHumeroUlnar_AxialMoment_E} \\
 & + 0.00016154 \text{RAcromioClavicular_InferoSuperiorForce_E}^2 \\
 & + 10.164 \text{RWrist_AbductionMoment_E} \\
 & - 0.04713 \text{RGlenoHumeral_ExternalRotation_E}^2 \\
 & + 0.14996 \text{RSternoClavicular_Elevation_E}^2 \\
 & + 33944 \text{MeMAct_RPectoralisMajorClavicularPart_F}^2 \\
 & + 15445 \text{MaMAct_RTrapeziusScapularPart_F}^2 - 0.8729 \text{Pmet_RArm_S} \\
 & + 0.175 \text{Pmet_LLeg_F}^2
 \end{aligned}$$

Regression models should only be applied if several mathematical assumptions are met (Rumsey, 2008). Those need to be reconfirmed before discussing the predictors and the prediction values.

The differences between the values derived from the study (target values/study values) and predictions are residuals. There are four statistical assumptions which should be met for the residuals (Costich-Sicker et al., 2002; Rumsey, 2008): normal distribution with the mean value 0, independency, constant variance for the predicted values and absence of patterns. All four assumptions were fulfilled; see Figure 14.32, p. 278.

9.2.2 Predictors

In Table 9.2 the factors are listed in the sequence of the steps in which they have been added. This also reflects the contribution of each factor to the variation of the discomfort value. Table 9.2 shows that the p-values of the first eight predictors indicate significant contribution, the 9th predictor is close to significant contribution ($p = 0.063$). The variance inflation factors (VIF), which characterize multicollinearity of predictors, are between 1 and 5. This indicates an acceptable degree of correlation between the factors (Costich-Sicker et al., 2002).

Table 9.2: Factors of the stepwise regression, ordered by the step in which they are added.

Factor	Factor group	Coefficient	p	VIF
RElbowHumeroUlnar_AxialMoment_E	joint reaction force	3.671	< 0.001	1.887
RAcromioClavicular_InferoSuperiorForce_E ²	joint reaction force	0.00016154	0.001	1.837
RWrist_AbductionMoment_E	joint moment measure	10.164	< 0.001	2.106
RGlenoHumeral_ExternalRotation_E ²	joint angle	-0.04713	< 0.001	3.086
RSternoClavicular_Elevation_E ²	joint angle	0.14996	< 0.001	1.58
MeMAct_RPectoralisMajorClavicularPart_F ²	mean muscle activity of right shoulder and arm	33944	< 0.001	2.13
MaMAct_RTrapeziusScapularPart_F	maximum muscle activity of right shoulder and arm	15445	0.002	1.526
Pmet_RArm_S	metabolic energy/power	-0.8729	0.016	1.713
Pmet_LLleg_F ²	metabolic energy/power	0.175	0.063	2.817
Constant	-	34.305	< 0.001	-

In analysis of variance calculations, the sum of squares (SS) value measures variation respectively deviations from the mean. The regression equation explains 96 % of the variation in the discomfort, see Table 9.3.

Table 9.3: Sources of variance calculates with analysis of variance.

Source	SS	% from total SS
Regression	5570.96	96.18 (= r^2)
Residual Error	221.07	3.6
Total	5792.03	100

The shares of the variation in discomfort explained by each factor (% of total SS) are listed in Table 9.4. Figure 9.1 illustrates the predictors, the numbers refer to Table 9.4.

Table 9.4: Percentage of variance in the data explained by each factor of the regression equation.

Factor group	No.	Factor	Sequen- tial SS	% total SS	Cum. % total SS
Joint reaction force	1	RElbowHumeroUlnar_AxialMoment_E	3029.39	52.30	52.3
Joint reaction force	2	RAcromioClavicular_InferoSuperiorForce_E ²	1350.78	23.32	75.62
Joint moment measure	3	RWrist_AbductionMoment_E	369.1	6.37	81.99
Joint angle	4	RGlenoHumeral_ExternalRotation_E ²	207	3.57	85.56
Joint angle	5	RSternoClavicular_Elevation_E ²	203.56	3.51	89.07
Mean muscle activity of shoulder/arm	6	MeMAct_RPectoralisMajorClavicularPart_F ²	159.18	2.75	91.82
Max. muscle activity of shoulder/arm	7	MaMAct_RTrapeziusScapularPart_F	147.6	2.55	94.37
Met. energy/power	8	Pmet_RArm_S	56.19	0.97	95.34
Met. energy/power	9	Pmet_LLeg_F ²	48.16	0.83	96.18

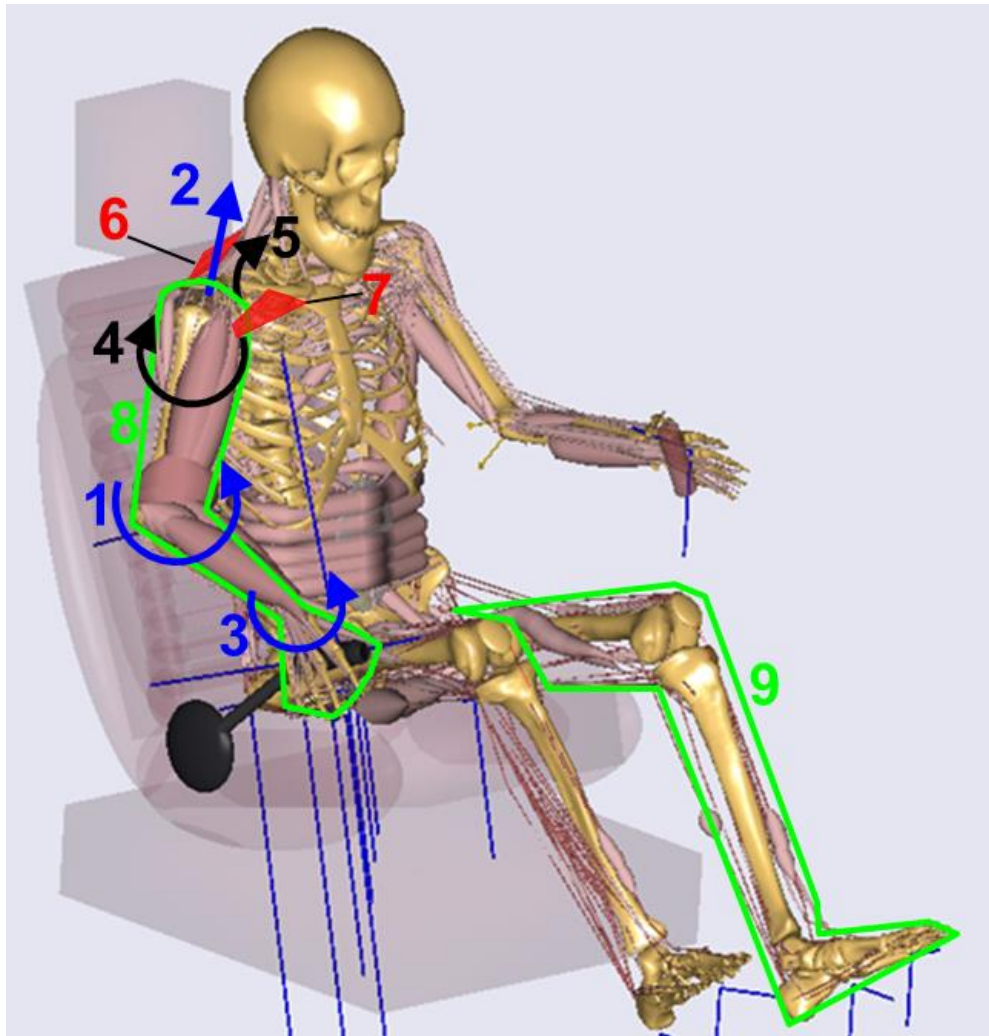


Figure 9.1: Illustration of the predictors which are numbered in Table 9.4.

In the following, the predictors are described shortly in order of their contribution to the discomfort variation.

The axial moment of the humeral ulnar joint at the start time step is explaining the major portion of variance (52.3 %) in the discomfort values is. A lower absolute value of external moment leads to increased discomfort (Figure 8.3, p. 180). A moment in internal direction is probably even more uncomfortable.

The squared inferior superior force of the right acromion clavicular joint at the end time step accounts for another 23.23 % of the variation. Figure 8.13 (p. 195) shows this factor versus discomfort. Higher values increase the perceived discomfort.

The right wrist abduction moment at the end time step explains 6.37 % of the discomfort variation. The higher the wrist abduction moment is, the higher is the perceived discomfort (Figure 8.17, p. 197).

The squared right glenohumeral external rotation angle at the end contributes with 3.57 % to the variation in discomfort. Rotations either in external and internal direction increase the discomfort as shown in Figure 8.19, p. 198.

The squared sternoclavicular elevation angle at the end (Figure 8.18, right, p. 198) accounts for 3.51 % of the discomfort variation. Larger elevation angles increase discomfort.

Further 2.75 % of the discomfort variation are explained by the squared mean muscle activity of the clavicular part of the right pectoralis major at the force time step (Figure 8.8, right, p. 190). This large pectoral muscle is involved in anteversion, adduction and inner rotation of the arm (Platzer et al., 2003). Low muscle activities with high discomfort for all four key percentiles at location 2 (rear up) are outliers. They indicate that the cause of the discomfort is not the right pectoralis major muscle activity. The cause is probably the chicken wing posture. The highest muscle activity values are achieved for location 5 (fore down).

Another 2.55 % of the discomfort variation is contributed by the squared maximum muscle activity of scapular part of the right trapezius muscle at the force time step (Figure 8.8, left, p. 190). This muscle stabilizes the shoulder girdle and pulls the scapula towards the vertebral column respectively rotates it (Platzer et al., 2003).

The last two predictors each contribute less than 1 % to the explanation of the discomfort variation. The metabolic power of the right arm and shoulder at the start (Figure 8.5, right, p. 183) is especially high for the rear up handbrake location (2) for the smaller percentiles of both genders and the fore down handbrake location (5) for the 95M. It correlates to the total metabolic energy ($r = 0.57$, $p = 0.002$) and metabolic power of the trunk ($r = 0.725$, $p < 0.001$) in that time step. It is an indicator of an uncomfortable posture at the start time step influencing the total perception of the handbrake application.

Similarly, higher squared metabolic power values of the left leg at the force time step (Figure 8.6, left, p. 185) are an indicator for handbrake location and percentile combinations for which the begin of the handbrake application seems to be perceived uncomfortable (rear up location for smaller percentiles, fore down location for larger percentiles), which influences the rating.

All in all, the 5 predictors from the end time step together explain 89 % of the variation in discomfort which is the major portion. They include 2 joint reaction forces (right axial moment of humeral ulnar joint and inferior superior force of acromioclavicular joint), a

joint moment measure (right wrist abduction moment) and 2 joint angles (right glenohumeral external rotation angle and sternoclavicular elevation angle).

The 4 remaining predictors contribute by another 7.1 % to the discomfort variation. They are from the start or force time steps and include muscle activities (right pectoralis major and trapezius) and metabolic power values (right arm and left leg).

It can be concluded that AMS results of the end time step cover a large portion of the discomfort perception for handbrake application with start body postures which are not too uncomfortable (marginal leaning forward, no chicken wings). In case of discomfort at the beginning of handbrake application, AMS results for the start and force time steps gain importance for discomfort prediction. Examples are the rear up handbrake location (2) for smaller percentiles (Figure 9.2, right) and the fore down handbrake location (5) for larger percentiles (Figure 9.3, right).

So, all three time steps are relevant for the prediction. It is not sufficient to focus on the end of the handbrake application only. This is in line with the primacy and recency effect (Atkinson & Shiffrin, 1968) and the peak-end rule (Redelmeier & Kahneman, 1996).

The first three predictors (RElbowHumeroUlnar_AxialMoment_E, RAcmioClavicular_InferoSuperiorForce_E², RWrist_AbductionMoment_E) explain 81.9 % of the discomfort prediction. The charts (factor versus discomfort) show an even distribution of the data points and no outliers.

However most of the other six factors have two patterns in common:

1. Most of the data points are at lower values of the predictor – often with a large spread of discomfort values.
2. There are some “outliers” for higher values of the predictor and higher discomfort ratings.

These patterns can indicate a spurious relationship. However, a causal relationship (dependency) between each of the factors and discomfort makes sense. It can be concluded that for the handbrake locations and percentiles, which lead to smaller values of these predictors, other predictors (i.e. the first three predictors) have a higher contribution to the discomfort rating. However, for higher values of these predictors, they gain influence on the discomfort rating.

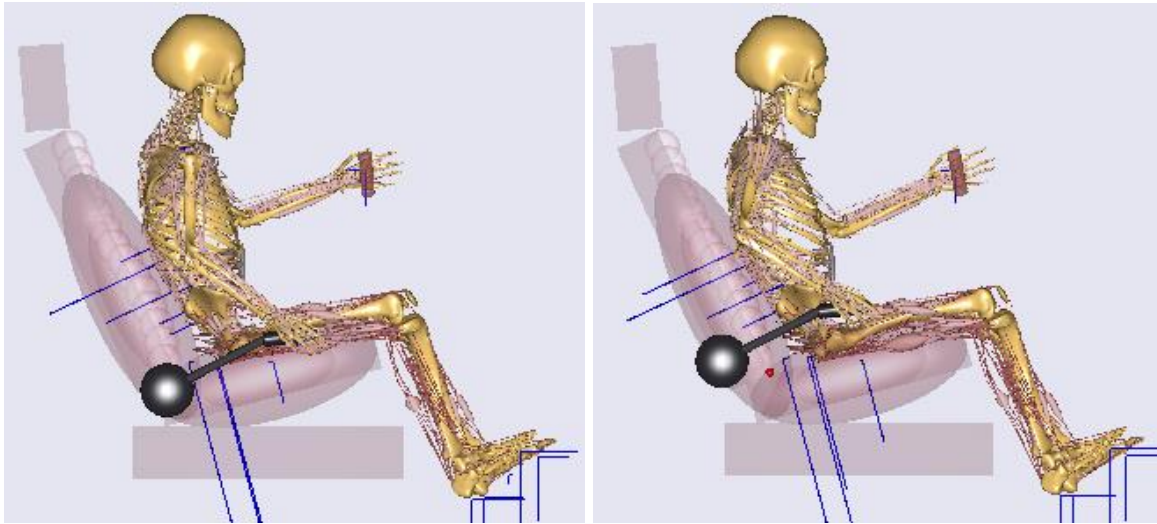


Figure 9.2: Start posture for 5F for mid handbrake location (1) (left) and for rear up handbrake location (2) (right).

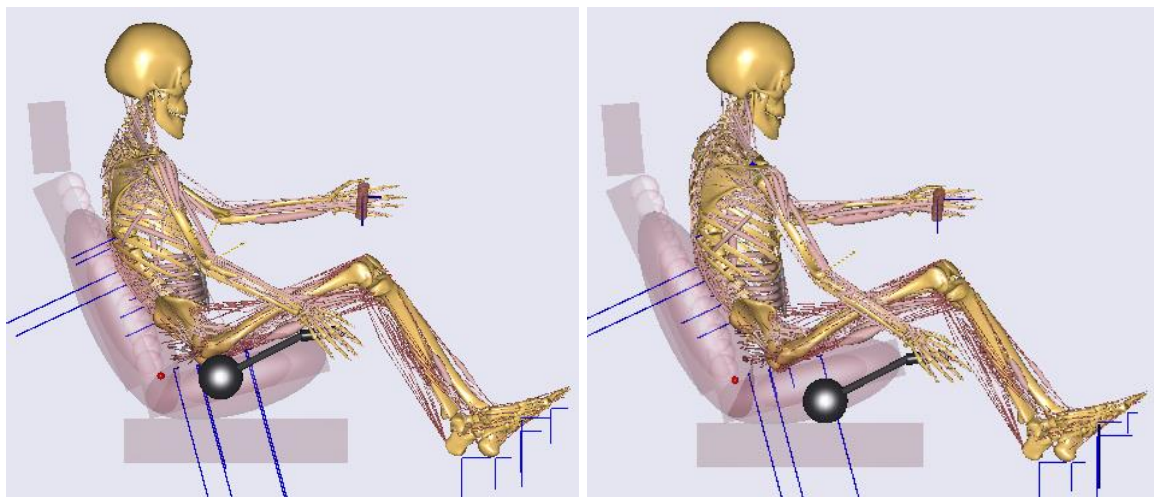


Figure 9.3: Start posture for 95M for mid handbrake location (1) (left) and for fore down handbrake location (5) (right).

9.2.3 Prediction quality

In the following, the predicted values are named discomfort index and discomfort values derived from the subjects are referred to discomfort ratings. Table 14.33 (p. 279) lists the discomfort ratings, indices and their delta for all locations and percentiles.

Figure 9.4 shows that the discomfort indices are in good agreement with the discomfort ratings. The ratings for location 1 are the average of the ratings for 1 and 6 which is the same location and leads to one discomfort index. So, location 6 is shown empty.

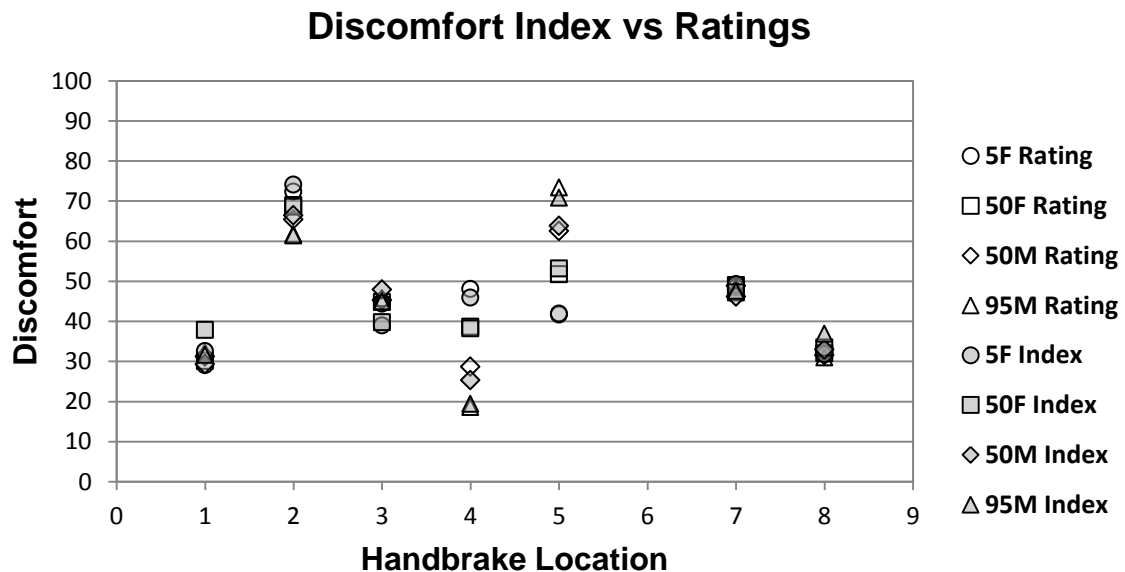


Figure 9.4: Discomfort index compared to the ratings.

In Figure 9.5 to Figure 9.8 the discomfort indices and ratings are compared separately for the 4 key percentiles.

Figure 9.5 illustrates that the discomfort indices for 5F are close to the ratings. Handbrake location 3 (fore up) results in the largest deviation: the predicted discomfort is slightly too low.

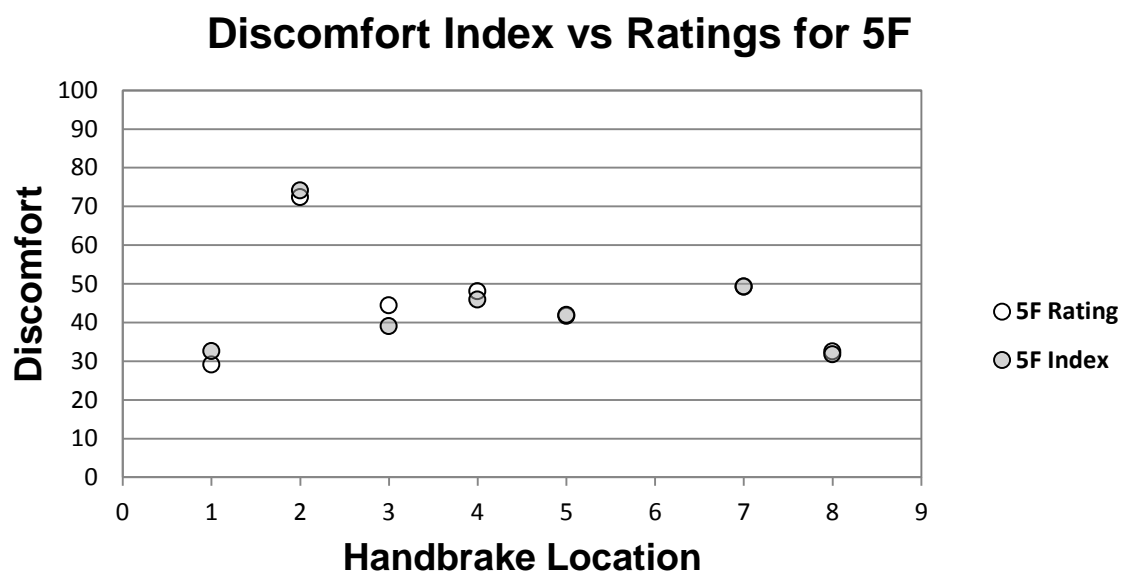


Figure 9.5: Discomfort index compared to the ratings for 5F.

Figure 9.6 shows good alignment of discomfort indices and ratings for 50F. The discomfort index for location 3 is predicted slightly too low. For location 1 the discomfort is predicted a bit too high.

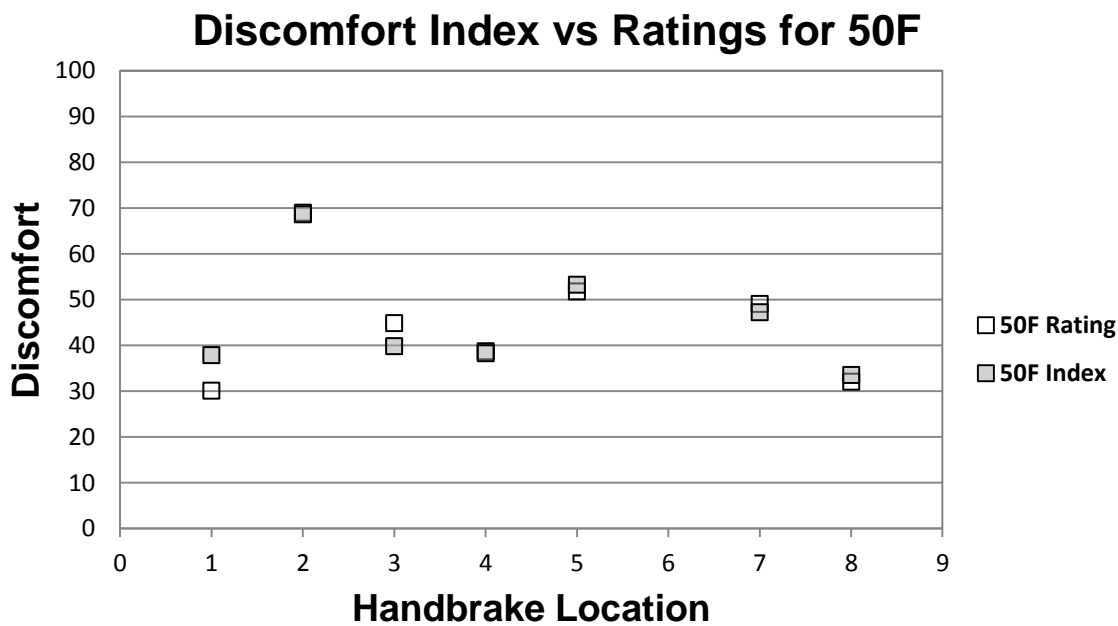


Figure 9.6: Discomfort index compared to the ratings for 50F.

The discomfort indexes for 50M are in very good alignment with the ratings as shown in Figure 9.7.

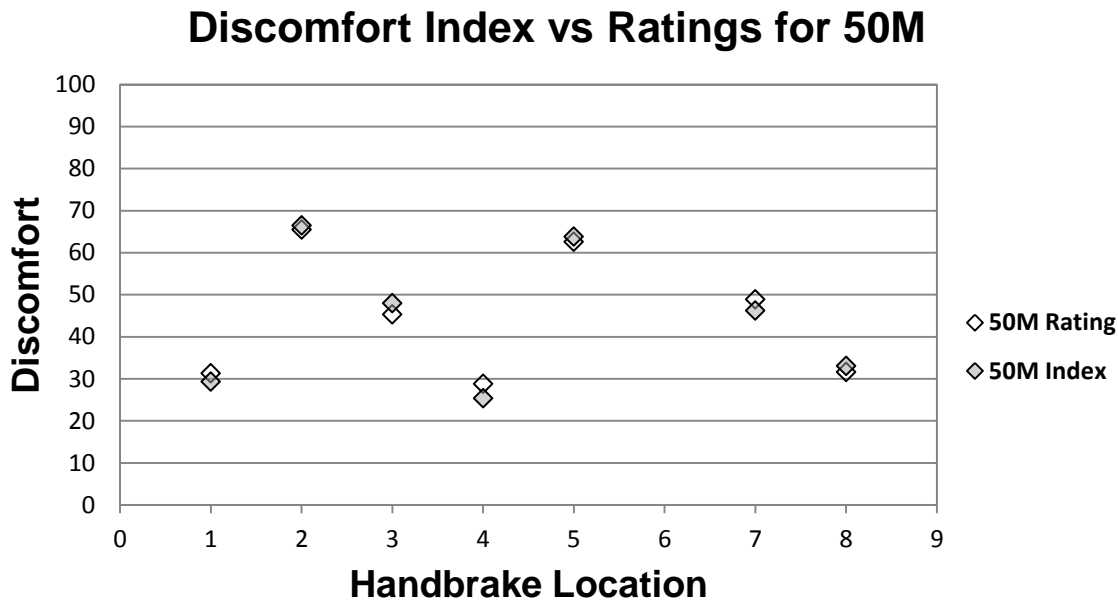


Figure 9.7: Discomfort index compared to the ratings for 50M.

Figure 9.8 illustrates also good alignment for 95M. For location 8 the discomfort index is slightly higher than the ratings.

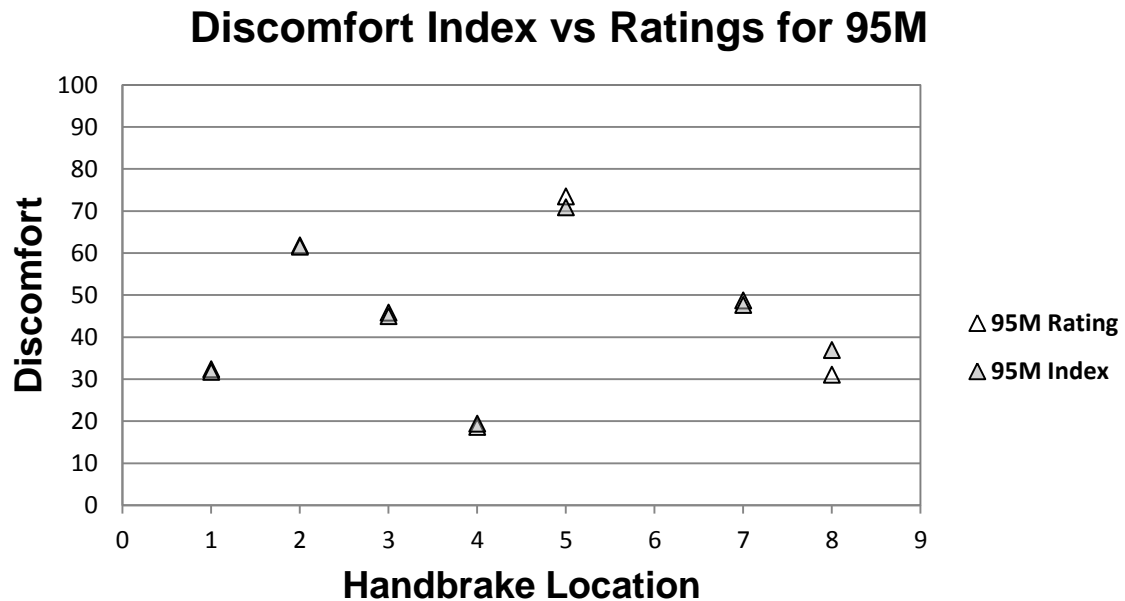


Figure 9.8: Discomfort index compared to the ratings for 95M.

So, all in all, the discomfort index is a very good prediction of the ratings. There are only minor, non-critical differences: The discomfort index is predicted slightly too high for location 1 for 50F and for location 8 for 95M. The discomfort index is predicted slightly too low for location 3 for 5F and 50F. The small differences are acceptable; especially when considering that the spread of subject's ratings is of the same magnitude for the handbrake location which was assessed twice (location 1 and 6, see Table 8.3, p. 177).

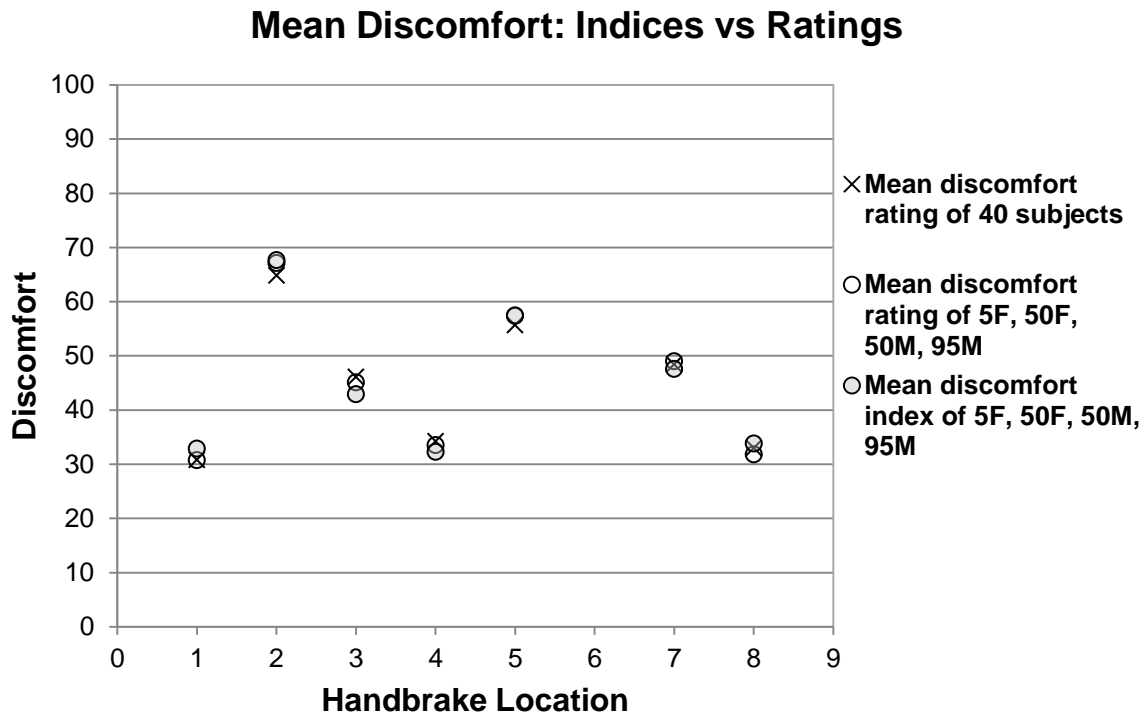


Figure 9.9: Mean discomfort indices compared to mean discomfort ratings.

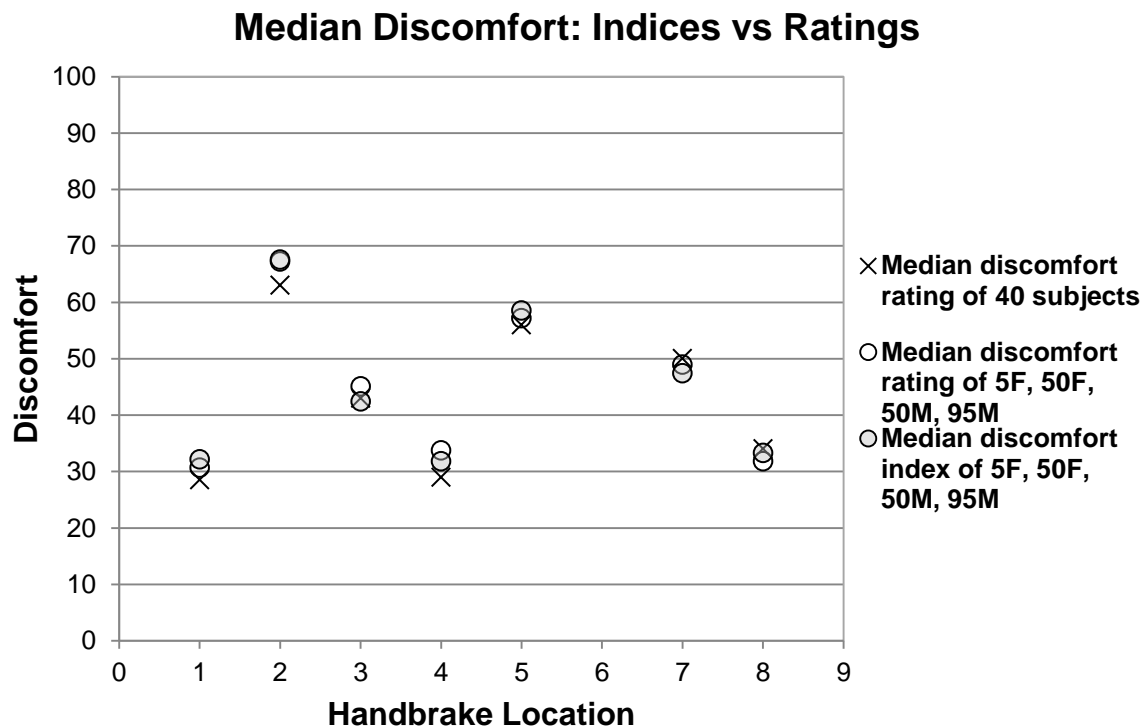


Figure 9.10: Median discomfort indices compared to median discomfort ratings.

In automotive industry, design variants often have to be compared based on one characteristic variable. In this case, mean and median discomfort ratings are suitable variables. The mean and median discomfort ratings and indices of the four key

percentiles well represent the mean and median ratings of the 40 subjects (as illustrated in Figure 9.9 and Figure 9.10). So the prediction equation fulfills its purpose.

9.3 Conclusions

In this chapter hypothesis 5 (combination of selected biomechanical parameters allows for discomfort prediction for the customer target population respectively key subgroups) was confirmed.

The aim of this doctoral thesis - to develop an equation to predict discomfort which is significant and explains a large portion of variation in the discomfort values – was successfully achieved with $r^2_{\text{adj}} = 0.943$ and $S = 3.5$ for the equation and p-values ≤ 0.063 for each predictor.

Deviations between the prediction and the ratings occur only for few combinations of key percentiles and handbrake locations and to a similar extent as the mean subjects' ratings for the same location differ (compare Table 8.3).

With the pre-selection of the factors depending on p-value and r value (see 9.2.1), there was a risk to exclude variables which are not significantly correlated to discomfort but may significantly enhance the prediction quality of a regression equation. The very good prediction quality of the established prediction equation confirms that accepting the risk was justified.

10 PROCEDURE TO PREDICT DISCOMFORT PERCEPTION

Aim of this work was to establish a procedure to predict discomfort of the handbrake application which meets the following demands:

- Reliable discomfort prediction which allows comparison of handbrake variants.
- Application of tools which are typically available in automotive development
- Ease of use.

Figure 10.1 shows the 5 step procedure established in this work. It fully meets the described demands.

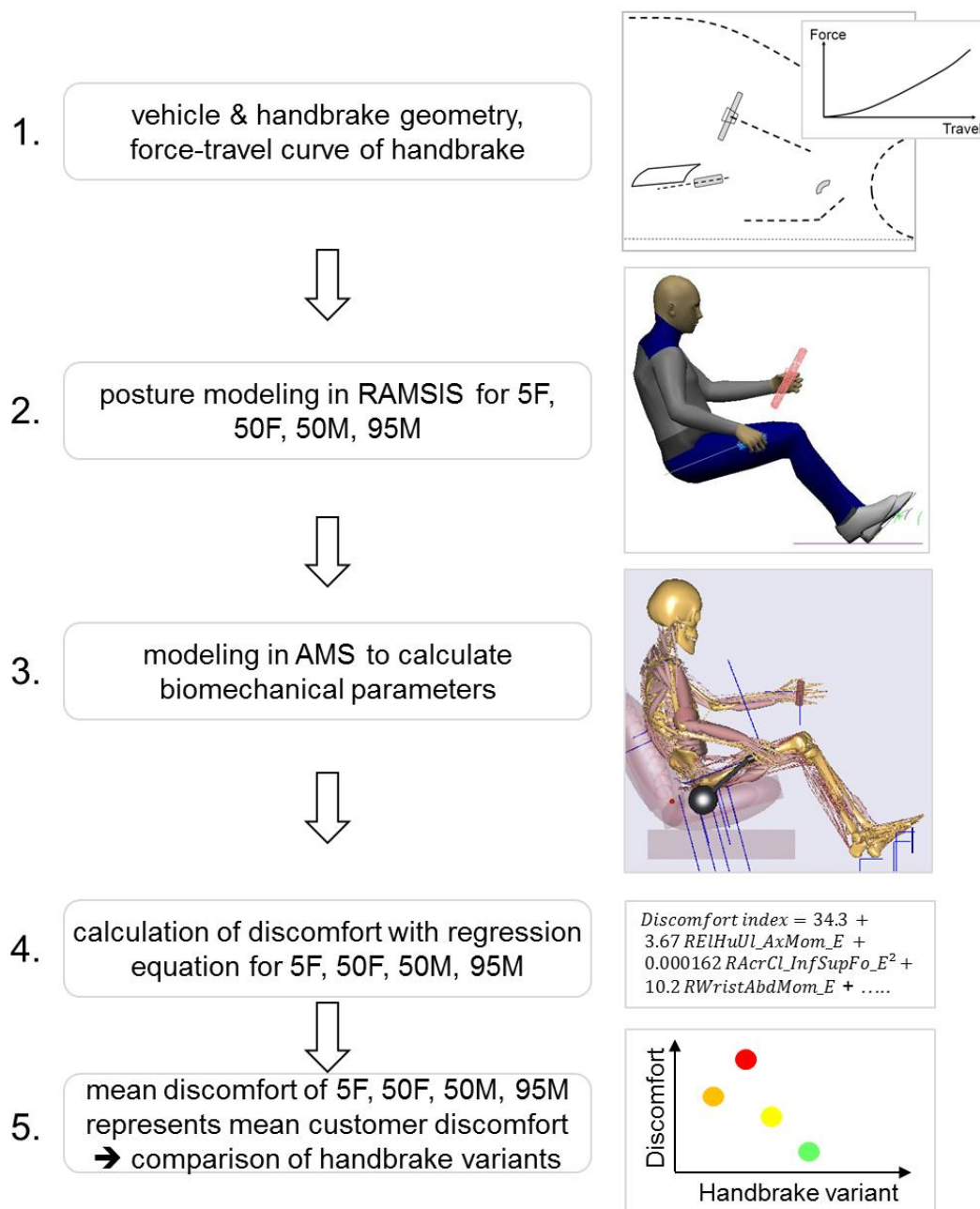


Figure 10.1: Procedure developed in this work.

For conducting a handbrake application discomfort assessment, the following five steps have to be completed:

The first step is the data compilation of:

- Geometric data of the vehicle (e.g. seat adjustment field, steering wheel and adjustment field, footrest, pedals).
- Geometric data of the handbrake (e.g. force application point, pivot point).
- Force-travel curve of the handbrake.

In **the second step**, RAMSIS is applied for posture prediction.

- Four manikins are created: 5F (5th body height percentile of the German female), 50F, 50M and 95M. For each of them, three postures are calculated.
- The driving posture is calculated by using the Car Driver Model in RAMSIS. This posture model is applied for all percentiles with the same set of constraints. The hip location (seat adjustment/position) and steering wheel adjustment/position of the driving posture are taken as a base for calculating the handbrake application postures.
- Then, the percentile specific User Defined Posture Models are applied to calculate the start and end postures of the handbrake application. Same constraints are used for all percentiles. The details are described in chapter 7.

In **the third step**, AMS is applied to calculate biomechanical parameters.

- RAMSIS output files for the start and end postures are used in AMS for scaling and modeling the handbrake application movement (kinematic analysis).
- The handbrake application movement and the force-travel curve of the handbrake are required as inputs for the calculation of biomechanical parameters in the inverse dynamic calculation. Details can be found in chapter 8.

In **the fourth step**, the regression equation (9.1), p. 202, is populated with the required biomechanical parameters calculated with AMS (in step 3) and the discomfort index is calculated for each key percentile.

In **the fifth step**, the mean (median) discomfort of the customer group is calculated. This is done by calculating the mean (median) discomfort of 5F, 50F, 50M and 95M.

Once this procedure is applied for several variants, they can be compared based on the mean (median) discomfort or individual discomfort of the key percentiles. The quantification of the handbrake discomfort allows optimizing handbrake ergonomics.

Vehicle development demands trade-offs between several components and attributes (e.g. handbrake discomfort, stowage accessibility, location of 2nd row air ducts, styling). If there is a choice of several center console layouts with differing handbrake designs respectively locations, the developed prediction/quantification of discomfort will help to find the best compromise between affected attributes and components.

11 DISCUSSION AND OUTLOOK

11.1 Discussion

This is the first published study which successfully demonstrates that for the handbrake application, the perceived discomfort can be reliably predicted based on postural, biomechanical and mathematical modelling. The discomfort can be predicted for key percentiles and also for the customer population.

A procedure was established based on application of RAMSIS for posture prediction, AMS for biomechanical modeling and a regression equation to predict a discomfort index for key percentiles and for the population based on AMS outputs. The procedure is readily available to be applied in vehicle development. As validation of the developed process was not included in this work, it is recommended to be completed first.

In the following the procedure applied in this work is discussed, its limitations are listed and thereby potential areas for future research are suggested.

The preliminary study with more than 100 subjects enabled a selection of subjects with reliable ratings and representative movements for the main study. The findings from the preliminary study also allowed major enhancements of the rating scale and suggested an extension of the handbrake location range to generate larger discomfort rating differences. This was essential for developing a CAE procedure which allows for differentiating within a large range of discomfort.

In the main study, the posture (“study posture”) and ratings (“study ratings”) of key body height percentiles (5F, 50F, 50M, 95M – the main percentiles typically used in automotive industry) were derived from the regression equation of the subjects’ joint angles / ratings and the body height. This procedure allows to include height depending behaviors but not to include behaviors very specific to a single subject.

Even individuals of the same body height partly demonstrated large variations in joint angles and ratings. It didn’t make sense to predict individual ratings / joint angles for automotive application and is neither possible to predict them with a CAE model.

Application of the standard Car Driver Posture Model in RAMSIS did not deliver realistic posture prediction for handbrake application. Good alignment between study joint angles and predicted joint angles was accomplished by developing dedicated User Defined Posture Models for each key percentile. These were applied for start and end posture. Increasing the number of posture models (i.e. one for start and one for end

posture) would have decreased the user-friendliness of the procedure. A minor and thus acceptable disadvantage of only one posture model per percentile is that the deltas between predicted start and end posture were found to be slightly smaller than the actual deltas. The obvious benefit is a time efficient procedure.

Based on the RAMSIS manikins and their posture as well as the force-travel curve of the handbrake, the handbrake application was biomechanically modeled in AMS. AMS outputs comprise factor groups such as joint reactions, joint moment measures (purely created by muscles), muscle activities, joint angles, metabolic power and energy consumption.

Highly significant correlations between factors of all factor groups and the study discomfort were found. In all groups, there are factors with at least moderate correlations with discomfort ratings. The highest r values for the best correlating factors of each group are between 0.54 and 0.723. As discomfort is a highly subjective experience, this correlation quality of numerous single predictors is considered very good. The factor with the best correlation to discomfort ($r = 0.723$, $p < 0.001$) is the right humeral ulnar axial moment at the end time step, a reaction moment. This correlation quality is similar to the one found by Dickerson et al. (2006) for the shoulder moment and perceived effort ($r = 0.71$, $p < 0.05$) in loaded reaches.

Using stepwise regression, predictors from the investigated groups were selected and combined to an equation for discomfort index calculation. The predicted discomfort index values match the study values very well and explain 96 % of the variation in the discomfort ratings ($r^2 = 96\%$, $r^2_{\text{adj}} = 94\%$). The calculated discomfort index for the different handbrake locations and percentiles is well in agreement with the study ratings.

In literature, no study was found which is directly comparable to this work. However, there are some studies which show major differences in set up but similarities in results (Zacher & Bubb, 2004; Dickerson et al., 2006; Wang & Trasbot, 2011). For example, there are differences regarding the task (i.e. reach instead of handbrake application), rating scale (i.e. 10 levels instead of 50), wording of the rating (e.g. perception of muscular effort), population (i.e. less than 10 subjects), calculation method of biomechanical measures respectively applied biomechanical modeling software and investigated predictors (i.e. biomechanical parameters and geometric parameters) (Dickerson et al., 2006). Another main difference is that in this work the posture/discomfort values for body height percentiles derived from regression equations

(between study body angles / ratings and discomfort) were used as prediction target – instead of specific values from single subjects.

So, it is conclusive that in literature the prediction of subjective perceptions (based on biomechanical, geometric and anthropometric parameters) often show lower accuracy as achieved in this study, for instance:

- The discomfort regression model based on selected joint angles and external load shows $r^2 = 0.78$ (Jung & Choe, 1996).
- The model for perceived effort in loaded reaches based on shoulder moment, shoulder flexion strength and geometric parameters has a prediction accuracy of $r^2 = 0.70$ (Dickerson et al., 2006).
- The prediction equation for reach discomfort based on stature, gender and geometric factors has an adjusted prediction accuracy of $r^2_{\text{adj}} = 0.51$ (Wang & Trasbot, 2011).

On the other hand, normalized discomfort for operating different controls was predicted based on joint angles and handedness with r^2 values up to 0.96 in the study (Kee, 2002) which is comparable to the value derived in this study.

11.2 Limitations and potential topics for future research

The result of this work is a procedure which comprises posture prediction, biomechanical modeling and calculation of discomfort indices to enable a CAE based assessment of the handbrake application. It has been demonstrated that there are highly significant correlations between perceived discomfort and biomechanical parameters. The developed procedure will be very beneficial for ergonomic design of the vehicle interior. It will help to avoid or reduce the number of studies with subjects during vehicle development to optimize handbrake design respectively compare variants. However, there are several limitations to this study, which have to be acknowledged and which suggest topics for future research.

11.2.1 Validation

Validation of the developed models and the proposed procedure with another sample of subjects was beyond the scope of this work. Thus, validation is an obvious topic for future research.

11.2.2 Subjects' demographics and anthropometry

All subjects were Germans living in Cologne. Their BMI had to be lower than 30 to enable motion analysis. The subject's age covers the age of the main driving population. So, research is required to clarify if the results of this work can still be applied to populations with different anthropometry (e.g. Asians), higher BMI (obese people) or differing age groups (e.g. drivers older than 80 years).

Age is known to significantly influence the reach posture (Chateauroux & Wang, 2008), so it may influence the handbrake application movement and discomfort perception, too.

11.2.3 Subjects' handbrake application habits

As the subjects live in Cologne, they are used to drive passenger vehicles mostly on level streets or slight grades. In this region, the handbrake is used mostly after parking the vehicle on level ground or slight grades (convenient handbrake application).

People who often park on grades, tend to apply higher handbrake forces than people usually parking on plane streets (Fetter et al., 2005).

In some regions such as UK, drivers are trained to apply the park brake anytime when they have stopped the vehicle at intersections or traffic lights on level ground.

The influence of the handbrake application/usage habits, experiences and thus expectations on the handbrake application movement and the discomfort perception would be worth studying.

Studies with larger number of subjects may allow deeper insights into the effects of subjects' characteristics (such as demographics, anthropometry and handbrake application habits) on the handbrake application movement and discomfort perception.

11.2.4 Handbrake and application characteristics

In this study, a conventional passenger vehicle handbrake with Ford typical geometry, kinematics and force characteristic (force travel curve) was utilized. The location of the handbrake was varied covering corner points and center of the range of typical handbrake locations of passenger vehicles. The accessibility was unrestricted as the ErgoBuck was not equipped with any components typically next to a handbrake such as armrest, shifter or bottles in cup holders. Only the seat could impair handbrake accessibility. The subjects applied the handbrake until they reached the target

application travel (respectively force) level which holds the vehicle on a slight slope (convenient application).

It is expected that the results of this study - handbrake application movement and discomfort – can be applied to convenient application of handbrakes with comparable geometry (lever length, handle design), kinematics and force characteristics within the investigated range of locations. This assumption is recommended to be validated in further studies.

More research is required to verify if – respectively to which extent – the results of this thesis can be applied to:

- Maximum handbrake application (which holds vehicle on steep grade).
- Handbrakes with different designs (e.g. shorter lever length, different kinematics, different force characteristics).
- Handbrake locations outside of the investigated range (e.g. in commercial vehicles).
- Handbrakes with impaired accessibility (e.g. by armrest).
- Other hand-operated controls (e.g. shifter).

It may be required to develop new (RAMSIS, AMS, Regression) models and/or procedures if there are large differences between the application of interest and the experimental set up in this study.

11.2.5 Subjective evaluation and motion analysis

The studies and motion analysis followed detailed procedures. It was attempted to avoid/reduce disruptive factors respectively sources affecting repeatability.

11.2.6 RAMSIS

In the RAMSIS User Defined Posture Models menu, the target joint angles (center of probability distribution) can be modified whereas the distribution curve cannot be changed. This is a restriction of the software. It would be beneficial and could increase prediction quality, if also the distribution curve itself could be modified.

A single User Defined Posture Model (UDPM) was used to predict the start and end handbrake application posture for each key percentile.

Using dedicated UDPMs for each, start and end, could increase accuracy of posture prediction. However, this approach would deteriorate ease of use and efficiency and thus was not followed.

11.2.7 AMS

AMS allows for modelling and adjusting a lot of details as well as to choose from many models (e.g. muscle, muscle recruitment, scaling models). The specific selections were done consciously by balancing advantages and disadvantages for each choice. It is not clear if different choices would have enhanced or deteriorated the prediction of discomfort.

11.2.8 Mathematical model

In this study, only the association between factors and discomfort was investigated and included in the stepwise regression. Interaction of the factors or interaction of the factors with other variables (e.g. gender, body height) was not studied and may be a topic of future research.

11.2.9 Pressure distribution

It has been shown that the combination of different types of parameters increases discomfort prediction accuracy compared to using only a single predictor type. The contact pressure distribution between the human and the vehicle environment (seat, handbrake, steering wheel, footrest, brake pedal) may influence the perception of physical discomfort. Thus, the discomfort prediction accuracy may be enhanced by including this factor. It is investigated e.g. in the UDASim project (Ulherr & Bengler, 2014) with regards to seat comfort.

11.2.10 Ergonomics and discomfort evaluation of other applications

Handbrake application has been chosen as one example to develop a procedure for the reliable prediction of discomfort based on RAMSIS, AMS and regression modeling.

There are numerous vehicle respectively driving related applications for which such a procedure would be beneficial for ergonomic evaluations, e.g. pedal operation or ingress and egress.

Developing similar procedures for other applications – related to vehicles, other products (e.g. tool usage) or workplace design – could be the focus of future research.

12 SUMMARY

Comfort is recognized as a major selling argument and an important factor in customers' product buying decisions. Therefore, vehicle manufacturers aim to develop ergonomic vehicles outperforming competitors by minimizing discomfort and maximizing comfort.

While in the past mainly subjective evaluation studies were conducted to assure an ergonomic design of vehicles, nowadays the use of Digital Human Models (DHMs) has increased offering several advantages. The application of DHMs decreases the number of resource intensive subjective evaluation studies. It enables objective assessments already at early stages of car development as well as quick evaluations and comparisons of several variants. So, the application of DHMs allows for optimization of vehicle ergonomics, increasing efficiency and decreasing development costs.

Numerous studies have shown that discomfort is linked to biomechanical parameters and the musculoskeletal system. Hence it is crucial that the evaluation with DHMs includes the analysis of the musculoskeletal load which is influenced by kinematics (posture, motion) and kinetics (external forces leading to internal loads).

A lot has been published on biomechanical parameters influencing reach posture, reach discomfort and its prediction with DHMs. In contrast to reach – and although the handbrake is an essential and security relevant control in vehicles – little has been published about handbrake application.

In some countries such as UK, learner drivers are trained to apply the handbrake every time the vehicle stops.

A handbrake is typically located in the center console and so exposed to trade-offs between many vehicle components and attributes. This makes it extremely important to understand and quantify how changes in the handbrake design influence the discomfort perception of the customers.

In this work, a multi-step approach was completed to achieve a reliable procedure to simulate handbrake application postures respectively movement and to predict the perceived discomfort, based on DHMs and mathematical analysis.

A vehicle mock-up (ErgoBuck) was prepared to represent major interior package dimensions of a passenger vehicle and to allow for variation of the handbrake location. At the beginning of the preliminary study, 117 subjects drove the corresponding vehicle and their seat and steering wheel positions were recorded and transferred to the mock-up. Then, the subjects evaluated the discomfort of handbrake application in the mock-up

using a visual analog scale. They assessed handbrake application of seven distinct handbrake locations with a randomized repetition of the central location. Their movements were recorded with video cameras.

40 of the participants also participated in the main study. Inclusion criteria were good repeatability of the ratings, representative movement patterns and a continuous distribution of body heights covering the main driving population. In the main study, the subjects evaluated the same number of handbrake variations. Aiming for more differing ratings in the main study – compared to the preliminary study – the range of handbrake locations was extended and a Category Partitioning Scale was used. To accurately capture the movements, a Vicon Nexus motion capturing and analysis system was used.

Analysis of the data revealed linear relationships between body height and discomfort as well as body height and joint angles. This suggested to focus on the key body height percentiles typically used in automotive development – 5F (5 percentile female), 50F, 50M and 95M – for further analysis.

The ratings (study ratings) and joint angles (study joint angles) for these key percentiles were derived from the regression equations of the subjects' ratings respectively joint angles and the body heights. This allowed to consider body height dependent characteristics, but to exclude characteristics very specific to a single subject.

RAMSIS is an ergonomic software used at many automotive companies. The joint angles predicted with RAMSIS were compared to the study joint angles. For this purpose, a dedicated User Defined Posture Model was created in RAMSIS for each key percentile and then applied with a common set of constraints for all percentiles. The predicted postures correspond well to the study postures.

AMS (AnyBody Modeling Software) is a biomechanical model which is also used by several automotive companies. Based on the anthropometry and predicted posture of the RAMSIS manikins, the vehicle and handbrake geometry and handbrake force, the handbrake application was modeled in AMS. The calculated biomechanical parameters include the groups joint reactions, joint moment measures (purely created by muscles), muscle activities, joint angles as well as metabolic power and energy. Values were calculated for the four key percentiles, all seven handbrake locations and for three time steps: start of handbrake application (with and without force transfer at the handle) and end of application.

In each factor group, there are several factors with highly significant correlations to discomfort ($p < 0.01$, $r = 0.54 - 0.723$). This confirms strong associations between the biomechanical parameters and the study discomfort ratings. Joint reactions, joint moment measures and muscle activities achieved highest correlation coefficients. By stepwise regression, nine factors were combined to a strong prediction model ($r^2 = 0.96$, $r^2_{\text{adj}} = 0.94$) for discomfort. The predicted discomfort values are well in line with the study discomfort ratings for all key percentiles and handbrake locations.

The five predictors, which explain the major portion (89 %) of the discomfort variation, are all related to the end time step. They include two joint reaction forces (axial moment of the right humeroulnar joint and vertical force of acromioclavicular joint), one joint moment measure (right wrist abduction moment) and two joint angles (right glenohumeral external rotation and sternoclavicular elevation). The four remaining predictors contribute by another 7.1 % to the discomfort variation. They are related to both start time steps, with and without force transfer. They comprise muscle activities of the right pectoralis major and the right trapezius muscle as well as metabolic power values of the right arm and the left leg.

To the best knowledge of the author, this work provides the first prove that the perceived discomfort of the handbrake application can be predicted reliably based on postural, biomechanical and mathematical modelling. A user-friendly procedure has been proposed to quantify handbrake discomfort with DHMs already in use in automotive development. The procedure can be applied at early stages of the development to enhance the ergonomics of the vehicle interior. Thereby it can increase efficiency and objectivity of the development procedure regarding handbrake ergonomics.

40 German subjects of a representative range of age and body height participated in the main study. The application of a typical handbrake lever was assessed for 7 locations covering the spread of typical handbrake locations in passenger vehicles.

Further work is required to validate the developed models and procedure. Future research may investigate to what extent the results of this work can be applied to differing driver populations. Examples are populations with different anthropometry (e.g. Asians or obese people), with other handbrake application habits (e.g. people who live in UK or in the mountains) or with differing age (e.g. drivers older than 80 years). Additionally, it will be interesting to understand how far the results can be applied to handbrakes with different designs, handbrake locations outside of the investigated

range (such as in commercial vehicles), handbrakes with restricted accessibility (e.g. by armrest) or other hand operated controls such as the gearshift lever.

Combinations of different types of biomechanical parameters may enhance the discomfort prediction accuracy. In future studies it could be investigated if the discomfort prediction accuracy can be further increased by including pressure distribution at the contact areas of the human and vehicle environment (such as the handbrake handle and the seat) as a factor.

Handbrake application has been chosen as one ergonomic example to develop a procedure for the reliable prediction of discomfort based on postural, biomechanical and mathematical modeling. Developing similar procedures for other applications – related to vehicle, other products or workplace design – could be a focus of future research.

13 GERMAN SUMMARY - DEUTSCHE ZUSAMMENFASSUNG

Komfort ist ein wichtiges Verkaufsargument und ein wesentlicher Faktor bei Kaufentscheidungen. Folglich setzen sich Fahrzeughersteller als Ziel, ergonomische Fahrzeuge zu entwickeln, welche sich gegenüber Mitbewerberfahrzeugen durch größeren Komfort und geringeren Diskomfort auszeichnen.

In der Vergangenheit wurden häufig Probandenstudien durchgeführt, um die Ergonomie von Fahrzeugen zu beurteilen und zu verbessern. Heutzutage werden oft digitale Menschmodelle eingesetzt, da ihre Anwendung zahlreiche Vorteile bietet: Die Anzahl an ressourcenaufwändigen und teuren Probandenstudien kann reduziert werden. Weiterhin werden objektive Beurteilungen bereits frühzeitig im Entwicklungsprozess ermöglicht. Schnelle Bewertungen und Vergleiche von mehreren Varianten können dazu beitragen, die Effizienz zu erhöhen, Entwicklungskosten zu senken und die Ergonomie zu optimieren.

Zahlreiche Studien belegen einen Zusammenhang zwischen empfundenen Diskomfort und biomechanischen Parametern bzw. dem muskuloskelettalen System (Bewegungsapparat). Folglich sollte die Evaluierung von Diskomfort mit digitalen Menschmodellen eine Analyse der muskuloskelettalen Belastungen beinhalten. Diese werden beeinflusst durch Kinematik (Haltung, Bewegung) und Kinetik (Analyse von Kräften und resultierenden Bewegungen oder inneren Belastungen).

Es gibt viele Veröffentlichungen über den Einfluss von biomechanischen Parametern auf Greifhaltungen und Greifdiskomfort sowie deren Vorhersage mit digitalen Menschmodellen. Im Gegensatz dazu wurde nur wenig veröffentlicht über die Betätigung der mechanischen Handbremse, obwohl diese nach wie vor ein wichtiges und sicherheitsrelevantes Bedienelement von Fahrzeugen ist.

In einigen Regionen, wie zum Beispiel in England, wird Fahrschülern beigebracht, die Handbremse jedes Mal anzuziehen, nachdem sie ein Fahrzeug zum Stehen gebracht haben – auch an Kreuzungen und Ampeln auf ebenen Straßen.

Eine Handbremse befindet sich typischerweise in der Mittelkonsole, wo Kompromisse bezüglich vieler Fahrzeugkomponenten und Attribute erforderlich sind. Deswegen ist es sehr wichtig, zu verstehen und zu quantifizieren, wie Veränderungen des Handbremsendesigns – insbesondere der Position der Handbremse – die Diskomfortwahrnehmung der Kunden beeinflussen.

In dieser Arbeit wurde eine zuverlässige Methode entwickelt zur Simulation der Bewegung bei der Betätigung der Handbremse und zur Berechnung des damit verbundenen Diskomforts. Die Methode basiert auf der Anwendung von digitalen Menschmodellen und mathematischer Modellierung.

Ein Fahrzeugmodell (ErgoBuck), welches den Innenraum eines PKWs abbildet, wurde mit einer Verstelleinheit für die Handbremsposition ausgestattet. Zu Beginn der Studie fuhren die Probanden den entsprechenden PKW, so dass Sitz- und Lenkradeinstellung erfasst und auf den ErgoBuck übertragen werden konnten.

In einer Vorstudie beurteilten 117 Probanden den Diskomfort der Handbremsbetätigung auf einer visuellen Analogskala für sieben unterschiedliche Handbremspositionen. Die zentrale Position wurde zweifach bewertet. Die Bewegung bei der Betätigung der Handbremse wurde mit Videokameras aufgezeichnet.

40 der Probanden nahmen auch an der Hauptstudie teil. Einschlusskriterien waren eine gute Reproduzierbarkeit bei der subjektiven Beurteilung, repräsentative Bewegungsmuster und das Erzielen einer gleichmäßigen Verteilung bezüglich der Körpergröße über den Bereich der Fahrerpopulation.

In der Hauptstudie beurteilten die Probanden erneut die Handbremsbetätigung für sieben unterschiedliche Handbremspositionen. Um eine größere Bandbreite an unterschiedlichen Beurteilungen als in der Vorstudie zu erzielen, wurde der Bereich der Handbremspositionen räumlich vergrößert und eine „Category Partitioning“ Skala zur Beurteilung verwendet. Zur präzisen Erfassung der Bewegungen wurde ein Vicon Nexus Bewegungsanalysesystem verwendet.

Die Datenanalyse ergab lineare Zusammenhänge zwischen der Körperhöhe und den Diskomfortwerten sowie zwischen der Körperhöhe und den Gelenkwinkeln. Dementsprechend wurden die weiteren Analysen für die Schlüsselperzentile durchgeführt, welche typischerweise in der Automobilbranche verwendet werden: 5F und 50F (5. und 50. Perzentil der Körpergröße, weiblich) sowie 50M und 95M (50. und 95. Perzentil der Körpergröße, männlich).

Die Gelenkwinkel (Studiengelenkwinkel) und Beurteilungen (Studiendiskomfort) der Perzentile wurden anhand der Regressionsgleichungen zwischen den Diskomfortratings bzw. Gelenkwinkeln der Probanden und ihrer Körperhöhe berechnet. So können Ausprägungen, die von der Körpergröße beeinflusst werden, berücksichtigt werden. Zudem wird der Einfluss von Ausprägungen, die nur für einen einzelnen Probanden gelten, minimiert.

Mit dem – in vielen Automobilkonzernen verwendeten – Menschmodell RAMSIS wurden Gelenkwinkel berechnet und mit den Studiengelenkwinkeln verglichen. Dazu wurde für jedes Schlüsselperzentil ein benutzerdefiniertes Haltungsmodell in RAMSIS entwickelt. Für alle Perzentile wurden die gleichen Restriktionen angewendet. Die vorhergesagten Haltungen stimmen gut mit den Studienhaltungen überein.

AMS (AnyBody Modellierungssoftware) ist ein biomechanisches Model, welches von mehreren Automobilkonzernen verwendet wird. Basierend auf Anthropometrie und Haltungen aus RAMSIS, der Fahrzeug- und Handbremsgeometrie sowie des Handbremskraftverlaufes wurde die Handbremsbetätigung in AMS modelliert.

Die berechneten biomechanischen Parameter umfassen die Gruppen Gelenkreaktionen, Gelenkmuskelmomente, Muskelaktivitäten, Gelenkwinkel sowie die metabolische Leistung und Energie. Die Werte wurden für die vier Schlüsselperzentile, die sieben Handbremspositionen und drei Zeitpunkte (Start der Handbremsbetätigung mit und ohne Kraftübertragung am Handbremsgriff, Ende der Handbremsbetätigung) berechnet.

In jeder Parametergruppe gibt es mehrere Faktoren mit hoch signifikanten Korrelationen zum Diskomfort ($p < 0.01$, $r = 0.54 - 0.723$). Dies bestätigt den Zusammenhang von Diskomfortempfinden und den biomechanischen Parametern. Gelenkreaktionen, Gelenkmuskelmomente und Muskelaktivitäten erzielten die höchsten Korrelationskoeffizienten.

Mittels schrittweiser Regression wurden neun Parameter zu einem präzisen Vorhersagemodell für den Diskomfort ($r^2 = 0.96$, $r^2_{\text{adj}} = 0.94$) kombiniert. Der berechnete Diskomfortwert, der Diskomfortindex, zeigt für die untersuchten Perzentile und Handbremspositionen eine gute Übereinstimmung mit dem Studiendiskomfort.

Die fünf Prädiktoren, welche den Hauptanteil (89 %) der Diskomfortvarianz aufklären, beziehen sich alle auf das Ende der Handbremsbetätigung. Sie beinhalten zwei Gelenkreaktionen (das axiale Moment des rechten Humeroulnargelenks (Teilgelenk des Ellenbogengelenks) und die vertikale Kraft im rechten Acromioclaviculargelenk (laterales Schlüsselbeingelenk, verbindet Schlüsselbein und Acromion des Schulterblatts)), ein Gelenkmuskelmoment (Abduktionsmoment im rechten Handgelenk) sowie zwei Gelenkwinkel (Außenrotation des rechten Arms und sternoclaviculare Anhebung, d.h. Anhebung von Schlüssel- und Brustbein).

Die vier verbleibenden Prädiktoren erklären weitere 7.1 % der Diskomfortvariation. Sie beziehen sich auf den Startzeitpunkt mit und ohne Kraftübertragung am Handbremsgriff.

Es sind die Muskelaktivitäten des rechten Pectoralis Major Muskels (großer Brustmuskel) und des rechten Trapezius Muskels (Rückenmuskel des Schultergürtels) sowie die metabolische Leistung des rechten Arms und linken Beins.

Nach Kenntnisstand der Autorin beinhaltet diese Arbeit den ersten Nachweis, dass der empfundene Diskomfort bei der Betätigung der Handbremse zuverlässig vorhergesagt werden kann durch Haltungssimulation sowie biomechanische und mathematische Modellierung.

Es wurde eine anwenderfreundliche Methode entwickelt, um den Diskomfort bei der Handbremsbetätigung durch die Anwendung von digitalen Menschmodellen, die in der Automobilentwicklung typischerweise verwendet werden, zu quantifizieren.

Diese Methode kann bereits in einem frühen Status in der Automobilentwicklung angewendet werden, um die Ergonomie des Fahrzeuginnenraums zu verbessern. Dadurch kann sie die Effizienz und Objektivität des Entwicklungsprozesses in Bezug auf die Handbremsergonomie erhöhen.

An der Hauptstudie haben 40 Probanden aus Köln mit repräsentativer Bandbreite an Körpergröße und Alter teilgenommen. Sie bewerteten die Betätigung eines konventionellen Handbremshebels für sieben unterschiedliche Positionen, welche den Bereich üblicher Handbremspositionen in PKWs abbilden.

Weitere Forschung ist erforderlich, um die entwickelten Modelle und die vorgeschlagene Methode zu validieren. Weiterhin ist es empfehlenswert zu untersuchen, wie gut die Ergebnisse dieser Arbeit auf andere Populationen anwendbar sind. Beispiele sind Populationen mit abweichender Körperanthropometrie (z.B. Asiaten oder adipöse Personen), mit anderen Handbremsgewohnheiten (Personen aus bergigen Regionen oder aus England) oder aus einer anderen Altersgruppe (z.B. älter als 80 Jahre).

Des Weiteren sind auch Untersuchungen von Interesse, inwieweit die Ergebnisse übertragbar sind: z.B. auf Handbremsen mit anderem Design oder erschwerter Zugänglichkeit, auf Handbremspositionen außerhalb des untersuchten Bereiches (z.B. in Nutzfahrzeugen) oder auch auf weitere handbetätigte Bedienelemente wie z.B. den Schalthebel.

Die Kombination verschiedener Arten von biomechanischen Parametern kann die Genauigkeit der Diskomfortvorhersage erhöhen. In weiteren Studien könnte untersucht werden, ob bzw. inwieweit die Vorhersagegenauigkeit gesteigert werden kann durch die

Einbeziehung zusätzlicher Parameter wie z.B. der Druckverteilung an den Kontaktflächen zwischen Mensch und Umgebung (Handbremsgriff, Sitz).

Die Handbremsbetätigung wurde als ein ergonomisches Beispiel ausgewählt, um eine Methode zu entwickeln mit der Diskomfort zuverlässig vorhergesagt werden kann basierend auf Haltungssimulation sowie biomechanischer und mathematische Modellierung. Die Entwicklung ähnlicher Methoden für andere Anwendungen – z.B. auch mit Bezug zu Fahrzeugen, oder aber auch für andere Produkte oder die Gestaltung von Arbeitsplätzen – könnten ein Schwerpunkt zukünftiger Forschung sein.

14 APPENDIX

14.1 Nomenclature

Abbreviations of muscles are listed in Table 14.21 (p. 264) and Table 14.22 (p. 265). Abbreviations of joint reaction forces and moment measures can be found in Table 14.23 (p. 270), Table 14.25 (p. 272) and Table 14.28 (p. 274). Abbreviations of joint angles (for the main study and subsequent modeling) are listed in Table 14.30 (p. 275). Abbreviations of posture variable used in the preliminary study are listed in Table 14.2 (p. 238) All other abbreviations are included in Table 14.1.

Table 14.1: Nomenclature.

Abbreviation	Meaning
#	Number of
2D	Two dimensional
3D	Three dimensional
A, _A	Point in time: at start of handbrake application
AAU	Aalborg University, Denmark
ABT	AnyBody Technology AS, Aalborg, Denmark
AC	Acromioclavicular joint
AFI	AnyFord Interface, Graphical user interface applied at Ford
AMMR	AnyBody Managed Model Repository
AMS	AnyBody Modeling System
A&U	Driving Environment - Accommodation & Usage, Department in the Ford Product
C	Coefficient matrix for unknown forces
CAE	Computer Aided Engineering
CDM	Car Driver Model
CG	Center of gravity
CNS	Central nervous system
Corr.	Correlation
CP	Category Partitioning
d	Vector of known applied loads and inertia forces
d	Perceived discomfort
dAbd	Range of abduction of the upper arm
DHM	Digital Human Modeling
DOF	Degree of freedom
e	Entry on the rating scale (in the main study)
E, _E	Point in time / time step: end of handbrake application, see Table 8.2., p. 174
EMG	Electromyography
Emet	Metabolic energy
FAP	Force application point
FDY	Maximum dynamic force
f	Force (inverse dynamics)
F	Scaled force
F ₀	Reference force
F, _F	Time step force, see Table 8.2, p. 174
FE	Finite elements
FE	Humeroulnar joint

Abbreviation	Meaning
FOCOPP	Force controlled posture prediction
FST	Maximal static force
G	Objective function
GH	Glenohumeral joint
H	Hypothesis
HPM	H-Point Machine
IAP	Industry advisory panel
IBO	Institute of Biomechanics and Orthopaedics, German Sport University Cologne,
K_L	Length scaling factor
K_M	Mass scaling factor
L	Location (of handbrake)
L_0	Original length
L_1	Scaled length
LCS	Local coordinate system
MAct	Muscle activity
MBS	Multi-body system
M_0	Original mass
M_1	Scaled mass
(M)	Muscle
Ma	Maximum
Me	Mean
MVC	Maximum voluntary contraction
N	Current strength of muscle
p	Power
p	Vector of four Euler parameters
$\Phi(q, t)$	Vector of kinematic constraints
Pmet	Metabolic power
PROCOPP	Probability controlled posture prediction
PS	Ulnoradial joint
q	Segment coordinate
Q	Question
r	Pearson correlation coefficient
r	Global position vector of the center of mass of a segment
r^2	Coefficient of determination
r^2_{adj}	Modified coefficient of determination, taking into account number of predictors in the
(R)	Joint reaction force
ρ	Spearman's rang correlation coefficient
RAMSIS	Rechnergestütztes Anthropometrisch-Mathematisches System zur Insassen-
ROM	Range of motion
s	Position vector of the node in local coordinate system
S	Scaling matrix
S_{11}, S_{22}, S_{33}	Scaling factors in x, y and z direction
$S, _S$	Time step start, see Table 8.2, p. 174
SAE	Society of Automotive Engineers
SAF	Seat adjustment field
SC	Sternoclavicular joint
SD	Standard deviation
SGRP	Seating Reference Point
ST	Scapula thoracic gliding plane
t	Time
v	Velocity
w'_i	Angular velocity in body-fixed reference frame
$\Phi(q, t)$	vector of kinematic constraints
VIT	Vehicle Interior Technologies, Department of Ford Research Center in Aachen,

14.2 Preliminary study

14.2.1 Pre-questionnaire

Subject ID: _____

Dear Subject,
thank you for participating in this Study. Your identity will remain anonymous and your answers will only be used for the purposes of this study.
Please answer the questions below. For comments and questions please use the reverse side and note the number of the question for reference.

Personal questions:

1 Gender ☐ f ☐ m Age: _____ Years Size: _____ cm Weight: _____ Kg

2 Occupation: ☐ Student ☐ Homemaker ☐ employed ☐ seeking work ☐ retirement
if applicable, please specify occupation: _____
Predominantly: ☐ seating (e.g. office, student ..)
☐ moderate activities (e.g. handcrafter, homemaker, ...)
☐ intense activities (e.g. construction worker)

3 Have you had injuries during the previous 12 month? ☐ yes ☐ no
If yes, please describe _____

5 Do you have muscle or joint troubles at the moment? ☐ yes ☐ no
If yes, please describe _____

6 Do you have back pain or muscular pain at the moment? Yes, I have got ☐ back pain ☐ muscular pain ☐ no
If yes, please describe _____
If yes, please describe in which body area _____

7 Do you have discomfort/impairments when seating? ☐ yes ☐ no
If yes, please describe _____
How long can you seat as a vehicle driver without discomfort/ ☐ less than 1h ☐ 1-2h ☐ more than 2h
How long can you seat as a vehicle passenger without discomfort/ ☐ less than 1h ☐ 1-2h ☐ more than 2h

8 Do you have discomfort/impairments when driving a car? ☐ no ☐ little ☐ medium ☐ severe
Kind of discomfort impairment (e.g. shoulder glance is difficult) _____

7 Have you ever participated in a posture training or a joint protection training? ☐ yes ☐ no
If yes, _____ years ago.

8 Do you regularly do sports? ☐ yes ☐ no Which sport: _____
If yes, which type: _____ times / week _____ minutes per session
If yes, which type: _____ times / week _____ minutes per session
If yes, which type: _____ times / week _____ minutes per session

9 Do you do additional physical activities additional to employment and sports? (e.g. gardening) ☐ yes ☐ no
If yes, which type: _____ times / week _____ minutes per session
If yes, which type: _____ times / week _____ minutes per session
If yes, which type: _____ times / week _____ minutes per session

Many thanks for your information!

To be filled by the study leader:

Steering: _____ Seat: _____ Backrest: _____ Headrest: _____

Group: _____ No. _____ Order: _____

Figure 14.1: Pre-questionnaire utilized in the preliminary study.

14.2.2 Variables from the video analysis

In this chapter, the variables which describe the posture or movement of handbrake application (see Table 14.2) are described briefly. This section (including figures) was extracted and only marginally modified from Rausch & Upmann (2015) which was based on Heinrich et al. (2014).

Table 14.2: Abbreviation of the variables from video analysis with reference to description text section and page. Abbreviations are in alphabetic sequence.

Abbreviation	Meaning	Section	Page
Abd	Abduction of the upper arm (glenohumeral abduction)	14.2.2.2	239
AntRet	Anteversion/retroversion of the arm (glenohumeral anteversion/retroversion)	14.2.2.1	238
dAbd	Range of abduction of the upper arm (range of glenohumeral abduction)	14.2.2.13	243
dAntRet	Range of anteversion/retroversion of the arm (range of glenohumeral anteversion/retroversion)	14.2.2.12	243
dEflex	Range of elbow flexion/extension	14.2.2.15	243
dESx	Dorsal-ventral movement of the elbow (determined in sagittal plan)	14.2.2.8	241
dESz	Vertical movement of the elbow	14.2.2.9	241
dETx	Dorsal-ventral movement of the elbow (determined in transversal plane)	14.2.2.10	242
dETz	Vertical shoulder movement	14.2.2.11	242
HG	Wrist abduction	14.2.2.4	239
SGh	Dorsal-ventral movement of the shoulder	14.2.2.6	240
SGv	Vertical position of the shoulder	14.2.2.5	240

14.2.2.1 Anteversion/retroversion of the Arm (AntRet)

The glenohumeral anteversion respectively retroversion characterizes the forward respectively backward position of the arm in sagittal plane. As shown in Figure 14.2, it was determined as the angle between the line from shoulder joint center to elbow joint center and the line from shoulder joint center to hip joint center. It was recorded for start and end of handbrake application.



Figure 14.2: Anteversion (left) and retroversion (right) of the arm (Heinrich et al., 2014, p. 59).

14.2.2.2 Abduction of the upper arm (Abd)

The glenohumeral abduction was determined as the front plane angle between the line from shoulder joint center to elbow joint center and the line from shoulder joint center to hip joint center (Figure 14.3), it. It was determined for start and end of handbrake application.

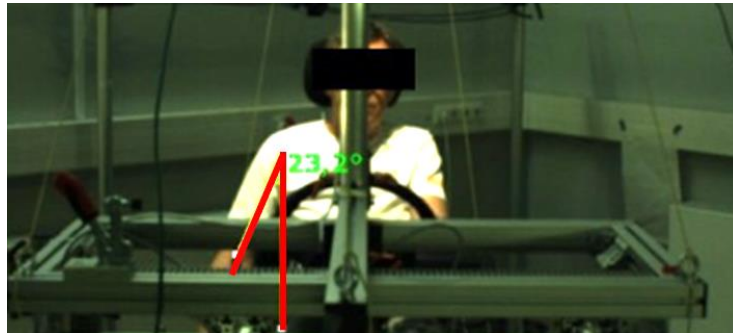


Figure 14.3: Abduction of the upper arm (Heinrich et al., 2014, p. 63).

14.2.2.3 Flexion of the elbow joint (Eflex)

The flexion of the elbow joint is indicated by the line from shoulder joint center to elbow joint center and the line from elbow joint center to wrist center in sagittal plane (Figure 14.4). Eflex was visually assessed for start and end position on a scale with 5 steps from 0 (straight, no flexion) to 4 (highly flexed).

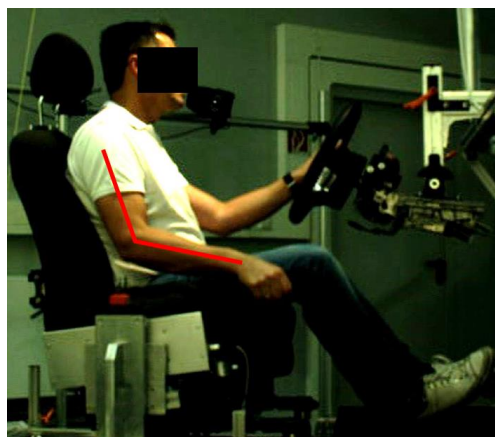


Figure 14.4: Elbow flexion is indicated by red lines.

14.2.2.4 Wrist abduction (HG)

The abduction of the wrist (HG) is indicated by the line from elbow joint center to wrist center and the line from wrist center to middle finger (Figure 14.5). It was visually assessed for start and end position on a scale with three steps: -1 (ulnar deviation, also referred to as adduction), 0 (no abduction/adduction) and 1 (radial deviation, abduction).

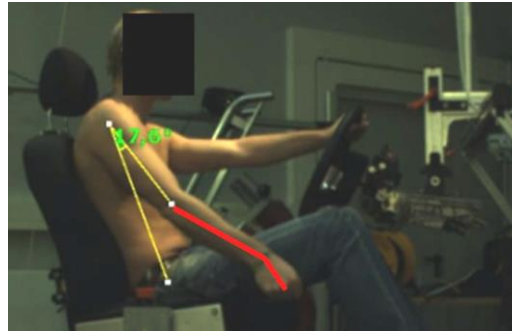


Figure 14.5: Adduction of the wrist is indicated by red lines (Heinrich et al., 2014, p. 61).

14.2.2.5 Vertical position of the shoulder (SGv)

The vertical position of the shoulder was determined along the vertical axis in frontal plane (Figure 14.6). It was visually assessed at the start and end position on a scale with three steps: 1 (cranial, upwards), 0 (neutral) and -1 (caudal, downwards).

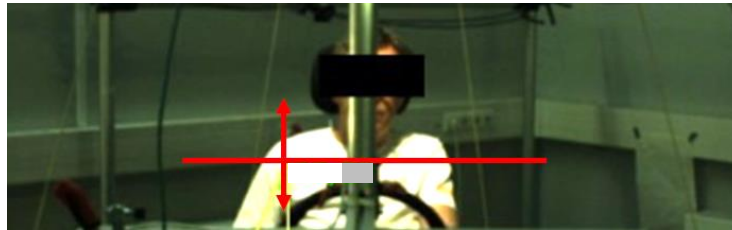


Figure 14.6: Vertical position of the shoulder is indicated by red arrows. Modified from Heinrich et al. (2014, p. 62).

14.2.2.6 Dorsal-ventral movement of the shoulder (SGh)

The dorsal-ventral movement of the shoulder joint was determined along the dorsal-ventral axis in the transversal plane (Figure 14.7). The change of the position from start to end of handbrake application was visually assessed on a scale with three steps: 1 (ventral, forwards), 0 (no change) and -1 (dorsal, backwards).

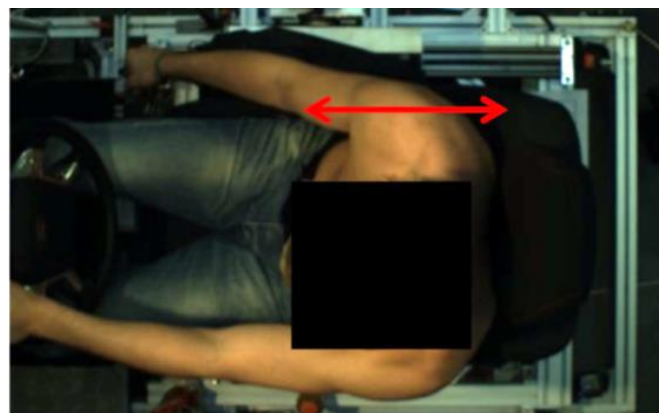


Figure 14.7: Dorsal-ventral movement of the shoulder joint is indicated by red arrows (Heinrich et al., 2014, p. 64).

14.2.2.7 Vertical shoulder movement (dSGv)

Vertical shoulder movement between start and end was determined along the vertical axis in frontal plane (Figure 14.8). It was assessed visually on a scale with two steps: 1 (for cranial, upwards) and 0 (no change).

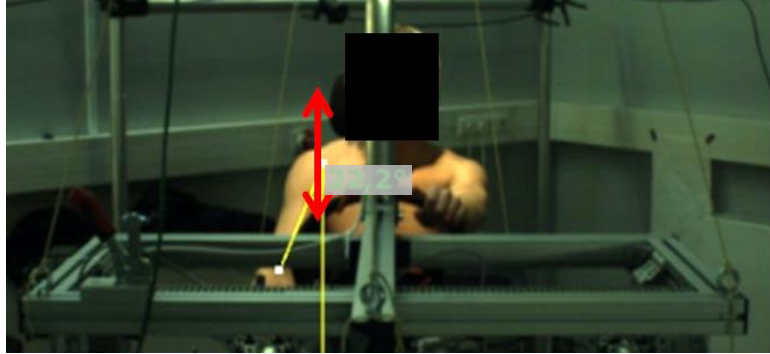


Figure 14.8: Vertical shoulder movement between start and end, indicated by red arrows (Heinrich et al., 2014, p. 69).

14.2.2.8 Dorsal-ventral movement of the elbow (dESx)

The horizontal movement of the elbow between start and end was determined on the dorsal-ventral axis in the sagittal plane (Figure 14.18). It was visually assessed on a scale with three steps: -1(dorsal, backwards), 0 (no change) and 1(ventral, forwards).

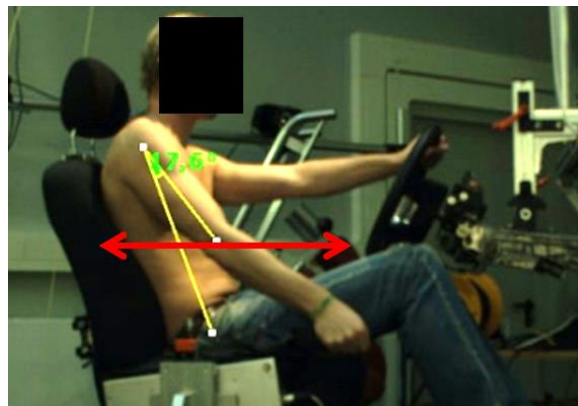


Figure 14.9: Dorsal-ventral movement of the elbow is indicated with arrows (Heinrich et al., 2014, p. 65).

14.2.2.9 Vertical movement of the elbow (dESz)

The vertical movement of the elbow from start to end was determined along the vertical axis in the sagittal plane (Figure 14.10). It was assessed visually on scale with three steps: 1 (cranial, upwards), 0 (no change) and -1 (caudal, downwards).



Figure 14.10: Change of the vertical elbow position between start and end, indicated by red arrows (Heinrich et al., 2014, p. 66).

14.2.2.10 Dorsal-ventral movement of the elbow (dETx)

The dorsal-ventral movement of the elbow from start to end was determined as the elbow position change along the dorsal-ventral axis in the transversal plane (Figure 14.11). It was visually assessed on a scale with 3 steps: 1 (ventral, forwards), 0 (no change) and -1 (dorsal, backwards).



Figure 14.11: Dorsal-ventral movement of the elbow is indicated with red arrows (Heinrich et al., 2014, p. 67).

14.2.2.11 Medio-lateral movement of the elbow (dETz)

The medio-lateral movement of the elbow was determined as the position change of the elbow along medio-lateral axis in the transversal plane (Figure 14.12) from start to end of handbrake application. It was visually assessed on a scale with 3 steps: 1 (lateral: to the right/outwards), 0 (no change), and -1 (medial: to the left/inwards).



Figure 14.12: Medio-lateral movement of the elbow is indicated with red arrows (Heinrich et al., 2014, p. 68).

14.2.2.12 Range of the anteversion/retroversion of the arm (dAntRet)

dAntRet describes the change of the anteversion/retroversion (see 14.2.2.1) between start and end position and is calculated as difference between AntRet_E and AntRet_A.

14.2.2.13 Range of abduction of the upper arm (dAbd)

dAbd describes the change of the glenohumeral abduction (see 14.2.2.2) between start and end position and is calculated as difference between Abd_E and Abd_A.

14.2.2.14 Range of dorsal-ventral position of the shoulder (dSGh)

dSGh describes the change of the dorsal-ventral position of the shoulder (14.2.2.6) between start and end and is calculated as difference between SG_E and SG_A.

14.2.2.15 Range of elbow flexion/extension (dEflex)

dEflex describes the change of the elbow flexion/extension (14.2.2.3) between start and end position and is calculated as difference between Eflex_E and Eflex_A.

14.2.2.16 Range of abduction of the wrist (dHG)

dHG describes the change of wrist abduction (14.2.2.4) between start and end position and is calculated as difference between HG_E and HG_A.

14.2.3 Post-questionnaire

Subject ID: _____

Dear Subject,
thank you for participating in this Study. Your identity will remain anonymous and your answers will only be used for the purposes of this study.
Please answer the questions below. For comments and questions please use the reverse side and note the number of the question for reference.

Questions about your vehicle, driving and park brake application habits

1 Driving Experience	_____	Years		
2 Which (private) vehicle do you drive ?	Manufacturer: _____	Model: _____	Constr. Year: _____	
3 Which kind of park brake is in your vehicle?	<input type="checkbox"/> Hand application (lever)	<input type="checkbox"/> Foot application	<input type="checkbox"/> Electronic (button)	
4 How many kilometers do you drive per year?	<input type="checkbox"/> below 10.000	<input type="checkbox"/> 10.000 to 20.000	<input type="checkbox"/> more than 20.000	
5 How often do you use the park brake while parking?	<input type="checkbox"/> never (next question 7)	<input type="checkbox"/> sometimes	<input type="checkbox"/> always (next question 7)	<input type="checkbox"/> I don't know
6 In which cases do you use the park brake while parking? Check all appropriate answers.	<input type="checkbox"/> on flat ground	<input type="checkbox"/> on slight slopes	<input type="checkbox"/> on steep slopes	<input type="checkbox"/> I don't know
7 How often do you use the park brake for when starting driving on a hill?	<input type="checkbox"/> never	<input type="checkbox"/> sometimes	<input type="checkbox"/> always	<input type="checkbox"/> I don't know
8 How often do you use the park brake at traffic lights?	<input type="checkbox"/> never (next question 10)	<input type="checkbox"/> sometimes	<input type="checkbox"/> always (next question 10)	<input type="checkbox"/> I don't know
9 In which cases do you use the park brake at traffic lights? Check all appropriate answers.	<input type="checkbox"/> on flat ground	<input type="checkbox"/> on slight slopes	<input type="checkbox"/> on steep slopes	<input type="checkbox"/> I don't know
10 Do you depress the brake pedal while applying the park brake?	<input type="checkbox"/> never	<input type="checkbox"/> sometimes	<input type="checkbox"/> always	<input type="checkbox"/> I don't know

If you have a hand applied park brake (hand brake), please answer the following details.

11 Do you depress the hand brake button before applying the handbrake?	<input type="checkbox"/> never	<input type="checkbox"/> sometimes	<input type="checkbox"/> always	<input type="checkbox"/> I don't know
12 Do you hold on the hand brake when entering/exiting the vehicle?	<input type="checkbox"/> never	<input type="checkbox"/> sometimes	<input type="checkbox"/> always	
13 How much do you apply the hand brake?	<input type="checkbox"/> lightly	<input type="checkbox"/> medium	<input type="checkbox"/> heavily	<input type="checkbox"/> I don't know

the following for questions, please check a number on a scale from 1 (extremely unsatisfied) to 10 (extremely satisfied)

14 How satisfied are you with the tactile/grip feeling of your hand brake?	<input type="checkbox"/> 1	<input type="checkbox"/> 2	<input type="checkbox"/> 3	<input type="checkbox"/> 4	<input type="checkbox"/> 5	<input type="checkbox"/> 6	<input type="checkbox"/> 7	<input type="checkbox"/> 8	<input type="checkbox"/> 9	<input type="checkbox"/> 10	<input type="checkbox"/> I don't know
15 How satisfied are you with the styling/design of your hand brake?	<input type="checkbox"/> 1	<input type="checkbox"/> 2	<input type="checkbox"/> 3	<input type="checkbox"/> 4	<input type="checkbox"/> 5	<input type="checkbox"/> 6	<input type="checkbox"/> 7	<input type="checkbox"/> 8	<input type="checkbox"/> 9	<input type="checkbox"/> 10	<input type="checkbox"/> I don't know
16 How satisfied are you with the application forces of your hand brake?	<input type="checkbox"/> 1	<input type="checkbox"/> 2	<input type="checkbox"/> 3	<input type="checkbox"/> 4	<input type="checkbox"/> 5	<input type="checkbox"/> 6	<input type="checkbox"/> 7	<input type="checkbox"/> 8	<input type="checkbox"/> 9	<input type="checkbox"/> 10	<input type="checkbox"/> I don't know
17 How satisfied are you with the position of your hand brake?	<input type="checkbox"/> 1	<input type="checkbox"/> 2	<input type="checkbox"/> 3	<input type="checkbox"/> 4	<input type="checkbox"/> 5	<input type="checkbox"/> 6	<input type="checkbox"/> 7	<input type="checkbox"/> 8	<input type="checkbox"/> 9	<input type="checkbox"/> 10	<input type="checkbox"/> I don't know
18 Has the hand brake always prevented the vehicle from driving away?	<input type="checkbox"/> yes	<input type="checkbox"/> no	<input type="checkbox"/> I don't know								

Many thanks for your information.

Figure 14.13: Post-questionnaire utilized in the preliminary study.

14.2.4 Preliminary study subjective evaluation

Table 14.3: p-values of Anderson-Darling Normality test for the five questions. $p > 0.05$ indicates that the data set follows a normal distribution. None of the data sets follows a normal distribution.

Question	Q1	Q2	Q3	Q4	Q5
p	< 0.005	< 0.005	< 0.005	< 0.005	< 0.005

Table 14.4: p-values of Anderson-Darling Normality test for all five questions and all eight handbrake locations. $p > 0.05$ indicates that the data set follows a normal distribution.

p	L1	L2	L3	L4	L5	L6	L7	L8
Q1	0.017	0.021	0.008	< 0.005	< 0.005	0.025	< 0.005	0.027
Q2	< 0.005	0.006	< 0.005	< 0.005	0.069	< 0.005	< 0.005	< 0.005
Q3	< 0.005	0.011	< 0.005	< 0.005	< 0.005	< 0.005	< 0.005	< 0.005
Q4	< 0.005	< 0.005	< 0.005	< 0.005	< 0.005	< 0.005	< 0.005	< 0.005
Q5	< 0.005	< 0.005	< 0.005	< 0.005	< 0.005	< 0.005	< 0.005	< 0.005

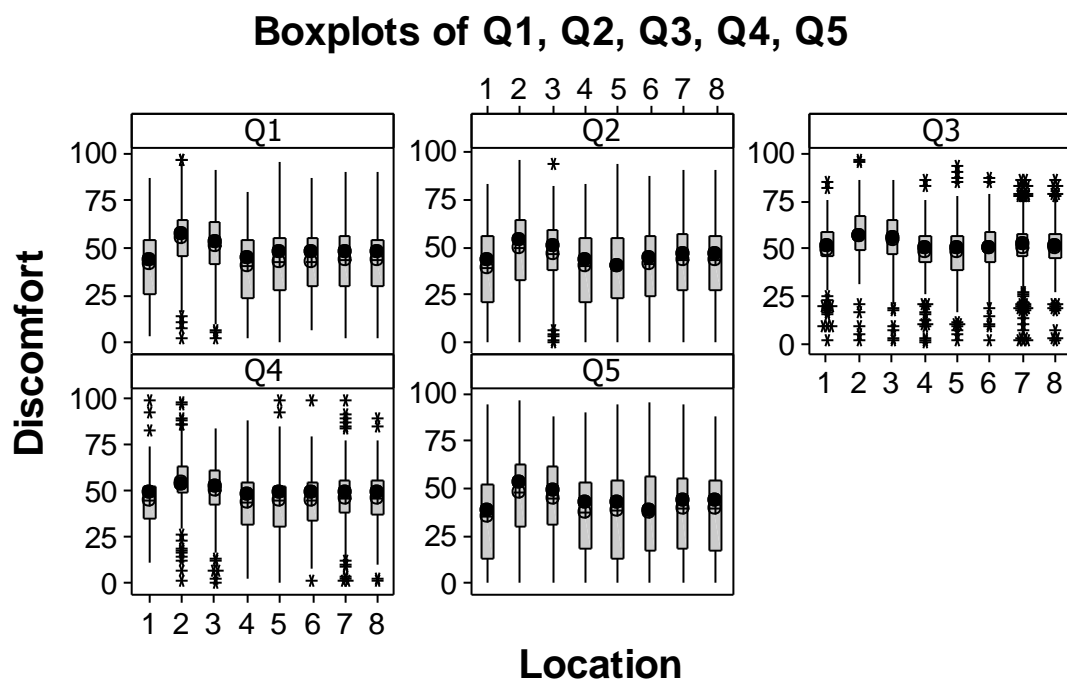


Figure 14.14: Boxplots of the ratings for all questions and handbrake locations.

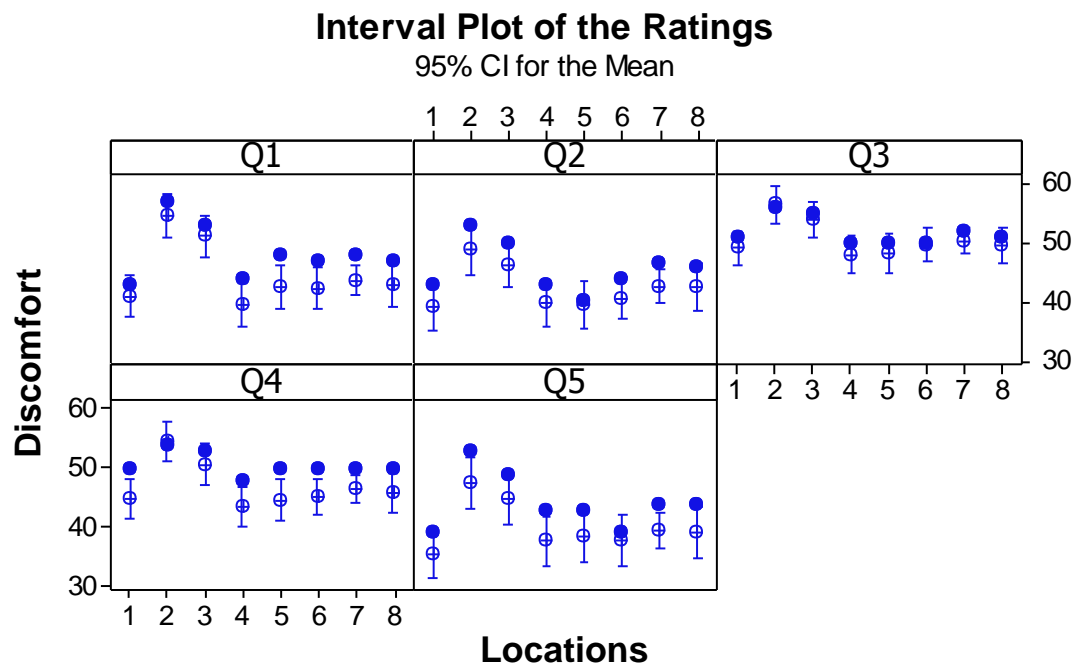


Figure 14.15: Subjective ratings of the preliminary study for all questions and handbrake locations. Increasing number indicates increasing discomfort. A blue dot represents the median. A Cross indicates the mean.

The bars represent the 95 % confidence intervals of means. This is based on the assumption that data sets are normally distributed which is not valid for all data subsets. Thus the chart needs to be considered only as a visual guide suggesting trends.

Table 14.5: Medians for all five questions and all eight handbrake locations with their descriptive statistics. p-values are calculated with Anderson-Darling normality test. $p > 0.05$ indicates that the data set follows a normal distribution.

Median	Q1	Q2	Q3	Q4	Q5
1	43.00	43.00	51.00	50.00	39.00
2	57.00	53.00	56.00	54.00	53.00
3	53.00	50.00	55.00	53.00	49.00
4	44.00	43.00	50.00	48.00	43.00
5	48.00	40.00	50.00	50.00	43.00
6	47.00	44.00	50.00	50.00	39.00
7	48.00	46.50	52.00	50.00	44.00
8	47.00	46.00	51.00	50.00	44.00
Analysis of the medians:					
Mean	48.38	45.69	51.88	50.63	44.25
SD	4.60	4.18	2.36	1.92	4.74
Min	43.00	40.00	50.00	48.00	39.00
Max	57.00	53.00	56.00	54.00	53.00
Range	14.00	13.00	6.00	6.00	14.00
p-value	0.223	0.612	0.031	0.010	0.215

Table 14.6: Means for the five questions and all eight handbrake locations with their descriptive statistics. p-values are calculated with Anderson-Darling normality test. $p > 0.05$ indicates that the data set follows a normal distribution.

Mean	Q1	Q2	Q3	Q4	Q5
1	40.95	39.14	49.14	44.86	35.53
2	54.68	48.78	56.54	54.64	47.65
3	51.13	46.18	53.88	50.68	44.74
4	39.57	39.79	47.99	43.56	37.76
5	42.55	39.50	48.25	44.62	38.42
6	42.23	40.66	49.61	45.14	37.86
7	43.67	42.62	50.38	46.59	39.55
8	42.72	42.43	49.61	45.92	39.05
Analysis of the means					
Mean	44.69	42.39	50.68	47.00	40.07
SD	5.31	3.46	2.99	3.76	4.04
Min	39.57	39.14	47.99	43.56	35.53
Max	54.68	48.78	56.54	54.64	47.65
Range	15.11	9.64	8.55	11.08	12.12
p-value	0.024	0.168	0.046	0.036	0.063

Table 14.7: Pearson correlation coefficient r of the mean ratings and median ratings for the locations (all p-values ≤ 0.009).

r	Q1-Q2	Q1-Q3	Q1-Q4	Q1-Q5
mean	0.96	0.98	0.99	0.97
median	0.84	0.89	0.92	0.91

Table 14.8: Spearman's correlation coefficient ρ of the mean ratings and median ratings for the locations.

ρ	Q1-Q2	Q1-Q3	Q1-Q4	Q1-Q5
mean	0.88	0.91	0.93	0.98
median	0.69	0.65	0.80	0.82

Table 14.9: Absolution differences of ratings for the identical handbrake locations and corresponding percentage of subjects. Discomfort range is from 0 to 100.

Absolute difference	Percentage of subjects	Cumulative percentage of subjects
0	6.31	6.31
1	8.11	14.42
2	5.41	19.83
3	4.50	24.33
4	6.31	30.64
5	6.31	36.95
6	6.31	43.26
7	3.60	46.86
8	5.41	52.27
9	4.50	56.77
10	3.60	60.37
11	4.50	64.87
12	4.50	69.37
13	0.90	70.27
14	4.50	74.77
15	2.70	77.47
16	0.00	77.47
17	1.80	79.27
18	1.80	81.07
19	0.90	81.97
20	0.90	82.87

14.2.5 Dendrogram for outlier selection

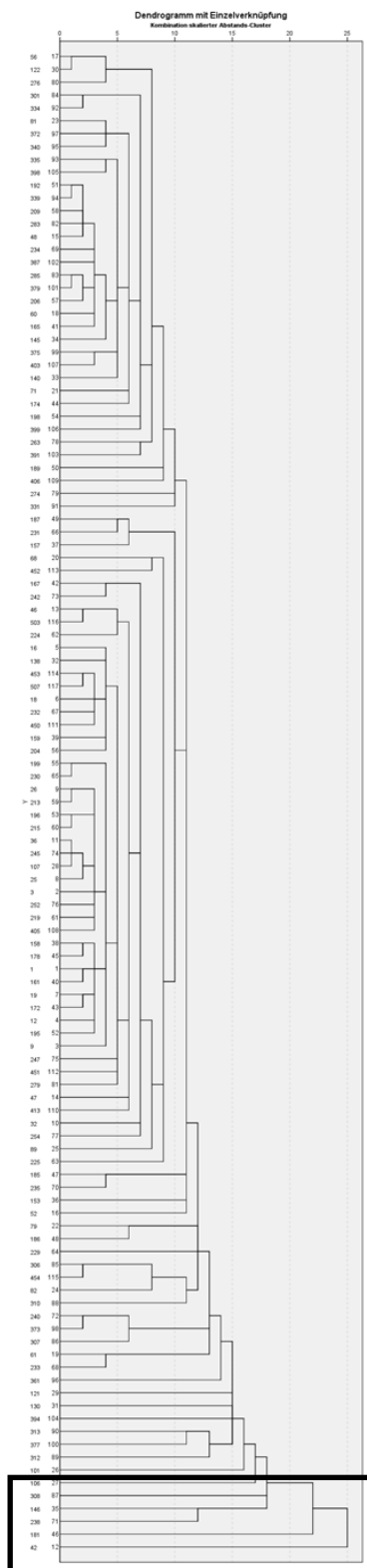


Figure 14.16: Dendrogram of the single linkage method. The six outliers are marked by a black box (Heinrich et al., 2014, p. 74).

14.2.6 Dendrogram for classification of subjects into clusters

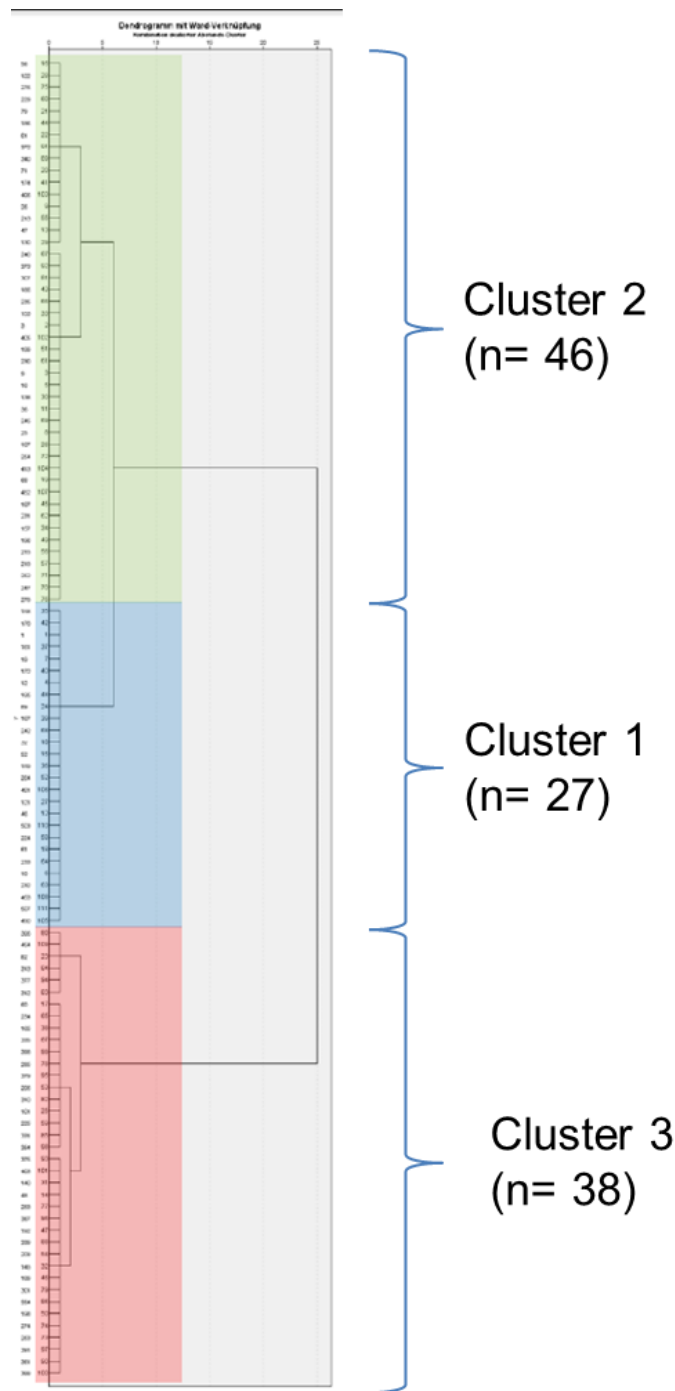


Figure 14.17: Dendrogram of the cluster analysis (ward method) with classification in three clusters (Heinrich et al., 2014, p. 81).

14.2.7 Correlation of movement variables and clusters

Table 14.10: Results of correlation analysis for movement variables and clusters (movement strategies). Ward groups and some of the movement variables are not normally distributed. Thus both, r and ρ , are shown. Both indicate similar strength of correlations.

Correlation to cluster	Pearson correlation coefficient r	p-value (related to r)	Spearman's rang correlation coefficient ρ
AntRet_E	-0.839	< 0.001	-0.885
Abd_E	0.836	< 0.001	0.845
AntRet_A	-0.814	< 0.001	-0.836
Abd_A	0.768	< 0.001	0.795
dESz	0.689	< 0.001	0.695
dAbd	0.608	< 0.001	0.603
Eflex_E	0.470	< 0.001	0.466
Eflex_A	0.440	< 0.001	0.434
dHG	0.415	< 0.001	0.425
HG_E	0.393	< 0.001	0.403
dETz	0.318	0.001	0.338
dAntRet	-0.213	0.025	-0.195
SGv_E	0.174	0.068	0.177
dEflex	0.143	0.134	0.169
dSGh	0.137	0.151	0.140
dSGv	0.134	0.161	0.146
SGh_E	0.109	0.253	0.111
HG_A	0.038	0.689	0.041
SGh_A	-0.028	0.767	-0.030
dETx	*	*	*
SGv_A	0.003	0.973	-0.000
dESx	*	*	*
*values identical for all subjects as all subjects move elbow in dorsal direction.			

14.2.8 Correlation of body height and further subject characteristics

Table 14.11: Results of correlation analysis for body height and other subject characteristics.

Correlation to body height	Pearson correlation coefficient R	p-value	Spearman's rang correlation coefficient ρ
Forearm with hand length	0.928	< 0.001	0.933
Upper arm length	0.903	< 0.001	0.907
Shoulder height seating	0.892	< 0.001	0.887
Seating height	0.884	< 0.001	0.927
Grip width	0.859	< 0.001	0.871
Seat adjustment in x	0.855	< 0.001	0.861
Hand length	0.809	< 0.001	0.811
Gender	-0.776	< 0.001	-0.78
F_{\max}	0.641	< 0.001	0.657
Seat adjustment in z	-0.48	< 0.001	-0.514
Steering wheel adj. in z	0.321	0.001	0.302
Steering wheel adj. in x	0.236	0.015	0.173
BMI	0.152	0.111	0.183
Age	-0.093	0.333	-0.098
Activity level	-0.08	0.406	-0.060

14.3 Main study

14.3.1 Marker setup

All tables (Table 14.12 to Table 14.16) in this subchapter are extracted from Rausch & Upmann (2015) which is based on Heinrich et al. (2014).

Table 14.12: Head markers (Heinrich et al., 2014, p. 111).

Marker	Description	Location
R_Stirnband_front	Front right head	Located approximately over the right temple
L_Stirnband_front	Front left head	Located approximately over the left temple
R_Stirnband_post	Back right head	Placed on the back of the head, roughly in a horizontal plane of the front head markers
L_Stirnband_post	Back left head	Placed on the back of the head, roughly in a horizontal plane of the front head markers

Table 14.13: Torso markers (Heinrich et al., 2014, p. 111).

Marker	Description	Location
C7 (only in calibration)	7th cervical vertebrae	Spinous process of the 7th cervical vertebrae
Sternum	Sternum	Placed on the sternum below the sternoclavicular joint

Table 14.14: Shoulder and arm markers (Heinrich et al., 2014, p. 111-112).

Marker	Description	Location
L_Acromion	Left acromion	Placed on acromion
L_Shoulder	Left shoulder	Placed on upper arm at height of the shoulder joint
L_Arm	Left upper arm	Placed on the vertical axis of the upper arm
L_Hum_lat	Left lateral elbow	Placed on the epicondylus lateralis
L_Hum_med	Left medial elbow	Placed on the epicondylus medialis
L_Uln	Left wrist marker on the ulna	Place on the distal end of the ulna below wrist joint
L_Rad	Left wrist marker on radius	Place on the distal end of the radius below wrist joint
L_HandTop	Left hand marker	Placed on distal end of the 3rd metacarpal (Os metacarpale tertium)
R_Acromion	Right acromion	Placed on the acromion
R_Shoulder	Right shoulder	Placed on upper arm at height of the shoulder joint
R_Arm	Right upper arm	Placed on the vertical axis of the upper arm
R_Hum_lat	Right lateral elbow	Placed on the epicondylus lateralis
R_Hum_med	Right medial elbow	Placed on the epicondylus medialis
R_Uln	Right wrist marker on the ulna	Place on the distal end of the ulna below wrist joint
R_Rad	Right wrist marker on radius	Place on the distal end of the radius below wrist joint
R_HandTop	Right hand marker	Placed on distal end of the 3rd metacarpal (Os metacarpale tertium)

Table 14.15: Hip markers (Heinrich et al., 2014, p. 112).

Marker	Description	Location
RASI (only in calibration)	Right ASIS	Placed on the anterior superior spina iliaca
LASI (only in calibration)	Left ASIS	Placed on the anterior superior spina iliaca
RPSI (only in calibration)	Right PSIS	Placed on the posterior superior spina iliaca
LPSI (only in calibration)	Left PSIS	Placed on the posterior superior spina iliaca
R_Belt1	First right belt marker	Placed on the right side of the belt, top marker
R_Belt2	Second right belt marker	Placed on the right side of the belt, left lower marker
R_Belt3	Third right belt marker	Placed on the right side of the belt, right lower marker
L_Belt1	First left belt marker	Placed on the right side of the belt, top marker
L_Belt2	Second left belt marker	Placed on the right side of the belt, left lower marker
L_Belt3	Third right left marker	Placed on the right side of the belt, right lower marker

Table 14.16: Leg and foot markers (Heinrich et al., 2014, p. 112-113).

Marker	Description	Location
R_Thigh1	First right thigh marker	Placed on the thigh, upper marker
R_Thigh2	Second right thigh marker	Placed on the thigh, lateral marker
R_Thigh3	Third right thigh marker	Placed on the thigh, medial marker
R_Knee	Right lateral knee marker	Placed on the lateralis epicondylus femoris
R_Knee_med	Right medial knee marker	Placed on the medialis epicondylus femoris
R_Ankle	Right lateral ankle marker	Placed on the malleolus lateralis
R_Mal_Med	Right medial ankle marker	Place on the malleolus medialis
R_Heel_Top	Right heel marker	Placed on the most distal point of the heel, right from the shoe
R_Meta5	Right lateral foot marker	Placed on the lateral side of the shoe (at os metatarsal 5)
R_Meta1	Right medial foot marker	Placed on the medial side of the shoe (at os metatarsal 1)
R_ToeTop	Right top foot marker	Placed on the top of the shoe (at phalanges distales 2)
L_Thigh1	First left thigh marker	Placed on the thigh, upper marker
L_Thigh2	Second left thigh marker	Placed on the thigh, lateral marker
L_Thigh3	Third left thigh marker	Placed on the thigh, medial marker
L_Knee	Left lateral knee marker	Placed on the lateralis epicondylus femoris
L_Knee_med	Left medial knee marker	Placed on the medialis epicondylus femoris
L_Ankle	Left lateral ankle marker	Placed on the malleolus lateralis
L_Mal_Med	Left medial ankle marker	Place on the malleolus medialis
L_Heel_Top	Left heel marker	Placed on the most distal point of the heel, right from the shoe
L_Meta5	Left lateral foot marker	Placed on the lateral side of the shoe (at os metatarsal 5)
L_Meta1	Left medial foot marker	Placed on the medial side of the shoe (at os metatarsal 1)
L_ToeTop	Left top foot marker	Placed on the top of the shoe (at phalanges distales 2)

14.3.2 Pre-questionnaire

Subject-ID: _____

Dear subject,
Thank you for participating in this Study. Your identity will remain anonymous and your answers will only be used for the purposes of this study. Please answer the questions below.

1. Information about your driving habits:

a. Do you regularly drive cars: ☐ yes How many hours per week? ____
☐ no

b. Have you ever done a safe driving training? ☐ yes
☐ no

c. How do you assess yourself regarding driving cars?

very experienced	<input type="checkbox"/> <input type="checkbox"/> <input type="checkbox"/> <input type="checkbox"/> <input type="checkbox"/> <input type="checkbox"/>	very inexperienced
smooth / calm driving style	<input type="checkbox"/> <input type="checkbox"/> <input type="checkbox"/> <input type="checkbox"/> <input type="checkbox"/> <input type="checkbox"/>	sporty / dynamic driving style
I enjoy driving	<input type="checkbox"/> <input type="checkbox"/> <input type="checkbox"/> <input type="checkbox"/> <input type="checkbox"/> <input type="checkbox"/>	driving is a necessary evil
I cope well with my vehicle	<input type="checkbox"/> <input type="checkbox"/> <input type="checkbox"/> <input type="checkbox"/> <input type="checkbox"/> <input type="checkbox"/>	in some situations I have difficulties to cope with my vehicle

2. Information about your health and feeling:

a. Do you feel sick?

not at all ☐ ☐ ☐ ☐ ☐ ☐ very sick

b. Do you feel pain? ☐ yes Where?
☐ no

c. At the moment, I am feeling

confident	<input type="checkbox"/> <input type="checkbox"/> <input type="checkbox"/> <input type="checkbox"/> <input type="checkbox"/> <input type="checkbox"/>	unconfident
awake	<input type="checkbox"/> <input type="checkbox"/> <input type="checkbox"/> <input type="checkbox"/> <input type="checkbox"/> <input type="checkbox"/>	tired
relaxed	<input type="checkbox"/> <input type="checkbox"/> <input type="checkbox"/> <input type="checkbox"/> <input type="checkbox"/> <input type="checkbox"/>	stressed
peaceful	<input type="checkbox"/> <input type="checkbox"/> <input type="checkbox"/> <input type="checkbox"/> <input type="checkbox"/> <input type="checkbox"/>	aggressive
happy	<input type="checkbox"/> <input type="checkbox"/> <input type="checkbox"/> <input type="checkbox"/> <input type="checkbox"/> <input type="checkbox"/>	sad

d. How do you assess your overall feeling?

very good ☐ ☐ ☐ ☐ ☐ ☐ very poor

To be filled by the study leader:

steering: _____ seat: _____ backrest: _____ headrest: _____
group: ____ No. ____ Order: _____

Figure 14.18: Pre-questionnaire utilized in the main study.

14.3.3 Post-questionnaire

Subject-ID: _____

Dear subject,

Thank you for participating in this Study. Your identity will remain anonymous and your answers will only be used for the purposes of this study. Please answer the questions below.

1. Information about the handbrake evaluation:

- a. The assessment of the handbrake application was
 very easy ☐ ☐ ☐ ☐ ☐ ☐ very difficult
- b. When assessing the handbrake application, I was
 very confident ☐ ☐ ☐ ☐ ☐ ☐ very unconfident
- c. The number of increments in the scale for the assessment of the handbrake application was
 much too low ☐ ☐ ☐ ☐ ☐ ☐ much too high

2. Information about the study:

- a. The study duration was
 much too short ☐ ☐ ☐ ☐ ☐ ☐ much too long
- b. The brakes were
 much too short ☐ ☐ ☐ ☐ ☐ ☐ much too long
- c. The study was
 not exhausting ☐ ☐ ☐ ☐ ☐ ☐ very exhausting

3. Information about your feeling:

- a. At the moment, I am feeling
- | | | |
|-----------|---|-------------|
| confident | <input type="checkbox"/> <input type="checkbox"/> <input type="checkbox"/> <input type="checkbox"/> <input type="checkbox"/> <input type="checkbox"/> | unconfident |
| awake | <input type="checkbox"/> <input type="checkbox"/> <input type="checkbox"/> <input type="checkbox"/> <input type="checkbox"/> <input type="checkbox"/> | tired |
| relaxed | <input type="checkbox"/> <input type="checkbox"/> <input type="checkbox"/> <input type="checkbox"/> <input type="checkbox"/> <input type="checkbox"/> | stressed |
| peaceful | <input type="checkbox"/> <input type="checkbox"/> <input type="checkbox"/> <input type="checkbox"/> <input type="checkbox"/> <input type="checkbox"/> | aggressive |
| happy | <input type="checkbox"/> <input type="checkbox"/> <input type="checkbox"/> <input type="checkbox"/> <input type="checkbox"/> <input type="checkbox"/> | sad |
- b. How do you assess your overall feeling?
- | | | |
|-----------|---|-----------|
| very good | <input type="checkbox"/> <input type="checkbox"/> <input type="checkbox"/> <input type="checkbox"/> <input type="checkbox"/> <input type="checkbox"/> | very poor |
|-----------|---|-----------|

Many thanks for your information!

Figure 14.19: Post-questionnaire applied in the main study.

14.3.4 Subjective evaluation

Table 14.17: p-values of Anderson-Darling normality test for the complete sample and each of the locations. p-values > 0.05 indicate that the data follow a normal distribution.

Location	all	L1	L2	L3	L4	L5	L6	L7	L8	L1, 6
p	< 0.005	0.007	0.179	0.006	0.079	0.055	0.056	0.007	0.531	0.215

Table 14.18: Significance levels of pairwise Mann-Whitney tests to test if medians are different. Significance levels with $p \leq 0.05$ (bold) indicate statistically significant differences.

Significance level	1	2	3	4	5	6	7	8
1		< 0.005	< 0.005	0.290	< 0.005	0.187	< 0.005	0.135
2			< 0.005	< 0.005	0.120	< 0.005	< 0.005	< 0.005
3				0.005	0.061	0.002	0.538	0.003
4					< 0.005	0.996	0.002	0.935
5						< 0.005	0.108	< 0.005
6							< 0.005	0.810
7								< 0.005
8								

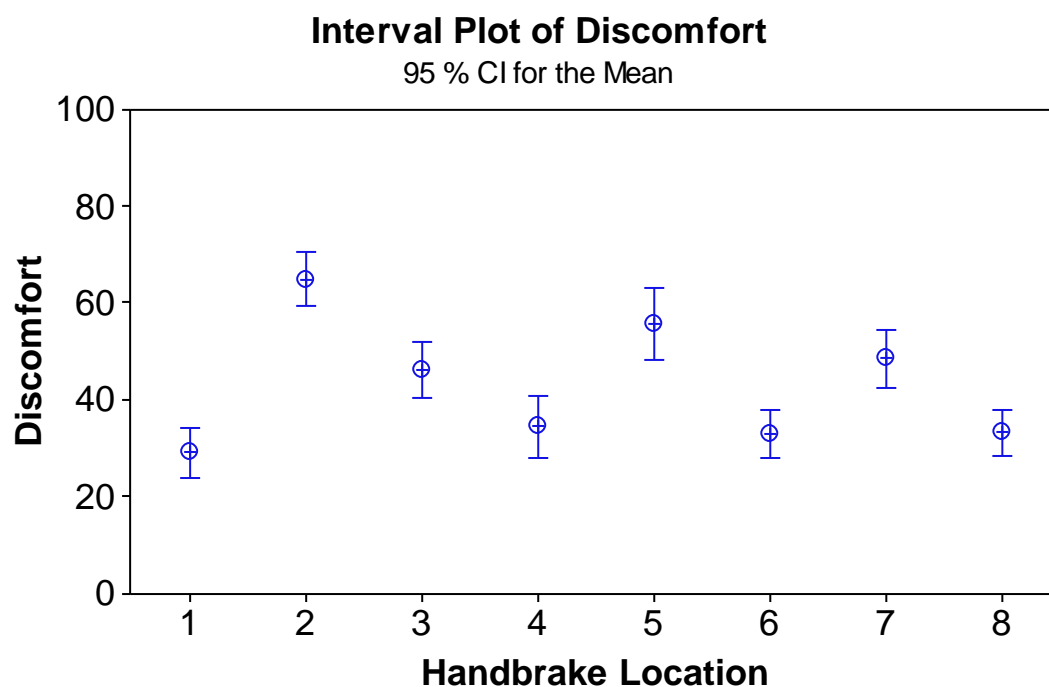


Figure 14.20: Mean with 95 %CI for the discomfort ratings. Note: For handbrake locations 1, 3 and 7 the data set are not normally distributed. For these handbrake locations the CI of the medians should be considered instead of the CI of the means.

Table 14.19: Results of analyzing the relationship of discomfort and body height.

Location	Description	p-value (Anderson -Darling)	Correlation to Body Height			Regression to Body Height (for p see correlation)	
			r	p	ρ	Equation	r^2_{adj}
L1	Central	0.007	-0.110	0.500	-0.046	Discomfort L1 = 52.7 - 13.6 Body Height [m]	< 0.001
L2	Rear up	0.179	-0.157	0.335	-0.228	Discomfort L2 = 102 - 21.2 Body Height [m]	< 0.001
L3	Fore up	0.006	0.023	0.888	0.042	Discomfort L3 = 40.4 + 3.2 Body Height [m]	< 0.001
L4	Rear down	0.079	-0.457	0.003	-0.45	Discomfort L4 = 160 - 72.0 Body Height [m]	0.188
L5	Fore down	0.055	0.356	0.024	0.337	Discomfort L5 = - 58.2 + 64.9 Body Height [m]	0.104
L6	Central	0.056	0.030	0.854	0.077	Discomfort L6 = 26.4 + 3.6 Body Height [m]	< 0.001
L7	Central with y shift	0.007	-0.069	0.674	-0.103	Discomfort L7 = 66.0 - 10.0 Body Height [m]	< 0.001
L8	Center of preliminary study	0.531	-0.007	0.968	0.027	Discomfort L8 = 34.3 - 0.8 Body Height [m]	< 0.001
L1,6	Mean of 1 and 6	0.215	-0.052	0.752	<0.001	Discomfort 1,6 = 39.5 - 5.0 Body Height [m]	< 0.001

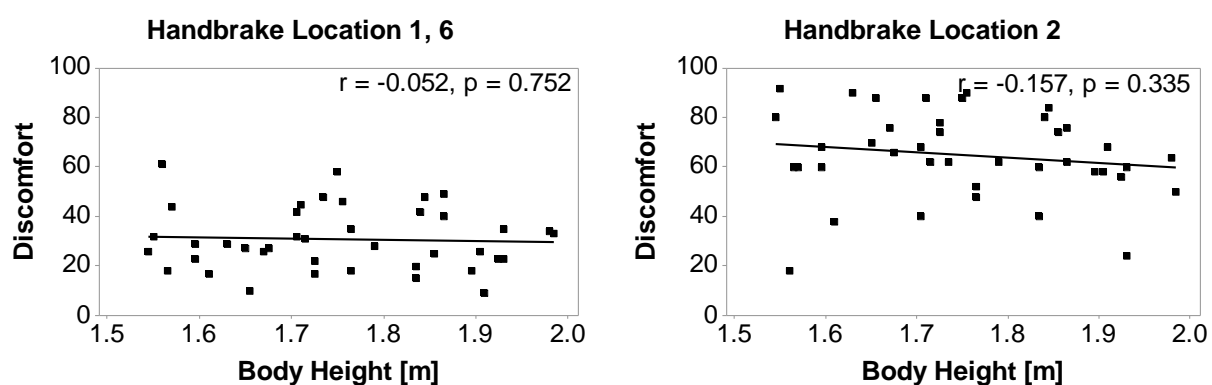


Figure 14.21: Left: Discomfort ratings versus body height for locations 1 and 6 (mean for each subject). Right: Discomfort ratings versus body height for location 2.

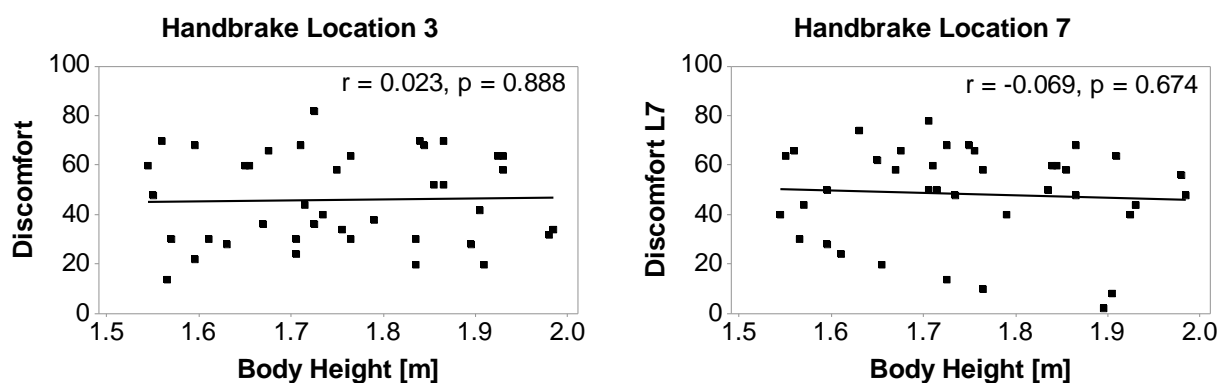


Figure 14.22: Left: Discomfort ratings versus body height for location 3. Right: Discomfort ratings versus body height for location 7.

14.4 Posture modeling

Chapter 14.4 was extracted from Raiber (2015) and only slightly modified. It is about the joints and joint angles relevant for posture analysis and posture modeling.

The angles between the segments describe the relative position of the segments in the three-dimensional space (e.g. the relative position of the upper arm to the upper body) and are defined with Euler angles in degrees.

14.4.1 Sternoclavicular joint

The sternoclavicular joint provides three degrees of freedom, which enable the elevation and depression of the shoulder girdle, its protraction and retraction (Figure 14.23) and the rotation around the clavicle.

The initial position (0°) of the sternoclavicular joint is defined as the location of the shoulder girdle referred to the shoulder axis in the neutral standing posture. The shoulder girdle movement in the horizontal plane is called protraction (positive angle) for forwards movements and retraction (negative angle) for backwards movements. The elevation (positive angle) characterizes the movement upwards in the frontal plane; the movement downwards is called depression (negative angle).

The rotational movement is rare and barely measurable with motion capture systems. Thus zero rotational movement is assumed in this study.

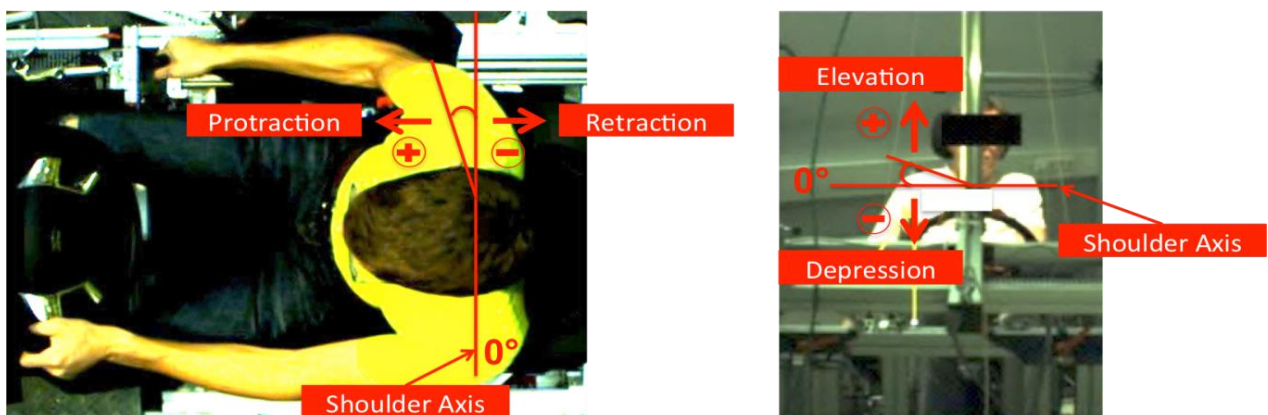


Figure 14.23: Sternoclavicular protraction/retraction and elevation/depression shown on frames of the videos recorded in the preliminary study (Raiber, 2015, p. 42).

14.4.2 Glenohumeral joint (shoulder joint)

The glenohumeral joint provides three degrees of freedom, which enable the anteversion and retroversion of the arm as well as its abduction and adduction and the external rotation (Figure 14.24). The initial position (0°) of the glenohumeral joint is

defined as the location of the upper arm referred to the position of the upper body in the neutral standing posture. The movement of the upper arm forwards in the sagittal plane with is called anteversion (positive angle, also called flexion). The backwards movement is referred to as retroversion (negative angle, also called extension). The abduction (positive angle) characterizes the movement of the upper arm away from the upper body center in the frontal plane. The movement towards the center of the upper body out of an abducted position is called adduction. The angle cannot get negative without an additional anteversion/retroversion, because the upper arm already touches the upper body in the initial position. The rotation of the upper arm around its longitudinal axis is called external rotation. The outward rotation of the arm results in a positive angle, the inward rotation has a negative angle.

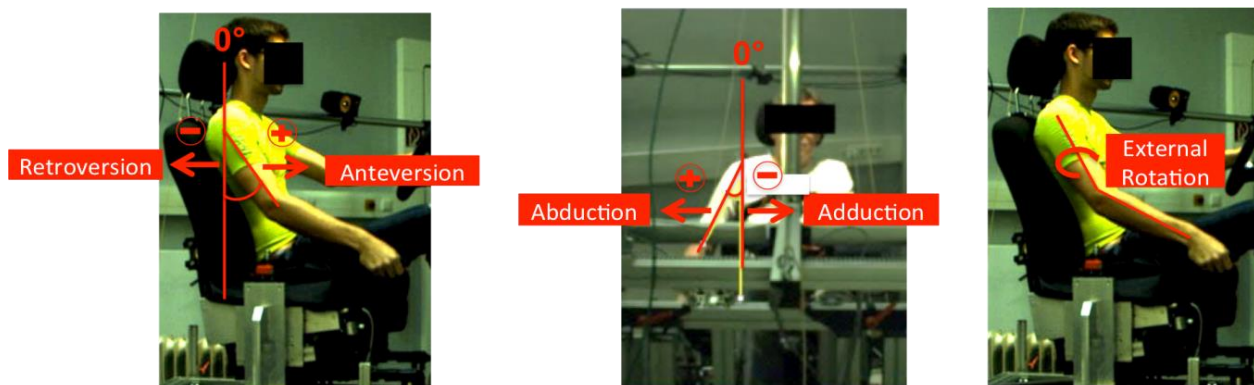


Figure 14.24: Glenohumeral anteversion/retroversion, abduction/adduction and external rotation shown on frames of the videos recorded in the preliminary study (Raiber, 2015, p. 43).

14.4.3 Elbow joint

The elbow joint consist of the humeroulnar and the proximal and distal radioulnar joints. It allows for flexion and extension of the elbow (Figure 14.25).

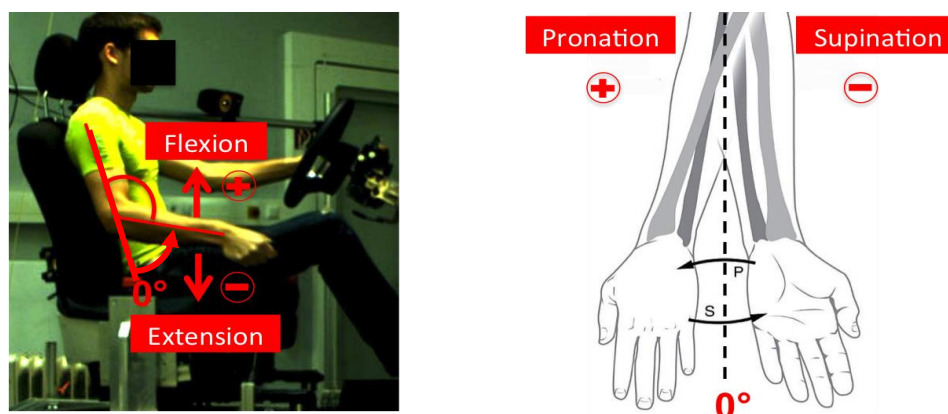


Figure 14.25: Left: Elbow flexion/extension shown on a frame of a video recorded in the preliminary study. Right: Radioulnar joint pronation/supination adapted from (OpenStax College, 2015); Sep. 17, 2014 (Raiber, 2015, p. 44).

The initial position (0°) of the elbow joint is defined as the stretched arm, when upper and lower arm build a straight line. The movement of the lower arm towards the upper arm is called flexion and is characterized by a positive angle. The anatomical conditions of the elbow joint usually do not permit an overstretching into a negative angle. Therefore, an extension can only occur out of a flexed elbow position. The proximal and distal radioulnar joints provide the pronation and supination (Figure 14.25). The pronation (positive angle) and supination (negative angle) is a movement of the elbow and influences the wrist/hand posture. Thereby, the lower arm is twisted inwards with the palm of the hand facing down (pronation) or outwards with the palm of the hand facing up (supination). The initial position (0°) is the untwisted lower arm with the thumb on top and the little finger at the bottom.

14.4.4 Wrist

The wrist provides two degrees of freedom, which provide the flexion (palmar flexion) and extension (dorsiflexion) of the wrist as well as its abduction and adduction (Figure 3.5). The initial position (0°) of the wrist is defined as the lower arm lying on a desk with the straight hand in extension of the lower arm. The flexion of the hand (the palm of the hand moving towards the lower arm) is called palmar flexion and has a positive angle; the extension (movement of the back of the hand towards the lower arm) is called dorsiflexion with a negative angle. The movement to the side where the thumb is placed is called abduction (positive angle); the movement to the other side is called adduction (negative angle).

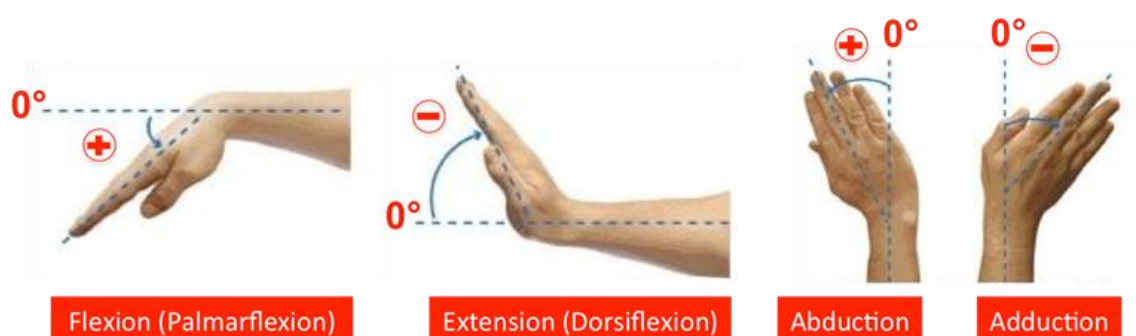


Figure 14.26: Wrist flexion/extension and abduction/adduction. Extracted from Raiber (2015, p. 44) who adapted from Papas (2015).

14.4.5 Vertebral column (spine / pelvis thorax angles)

The vertebral column provides upper body movements in three directions: 1. inclination (flexion) and reclination (extension), 2. lateral flexion (or lateral bending) and 3. rotation of the upper body (Figure 14.27). The initial position (0°) of the spine is defined as the

neutral standing posture with straight upper body (aligned along the vertical axis). Bending forward in the sagittal plane characterizes the inclination or flexion with a negative angle; leaning back is called reclination or extension (positive angle). Lateral bending of the upper body in the frontal plane is called lateral flexion with positive angles to the right side (towards the handbrake) and negative angles to the left. The rotation to the left in the horizontal plane is characterized by a positive angle, the rotation to the right is characterized by a negative angle. In AMS, the terms PelvisThorax_Extension, PelvisThorax_LateralBending and PelvisThorax_Rotation are utilized.

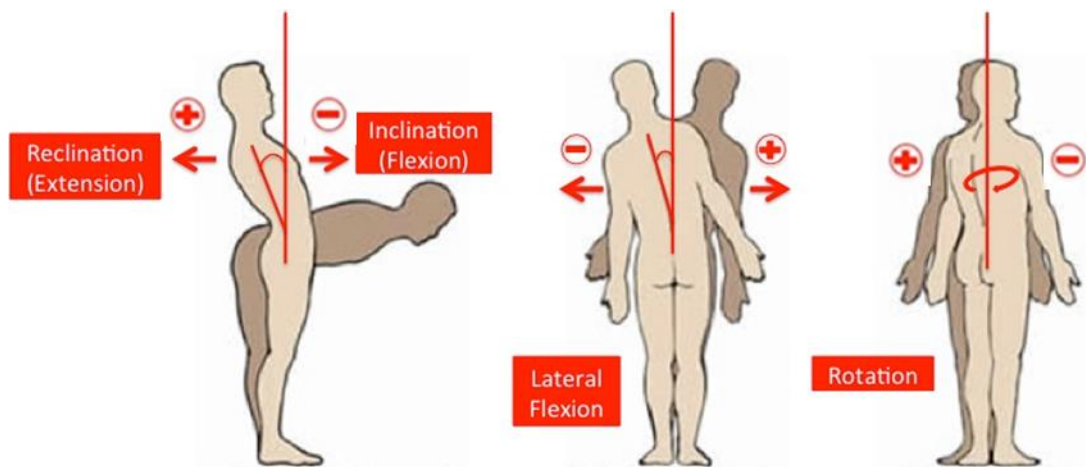


Figure 14.27: Spine inclination/reclination (PelvisThorax_Extension), lateral flexion (PelvisThorax_LateralBending) and rotation (PelvisThorax_Rotation). Modified from Raiber (2015, p. 44) who adapted from Pope (2015).

14.4.6 Changes in joint angles during the handbrake application

Table 14.20: Changes in joint angles during handbrake application (between start and end) for all key percentiles and handbrake locations. Extracted and modified from Raiber (2015, p.59).

	Joint Angle	5F	50F	50M	95M		5F	50F	50M	95M
Location 1 (same as 6)	RGlenohumeral_Anteversion	-15.2	-16.3	-17.4	-18.6	Location 5	-17	-16.6	-16.1	-15.7
	RGlenohumeral_Abduction	12.9	10	6.9	3.7		5	3.4	1.8	0.1
	RElbow_Flexion	32.3	31.8	31.3	30.8		29.1	29.5	29.9	30.3
	RWrist_Flexion	20.7	16.8	12.7	8.5		12.7	10.5	8.1	5.6
	RWrist_Abduction	4.5	3.5	2.4	1.3		3.3	3	2.7	2.3
	RSternoClavicular_Protraction	-4	-4.1	-4.1	-4.2		-6.8	-7.5	-8.2	-9
	RSternoClavicular_Elevation	4.4	4.3	4.2	4.1		7.5	6.7	5.7	4.8
	PelvisThorax_Extension	1.2	1.1	0.9	0.8		4.6	3.5	2.4	1.3
	PelvisThorax_LateralBending	-1.3	-1.4	-1.4	-1.5		-5.3	-4.6	-3.9	-3.2
	PelvisThorax_Rotation	0.9	1.2	1.5	1.7		0.7	0.4	0.1	-0.2
Location 2	RGlenohumeral_Anteversion	-14.7	-14.8	-14.8	-14.8	Location 7	-17.9	-18.2	-18.5	-18.9
	RGlenohumeral_Abduction	10.4	8.5	6.4	4.3		13.1	9.9	6.6	3.2
	RElbow_Flexion	26.1	25.5	24.8	24.1		33.5	32.8	32.1	31.3
	RWrist_Flexion	19.2	16.4	13.5	10.5		17.6	14.2	10.6	6.9
	RWrist_Abduction	6.4	5.2	4	2.7		4.2	3.2	2.2	1.2
	RSternoClavicular_Protraction	-7.8	-6	-4.1	-2.1		-5.7	-5.6	-5.5	-5.3
	RSternoClavicular_Elevation	5	4.4	3.8	3.1		5.6	5	4.5	4
	PelvisThorax_Extension	1.7	1.5	1.2	0.9		1.9	1.6	1.2	0.8
	PelvisThorax_LateralBending	-2.6	-1.8	-1	-0.2		-2.2	-1.9	-1.5	-1.2
	PelvisThorax_Rotation	2.3	2.2	2	1.9		1.9	1.9	2	2.1
Location 3	RGlenohumeral_Anteversion	-16.3	-16.8	-17.3	-17.9	Location 8	-14.6	-15.8	-17	-18.2
	RGlenohumeral_Abduction	12	8.8	5.4	2		12.5	9.7	6.6	3.6
	RElbow_Flexion	30.7	31.4	32.2	33		30.8	31.5	32.1	32.8
	RWrist_Flexion	19.1	14.7	10.2	5.5		21	16.8	12.3	7.7
	RWrist_Abduction	3.4	2.8	2.2	1.5		4.2	3.3	2.4	1.4
	RSternoClavicular_Protraction	-5.2	-5.2	-5.3	-5.4		-3.8	-4	-4.2	-4.4
	RSternoClavicular_Elevation	4.7	4.7	4.8	4.8		7	6	4.9	3.9
	PelvisThorax_Extension	0.9	0.9	1	1		1.3	1	0.6	0.3
	PelvisThorax_LateralBending	-2.1	-2	-1.8	-1.6		-2.9	-2.3	-1.6	-1
	PelvisThorax_Rotation	1.7	1.7	1.7	1.7		1.3	1.4	1.5	1.5
Location 4	RGlenohumeral_Anteversion	-14	-15.2	-16.5	-17.8	Location 9	-14.6	-15.8	-17	-18.2
	RGlenohumeral_Abduction	14.1	11.9	9.7	7.4		12.5	9.7	6.6	3.6
	RElbow_Flexion	33.7	32.5	31.2	29.8		30.8	31.5	32.1	32.8
	RWrist_Flexion	23.3	19.8	16.1	12.3		21	16.8	12.3	7.7
	RWrist_Abduction	6.2	5.1	4	2.9		4.2	3.3	2.4	1.4
	RSternoClavicular_Protraction	-4.6	-4.2	-3.7	-3.3		-3.8	-4	-4.2	-4.4
	RSternoClavicular_Elevation	4.6	4.7	4.7	4.7		7	6	4.9	3.9
	PelvisThorax_Extension	2	1.6	1.3	0.9		1.3	1	0.6	0.3
	PelvisThorax_LateralBending	-3.2	-2.6	-1.9	-1.2		-2.9	-2.3	-1.6	-1
	PelvisThorax_Rotation	1.6	1.6	1.7	1.7		1.3	1.4	1.5	1.5

14.5 Biomechanical modeling and correlation to discomfort

14.5.1 Muscles

In AMS, muscles are often modeled as a group of muscle bundles with differing load paths. The muscles in the table partly refer to several muscle bundles.

Table 14.21: Arm and shoulder muscles selected for analyses.

Arm/shoulder muscle	Abbreviation 1	Abbreviation 2
RBicepsBrachiiCaput	RBicepsBC	
RCoracobrachialis	RCoracobrachialis	
RDeltoidScapularPart	RDeltoidSP	
RDeltoidClavicularPart	RDeltoidCP	
RInfraspinatus	RInfraspinatus	
RLatissimusDorsi	RLatissimusDorsi	
RElevatorScapulae	RElevatorScapulae	
RPectoralisMajorThoracicPart	RPectoralisMajorTP	
RPectoralisMajorClavicularPart	RPectoralisMajorCP	RPectMajorClav
RPectoralisMinor	RPectoralisMinor	
RRhomboideus	RRhomboideus	
RSerratusAnterior	RSerratusAnterior	
RSternocleidomastoid	RSternocleidomastoid	
RSubscapularis	RSubscapularis	
RSupraspinatus	RSupraspinatus	
RTeresMajor	RTeresMajor	
RTeresMinor	RTeresMinor	
RTrapeziusScapularPart	RTrapeziusSP	RTrapScap
RTrapeziusClavicularPart	RTrapeziusCP	
RBrachialis	RBrachialis	
RTricepsLongHead	RTricepsLH	
RTricepsMedialHead	RTricepsME	
RTricepsLateralHead	RTricepsLA	
RBrachioradialis	RBrachioradialis	
RAnconeus	RAnconeus	
RPronatorTeresHumeralHead	RPronatorTeresHu	
RPronatorTeresUlnarHead	RPronatorTeresUI	
RSupinatorHumeralPart	RSupinatorHu	
RSupinatorUlnarPart	RSupinatorUI	
RPronatorQuadratus	RPronatorQuadr	
RExtensorIndicis	RExtensorIndicis	
RAbductorPollicis	RAbductorPollicis	
RExtensorPollicis	RExtensorPollicis	
RExtensorCarpiRadialis	RExtensorCarpiRa	
RExtensorCarpiUlnaris	RExtensorCarpiUI	
RFlexorCarpi	RFlexorCarpi	
RPalmarisLongus	RPalmarisLongus	
RFlexorDigitorumSuperficialis	RFlexorDigitorumSu	
RFlexorDigitorumProfundus	RFlexorDigitorumPr	
RExtensorDigitorum	RExtensorDigitorum	
RExtensorDigitiMinimi	RExtensorDigitiMinimi	
RFlexorPollicis	RFlexorPollicis	

Table 14.22: Trunk muscles selected for analysis.

Trunk muscles	Abbreviation
RMultifidi	RMultifidi
RErectorSpinae	RErectorSpinae
RPsoasMajor	RPsoasMajor
RQuadratusLumborum	RQuadratusLumb
RObliquusExternus	RObliquusExt
RObliquusInternus	RObliquusInt
RSemispinalis	RSemispinalis
RThoracicMultifidi	RThoracicMultifidi
LMultifidi	LMultifidi
LErectorSpinae	LErectorSpinae
LPsoasMajor	LPsoasMajor
LQuadratusLumborum	LQuadratusLumbo
LObliquusExternus	LObliquusExt
LObliquusInternus	LObliquusInt
LSemispinalis	LSemispinalis
LThoracicMultifidi	LThoracicMultifidi
RectusAbdominis	RectusAbdominis
Spinalis	Spinalis
Transversus	Transversus

14.5.2 Muscle anatomy

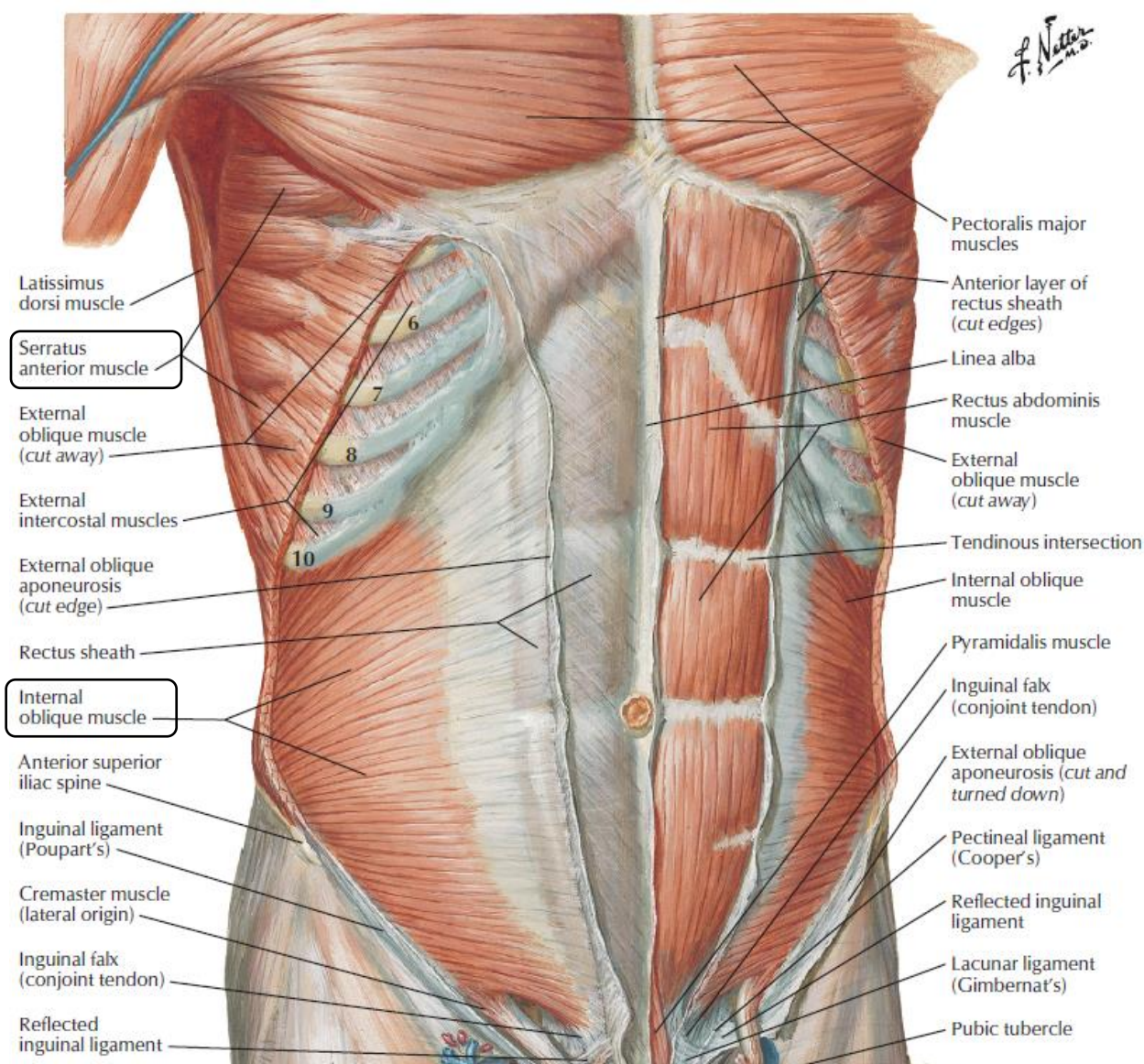


Figure 14.28: Intermediate dissection of anterior abdominal wall. Extracted and modified from Netter (2014, p. 246).

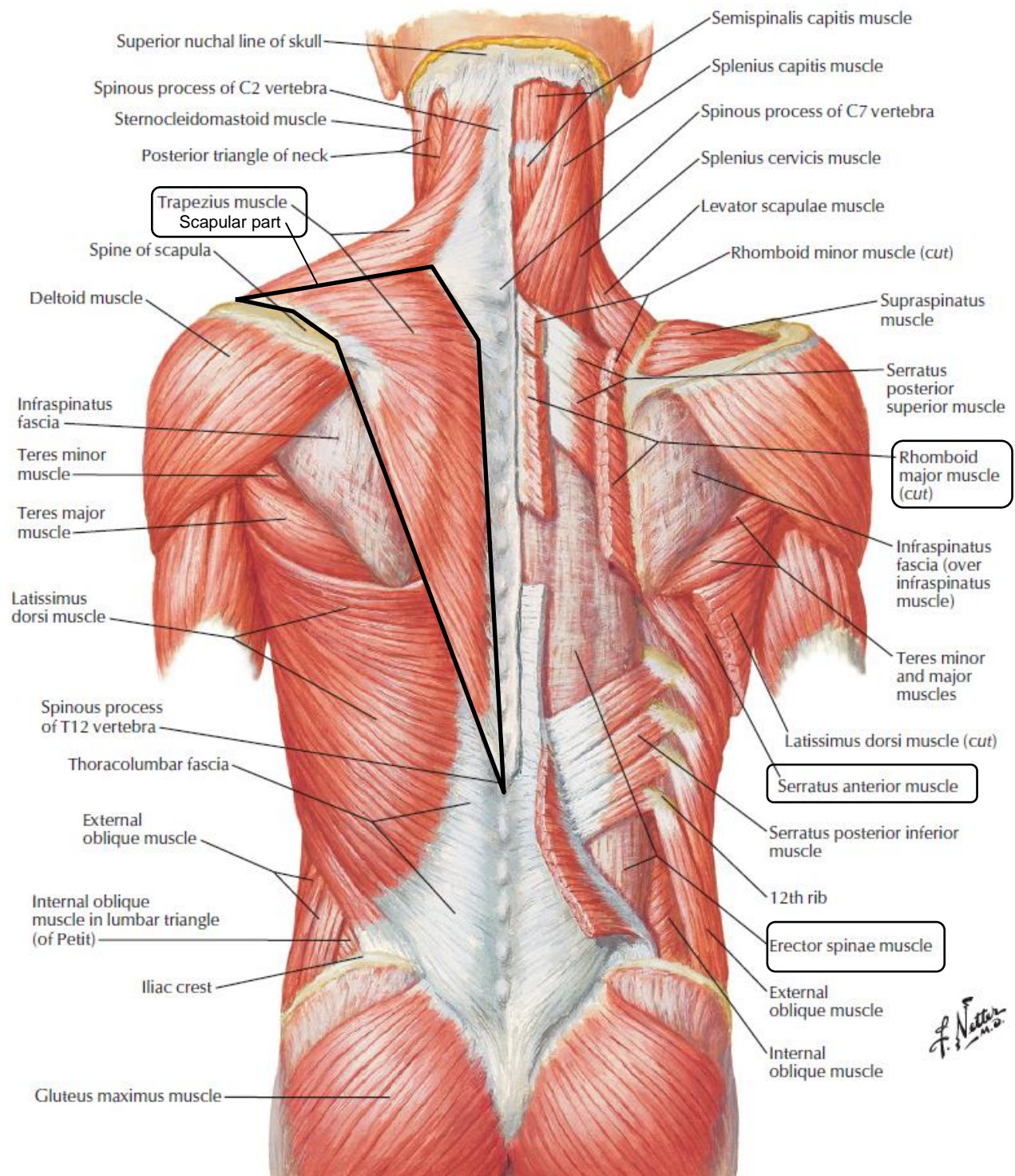


Figure 14.29: Superficial layers of muscles of the back. Extracted and modified from Netter (2014, p. 171).

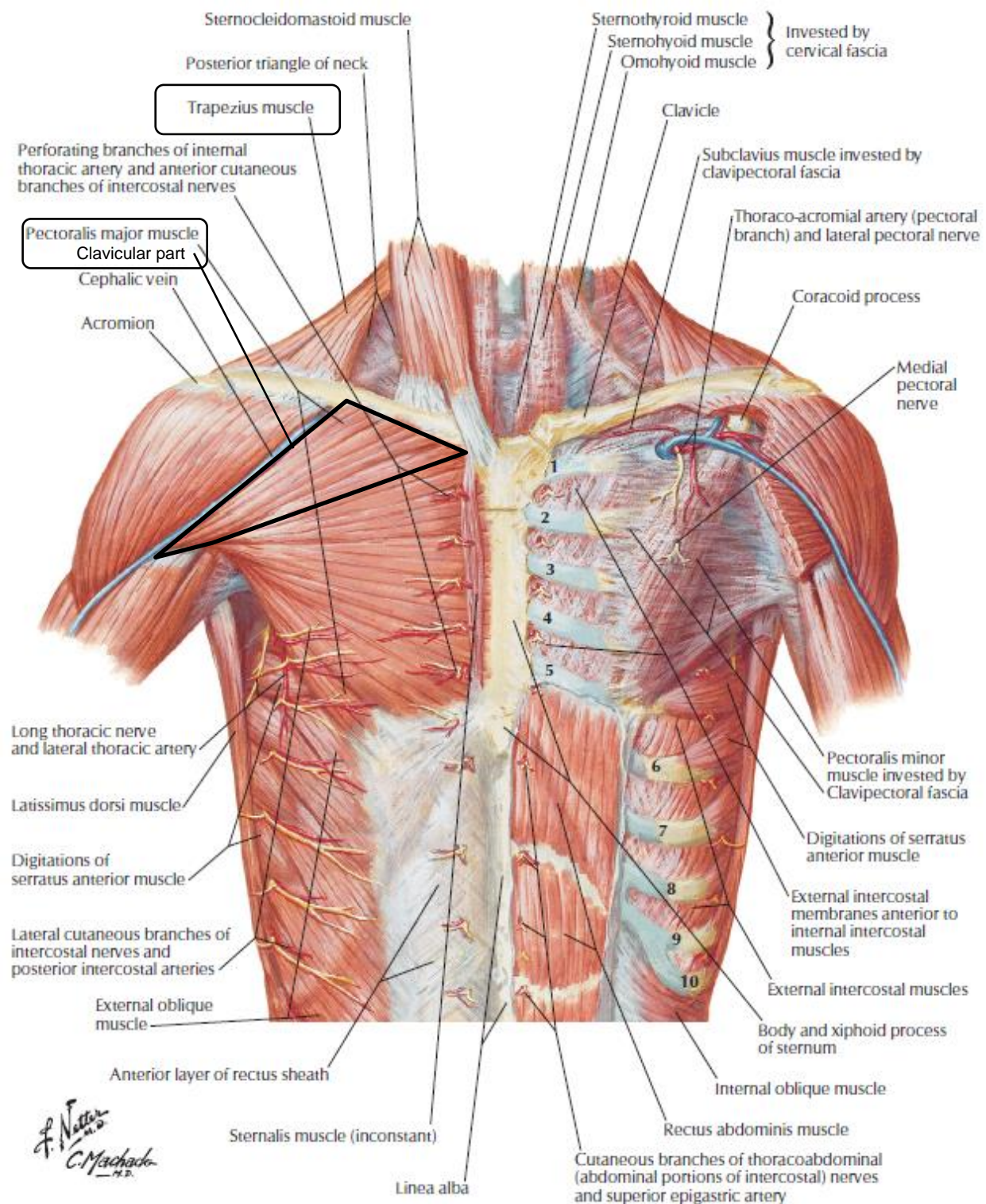


Figure 14.30: Anterior thoracic wall. Extracted and modified from Netter (2014, p. 185).

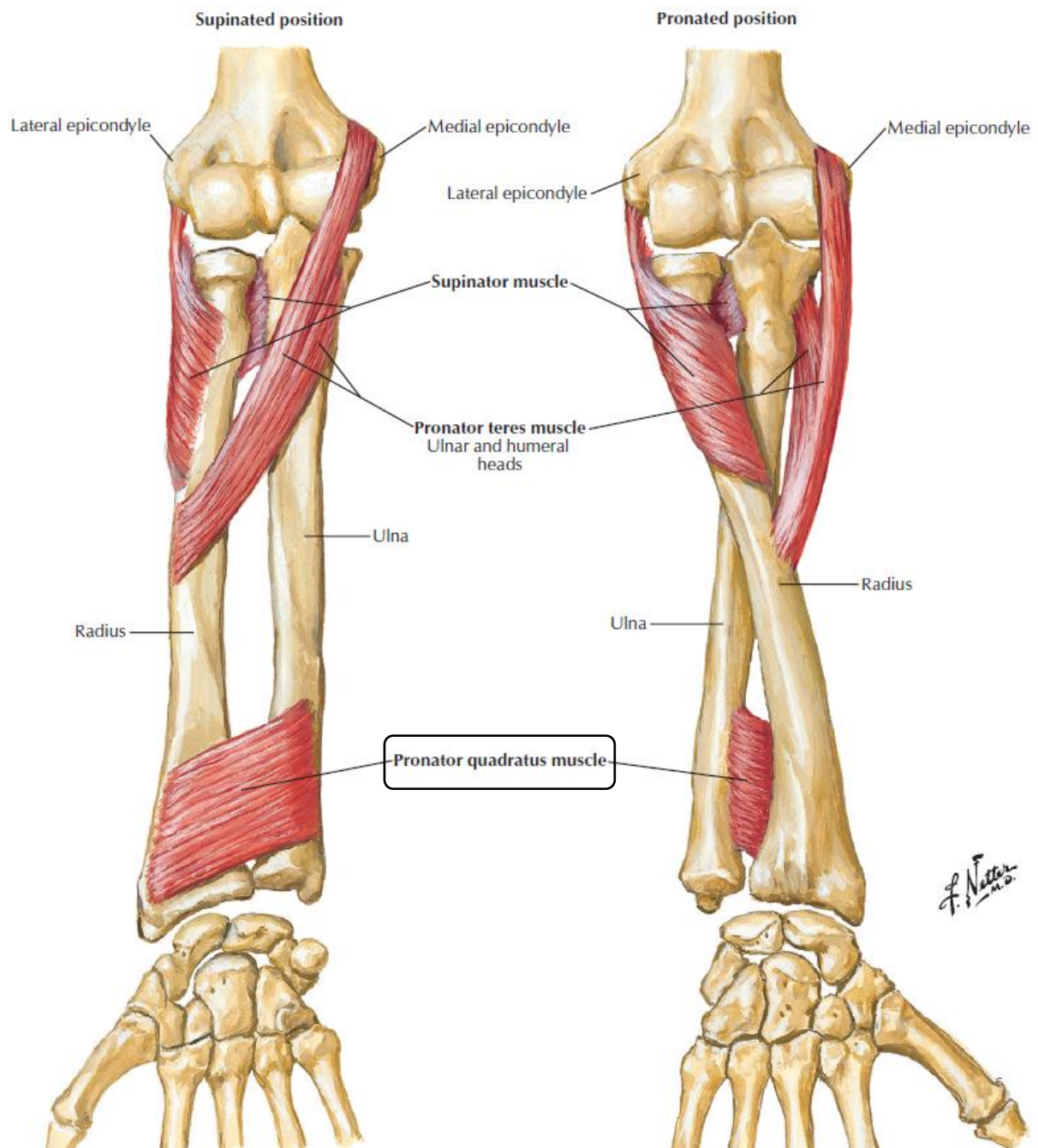


Figure 14.31: Muscles of the forearm: Rotators of the radius. Extracted and modified from Netter (2014, p. 426).

14.5.3 Joint reactions and joint moment measures

In the tables in section 14.5.3, joint reactions and joint moment measures selected for analyses are listed.

Table 14.23: Joint reactions of right shoulder and arm with abbreviations.

Right shoulder and arm joint reaction	Abbreviation 1	Abbreviation 2
RSternoClavicular_InferoSuperiorForce	RSternoClavicular_InSuFo	RStCl_InSuFo
RSternoClavicular_AnteroPosteriorForce	RSternoClavicular_AnPoFo	RStCl_AnPoFo
RSternoClavicular_MedioLateralForce	RSternoClavicular_MeLaFo	RStCl_MeLaFo
RAcromioClavicular_MedioLateralForce	RAcromioClavicular_MeLaFo	RAcCl_MeLaFo
RAcromioClavicular_InferoSuperiorForce	RAcromioClavicular_InSuFo	RAcCl_InSuFo
RAcromioClavicular_AnteroPosteriorForce	RAcromioClavicular_AnPoFo	RAcCl_AnPoFo
RGlenoHumeral_DistractionForce	RGlenoHumeral_DiFo	RGIHu_DiFo
RGlenoHumeral_InferoSuperiorForce	RGlenoHumeral_InSuFo	RGIHu_InSuFo
RGlenoHumeral_AnteroPosteriorForce	RGlenoHumeral_AnPoFo	RGIHu_AnPoFo
RElbowHumeroUlnar_MedioLateralForce	RHumeroUlnar_MeLaFo	RHuUI_MeLaFo
RElbowHumeroUlnar_ProximoDistalForce	RHumeroUlnar_PrDiFo	RHuUI_PrDiFo
RElbowHumeroUlnar_AnteroPosteriorForce	RHumeroUlnar_AnPoFo	RHuUI_AnPoFo
RElbowHumeroUlnar_AxialMoment	RHumeroUlnar_AxMo	RHuUI_AxMo
RElbowHumeroUlnar_LateralMoment	RHumeroUlnar_LaMo	RHuUI_LaMo
RProximalRadioUlnar_RadialForce	RProximalRadioUlnar_RaFo	RPrRaUI_RaFo
RProximalRadioUlnar_DorsoVolarForce	RProximalRadioUlnar_DoVoFo	RPrRaUI_DoVoFo
RRadioHumeral_ProximoDistalForce	RRadioHumeral_PrDiFo	RRaHu_PrDiFo
RDistalRadioUlnar_RadialForce	RDistalRadioUlnar_RaFo	RDiaRaUI_RaFo
RDistalRadioUlnar_DorsoVolarForce	RDistalRadioUlnar_DoVoFo	RDiaRaUI_DoVoFo
RWristRadioCarpal_RadialForce	RWristRadioCarpal_RaFo	RWrRaCa_RaFo
RWristRadioCarpal_ProximoDistalForce	RWristRadioCarpal_PrDiFo	RWrRaCa_PrDiFo
RWristRadioCarpal_DorsoVolarForce	RWristRadioCarpal_DoVoFo	RWrRaCa_DoVoFo
RWristRadioCarpal_AxialMoment	RWristRadioCarpal_AxMo	RWrRaCa_AxMo

Table 14.24: Joint reactions of right shoulder and arm with sign conventions (AnyBody Technology A/S, 2015a). The reactions are calculated in the coordinate system of the 1st node and act from the 1st node on the 2nd node.

Right shoulder and arm joint reaction	Reaction from (1 st node)	Reaction on (2 nd node)	Sign convention
RSternoClavicular_InferoSuperiorForce	Thorax_sc	Clavicula_sc	Superior positive
RSternoClavicular_AnteroPosteriorForce	Thorax_sc	Clavicula_sc	Posterior positive
RSternoClavicular_MedioLateralForce	Thorax_sc	Clavicula_sc	Lateral positive
RAcromioClavicular_MedioLateralForce	Clavicula_ac	Scapula_ac	Lateral positive
RAcromioClavicular_InferoSuperiorForce	Clavicula_ac	Scapula_ac	Superior positive
RAcromioClavicular_AnteroPosteriorForce	Clavicula_ac	Scapula_ac	Posterior positive
RGlenoHumeral_DistractionForce	Scapula_gh	Humerus_gh	Distraction positive
RGlenoHumeral_InferoSuperiorForce	Scapula_gh	Humerus_gh	Superior positive
RGlenoHumeral_AnteroPosteriorForce	Scapula_gh	Humerus_gh	Posterior positive
RElbowHumeroUlnar_MedioLateralForce	HumerusFE	UlnaFE	Medial positive
RElbowHumeroUlnar_ProximoDistalForce	HumerusFE	UlnaFE	Proximal positive
RElbowHumeroUlnar_AnteroPosteriorForce	HumerusFE	UlnaFE	Anterior positive
RElbowHumeroUlnar_AxialMoment	HumerusFE	UlnaFE	Internal positive
RElbowHumeroUlnar_LateralMoment	HumerusFE	UlnaFE	Medial positive
RProximalRadioUlnar_RadialForce	UlnaPs	RadiusPs	Ulnar positive
RProximalRadioUlnar_DorsoVolarForce	UlnaPs	RadiusPs	Dorsal positive
RRadioHumeral_ProximoDistalForce	Radius	Humerus	Distal Positive
RDistalRadioUlnar_RadialForce	UlnaPs	RadiusPs	Ulnar positive
RDistalRadioUlnar_DorsoVolarForce	UlnaPs	RadiusPs	Volar positive
RWristRadioCarpal_RadialForce	Radius	Hand	Ulnar positive
RWristRadioCarpal_ProximoDistalForce	Radius	Hand	Proximal positive
RWristRadioCarpal_DorsoVolarForce	Radius	Hand	Dorsal positive
RWristRadioCarpal_AxialMoment	Radius	Hand	Internal positive

Table 14.25: Joint reactions of the trunk with abbreviations.

Trunk joint reaction	Abbreviation 1	Abbreviation 2
SacrumPelvis_MedioLateralForce	SacrumPelvis_MeLaFo	SaPe_MeLaFo
SacrumPelvis_ProximoDistalForce	SacrumPelvis_PrDiFo	SaPe_PrDiFo
SacrumPelvis_AnteroPosteriorForce	SacrumPelvis_AnPoFo	SaPe_AnPoFo
L5Sacrum_MedioLateralForce	L5Sacrum_MeLaFo	L5Sa_MeLaFo
L5Sacrum_ProximoDistalForce	L5Sacrum_PrDiFo	L5Sa_PrDiFo
L5Sacrum_AnteroPosteriorForce	L5Sacrum_AnPoFo	L5Sa_AnPoFo
L4L5_MedioLateralForce	L4L5_MeLaFo	L4L5_MeLaFo
L4L5_ProximoDistalForce	L4L5_PrDiFo	L4L5_PrDiFo
L4L5_AnteroPosteriorForce	L4L5_AnPoFo	L4L5_AnPoFo
L3L4_MedioLateralForce	L3L4_MeLaFo	L3L4_MeLaFo
L3L4_ProximoDistalForce	L3L4_PrDiFo	L3L4_PrDiFo
L3L4_AnteroPosteriorForce	L3L4_AnPoFo	L3L4_AnPoFo
L2L3_MedioLateralForce	L2L3_MeLaFo	L2L3_MeLaFo
L2L3_ProximoDistalForce	L2L3_PrDiFo	L2L3_PrDiFo
L2L3_AnteroPosteriorForce	L2L3_AnPoFo	L2L3_AnPoFo
L1L2_MedioLateralForce	L1L2_MeLaFo	L1L2_MeLaFo
L1L2_ProximoDistalForce	L1L2_PrDiFo	L1L2_PrDiFo
L1L2_AnteroPosteriorForce	L1L2_AnPoFo	L1L2_AnPoFo
T12L1_MedioLateralForce	T12L1_MeLaFo	T12L1_MeLaFo
T12L1_ProximoDistalForce	T12L1_PrDiFo	T12L1_PrDiFo
T12L1AnteroPosteriorForce	T12L1_AnPoFo	T12L1_AnPoFo
C0C1_MedioLateralForce	C0C1_MeLaFo	C0C1_MeLaFo
C0C1_ProximoDistalForce	C0C1_PrDiFo	C0C1_PrDiFo
C0C1_AnteroPosteriorForce	C0C1_AnPoFo	C0C1_AnPoFo
C0C1_AxialMoment	C0C1_AxMo	C0C1_AxMo
C0C1_LateralMoment	C0C1_LaMo	C0C1_LaMo

Table 14.26: Joint reactions of the trunk with sign conventions (AnyBody Technology A/S, 2015a). The reactions are calculated in the coordinate system of the 1st node and act from the 1st node on the 2nd node.

Trunk joint reaction	Reaction from (1 st node)	Reaction on (2 nd node)	Sign convention
SacrumPelvis_MedioLateralForce	Pelvis	Sacrum	Lateral positive
SacrumPelvis_ProximoDistalForce	Pelvis	Sacrum	Distal (superior) positive
SacrumPelvis_AnteroPosteriorForce	Pelvis	Sacrum	Anterior positive
L5Sacrum_MedioLateralForce	Sacrum	L5	Lateral positive
L5Sacrum_ProximoDistalForce	Sacrum	L5	Distal (superior) positive
L5Sacrum_AnteroPosteriorForce	Sacrum	L5	Anterior positive
L4L5_MedioLateralForce	L5	L4	Lateral positive
L4L5_ProximoDistalForce	L5	L4	Distal (superior) positive
L4L5_AnteroPosteriorForce	L5	L4	Anterior positive
L3L4_MedioLateralForce	L4	L3	Lateral positive
L3L4_ProximoDistalForce	L4	L3	Distal (superior) positive
L3L4_AnteroPosteriorForce	L4	L3	Anterior positive
L2L3_MedioLateralForce	L3	L2	Lateral positive
L2L3_ProximoDistalForce	L3	L2	Distal (superior) positive
L2L3_AnteroPosteriorForce	L3	L2	Anterior positive
L1L2_MedioLateralForce	L2	L1	Lateral positive
L1L2_ProximoDistalForce	L2	L1	Distal (superior) positive
L1L2_AnteroPosteriorForce	L2	L1	Anterior positive
T12L1_MedioLateralForce	L1	T12	Lateral positive
T12L1_ProximoDistalForce	L1	T12	Distal (superior) positive
T12L1_AnteroPosteriorForce	L1	T12	Anterior positive
C0C1_MedioLateralForce	C1	C0	Lateral positive
C0C1_ProximoDistalForce	C1	C0	Distal (superior) positive
C0C1_AnteroPosteriorForce	C1	C0	Anterior positive
C0C1_AxialMoment	C1	C0	Left positive
C0C1_LateralMoment	C1	C0	Right positive

Table 14.27: Joint moment measures of the right shoulder and arm with abbreviations.
Positive direction is indicated by the name.

Right shoulder and arm joint moment measure	Abbreviation 1	Abbreviation 2
RGlenoHumeral_AbductionMoment	RGlenoHumeral_AbMo	RGIHu_AbMo
RGlenoHumeral_FlexionMoment	RGlenoHumeral_FIMo	RGIHu_FIMo
RGlenoHumeral_ExternalRotationMoment	RGlenoHumeral_ExRoMo	RGIHu_ExRoMo
RElbow_FlexionMoment	RElbow_FIMo	RElbow_FIMo
RElbow_PronationMoment	RElbow_PrMo	RElbow_PrMo
RWrist_FlexionMoment	RWrist_FIMo	RWrist_FIMo
RWrist_AbductionMoment	RWrist_AbMo	RWrist_AbMo

Table 14.28: Joint moment measures of the trunk with abbreviations.

Trunk joint moment measure	Abbreviation 1	Abbreviation 2
SacrumPelvis_FlexionExtensionMoment	SacrumPelvis_FIMo	SaPe_FIMo
SacrumPelvis_AxialMoment	SacrumPelvis_AxMo	SaPe_AxMo
SacrumPelvis_LateralMoment	SacrumPelvis_LaMo	SaPe_LaMo
C0C1_FlexionExtensionMoment	C0C1_FleMo	C0C1_FIMo

Table 14.29: Joint moment measures of the trunk with sign convention.

Trunk joint moment measure	Sign convention
SacrumPelvis_FlexionExtensionMoment	Extension positive
SacrumPelvis_AxialMoment	Rotation to the left (counter clockwise) positive
SacrumPelvis_LateralMoment	Lateral flexion to the right positive
C0C1_FlexionExtensionMoment	Extension positive

14.5.4 Joint angles

Table 14.30: Joint angles selected for analyses are listed. For most of the joint angles the name indicates the positive direction. Otherwise the positive direction is specified in brackets.

Joint angles	Abbreviation 1	Abbreviation 2
RGlenohumeral_Flexion	RGlenohumeral_Fl	RGIHu_Fl
RGlenohumeral_ExternalRotation	RGlenohumeral_ExRo	RGIHu_ExRo
RGlenohumeral_Abduction	RGlenohumeral_Ab	RGIHu_Ab
RElbow_Flexion	RElbow_Fl	RElbow_Fl
RElbow_Pronation	RElbow_Pro	RElbow_Pro
RWrist_Flexion	RWrist_Fl	RWrist_Fl
RWrist_Abduction	RWrist_Ab	RWrist_Ab
RSternoClavicular_Protraction	RSternoClavicular_Pr	RStCl_Pr
RSternoClavicular_Elevation	RSternoClavicular_El	RStCl_El
RSternoClavicular_AxialRotation (+upwards rotation of anterior part)	RSternoClavicular_AxRo	RStCl_AxRo
Pelvis_RotationX* (+ left, "lateral tilting/flexion")	Pelvis_RotX	Pe_RotX
Pelvis_RotationY* (+ backward, "extension")	Pelvis_RotY	Pe_RotY
Pelvis_RotationZ* (+ axial rotation to the left, counter clockwise)	Pelvis_RotZ	Pe_RotZ
PelvisThorax_Extension	PelvisThorax_Ex	PeTh_Ex
PelvisThorax_LateralBending (+ to the right)	PelvisThorax_La_Be	PeTh_La_Be
PelvisThorax_Rotation (+ axial rotation to the left, counter clockwise)	PelvisThorax_Ro	PeTh_Ro

* For pelvis rotation, there is an influence of the order of rotation as the pelvis location and rotation define the location and orientation of the manikin within its environment. The pelvis is rotated first about z, then about y, then about x axis. So, the orientation of the x rotation in the vehicle coordinate system depends on how the pelvis was rotated about z and y before. The directions in the table each refer to the case, when both other rotations are 0 degrees. (Jung, M., 2015)

14.5.5 Correlations with $p \leq 0.06$

Table 14.31: Overview of selected power and energy consumption values.

Handbrake Location	Percentile	Discomfort	Pmet_Trunk_S	Pmet_LLeg_F ²	Pmet_RArm_S	Pmet_RArm_E
1	5F	29.14	0.33	5.11	1.67	114.11
1	50F	30.15	0.13	1.35	1.31	119.21
1	50M	31.23	0.47	1.46	3.29	111.47
1	95M	32.32	0.88	0.34	6.32	102.56
2	5F	72.39	1.03	60.01	8.45	101.72
2	50F	69.01	0.78	0.37	3.60	98.30
2	50M	65.42	0.80	1.36	10.50	84.19
2	95M	61.78	1.24	1.17	5.60	107.58
3	5F	44.43	0.31	2.15	2.05	112.40
3	50F	44.85	0.16	0.34	1.43	97.33
3	50M	45.31	0.44	0.64	4.21	106.51
3	95M	45.77	0.95	0.87	4.45	78.88
4	5F	48.09	0.69	27.14	2.40	136.52
4	50F	38.71	1.15	2.65	3.62	122.30
4	50M	28.74	0.75	1.42	5.10	123.99
4	95M	18.61	0.52	1.14	7.07	109.20
5	5F	41.68	1.22	2.62	5.28	131.84
5	50F	51.78	1.15	1.22	2.86	83.78
5	50M	62.53	1.20	0.52	4.20	106.74
5	95M	73.44	2.99	30.21	12.28	79.52
7	5F	49.24	0.55	2.05	2.54	119.84
7	50F	49.06	0.80	3.93	4.02	101.98
7	50M	48.88	0.43	0.91	3.71	103.31
7	95M	48.69	0.13	10.93	1.15	73.30
8	5F	32.54	0.30	2.53	1.63	112.96
8	50F	32.07	0.81	1.88	4.48	96.15
8	50M	31.56	0.50	1.42	2.82	106.96
8	95M	31.05	0.59	6.25	5.20	95.81

14.6 Discomfort modeling

14.6.1 Stepwise regression

Table 14.32: Stepwise regression results: Overview of coefficients and p-values of predictors for discomfort ($\alpha_{\text{enter}} = 0.1$, $\alpha_{\text{remove}} = 0.1$). S, r^2 , r^2_{adj} of resulting equations.

Step	1	2	3	4	5	6	7	8	9
Constant	84.56	72.15	44.93	37.45	38.01	28.8	29	33.13	34.31
RHuUI_AxMo_E	4.2	3.61	3.75	4.24	4.27	3.81	3.43	3.7	3.67
p-value	< 0.001	< 0.001	< 0.001	< 0.001	< 0.001	< 0.001	< 0.001	< 0.001	< 0.001
RAcCI_InSuFo_E²		0.00031	0.00021	0.00024	0.00022	0.00018	0.00016	0.00018	0.00016
p-value		< 0.001	0.003	0.001	< 0.001	0.002	0.002	< 0.001	0.001
RWrist_AbMo_E			8.8	12.9	11.6	12.1	10.3	10.5	10.2
p-value			0.008	0.001	0.001	< 0.001	< 0.001	< 0.001	< 0.001
RGIHu_ExRo_E²				-0.036	-0.039	-0.037	-0.0324	-0.0343	-0.0471
p-value				0.026	0.01	0.006	0.005	0.002	< 0.001
RStCI_EI_E²					0.094	0.14	0.14	0.137	0.15
p-value					0.014	0.001	< 0.001	< 0.001	< 0.001
MeMAAct_RPect MajorClav_F²						20593	29635	31890	33944
p-value						0.015	0.001	< 0.001	< 0.001
MaMAAct_RTrap Scap_F²							14344	15570	15445
p-value							0.007	0.003	0.002
Pmet_RArm_S								-0.67	-0.87
P-value								0.061	0.016
Pmet_LLleg_F²									0.175
p-value									0.063
S	10.3	7.51	6.59	6.03	5.36	4.75	4.03	3.76	3.50
r^2	52.3	75.62	82	85.57	89.09	91.83	94.38	95.35	96.18
r^2_{adj}	50.47	73.67	79.75	83.06	86.6	89.5	92.42	93.39	94.27

Residual Plots for Discomfort

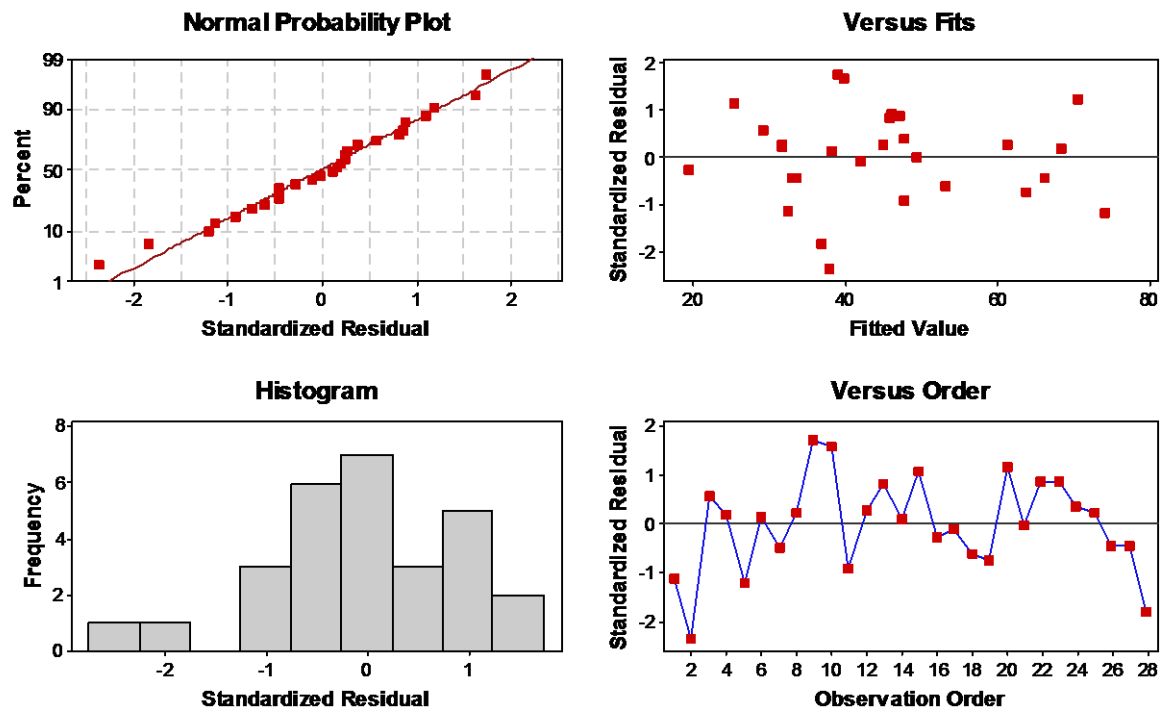


Figure 14.32: Residual Plot for prediction equation (9.1).

14.6.2 Discomfort index

Table 14.33: Discomfort ratings, indices and their delta.

Handbrake location	Percentile	Discomfort rating	Discomfort index	Delta (index-rating)
1	5F	29.141	32.587	3.446
1	50F	30.153	37.891	7.738
1	50M	31.23	29.311	-1.919
1	95M	32.324	31.691	-0.633
2	5F	72.386	74.154	1.768
2	50F	69.011	68.66	-0.351
2	50M	65.42	66.444	1.024
2	95M	61.775	61.481	-0.294
3	5F	44.429	39.006	-5.423
3	50F	44.854	39.83	-5.024
3	50M	45.306	47.917	2.611
3	95M	45.765	44.974	-0.791
4	5F	48.085	45.945	-2.14
4	50F	38.71	38.318	-0.392
4	50M	28.735	25.354	-3.381
4	95M	18.61	19.407	0.797
5	5F	41.682	41.981	0.299
5	50F	51.782	53.247	1.465
5	50M	62.528	63.799	1.271
5	95M	73.436	70.832	-2.604
7	5F	49.239	49.305	0.066
7	50F	49.064	47.226	-1.838
7	50M	48.878	46.155	-2.723
7	95M	48.689	47.656	-1.033
8	5F	32.541	31.785	-0.756
8	50F	32.066	33.532	1.466
8	50M	31.561	33.033	1.472
8	95M	31.048	36.926	5.878

15 REFERENCES

References

- Akerblom, B. (1948). *Standing and sitting posture. With special reference to the construction of chairs* (Dissertation). Stockholm, Sweden: Nordiska bokhandeln.
- Alexander, T. & Conradi, J. (2001). *Analysis of anthropometry and range validity of the Digital Human Model RAMSIS*. Digital Human Modeling for Design and Engineering Conference and Exposition, Arlington, Virginia, USA, June, 26-28, 2001. SAE Technical Paper Series No. 2001-01-2104. Warrendale, Pennsylvania, USA: Society of Automotive Engineers.
- Ambike, S. & Schmiedeler, J. P. (2013). The leading joint hypothesis for spatial reaching arm motions. *Experimental brain research*, 224(4), 591–603.
- Andreoni, G., Rabuffetti, M. & Pedotti, A. (1999). *A methodological approach for the analysis of the car driver's posture*. Digital Human Modeling for Design and Engineering, International Conference and Exposition, The Hague, The Netherlands, May, 18-20, 1999. SAE Technical Paper Series No. 1999-01-1927. Warrendale, Pennsylvania, USA: Society of Automotive Engineers.
- Annegarn, J. (2006). *Scaling in human simulation models. The development of an isometric strength scaling method which needs easy accessible data only* (Master Thesis). Maastricht, the Netherlands: Maastricht University.
- Annett, J. (2002). Subjective rating scales: science or art? *Ergonomics*, 45(14), 966–987.
- AnyBody Technology A/S. (2014). *AnyScript Community: AnyScript Support Wiki*. Retrieved March, 23, 2014 from <http://wiki.anyscript.org/>.
- AnyBody Technology A/S. (2015a). *AnyBody (Source Code)*. Aalborg, Denmark: AnyBody Technology A/S.
- AnyBody Technology A/S. (2015b). *AnyBody Technology Company Website*. Retrieved February 23, 2015 from <http://www.anybodytech.com/>.
- Arjmand, N. & Shirazi-Adl, A. (2006). Sensitivity of kinematics-based model predictions to optimization criteria in static lifting tasks. *Medical Engineering & Physics*, 28(6), 504–514.
- Atkinson, R. C. & Shiffrin, R. M. (1968). Human Memory: A proposed system and its control processes. In K. W. Spence & J. T. Spence (Eds.), *Psychology of Learning and Motivation: Vol. 2. The Psychology of Learning and Motivation* (pp. 89–195). New York, New York, USA: Academic Press.
- Augsburg, K., Heimann, S. & Fetter, R. (2004). *Handbremsen DNA*. Ilmenau, Germany: Technische Universität Ilmenau, Fachgebiet für Kraftfahrzeugtechnik.
- Backhaus, K., Erichson, B., Plinke, W. & Weiber, R. (2006). *Multivariate Analysemethoden: Eine anwendungsorientierte Einführung* (11., überarbeitete Auflage). Berlin, Germany: Springer.
- Badler, N. I., Phillips, C. B. & Webber, B. L. (1993). *Virtual humans and simulated agents*. New York, New York, USA: Oxford University Press.
- Barre, A. & Armand, S. (2014). Biomechanical ToolKit: Open-source framework to visualize and process biomechanical data. *Computer Methods and Programs in Biomedicine*, 114(1), 80–87.

- Bassett, D. R. (2002). Scientific contributions of A. V. Hill: exercise physiology pioneer. *Journal of Applied Physiology*, 93(5), 1567–1582.
- Bergmann, G., Graichen, F., Bender, A., Kääb, M., Rohlmann, A. & Westerhoff, P. (2007). In vivo glenohumeral contact forces - Measurements in the first patient 7 months postoperatively. *Journal of Biomechanics*, 40(10), 2139–2149.
- Bernstein, N. A. (1967). *The co-ordination and regulation of movements*. Oxford, New York, New York, USA: Pergamon Press.
- Bhise, V. D. (2012). *Ergonomics in the automotive design process*. Boca Raton, Florida, USA: CRC Press.
- Bonin, D., Wischniewski, S., Paul, G., Wirsching, H.-J., Upmann, A. & Rausch, J. (2014). *Exchanging data between Digital Human Modeling systems - A review of data formats*. 3rd International Digital Human Modeling Symposium. Tokyo, Japan.
- Borot, C., Cabane, C. & Marca, C. (2014). *Prediction of the driver posture and muscular activity*. 5th International Symposium of Human Modeling and Simulation in Automotive Engineering. Munich, Germany.
- Bortz, J. (1999). *Statistik: Für Sozialwissenschaftler* (5. vollständig überarbeitete Auflage). Berlin, Germany: Springer.
- Boston, J. R., Rudy, T. E., Mercer, S. R. & Kubinski, J. A. (1993). A measure of body movement coordination during repetitive dynamic lifting. *IEEE Transactions on Rehabilitation Engineering*, 1(3), 137–144.
- Braune, C. W. (1877). *An atlas of topographical anatomy; After plane sections of frozen bodies: Translated by Edward Bellamy*. Philadelphia, Pennsylvania, USA: Lindsay and Blakiston.
- Braune, W. & Fischer, O. (1988). *Determination of the moments of inertia of the human body and its limbs*. Berlin, Deutschland: Springer.
- Brüggemann, G. P. (2005). *Grundlagen der Biomechanik des muskulo-skelettalen Systems: Material zur Vorlesung* (4., verb. Aufl.). Cologne, Germany: Sport und Buch Strauß GmbH.
- Bubb, H. (2004). Ergonomie und Sitzgestaltung. In H.-J. Wilke (Ed.), *Ergomechanics. Interdisziplinärer Kongress Wirbelsäulenforschung*. Aachen, Deutschland: Shaker.
- Bubb, H. (2007). Ergonomie und Design. In H. H. Braess & U. Seiffert (Eds.), *Automobildesign und Technik. Formgebung, Funktionalität, Technik* (1st ed., pp. 240–263). Wiesbaden, Germany: Vieweg.
- Bubb, H. (2013). Entwicklung digitaler Menschmodell am Beispiel RAMSIS. In S. Wischniewsky & L. Adolph (Eds.), *Digitale Ergonomie – Trends und Strategien für den Einsatz digitaler Menschmodelle. Tagungsdokumentation Symposium vom 20. November 2012 in Dortmund*. Dortmund, Germany: Bundesanstalt für Arbeitsschutz und Arbeitsmedizin.
- Bubb, H. & Fritzsche, F. (2009). A scientific perspective of Digital Human Models: Past, present and future. In V. G. Duffy (Ed.), *Handbook of Digital Human Modeling. Research for Applied Ergonomics and Human Factors Engineering* (p.3-1–3-30). Boca Raton, Florida, USA: CRC Press.
- Bühner, M. (2004). *Einführung in die Test- und Fragebogenkonstruktion. ps psychologie*. München, Germany: Pearson Studium.
- Bulle, J., Dominioni, G. C., Wang, X. & Compigne (2013). *Comparing RAMSIS driving posture predictions with experimental observations for defining optimum task constraints*. 2nd International Digital Human Modeling Symposium. Ann Arbor, Michigan, USA.

- Burgess-Limerick, R., Abernethy, B. & Neal, R. J. (1993). Relative phase quantifies interjoint coordination. *Journal of Biomechanics*, 26(1), 91–94.
- Byun, S. N. (1991). *A computer simulation using a multivariate biomechanical posture prediction model for manual materials handling tasks* (Dissertation). Ann Arbor, Michigan, USA: University of Michigan.
- Caldwell, L. S., Chaffin, D. B., Dukes-Dobos, F. N., Kroemer, K. H., Laubach, L. L., Snook, S. H. & Wasserman, D. E. (1974). A proposed standard procedure for static muscle strength testing. *American Industrial Hygiene Association journal*, 35(4), 201–206.
- Case, K., Porter, J. M. & Bonney, M. C. (1990). SAMMIE: A man and workplace modelling system. In W. Karwowski, A. M. Genaidy & S. S. Asfour (Eds.), *Computer-aided ergonomics* (pp. 31–56). London, UK: Taylor & Francis.
- Cavanaugh, J. T., Shinberg, M., Ray, L., Shipp, K. M., Kuchibhatla, M. & Schenkman, M. (1999). Kinematic characterization of standing reach: comparison of younger vs. older subjects. *Clinical Biomechanics*, 14(4), 271–279.
- Chaffee, J. (1969). *Methods for determining driver reach capability*. International Automotive Engineering Congress and Exposition, Detroit, Michigan, USA, January, 13, 1969. SAE Technical Paper Series No. 690105. Warrendale, Pennsylvania, USA: Society of Automotive Engineers.
- Chaffin, D. B. (2001). *Digital Human Modeling for vehicle and workplace design*. Warrendale, Pennsylvania, USA: Society of Automotive Engineers.
- Chaffin, D. B., Andersson, G. & Martin, B. J. (1999a). *Occupational biomechanics* (3rd edition). New York, New York, USA: John Wiley and Sons.
- Chaffin, D. B., Faraway, J. & Zhang, X. (1999b). *Simulating Reach Motions* (SAE Technical Paper Series No. 1999-01-1916). Warrendale, Pennsylvania, USA: Society of Automotive Engineers.
- Chaffin, D. B., Faraway, J. J., Zhang, X. & Woolley, C. (2000). Stature, Age, and Gender Effects on Reach Motion Postures. *Human Factors*, 42(3), 408–420.
- Chateauroux, E. & Wang, X. (2008). Effects of Age, Gender, and Target Location on Seated Reach Capacity and Posture. *Human Factors*, 50(2), 211–226.
- Chateauroux, E. & Wang, X. (2012). Comparison between static maximal force and handbrake pulling force. *Work*, 41(Suppl. 1), 1305–1310.
- Chevalot, N. & Wang, X. (2004). *An experimental investigation of the discomfort of arm reaching movements in a seated position*. Digital Human Modeling for Design and Engineering Symposium, Rochester, Michigan, USA, June, 15–17, 2004. SAE Technical Paper Series No. 2004-01-2141. Warrendale, Pennsylvania, USA: Society of Automotive Engineers.
- Choudry, M. U., Beach, T. A., Callaghan, J. P. & Kulic, D. (2013). A stochastic framework for movement strategy identification and analysis. *IEEE Transactions on Human-Machine Systems*, 43(3), 314–327.
- Congleton, J. J. (1983). *Design and evaluation of a neutral posture chair* (Dissertation). Lubbock, Texas, USA: Texas Tech University.
- Corlett, E. N. & Bishop, R. P. (1976). A technique for assessing postural discomfort. *Ergonomics*, 19(2), 175–182.
- Costich-Sicker, T., Sheehy, P., Samuel, P., Navarro, D., Ziemer, T., Silvers, R., ... (2002). *The black belt memory jogger: A pocket guide for six sigma success* (1st edition). Salem, New Hampshire, USA: Goal/QPC and Six Sigma Academy.

- Crowninshield, R. D. & Brand, R. A. (1981). A physiologically based criterion of muscle force prediction in locomotion. *Journal of Biomechanics*, 14(11), 793–801.
- Cruse, H., Wischmeyer, E., Brüwer, M., Brockfeld, P. & Dress, A. (1990). On the cost functions for the control of the human arm movement. *Biological Cybernetics*, 62(6), 519–528.
- Damon, A., Stoudt, H. W. & McFarland, R. A. (1966). *The human body in equipment design*. Cambridge, UK: Harvard University Press.
- Damsgaard, M., Rasmussen, J., Christensen, S. T., Surma, E. & Zee, M. de. (2006). Analysis of musculoskeletal systems in the AnyBody Modeling System. *Simulation Modelling Practice and Theory*, 14(8), 1100–1111.
- De Leonardis, D. M., Ferguson, S. A. & Pantula, J. F. (1998). *Survey of driver seating positions in relation to the steering wheel*. International Congress and Exposition Detroit, Michigan, USA, February, 23-26, 1998. SAE Technical Paper Series No. 980642. Warrendale, Pennsylvania, USA: Society of Automotive Engineers.
- De Looze, M. P., Kuijt-Evers, L. F. M. & van Dieën, J. (2003). Sitting comfort and discomfort and the relationships with objective measures. *Ergonomics*, 46(10), 985–997.
- De Luca, C. J. (1997). The use of surface electromyography in biomechanics. *Journal of Applied Biomechanics* 13(2), 135–163.
- Delleman, N. J. (1999). *Working postures: prediction and evaluation* (Dissertation). Amstelveen, The Netherlands: Vrije Universiteit Amsterdam.
- Delleman, N. J. & Hin, A. J. S. (2000). *Postural behaviour in static gazing upwards and downwards*. Digital Human Modeling for Design and Engineering Conference and Exposition Dearborn, Michigan, USA, June, 6-8, 2000. SAE Technical Paper Series No. 2000-01-2173. Warrendale, Pennsylvania, USA: Society of Automotive Engineers.
- Delleman, N. J., Hin, A. J. S. & Tan, K. T. (2003). *Postural behavior in static reaching sideways*. Digital Human Modeling for Design and Engineering Conference and Exposition, Montreal, Canada, June, 16-19, 2003. SAE Technical Paper Series No. 2003-01-2230. Warrendale, Pennsylvania, USA: Society of Automotive Engineers.
- Delleman, N. J., Huysmans, M. A. & Kuijt-Evers, L. F. M. (2001). *Postural behaviour in static gazing sideways*. Digital Human Modeling for Design and Engineering Conference and Exposition Arlington, Virginia, USA, June, 26-28, 2001. SAE Technical Paper Series No. 2001-01-2093. Warrendale, Pennsylvania, USA: Society of Automotive Engineers.
- Desmurget, M., Grea, H. & Prablanc, C. (1998). Final posture of the upper limb depends on the initial position of the hand during prehension movements. *Experimental Brain Research*, 119(4), 511–516.
- Dickerson, C. R., Martin, B. J. & Chaffin, D. B. (2006). The relationship between shoulder moments and the perception of muscular effort in loaded reaches. *Ergonomics*, 49(11), 1036–1051.
- DIN 33411-4 (1987). Berlin, Deutschland: Beuth Verlag GmbH.
- Divivier, A. & Wirsching (2015). Phone conversation on RAMSIS Car Driver Model. January, 15, 2015.
- Doriot, N. & Wang, X. (2006). Effects of age and gender on maximum voluntary range of motion of the upper body joints. *Ergonomics*, 49(3), 269–281.
- Dounskaia, N. (2010). Control of human limb movements: the leading joint hypothesis and its practical applications. *Exercise and Sport Sciences Reviews*, 38(4), 201–208.

- Dounskaia, N. & Wang, W. (2014). A preferred pattern of joint coordination during arm movements with redundant degrees of freedom. *Journal of Neurophysiology*, 112(5), 1040–1053.
- Duffy, V. G. (Ed.). (2009). *Handbook of Digital Human Modeling: Research for applied ergonomics and human factors engineering*. Boca Raton, Florida, USA: CRC Press.
- Dufour, F. & Wang, X. (2005). *Discomfort assessment of car ingress/egress motions using the concept of neutral movement*. Digital Human Modeling for Design and Engineering Symposium Iowa City, Iowa, USA, June, 14-16, 2005. SAE Technical Paper Series No. 2005-01-2706. Warrendale, Pennsylvania, USA: Society of Automotive Engineers.
- Dysart, M. J. & Woldstad, J. C. (1996). Posture prediction for static sagittal-plane lifting. *Journal of Biomechanics*, 29(10), 1393–1397.
- ECE 13 – H. Status of United Nations Regulation, Uniform provisions concerning the approval of passenger cars with regard to braking. February, 13, 2014. United Nations.
- ECE 13 –11 Suppl. 11. Status of United Nations Regulation, Uniform provisions concerning the approval of vehicles of categories M, N and O with regard to braking. October, 17, 2014. United Nations.
- Ehrlenspiel, K., Kiewert, A. & Lindemann, U. (1998). *Kostengünstig entwickeln und konstruieren: Kostenmanagement bei der integrierten Produktentwicklung* (2. Auflage). VDI. Berlin, Heidelberg, Germany: Springer.
- Evershed, D. G. (1970). *A computer model of man for workspace assessment* (Dissertation). Nottingham, UK: University of Nottingham.
- Farahani, S. D. (2014). *Human posture and movement prediction based on musculoskeletal modeling* (Dissertation). Aalborg, Denmark: Aalborg University.
- Faraway & Julian J. (2003). *Data-based motion prediction*. Digital Human Modeling for Design and Engineering Conference and Exposition, Montreal, Canada, June, 16-19, 2003. SAE Technical Paper Series No. 2003-01-2229. Warrendale, Pennsylvania, USA: Society of Automotive Engineers.
- Fetter, R., Heimann, S. & Augsburg, K. (2005). Konzeption und Konstruktion eines Ergonomie-Prüfstandes zur Variation der Handbremshebel-Orientierung. In P. Scharff (Ed.), 50. *Internationales wissenschaftliches Kolloquium, September, 19-23, 2005*. Ilmenau, Germany: Isle.
- Fischer, M. H., Rosenbaum, D. A. & Vaughan, J. (1997). Speed and sequential effects in reaching. *Journal of Experimental Psychology: Human Perception and Performance*, 23(2), 404–428.
- FMVSS 105. Federal Motor Vehicle Safety Standard - Hydraulic and electric brake systems. January, 6, 2012. U.S. Department of Transportation.
- FMVSS 135. Federal Motor Safety Standard - Light vehicle brake systems. January, 6, 2012. U.S. Department of Transportation.
- Fröhmel, C. (2010). *Validierung des RAMSIS-Krafthaltungsmodells* (Dissertation). Munich, Germany: Technische Universität München.
- Geuß, H. (1995). Entwicklung eines anthropometrischen Meßverfahrens für das CAD-Menschmodell RAMSIS. In H. Geuß, R. Krist & A. Seidl (Eds.), Forschungsvereinigung Automobiltechnik E.V. (FAT) (FAT): Vol. 123. *RAMSIS - Ein System zur Erhebung und Vermessung dreidimensionaler Körperhaltungen von Menschen zur ergonomischen Auslegung von Bedien- und Sitzplätzen im Auto*. Frankfurt, Germany: Forschungsvereinigung Automobiltechnik E.V. (FAT).

- Geuss, H. (1998). *Optimizing the product design process by Computer Aided Ergonomics*. Digital Human Modeling for Design and Engineering Conference and Exposition Dayton, Ohio, USA, April, 28-29, 1998. SAE Technical Paper Series No. 981310. Warrendale, Pennsylvania, USA: Society of Automotive Engineers.
- Geuß, H., Krist, R. & Seidl, A. (1995). *FORSCHUNGSVEREINIGUNG AUTOMOBILTECHNIK E.V. (FAT): Vol. 123. RAMSIS - Ein System zur Erhebung und Vermessung dreidimensionaler Körperhaltungen von Menschen zur ergonomischen Auslegung von Bedien- und Sitzplätzen im Auto*. Frankfurt, Deutschland: Forschungsvereinigung Automobiltechnik E.V. (FAT).
- Gielen, C., van Bolhuis, B. M. & Theeuwen, M. (1995). On the control of biologically and kinematically redundant manipulators. *Human Movement Science*, 14(4-5), 487–509.
- Gielen, C., Vrijenoek, E., Flash, T. & Neggers, S. F. W. (1997). Arm position constraints during pointing and reaching in 3-D space. *Journal of Neurophysiology*, 78(2), 660–673.
- Gielen, S. (2009). Review of models for the generation of multi-joint movements in 3-D. *Advances in Experimental Medicine and Biology*, (629), 523–550.
- Gielen, S., van Bolhuis, B. & Vrijenoek, E. (1998). On the number of degrees of freedom in biological limbs. In M. L. Latash (Ed.), *Progress in Motor Control - Bernstein's Tradition in Movement*. Champaign, Illinois, USA: Human Kinetics.
- Gkikas, N. (Ed.) (2013). *Automotive ergonomics: Driver-vehicle interaction*. Boca Raton, Florida, USA: CRC Press.
- Godil, A. & Ressler, S. (2009). Shape and size analysis and standards. In V. G. Duffy (Ed.), *Handbook of Digital Human Modeling. Research for applied ergonomics and human factors engineering* (pp. 14-1–14-15). Boca Raton, Florida, USA: CRC Press.
- Grandjean, E. (1988). *Fitting the task to the man: A textbook of occupational ergonomics* (4th ed). London, UK: Taylor & Francis.
- Grehn, J. & Krause, J. (2006). *Metzler Physik* (3. Auflage). Stuttgart, Germany: Metzler.
- Grosser, M. (1987). *Die sportliche Bewegung: Anatomische und biomechanische Grundlagen* (BLV Sportwissen: Vol. 415). Munich, Germany: BLV.
- Gunzelmann, G., Gaughan, C., Huiskamp, W., Van den Bosch, K., Alexander, T., de Jong, S., Bruzzone, A. G. & Tremori, A. (2014). *In search of interoperability standards for human behavior representations*. Interservice/Industry Training, Simulation, and Education Conference (IIITSEC), November, 24, to December, 4, 2014. Paper No. 14216 .
- Gutfleisch, R. (2008). *Leitfaden Clusteranalyse – Teil 2*. Retrieved June, 2, 2015 from http://www.staedtestatistik.de/fileadmin/vdst/ag-methodik/Leitfaeden/2008_AGMethodik_LeitfadenClusteranalyse_Teil2.pdf.
- Gyr, M. (2011). *Isometrische Maximalkraftstudie und Validierung einer Datenskalierung in einer Mehrkörpersimulationssoftware. Adduktion und Abduktion im Schultergelenk* (Bachelorarbeit). Jülich, Germany: Fachhochschule Aachen,
- Hamfeld, H., Hansen, G., Trieb, R. & Seidl, A. (1999). *RAMSIS/SCAN --A new approach to 3D-body scanning for automated anthropometric measuring and individual product design*. Digital Human Modeling for Design and Engineering International Conference and Exposition The Hague, The Netherlands May, 18-20, 1999. SAE Technical Paper Series No. 1999-01-1890. Warrendale, Pennsylvania, USA: Society of Automotive Engineers.

- Hamill, J., Knutzen, K. M. & Derrick, T. R. (2015). *Biomechanical basis of human movement* (fourth edition). Philadelphia, Pennsylvania, USA, Baltimore, Maryland, USA: Lippincott Williams & Wilkins, a Wolters Kluwer business.
- Hanson, L., Sperling, L. & Akselsson, R. (2006). Preferred car driving posture using 3-D information. *International Journal of Vehicle Design*, 42(1/2), 154.
- Hartung, J. (2006). *Objektivierung des statischen Sitzkomforts auf Fahrzeugsitzen durch die Kontaktkräfte zwischen Mensch und Sitz* (Dissertation). Munich, Germany: Technische Universität München.
- Haywood, K. M., Williams, K. & VanSant, A. (1991). Qualitative assessment of the backswing in older adult throwing. *Research Quarterly for Exercise and Sport*, 62(3), 340–343.
- He, J., Xia, C., Chen, S. & Cui, G. (2008). *Evaluation and optimization of driver posture*. Digital Human Modeling for Design and Engineering Conference and Exhibition Pittsburgh, Pennsylvania, USA, June, 17-19, 2008. SAE Technical Paper Series No. 2008-01-1865. Warrendale, Pennsylvania, USA: Society of Automotive Engineers.
- Heidinger, F. (1990). Ergonomische Sitzgestaltung zur Praevention sitzhaltungsbedingter Wirbelsaeulenschaedigungen. *Arbeitsmedizin Sozialmedizin Praeventivmedizin*, 25(3), 123–126.
- Heinrich, K., Upmann, A., Rausch, J., Lietmeyer, J., Rzepka, P., Fischbein, I. & Brüggemann, G.-P. (2014). *Projektbericht: Analyse und Beurteilung der Handbremsbetätigung*. Cologne, Germany.
- Helander, M. G. & Zhang, L. (1997). Field studies of comfort and discomfort in sitting. *Ergonomics*, 40(9), 895–915.
- Heller, O. (1985). Hörfeldaudiometrie mit dem Verfahren der Kategorienunterteilung (KU). *Psychologische Beiträge*, 27(4), 478–493.
- Hepp, K., Haslewanter, T., Straumann, D., Hepp-Reymond, M.-C. & Henn, V. (2012). The control of arm-, gaze-, and head-movements by Listings's law. In R. Caminiti, P. B. Johnson & Y. Burnod (Eds.), *Control of arm movement in space. Neurophysiological and computational approaches* (Experimental Brain Research Series Vol. 22.). Berlin, Germany: Springer.
- Houglum, P. A., Bertoti, D. & Brunnstrom, S. (2012). *Brunnstrom's clinical kinesiology* (6th edition). Philadelphia, Pennsylvania, USA: F.A. Davis.
- Hsiao, H. & Keyserling, W. M. (1991). Evaluating posture behavior during seated tasks. *International Journal of Industrial Ergonomics*, 8(4), 313–334.
- Human Solutions GmbH (2014a). *RAMSIS NextGen BodyBuilder User Guide*. Kaiserslautern, Germany: Human Solutions GmbH.
- Human Solutions GmbH (2014b). *RAMSIS NextGen Ergonomics User Guide*. Kaiserslautern, Germany: Human Solutions GmbH.
- Human Solutions GmbH (2014c). *RAMSIS NextGen Framework User Guide*. Kaiserslautern, Germany: Human Solutions GmbH.
- Human Solutions GmbH (2014d). *Human Solutions bringt RAMSIS NextGen auf den Markt: Gute Ergonomie ist gleichbedeutend mit Komfort und Sicherheit*. Kaiserslautern, Deutschland. Retrieved March, 10, 2015 from http://www.human-solutions.com/group/upload/Pressemitteilungen/Deutsch/08_14_RAMSIS_NextGen.pdf.
- Human Solutions GmbH (2015). *Human Solutions: Products mobility website*. Retrieved March, 10, 2015 from <http://www.human-solutions.com/>.

- Huston, R. L. (2009). *Principles of biomechanics* (Mechanical engineering: Vol. 213). Boca Raton, Florida, USA: CRC Press.
- Huxley, A. (1980). *Reflections on muscle* (Sherrington lectures: Vol. 14). Liverpool, UK: Liverpool University Press.
- Jonsson, B. (2011). Hand position on steering wheel during driving. *Traffic Injury Prevention*, 12(2), 187–190.
- Jonsson, B., Stenlund, H., Svensson, M. Y. & Björnstig, U. (2008). Seat adjustment-capacity and repeatability among occupants in a modern car. *Ergonomics*, 51(2), 232–241.
- Jung, E. S. & Choe, J. (1996). Human reach posture prediction based on psychophysical discomfort. *International Journal of Industrial Ergonomics*, 18(2-3), 173–179.
- Jung, E. S., Choe, J. & Kim, S. H. (1994). Psychophysical cost function of joint movement for arm reach posture prediction. *Proceedings of the Human Factors and Ergonomics Society Annual Meeting*, 38(10), 636–640.
- Jung, M. (2015). Telephone conversation about AMS details. December, 16, 2016.
- Jung, M., Damsgaard, M., Andersen, M.S. & Rasmussen, J. (2013). *Integrating biomechanical manikins into a CAD environment*. 2nd International Digital Human Modeling Symposium. Ann Arbor, Michigan, USA .
- Kaminski, T. R., Bock, C. & Gentile, A. M. (1995). The coordination between trunk and arm motion during pointing movements. *Experimental Brain Research*, 106(3), 457–466.
- Karhu, O., Kansi, P. & Kuorinka, I. (1977). Correcting working postures in industry: A practical method for analysis. *Applied Ergonomics*, 8(4), 199–201.
- Karst, G. M. & Hasan, Z. Direction-dependent strategy for control of multi-joint arm movement. In J. M. Winters & s L. Y. Woo (Eds.), *Multiple muscle systems: Biomechanics and movement organization* (pp. 268-281). New York, USA: Springer.
- Kee, D. (2002). A method for analytically generating three-dimensional isocomfort workspace based on perceived discomfort. *Applied Ergonomics*, 33(1), 51–62.
- Kee, D. & Karwowski, W. (2001a). LUBA: an assessment technique for postural loading on the upper body based on joint motion discomfort and maximum holding time. *Applied Ergonomics*, 32(4), 357–366.
- Kee, D. & Karwowski, W. (2001b). The boundaries for joint angles of isocomfort for sitting and standing males based on perceived comfort of static joint postures. *Ergonomics*, 44(6), 614–648.
- Kee, D. & Lee, I. (2012). Relationships between subjective and objective measures in assessing postural stresses. *Applied Ergonomics*, 43(2), 277–282.
- Kennedy, K. W. (1964). *Reach capability of the USAF population.: Phase I. The outer boundaries of grasping reach envelopes for the shirt-sleeved, seated operator* (AMRL-TR64-59). Wright Patterson Air Force Base, Ohio, USA: Aerospace Medical Research Laboratories.
- Kim, S. H. & Lee, K. (2009). Development of discomfort evaluation method for car ingress motion. *International Journal of Automotive Technology*, 10(5), 619–627.
- Kim, K. H., Martin, B. J., Dukic, T. & Hanson, L. (2006). *The role of visual and manual demand in movement and posture organization*. Digital Human Modeling for Design and Engineering Conference; Lyon, France, July, 04 - 06, 2006. SAE Technical Paper Series No. 2006-01-2331. Warrendale, Pennsylvania, USA: Society of Automotive Engineers.

- Kladroba, A. & Stenke, G. (2013). *FuE-Datenreport 2013 Analysen und Vergleiche: Wissenschaftsstatistik*. Essen, Germany: Wissenschaftsstatistik GmbH.
- Koch, J. (2013). *Eine isometrische Maximalkraftstudie der oberen Extremitäten zur Validierung einer alters- und geschlechtsspezifischen Stärkeskalierung in der Mehrkörpersimulationssoftware AnyBody* (Masterarbeit). Cologne, Germany: Deutsche Sporthochschule Köln.
- Koh, T. J., Grabiner, M. D. & De Swart, Robert J. (1992). In vivo tracking of the human patella. *Journal of Biomechanics*, 25(6), 637–643.
- Kolich, M. (2008). A conceptual framework proposed to formalize the scientific investigation of automobile seat comfort. *Applied Ergonomics*, 39(1), 15–27.
- Kolling, J. (1997). *Validierung und Weiterentwicklung eines CAD-Menschmodells für die Fahrzeuggestaltung* (Dissertation). Munich, Germany: Technische Universität München.
- Komi, P. V. (1990). Relevance of in vivo force measurements to human biomechanics. *Journal of Biomechanics*, 23 (Suppl. 1), 23–34.
- Korein, J. U. (1984) *A geometric investigation of reach* (Dissertation). Philadelphia, Pennsylvania, USA: University of Pennsylvania.
- Krist, R. (1993). *Modellierung des Sitzkomforts. Eine experimentelle Studie* (Dissertation). Eichstätt, Germany: Katholische Universität Eichstätt.
- Kroemer, K. H. E., Kroemer, H. J. & Kroemer-Elbert, K. E. (2010). *Engineering physiology: Bases of human factors engineering/ergonomics* (Fourth edition). Heidelberg, Germany: Springer.
- Kuijt-Evers, L. F. M., Groenesteijn, L., de Looze, M. P. & Vink, P. (2004). Identifying factors of comfort in using hand tools. *Applied Ergonomics*, 35(5), 453–458.
- Kulwicki, P. V., Schlei, E. J. & Vergamini, P. L. (1962). *Weightless man: Self-rotation techniques* (AMRL-TDR, 62-129). Wright-Patterson Air Force Base, Ohio, USA: Aerospace Medical Research Laboratories.
- Kyung, G. (2008). *An integrated human factors approach to design and evaluation of the driver workspace and interface: Driver Perceptions, Behaviours, and Objective Metrics* (Dissertation). Blacksburg, Virginia, USA: Virginia Polytechnic Institute and State University.
- Kyung, G. & Nussbaum, M. A. (2009). Specifying comfortable driving postures for ergonomic design and evaluation of the driver workspace using Digital Human Models. *Ergonomics*, 52(8), 939–953.
- Kyung, G., Nussbaum, M. A. & Babski-Reeves, K. L. (2010). Enhancing digital driver models: identification of distinct postural strategies used by drivers. *Ergonomics*, 53(3), 375–384.
- Laubach, L. L. (1978). Human muscular strength. In Webb Associates (Ed.), *Anthropometric source book* (Volume 1: Anthropometry for designers, NASA Ref. 1024). Houston, Texas, USA: NASA Scientific and Technical Information Office.
- Laursen, B., Jensen, B. R., Németh, G. & Sjøgaard, G. (1998). A model predicting individual shoulder muscle forces based on relationship between electromyographic and 3D external forces in static position. *Journal of Biomechanics*, 31(8), 731–739.
- Lawton, M. P. (1990). Aging and performance of home tasks. *Human Factors*, 32(5), 527–536.
- Lee, K. S. & Ferraiuolo, P. (1993). *Seat comfort*. SAE International Congress and Exposition; Detroit, Michigan, USA, March, 01, 1993. SAE Technical Paper Series No. 930105. Warrendale, Pennsylvania, USA: Society of Automotive Engineers.

- Lee, K. S. & Jung, M. C. (2015). Investigation of hand postures in manufacturing industries according to hand and object properties. *International Journal of Industrial Ergonomics*, 46, 98–104.
- Lestrelin, D. & Trasbot, J. (2005). *The REAL MAN project: Objectives, results and possible follow-up*. Digital Human Modeling for Design and Engineering Symposium Iowa City, Iowa June 14-16, 2005. SAE Technical Paper Series No. 2005-01-2682. Warrendale, Pennsylvania, USA: Society of Automotive Engineers.
- Li, Z. (2014). *The synergy of human arm and robotic system* (Dissertation). Santa Cruz, California, USA: University of California.
- Lietmeyer, J. (2013). *Determinanten von Diskomfort bei Betätigung der Feststellbremse im Pkw* (Masterarbeit). Cologne, Germany: Deutsche Sporthochschule Köln.
- Loczi, J., Dietz, M. & Nielson, G. *Validation and application of the 3-D CAD manikin RAMSIS in automotive design*. International Congress and Exposition, Detroit, Michigan, USA, March, 1-4, 1999. SAE Technical Paper Series No. 1999-01-1270. Warrendale, Pennsylvania, USA: Society of Automotive Engineers.
- Macey, S. & Wardle, G. (2009). *H-Point: The fundamentals of car design & packaging* (1st edition). Pasadena, Culver City California, USA: Art Center College of Design and Design Studio Press.
- Majid, N. A. b. A. (2011). *Musculoskeletal analysis of driving fatigue: The influence of seat condition* (Master Thesis). Ikuta, Japan: Meiji University.
- Mark, L. S., Nemeth, K., Gardner, D., Dainoff, M. J., Paasche, J., Duffy, M. & Grandt, K. (1997). Postural dynamics and the preferred critical boundary for visually guided reaching. *Journal of Experimental Psychology: Human Perception and Performance*, 23(5), 1365–1379.
- Marler, T., Arora, J., Beck, S., Lu, J., Mathai, A., Patrick, A. & Swan, C. (2009). Computational approaches in Digital Human Modeling. In V. G. Duffy (Ed.), *Handbook of Digital Human Modeling. Research for applied ergonomics and human factors engineering* (pp.10-1–10-33). Boca Raton, Florida, USA: CRC Press.
- Marshall, R. N., Wood, G. A. & Jennings, L. S. (1986). Performance criteria in normal human locomotion. *Journal of Biomechanics*, 19(6), 487.
- Maslow, A. H. (1943). A theory of human motivation. *Psychological Review*, 50(4), 370–396.
- Maslow, A. H. (1978). *Motivation und Persönlichkeit* (2. erweiterte Auflage). Olten, Swiss: Walter-Verlag.
- McAtamney, L. & Corlett, N. E. (1993). RULA: a survey method for the investigation of work-related upper limb disorders. *Applied Ergonomics*, 24(2), 91–99.
- Mense, S. (2010). Functional anatomy of muscle: Muscle, nociceptors and afferent fibers. In S. Mense & R. D. Gerwin (Eds.), *Muscle Pain: Understanding the Mechanisms* (pp. 17–48). Berlin, Germany: Springer.
- Mergl, C. (2006). *Entwicklung eines Verfahrens zur Optimierung des Sitzkomforts auf Automobilsitzen* (Dissertation). München, Deutschland: Technische Universität München.
- Mergl, C., Klendauer, M., Mangen, C. & Bubb, H. (2005). *Predicting long-term riding comfort in cars by contact forces between human and seat*. Digital Human Modeling for Design and Engineering Symposium Iowa City, Iowa June 14-16, 2005. SAE Technical Paper Series No. 2005-01-2690. Warrendale, Pennsylvania, USA: Society of Automotive Engineers.

- Miller, D. I. & Nelson, R. C. (1973). *Biomechanics of sport: A research approach [by] Doris I. Miller [and] Richard C. Nelson* (Health education, physical education, and recreation series). Philadelphia, USA: Lea & Febiger.
- Minitab (2015). *Minitab 15 Software including Help Menu*: Minitab, Inc.
- Moes, N. C. (2005). Analysis of sitting discomfort, a review. In P. D. Bust & P. T. McCabe (Eds.), *Contemporary Ergonomics 2005* (pp. 200–204). London, UK: Taylor & Francis.
- Mohamad, D., Deros, B. M., Wahab, D. A., Daruis, D. D. I. & Ismail, A. R. (2010). Integration of comfort into a drivers car seat design using image analysis. *American Journal of Applied Sciences*, 7(7), 937–942.
- Monnier, G., Renard, F., Chameroy, A., Wang, X. & Trasbot, J. (2006). *A motion simulation approach integrated into a design engineering process: Digital Human Modeling for Design and Engineering Conference, Lyon, France, July, 4-6, 2006*. SAE Technical Paper Series No. 2006-01-2359. Warrendale, Pennsylvania, USA: Society of Automotive Engineers.
- Monnier, G., Wang, X. & Trasbot, J. (2009). A motion simulation tool for automotive interior design. In V. G. Duffy (Ed.), *Handbook of Digital Human Modeling. Research for applied ergonomics and human factors engineering* (pp. 31-1–31-14). Boca Raton, Florida, USA: CRC Press.
- Montgomery, D. C. (2013). *Design and analysis of experiments* (eighth edition). Hoboken, New Jersey, USA: Wiley.
- Mossey, M. E., Xi, Y., McConomy, S. K., Brooks, J. O., Rosopa, P. J. & Venhovens, P. J. (2014). Evaluation of four steering wheels to determine driver hand placement in a static environment. *Applied Ergonomics*, 45(4), 1187–1195.
- Naddeo, A., Cappetti, N., Vallone, M. & Califano, R. (2014). New trend line of research about comfort evaluation: proposal of a framework for weighing and evaluating contributes coming from cognitive, postural and physiologic comfort perceptions. In P. Vink (Ed.), *Proceedings of the 5th International Conference on Applied Human Factors and Ergonomics AHFE 2014*, Krakow, Poland, July, 19-23, 2014.
- Naumann & Rötting. (2007). Digital Human Modeling for design and evaluation of human-machine systems. *MMI-Interaktiv*, 12 (April 2007).
- Nelson, W. L. (1983). Physical principles for economies of skilled movements. *Biological Cybernetics*, 46(2), 135–147.
- Netter, F. H. (2014). *Atlas of human anatomy* (Sixth edition). Philadelphia, Pennsylvania, USA: Saunders Elsevier.
- Nigg, B. M. & Herzog, W. (Eds.) (1999). *Biomechanics of the Musculo-skeletal system* (second edition). Chichester, UK: John Wiley & Sons LTD.
- Nilsson, G. *Validity of comfort assessment in RAMSIS*. Digital Human Modeling for Design and Engineering International Conference and Exposition The Hague, The Netherlands, May, 18-20, 1999. SAE Technical Paper Series No. 1999-01-1900. Warrendale, Pennsylvania, USA: Society of Automotive Engineers.
- OICA. (2016). *Sales of new vehicles 2005-2015*. Retrieved April, 10, 2016 from <http://www.oica.net/category/sales-statistics/>.
- OpenStax College. (2015). *Types of Body Movements*. Retrieved June, 30, 2015 from <http://cnx.org/contents/a829ec63-2bac-4a7c-aaf4-87a10e71c27f@3/Types-of-Body-Movements>.

- Pannetier, R. & Wang, X. (2014). A comparison of clutching movements of freely adjusted and imposed pedal configurations for identifying discomfort assessment criteria. *Applied Ergonomics*, 45(4), 1010–1018.
- Papas, M. (2015). *Wrist and hand*. Retrieved June, 30, 2015 from <http://www.revolutionarytennis.com/Resources/wristandhandterm.jpeg>.
- Park, J., Jung, K., Chang, J., Kwon, J. & You, H. (2011). Evaluation of driving posture prediction in digital human simulation using RAMSIS. *Proceedings of the Human Factors and Ergonomics Society Annual Meeting*, 55(1), 1711–1715.
- Park, K. S. (1973). *Computerized simulation model of posture during manual material handling* (Dissertation). Ann Arbor, Michigan, USA: University of Michigan.
- Park, S. J., Kim, C.-B., Kim, C. J. & Lee, J. W. (2000). Comfortable driving postures for Koreans. *International Journal of Industrial Ergonomics*, 26(4), 489–497.
- Parkin, S., Mackay, G. M. & Cooper, A. (1995). How drivers sit in cars. *Accident Analysis and Prevention*, 27(6), 777–783.
- Parkinson, M. B., Chaffin, D. B. & Reed, M. P. (2006). Center of pressure excursion capability in performance of seated lateral-reaching tasks. *Clinical Biomechanics*, 21(1), 26–32.
- Paul, G. & Lee, W. C. (2011). *Interfacing Jack and AnyBody: Towards anthropometric musculoskeletal Digital Human Modeling*. 1st International Symposium on Digital Human Modeling. Lyon, France.
- Platzer, W., Fritsch, H., Kühnel, W., Kahle, W. & Frotscher, M. (2003). *Taschenatlas Anatomie: In 3 Bänden. (1 Bewegungsapparat, 8. korrigierte und ergänzte Auflage)*. Stuttgart, Germany: Thieme.
- Pope, R. (2015). *Spinal anatomy: movements*. Retrieved June, 30, 2015 from http://www.spinesurgeon.com.au/Neurological_Conditions/images/movements.jpg.
- Raiber, P. (2015). *Simulation of the handbrake application in RAMSIS NextGen. Body Posture Prediction for Different Handbrake Locations and Customer Groups* (Master Thesis). Cologne, Germany: German Sport University Cologne.
- Rasmussen, J., Dahlquist, J., Damsgaard, M., Zee, M. de & Christensen, S. T. (2003). *Musculoskeletal modeling as an ergonomic design method*. International Ergonomics Association XVth Triennial Conference. Seoul, Korea.
- Rasmussen, J., Damsgaard, M. & Voigt, M. (2001). Muscle recruitment by the min/max criterion — a comparative numerical study. *Journal of Biomechanics*, 34(3), 409–415.
- Rasmussen, J., Zee, M. de, Damsgaard, M., Christensen, S. T., Marek, C. & Siebertz, K. (2005). *A general method for scaling musculo-skeletal models*. International Symposium on Computer Simulation in Biomechanics. Cleveland, Ohio, USA.
- Rausch, J. R., Siebertz, K., Christensen, S. T. & Rasmussen, J. (2006). Simulation des menschlichen Bewegungsapparates zur Innenraumgestaltung von Fahrzeugen. *VDI Bericht*, 1967(2), 1027–1048.
- Rausch, J. R. (2005). *Optimierung der Fahrzeuginnenraumgestaltung durch Bewertung der Muskelkräfte mit Hilfe eines biomechanischen Modells* (Diplomarbeit). Aachen, Germany: Fachhochschule Aachen.
- Rausch, J. R. (2010). *AnyBody AR-gateway review presentation*. Aachen, Germany: Ford.
- Rausch, J. R. (2015a). *Biomechanical model to analyze comfort prediction*. 10th International Conference Innovative Seating. Berlin, Germany.
- Rausch, J. R. (2015b). Phone conversation about AnyBody Details. April, 23, 2015.

- Rausch, J. R., Popovic, N. & Upmann, A. (2014). *AnyBody Handbrake IR Gateway Review*. Aachen, Germany: Ford.
- Rausch, J. R. & Upmann, A. (2015a). *AnyFord Interface: Manual V4.4*. Cologne, Aachen, Germany: Ford.
- Rausch, J. R. & Upmann, A. (2015b). *Technical report: Handbrake study*. Aachen, Cologne, Germany: Ford.
- Reddy, B. D. (2016). Functional analysis, boundary value problems and Finite Elements. In J. Schröder & P. Wriggers (Eds.), *Advanced finite element technologies*. (pp. 1-15). Vol. 556 [S.L.]: Springer (CISM International Centre for Mechanical Sciences).
- Redelmeier, D. A. & Kahneman, D. (1996). Patients' memories of painful medical treatments: real-time and retrospective evaluations of two minimally invasive procedures. *Pain*, 66(1), 3–8.
- Reed, M. P., Manary, M. A., Flannagan, C. A. C. & Schneider, L. W. (2000). Effects of vehicle interior geometry and anthropometric variables on automobile driving posture. *Human Factors: The Journal of the Human Factors and Ergonomics Society*, 42(4), 541–552.
- Reed, M. P., Manary, M. A., Flannagan, C. A. C. & Schneider, L. W. (2002). A statistical method for predicting automobile driving posture. *Human Factors: The Journal of the Human Factors and Ergonomics Society*, 44(4), 557–568.
- Reed, M. P., Manary, M. A., Flannagan, C. A. C. & Schneider, L. W. (2000). *Comparison of methods for predicting automobile driver posture*. Digital Human Modeling for Design and Engineering Conference and Exposition, Dearborn, Michigan, June, 6-8, 2000. SAE Technical Paper Series No. 2000-01-2180. Warrendale, Pennsylvania, USA: Society of Automotive Engineers.
- Reed, M. P., Parkinson, M. B. & Chaffin, D. B. (2003a). *A new approach to modeling driver reach* (SAE Technical Paper Series No. 2003-01-0587). Warrendale, Pennsylvania, USA: Society of Automotive Engineers.
- Reed, M. P., Parkinson, M. B. & Klinkenberger, A. L. (2003b). *Assessing the validity of kinematically generated reach envelopes for simulations of vehicle operators*. Digital Human Modeling for Design and Engineering Conference and Exposition, Montreal, Canada, June 16-19, 2003. SAE Technical Paper Series No. 2003-01-2216. Warrendale, Pennsylvania, USA: Society of Automotive Engineers.
- Reed, M. P., Parkinson, M. B. & Wagner, D. W. (2004). *Torso kinematics in seated reaches* (SAE Technical Paper Series No. 2004-01-2176). Warrendale, Pennsylvania, USA: Society of Automotive Engineers.
- Reif, K. (Ed.). (2014). *Fundamentals of automotive and engine technology*. Wiesbaden, Germany: Springer Fachmedien.
- Richards, L. G. (1980). On the psychology of passenger comfort. In D. J. Osborne & J. A. Levis (Eds.), *Human factors in transport research*. London, UK: Academic Press.
- Rim, Y. H., Moon, J. H., Kim, G. Y. & Noh, S. D. (2008). Ergonomic and biomechanical analysis of automotive general assembly using XML and Digital Human Models. *International Journal of Automotive Technology*, 9(6), 719–728.
- Romain, P. & Xuguang, W. (2012). Development of objective discomfort evaluation indicators for a task-oriented motion using less constrained motion concept: application to automotive pedal clutching task. *Work*, 41(Suppl 1), 1461–1465.

- Römer, A., Pache, M., Weißhahn, G., Lindemann, U. & Hacker, W. (2001). Effort-saving product representations in design—results of a questionnaire survey. *Design Studies*, 22(6), 473–491.
- Rosenbaum, D. A., Loukopoulos, L. D., Meulenbroek, R. G. J., Vaughan, J. & Engelbrecht, S. E. (1995). Planning reaches by evaluating stored postures. *Psychological Review*, 102(1), 28–67.
- Rumsey, D. (2008). *Wenn es mehr als die Grundlagen sein sollen*. Weiterführende Statistik (1. Auflage). Weinheim, Germany: Wiley-VCH.
- Ryan, P. W. (1972). *Cockpit geometry evaluation* (Joint Army-Navy Aircraft Instrumentation Research Report 700201). Seattle, Washington, USA: The Boeing Company.
- Rzepka, P. (2015). *Identifizierung und Klassifizierung von Bewegungsstrategien zur Betätigung einer Handbremse* (Masterarbeit). Cologne, Germany: Deutsche Sporthochschule Köln.
- SAE J287 (2007). *Driver hand control reach* (Surface Vehicle Recommended Practice No. J287 REV. FEB2007). Warrendale, Pennsylvania, USA: Society of Automotive Engineers.
- SAE J826 (2008). *Devices for use in defining and measuring vehicle seating accommodation* (Surface Vehicle Standard No. J826 REV. NOV2008). Warrendale, Pennsylvania, USA: Society of Automotive Engineers.
- SAE J1100 (2009). *Motor vehicle dimensions* (Surface Vehicle Recommended Practice No. J1100 REV. NOV2009). Warrendale, Pennsylvania, USA: Society of Automotive Engineers.
- Sanctis, T. de, Tarantino, V., Straulino, E., Begliomini, C. & Castiello, U. (2013). Co-registering kinematics and evoked related potentials during visually guided reach-to-grasp movements. *PloS one*, 8(6), e65508, 1-10.
- Saziorski, W. M., Aruin, A. S. & Selujanow, W. N. (1984). *Biomechanik des menschlichen Bewegungsapparates* (Übersetzung aus dem Russischen von Günter Friedrich, fachliche Bearbeitung der deutschsprachigen Fassung von Jürgen Sperlich). Berlin, Germany: Sportverlag.
- Schaefer, P., Rudolph, H. & Schwarz, W. (2000). *Digital man models physical strength - a new approach in strength simulation*. Digital Human Modeling for Design and Engineering Conference and Exposition, Dearborn, Michigan, June, 6-8, 2000. SAE Technical Paper Series No. 2000-01-2168. Warrendale, Pennsylvania, USA: Society of Automotive Engineers.
- Schmidt, S., Amereller, M., Franz, M., Kaiser, R. & Schwirtz, A. (2014). A literature review on optimum and preferred joint angles in automotive sitting posture. *Applied Ergonomics*, 45(2), 247–260.
- Schmidtke, H. (Ed.) (1993). *Handbuch der Ergonomie* (3. neubearbeitete und erweiterte Auflage). München, Germany: Carl Hanser.
- Schünke, M. (2000). *Funktionelle Anatomie - Topographie und Funktion des Bewegungssystems*. Stuttgart, Germany: Thieme.
- Schwarz, W. (1997). *3D-Video-Lastungsanalyse: Ein neuer Ansatz zur Kraft- und Haltungsanalyse* (Dissertation, VDI Fortschrittberichte VDI Reihe 17, Nr. 166). Düsseldorf, Germany: VDI.
- Seidl, A. (1997) *RAMSIS - A new CAD-tool for ergonomic analysis of vehicles developed for the German automotive industry* (Automotive Concurrent/Simultaneous

- Engineering SP-1233, SAE Technical Paper Series No. 970088). Warrendale, Pennsylvania, USA: Society of Automotive Engineers.
- Seidl, A. (1995). Das Menschmodell RAMSIS - Analyse, Synthese und Simulation dreidimensionaler Körperhaltungen des Menschen. In H. Geuß, R. Krist & A. Seidl (Eds.), *FORSCHUNGSVEREINIGUNG AUTOMOBILTECHNIK E.V. (FAT): Vol. 123. RAMSIS - Ein System zur Erhebung und Vermessung dreidimensionaler Körperhaltungen von Menschen zur ergonomischen Auslegung von Bedien- und Sitzplätzen im Auto*. Frankfurt, Germany: Forschungsvereinigung Automobiltechnik E.V. (FAT).
- Seitz, T. (2003). *Videobasierte Messung menschlicher Bewegungen konform zum Menschmodell RAMSIS* (Dissertation). München, Germany: Technische Universität München.
- Seitz, T., Recluta, D., Zimmermann, D. & Wirsching, H.-J (2005). *FOCOPP - An Approach for a human posture prediction model using internal/external forces and discomfort* (SAE Technical Paper Series No. 2005-01-2694). Warrendale, Pennsylvania, USA: Society of Automotive Engineers.
- Sendler, J. & Kirchner, S. (2012). *Ergonomieprüfstand (Ergobuck)*. Ilmenau, Germany: Technische Universität Ilmenau.
- Sengupta, A. K. & Das, B. Maximum reach envelope for the seated and standing male and female for industrial workstation design. *Ergonomics*, 43(9), 1390–1404.
- Senner, V. (2001). *Biomechanische Methoden am Beispiel der Sportgeräteentwicklung* (Dissertation). Munich, Germany: Technische Universität München.
- Shen, W. & Parsons, K. C. (1997). Validity and reliability of rating scales for seated pressure discomfort. *International Journal of Industrial Ergonomics*, 20(6), 441–461.
- Siebertz, K., Christensen, S. T., Damsgaard, M. & Rasmussen, J. (2004). *The AnyBody Car-Driver, a biomechanical model of the human musculoskeletal system* (Technical Report No. SRR-2004-0153). Aachen, Germany: Ford.
- Siebertz, K. & Rausch, J. R. (2006). *AnyBody Car Driver Model, revision 2*: (Technical Report No. SRR-2006-0067). Aachen, Germany: Ford.
- Siefert, A. & Nuber, A. (2014). *Comprehensive software platform for driver's discomfort: UDASim project outline and goals presentation*. Höchberg, Deutschland: Wölfel.
- Simons, D. G., Travell, J. G. & Simons, L. S. (1999). *Travell & Simons' myofascial pain and dysfunction: The trigger point manual* (2nd edition). Baltimore, Maryland, USA: Williams & Wilkins.
- SizeGERMANY (2012). *Human Solutions GmbH: SizeGermany – Die deutsche Reihenmessung*. Retrieved July, 4, 2012 from <https://portal.sizegermany.de/>.
- Snyder, R. G., Chaffin, D. B. & Schutz, R. K. (1972). *Link system of the human torso (Technical Report AMRL-TR071-88)*. Wright-Patterson Air Force base, Ohio, USA: Aerospace Medical Research Laboratory.
- Soechting, J. F., Buneo, C. A., Herrmann, U. & Flanders, M. (1995). Moving effortlessly in three dimensions: does Donders' law apply to arm movement? *Journal of Neuroscience*, 15(9), 6271–6280.
- Soechting, J. F. & Flanders, M. (1993). Parallel, interdependent channels for location and orientation in sensorimotor transformations for reaching and grasping. *Journal of Neurophysiology*, 70(3), 1137–1150.
- Statistisches Bundesamt (2015). *Statistisches Jahrbuch Deutschland 2015*. Wiesbaden, Germany: Statistisches Bundesamt.

- Steinberg, U., Caffier, G., Schultz, K., Jakob, M. & Behrendt, S. (2007). *Leitmerkalmethode manuelle Arbeitsprozesse. Erarbeitung und Anwendungserprobung einer Handlungshilfe zur Beurteilung der Arbeitsbedingungen* (Forschung Projekt F 1994). Dortmund, Germany: Bundesanstalt für Arbeitsschutz und Arbeitsmedizin (BAuA).
- Sternad, D., Abe, M. O., Hu, X. & Müller, H. (2011). Neuromotor noise, error tolerance and velocity-dependent costs in skilled performance. *PLoS Computational Biology*, 7(9), e1002159, 1-15.
- Tabachnick, B. G. & Fidell, L. S. (2007). *Using multivariate statistics* (5th edition). Boston, Massachusetts, USA: Pearson.
- Tillery, S., Ebner, T. & Soechting, J. (1995). Task dependence of primate arm postures. *Experimental Brain Research*, 104(1), 1-11.
- Todorov, E. (2004). Optimality principles in sensorimotor control. *Nature Neuroscience*, 7(9), 907–915.
- Ulherr, A. & Bengler, K. (2014). *Global discomfort assessment for vehicle passengers by simulation (UDASim)*. 3rd International Digital Human Modeling Symposium. Tokyo, Japan.
- Upmann, A. (2014). *Handbrake Location: Design for Six Sigma 6-Panel for the Black Belt project #64415*. Cologne, Germany: Ford.
- Upmann, A. & Raiber, P. (2014). *Simulation of handbrake application*. RAMSIS User Conference 2014. Kaiserslautern, Germany.
- Van der Meulen, P. & Seidl, A. (2007). RAMSIS - The leading cad tool for ergonomic analysis of vehicles. In V. G. Duffy (Ed.), *Digital Human Modeling. First International Conference on Digital Human Modeling, ICDHM 2007, held as part of HCI International 2007, Beijing, China, July 22-27, 2007: proceedings*. Berlin, Germany: Springer.
- Vandenbergh, A., Levin, O., Schutter, J. de, Swinnen, S. & Jonkers, I. (2010). Three-dimensional reaching tasks: effect of reaching height and width on upper limb kinematics and muscle activity. *Gait & Posture*, 32(4), 500–507.
- Vaughan, J., Rosenbaum, D. A., Harp, C. J., Loukopoulos, L. D. & Engelbrecht, S. (1998). Finding final postures. *Journal of Motor Behavior*, 30(3), 273–284.
- Vink, P. & Hallbeck, S. (2012). Editorial: Comfort and discomfort studies demonstrate the need for a new model. *Applied Ergonomics*, 43(2), 271–276.
- Wallentowitz, H. (2005). *Längsdynamik von Kraftfahrzeugen: Verkehrssystem Kraftfahrzeug, Leistungs- und Energiebedarf, Antriebsstrang, Fahrzeugdynamik ; Umdruck zur Vorlesung Kraftfahrzeuge I* (12. Auflage). Aachen, Germany: Forschungsgesellschaft Kraftfahrwesen.
- Walton, D. & Thomas, J. A. (2005). Naturalistic observations of driver hand positions. *Transportation Research Part F: Traffic Psychology and Behaviour*, 8(3), 229–238.
- Wang, X. (2009). Discomfort evaluation and motion measurement. In V. G. Duffy (Ed.), *Handbook of Digital Human Modeling. Research for applied ergonomics and human factors engineering* (pp. 25-1–25-8). Boca Raton, Florida, USA: CRC Press.
- Wang, X., Chateauroux, E. & Chevalot, N. (2007). A data-based modeling approach of reach capacity and discomfort for Digital Human Models. *Lecture Notes in Computer Science*, 4561, 215-223.
- Wang, X., Chevalot, N., Monnier, G. & Trasbot, J. (2006). *From motion capture to motion simulation: An in-vehicle reach motion database for car design*. Digital Human Modeling for Design and Engineering Conference, Lyon, France, July, 4-6, 2006.

- SAE Technical Paper Series No. 2006-01-2362. Warrendale, Pennsylvania, USA: Society of Automotive Engineers.
- Wang, X., Chevalot, N. & Trasbot, J. (2008). *Prediction of in-vehicle reach surfaces and discomfort by Digital Human Models*. Digital Human Modeling for Design and Engineering Conference and Exhibition, Pittsburgh, Pennsylvania, USA, June, 17-19, 2008. SAE Technical Paper Series No 2008-01-1869. Warrendale, Pennsylvania, USA: Society of Automotive Engineers.
- Wang, X., Le Breton-Gadegbeku, B. & Bouzon, L. (2004). Biomechanical evaluation of the comfort of automobile clutch pedal operation. *International Journal of Industrial Ergonomics*, 34(3), 209–221.
- Wang, X. & Trasbot, J. (2011). Effects of target location, stature and hand grip type on in-vehicle reach discomfort. *Ergonomics*, 54(5), 466–476.
- Wang, X. & Verriest, J. P. (1998). A geometric algorithm to predict the arm reach posture for Computer-aided Ergonomic evaluation. *Journal of Visualization and Computer Animation*, 9(1), 33–47.
- Wang, X., Verriest, J. P., Lebreton-Gadegbeku, B., Tessier, Y. & Trasbot, J. (2000). Experimental investigation and biomechanical analysis of lower limb movements for clutch pedal operation. *Ergonomics*, 43(9), 1405–1429.
- Webb Associates (Ed.). (1978). *Anthropometric source book: Volume 1: Anthropometry for designers* (NASA Ref. 1024). Houston, Texas, USA: NASA Scientific and Technical Information Office.
- Welsh, R., Clift, L., Morris, A., Cook, S. & Watson, J. (2003). *An assessment of cars for small drivers*. Loughborough, UK: Loughborough University.
- Wing, A. M., Lederman, S. J., Nowak, D. A. & Hermsdörfer, J. (2001). Points for precision grip. In D. A. Nowak & J. Hermsdörfer (Eds.), *Sensorimotor Control of Grasping* (pp. 193–203). Cambridge, UK: Cambridge University Press.
- Wirsching, H.-J. (2013). Quo Vadis RAMSIS? In S. Wischniewsky & L. Adolph (Eds.), *Digitale Ergonomie – Trends und Strategien für den Einsatz digitaler Menschmodelle*. Tagungsdokumentation Symposium vom 20. November 2012 in Dortmund (pp. 90–100). Dortmund, Germany: Bundesanstalt für Arbeitsschutz und Arbeitsmedizin.
- Wirsching, H.-J. & Engstler, F. (2012). New enhancements and validation of force based posture and discomfort predictions. *Work*, 41(Suppl 1), 2232–2237.
- Wirsching, H.-J. & Premkumar, S. *Statistical representations of human populations in ergonomic design*. Digital Human Modeling for Design and Engineering Conference and Exhibition, Seattle, Washington, June, 12-14, 2007. SAE Technical Paper Series No. 2007-01-2451. Warrendale, Pennsylvania, USA: Society of Automotive Engineers.
- Yilmaz, T. D., Heimann, J., Fingberg, U., Marek, C. & Fischbein, I. (2012). *Hand operated mechanical park brake DNA*. Cologne, Germany: Ford.
- Zacher, I. & Bubb, H. *Strength based discomfort model of posture and movement*. Digital Human Modeling for Design and Engineering Symposium, Rochester, Michigan, USA, June, 15-17, 2004. SAE Technical Paper Series No. 2004-01-2139. Warrendale, Pennsylvania, USA: Society of Automotive Engineers.
- Zander, T., Dreischarf, M., Schmidt, H., Bergmann, G. & Rohlmann, A. (2015). Spinal loads as influenced by external loads: A combined in vivo and in silico investigation. *Journal of Biomechanics*. 48(4).578-584.
- Zee, M. de, Hansen, L., Wong, C., Rasmussen, J. & Simonsen, E. B. (2007). A generic detailed rigid-body lumbar spine model. *Journal of Biomechanics*, 40(6), 1219–1227.

- Zhang, L., Helander, M. G. & Drury, C. G. (1996). Identifying factors of comfort and discomfort in sitting. *Human Factors: The Journal of the Human Factors and Ergonomics Society*, 38(3), 377–389.
- Zhang, X. *Biomechanical realism versus algorithmic efficiency: A trade-off in human motion simulation modeling* (SAE Technical Paper Series No. 2001-01-2090). Warrendale, Pennsylvania, USA: Society of Automotive Engineers.
- Zhang, X. & Chaffin, D. (2000). A three-dimensional dynamic posture prediction model for simulating in-vehicle seated reaching movements: development and validation. *Ergonomics*, 43(9), 1314–1330.
- Zhang, X. & Chaffin, D. B. (1997). Task effects on three-dimensional dynamic postures during seated reaching movements: an investigative scheme and illustration. *Human Factors*, 39(4), 659–671.
- Zhang, X. & Chaffin, D. B. (2005). Digital Human Modeling for computer-aided ergonomics. In W. Karwowski & W. S. Marras (Eds.), *Handbook of Occupational Ergonomics* (pp. 10-1–10-20). London, UK: CRC Press.

16 CURRICULUM VITAE

Andrea Upmann was born on the 24th of March 1983 in Rheine, Germany. In 2002, she took the final examination at the Gymnasium Dionysianum in Rheine and started to study Mechanical Engineering at RWTH Aachen University in Aachen, Germany. She graduated in 2007 and joined Ford-Werke GmbH in Cologne, Germany, as a vehicle development engineer.

In her first position at Ford, she was responsible for the Exterior Visibility Attribute.

In 2010, she moved to a new position as Attribute Leader for Postural Comfort. Since 2011, she has established a close cooperation on research projects with the Institute of Biomechanics and Orthopaedics at the German Sport University, Cologne.

In 2013, she registered at this university for doctoral studies and started to work on her doctoral thesis which was supervised by Univ.-Prof. Dr. Gert-Peter Brüggemann and is presented herewith.